The Impact of Phase Behaviour on Coke Formation in Delayed Cokers

By

Vieman A. Ali

A thesis submitted in conformity with the requirements
for the degree of Master of Applied Science,
Graduate Department of Chemical Engineering and Applied Chemistry,
University of Toronto

Abstract

In addition to valuable light products, delayed cokers produce shot and sponge coke. Shot coke is an undesirable by-product because represents safety problems and profit loss. The production of these coke structures in delayed cokers has not been studied extensively. In this thesis, a laboratory delayed coker was constructed and the impact of the phase behaviour of the phase(s) where coking reactions take place on the formation of these two cokes and on the amount of coke produced was investigated. A test to discriminate shot and sponge coke was developed. The results showed that the production of shot vs. sponge coke was not linked to phase behaviour, even for residues known to produce shot coke in delayed cokers. However, the amount of coke produced was linked to this variable. Shot coke formation would appear to be linked to overheating of surfaces. These and other issues are discussed in the thesis.

Acknowledgments

I wish to thank PDVSA-Intevep for its financial support and for giving me the opportunity to work with outstanding professionals who moulded my technical career and influenced my motivation to work. Also, I've had the chance to make many friends. Special thanks to Carola, Gustavo "El Gordo", Jorge "El Bicho", Juan Francisco "El Cisco" and Eusebio for their friendship and advice.

I also wish to thank Professor John Shaw for his advice, trust and help through the development of this experimental program and data interpretation. I enjoy working with you. This was a valuable experience that enriched my technical career.

I will always remember the friends I have made at the University of Toronto. Special thanks goes to Xiang Yang and Dimitri. Xiang Yang, thank you for your advice. I'll always remember our conversations in the lab and the office. Dimitri, thank you for sharing lunchtime. I will always miss the "Spanish-Greek vocabulary cross-checking" and the arm wrestling matches. Also, I wish to thank the guys at the machine shop, especially Eric Close, who helped me troubleshoot the apparatus.

To my brothers Carlos and Paul and our parents Rosa and Gerardo, who gave us strong values and the best legacy: education; and encourage us to work hard for what we want.

To my wife Verónica for her love, patience and comprehension. I love you. Also, you gave us the two main reasons of our lives: Sarah and Samuel. This thesis is specially dedicated to them, and to Zuni, Suhail, Daniel, Natasha and Carlos Jr. Your legacy will be education. It's up to you.

Table of Contents

Abstract ii

Acknowledgments iii

Table of Contents iv

List of Figures vii

List of Tables x

Chapter 1 - Introduction 11
  Background 11
    Delayed Coking Process 13
    Coke 14
    Shot Coke in Delayed Coking Units 15
  Motivation 16
  A Link Between Phase Behaviour and Coke Formation 17
  Objectives and Scope 17
    Importance 18
    Organization of Thesis 18

Chapter 2 – Literature Review 19
  Variables Affecting Shot Coke Formation 19
    Feedstock Quality 19
    Operating Variables 20
  Coking Mechanism 22
  Phase Behaviour 24
    Phase Diagrams 25
    The Phase Rule 25
    Behaviour Classification Scheme of Scott and van Konyneburg 27
    Solid Interference 30
    Phase Diagrams for Multi-component Systems: 32
  Delayed coking Models 34
  Summary 37

Chapter 3 – Materials, Apparatus and Methodology 38
  Feedstocks 38
  Laboratory Apparatus 39
    Laboratory Unit Design Premises 39
    Apparatus Description 40
    Methodology 43
  Operating Conditions 45
    One component ABVB model 46
    Two pseudo-component ABVB model 47
  Summary 49

Chapter 4 – Experimental 50

  Experimental Matrix 50
  Evaluation of Experimental and Product Analysis Techniques 52
    Data Acquisition and Mass Balances 53
    Coke Type Evaluation 56
  Equipment Performance Evaluation 60
    Coker Operating Conditions 60
    Performance of the feed pump 61
    Performance of the Coker effluent condenser 62
  Summary 63

Chapter 5 – Results and Discussion 64
  Evaluation of the Laboratory Apparatus 64
    Reproducibility of Mass Balances 64
    Comparison of Product Yields with Delayed Coking Models 66
  Coke Type Evaluation 68
    Surface Morphology and Particle Breakage Test Results 68
    Microscopic Examination of Particle Sections 74
  Coke Formation and Phase Behaviour 77
    Variation of Coke Yield with Pressure 78
    Variation of Coke Yield with Feedstock Composition 80
  Coke Yield and the Impact of n-Dodecane 82
  Summary 82

Chapter 6 – Summary and Conclusions 84

Chapter 7 – Recommendations for Future Work 87

Nomenclature 89
  Variables 89
  Subscripts 90
  Superscripts 91
  Acronyms 91

References 92

Appendix A: Product Yields and Properties 97

Appendix B: Laboratory Unit Design 102

Appendix C: Feed Pump Calibration 115

Appendix D: Coker Effluent Condenser 125

Appendix E: Data Acquisition System Configuration 134

Appendix F: Operating Procedure 140

Appendix G: Operating Data 146

Appendix H: Mass Balances 175

Appendix I: Coke Breakage Method 205

Appendix J: Coke Analyses 210

List of Figures

Figure 1.1: Delayed coking process 13

Figure 1.2: Samples of different cokes obtained from vacuum residue processing. Left: shot coke. Right: sponge coke (Elliot, 2001). 14

Figure 2.1: Coke products from petroleum fractions (Speight, 1998) 22

Figure 2.2: Pressure – Temperature projections illustrating the classification of the phase behaviour of binary mixtures. 28

Figure 2.3: solid interference with a continuous critical line 31

Figure 2.4: solid interference diagram derived from a type III diagram. 31

Figure 2.5: P-T phase diagram for Type V phase behaviour. Expansion from binary to ternary system. 32

Figure 2.6: P-T diagrams of n-decylbenzene + ethane + carbon dioxide I) 40 mole % carbon dioxide, II) 20 mole % carbon dioxide, III) 10 mole carbon dioxide and IV) n-decylbenzene + ethane. 33

Figure 3.1: Apparatus schematic 40

Figure 3.2: Coker design versions. A: lateral inlet version. B: bottom inlet version. 1: feedstock inlet; 2: vapor outlet; 3: thermocouple connection; 4: pressure transducer connection. 41

Figure 3.3: Comparison of bubble pressure data and calculations where ABVB is considered as one component for mixtures of ABVB and n-C_{12} at 523 K and 613 K (250 °C and 340 °C). 46

Figure 3.4: Comparison of bubble pressure data and calculations for mixtures of ABVB and n-C_{12} at 523 K and 613 K (250 °C and 340 °C) where ABVB is considered as two pseudo-components. 47

Figure 3.5: Calculated bubble pressures for mixtures of ABVB and n-dodecane at 698 K. 48

Figure 4.1: Phases diagram at 613 K (340 ºC) for mixtures of n-C_{12} + ABVB (Zou, 2002). 50

Figure 4.2: Shot coke particles produced in a commercial delayed coking unit. Feedstock: Heater Feedstock (Morin, 2002). 58

Figure 4.3: Shot coke particles produced in a delayed coking pilot plant. Feedstock: Heater Feedstock (Morin, 2002). 58

Figure 4.4: Shot coke (left) and sponge coke (right) produced in a delayed coking pilot plant. Feedstock: Heater Feedstock (Morin, 2002). 59

Figure 4.5: Breakage mass for shot coke and sponge coke particles. 59

Figure 4.6: Coker variables (temperature and pressure) for experiment 43. 61

Figure 4.7: Feed pump. Flow rate error represents the difference between the actual flow and the expected flow. 62

Figure 4.8: Experiment 41: condenser inlet and outlet temperatures. 62

Figure 5.1: Coke yield as function of pressure for different mixtures of ABVB + n-dodecane. 67

Figure 5.2: Experiments with mixtures of ABVB and n-dodecane at low pressure. Coke yields based on the residue processed (E_{34}: ABVB 50 wt%, P=238 kPa, T=699 K; E_{35}: ABVB 50 wt%, P=239 kPa, T=699 K; E_{41}: ABVB 30 wt%, P=239 kPa, T=699 K). 68

Figure 5.3: E_{19} (ABVB: 60 wt%; 6100 kPa): photomicrographs of coke samples. 69

Figure 5.4: E_{20} (ABVB: 60 wt%; 3550 kPa): photomicrographs of coke samples. 69

Figure 5.5: E_{21} (ABVB: 40 wt%; 6100 kPa): photomicrographs of coke samples. 70

Figure 5.6: E_{22} (ABVB: 40 wt%; 3550 kPa): photomicrographs of coke samples. 70

Figure 5.7: E_{27} (ABVB: 45 wt%; 6100 kPa): photomicrographs of coke samples. 70

Figure 5.8: E_{28} (ABVB: 45 wt%; 6100 kPa): photomicrographs of coke samples. 70

Figure 5.9: E_{29} (ABVB: 50 wt%; 6100 kPa): photomicrographs of coke samples. 71

Figure 5.10: E_{30} (ABVB: 50 wt%; 3550 kPa): photomicrographs of coke samples. 71

Figure 5.11: E_{38} (ABVB: 50 wt%; 2240 kPa): photomicrographs of coke samples. 71

Figure 5.12: Breakage mass average values for coke samples produced in different experiments and reference values for shot coke and sponge coke. Error bars represent the 95% confidence limits. 72

Figure 5.13: E_{25} (Heater Feedstock; 698 K; 240 kPa): photomicrographs of coke samples. 73

Figure 5.14: E_{26} (Heater Feedstock; 718 K; 240 kPa): photomicrographs of coke samples. 73

Figure 5.15: E_{36} (Heater Feedstock; 720 K; 178 kPa): photomicrographs of coke samples. 73

Figure 5.16: SEM. A, B: shot coke produced in a delayed coking pilot plant. C, D: coke sample produced in experiment 36. 75

Figure 5.17: Polarized Light Microscope. Pictures A and C: non-polarized light. Pictures B and D: polarized light. Sample from experiment 36. 76

Figure 5.18: Coke yield from ABVB in ABVB + n-dodecane mixtures at 698 K. 78

Figure 5.19: Phase diagram represents a coke yield model as function of feedstock composition and pressure. 81

List of Tables

Table 2.1: Degrees of freedom and features ... 27

Table 2.2: Delayed coking product yields (wt%) ... 35

Table 2.3: Variables in the delayed coking models used to design and evaluate the apparatus (Cabrera, Sanoja, & Ali, 1997 and Cabrera, Guerrero, & Ali, 1998). ... 36

Table 3.1: Properties of different vacuum residue samples and n-dodecane. ... 38

Table 3.2: Physical and critical properties of the ABVB pseudo-components ... 47

Table 3.3: Bubble pressure, for mixtures of ABVB and n-dodecane at 698 K, calculated with two different models. ... 48

Table 4.1: Experimental matrix for evaluation of mixtures of ABVB and n-Dodecane. . 51

Table 4.2: Experimental matrix for evaluation of other vacuum residues. Composition is related to ABVB content (wt fraction) on the mixture and pressure in kPa. ... 52

Table 4.3: Mass balance equations. ... 54

Table 4.4: Mass balance calculation for experiment 33. ... 55

Table 4.5: Properties of samples of shot and sponge coke gathered from the same source (Ellis & Bacha, 1996). ... 56

Table 4.6: Standard deviations for temperature and pressure in the coker. ... 60

Table 5.1: Reproducibility of General and Petroleum Mass Balances. ... 65

Table 5.2: Comparison of product yields obtained in the new apparatus and the expected values according to the delayed coking models. ... 66

Table 5.3: Breakage weights average values for experiments carried out with Heater Feedstock. ... 74

Chapter 1 - Introduction

Background

Crude oils are classified according to their API gravity (Petróleos de Venezuela, 2000) as light crude oils (30 – 49.9), medium crude oils (22.0 29.9), heavy oils A (14 – 21.9), heavy oils B (10 – 13.9) and extra-heavy oils (bellow 9.9). The lighter the crude oil the easier the production of light valuable hydrocarbon products like naphtha, gasoline and diesel by separation methods (for example distillation); moreover, high yields of these products are achieved without using deep conversion technologies. On the other hand, heavy oil characteristics are: low hydrogen to carbon ratio (H/C ratio), high content of contaminants (Sulphur, Nitrogen, Nickel, Vanadium) and low yields of light hydrocarbon products when they are distilled or physically separated. For example, only 50% of the bitumen can be recovered by vacuum distillation (Gray, 2002). Therefore, the use of deep conversion technologies is necessary to transform the heavy petroleum fractions, also called residue, into more valuable hydrocarbon products.

Processes for conversion of heavy petroleum fractions into more valuable liquid products with carbon rejection can be classified into three groups: first, catalytic cracking which includes the use of catalyst and heat to produce smaller molecules than those existing in the feedstock; second, hydrocracking which involves the use of hydrogen in the presence of a catalyst to produce compounds with higher H/C ratio; and third, thermal cracking which comprises the use of energy (high temperatures) to produce lighter compounds (Gray, 1994).

In catalytic cracking the advances have been related to increase the fraction of residue in the throughput to Fluid Catalytic Cracking (FCC) units; chiefly by designing more resistant catalysts with traps for metals and catalyst poisons. However, the large amount of contaminants in residues from heavy oils make these feedstocks unsuitable for processing in these units; moreover, the amount of residue processed is too low (between 5 and 10 wt%) and this alternative cannot be considered as the best option for processing of residues from heavy oils.

In hydrocracking, research activities are oriented to develop new processes and technologies to upgrade heavy oils; to improve required procedures like catalyst regeneration; and to develop new effective catalysts and to understand the behaviour of these heavy hydrocarbons when processed under hydrogen donor catalyzed conditions (Dew, Wang, & Seon, 1996; Weissman, 1997; Yang, Nakamura & Fujimoto, 1998; McGrath, 1999, Gray, Zhao & McKnight, 2000, Chen & Tsai, 1999, Mirzayeva et al., 1995; Butz & Oelert, 1995; Martinez, Benito & Callejas, 1997b, 1997c; Nuñez, Pachon, Kaparov & Resasco, 2000; Callejas & Martinez, 2000a, 2000b); therefore, hydrocracking is considered the most promising alternative to process heavy oils and their residues; but the difficulties associated with hydro-conversion processes such as the costs of hydrogen and catalysts, high pressure vessels and the intolerance of coke formation that causes poisoning of catalysts make these technologies less suitable than thermal cracking technologies.

Thermal cracking technologies are still the most frequently selected alternatives for heavy oil residues because of the comprehensive knowledge of these technologies. They can be classified as coke free processes (i.e. Visbreaking), and coke rejection processes (i.e. Delayed Coking, Fluidcoking and Flexicoking). Until 1994, 64% of the total world residue conversion capacity was based on thermal cracking technologies. In North America, more than 50% of residue processing capacity was based on coke rejection processes (Petróleos de Venezuela-Intevep [PDVSA-Intevep], 1999). Until 1995, there were 136 delayed coking units around the world, which represented 3228 MBD (Thousand Barrels per Day) total processing capacity, 8 Fluidcoking units with 370 MBD total capacity and 5 Flexicoking units that processed 165 MBD. Between the 1st quarter of 1999 and the 3rd quarter of 2000, up to 12 new delayed coking units were expected to start up, with a total processing capacity of 435 MBD (PDVSA-Intevep, 1999). This represents almost 14% of delayed coking capacity that existed prior to 1995. All these units except one are oriented to process vacuum residues, and considering the availability of heavy crude oils with the scarcity of light crude oils, there is a high probability that these units are oriented to process vacuum residues from heavy oils. This shows that the most popular alternative among coke rejection processes is the delayed coking process.

The Canadian industry has been using delayed and fluid coking technologies for more than 35 years to upgrade oil sands bitumen into synthetic crude oil. Nowadays, the production is over 300000 barrels per day and there are plans to more than double this total (Parker et al, 2002). Moreover, SUNCOR, which makes use of delayed coking technology, is arguably the most profitable of the bitumen producer/refiners.

Delayed Coking Process

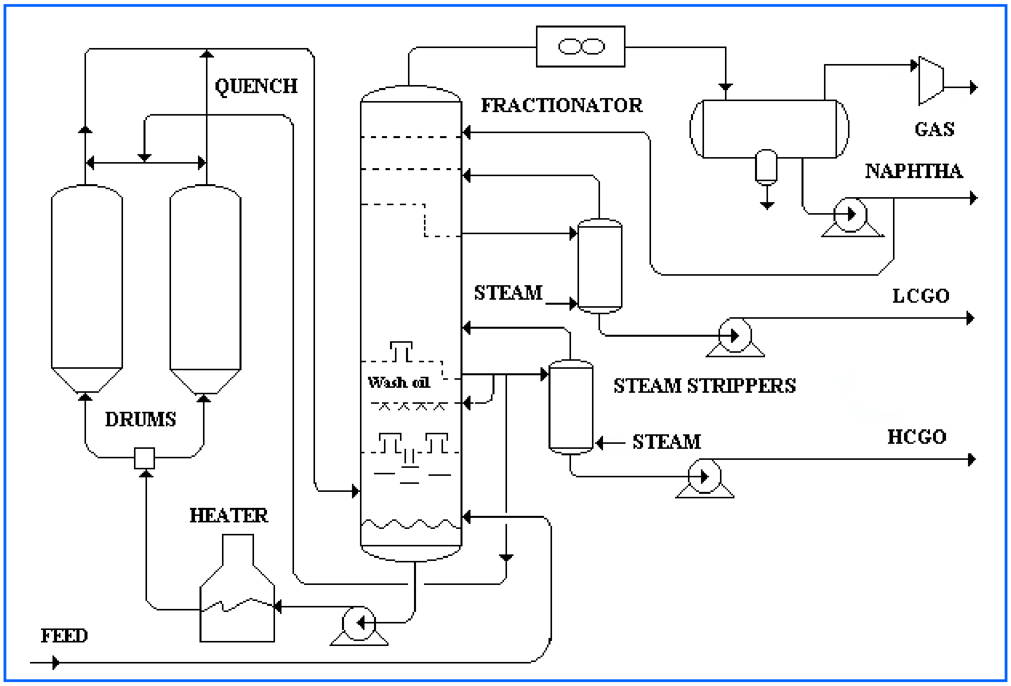

Figure 1.1: Delayed coking process

Figure 1.1 shows a flow diagram of the delayed coking technology. This technology is a batch-continuous process where the feedstock is pumped through a continuous operating heater. In this equipment the feedstock is heated up to reaction temperature (760 – 780 K), and afterwards, it is switched between two reactors (called drums) that work at pressures between 240 kPa and 1100 kPa. The higher pressure is typical of units where special cokes (needle or anode coke) are produced. While one drum is filling (the filling cycle is between 11 and 24 hours), the other drum is subject to steam stripping, cooling, decoking, pressure testing and warming up. The vapor, from the top of the coking drum, is sent to the main fractionator where gases (C_1 – C_4's) and light products, typically naphtha, light gas oil (LCGO) and heavy gas oil (HCGO) are obtained. The heavy components in the vapor leaving the drums are condensed in the bottom of the main fractionator, mixed with fresh feed, and recycled to the reaction zone. The heavy hydrocarbons that remain in the drums condense and polymerize to form coke. These units are essentially used to process the “bottom of the barrel” looking for higher yields of more valuable light products. Coke is an undesired by-product.

Coke

In a delayed coking unit, condensation and polymerization reactions that take place on the material that remains in the reactor form coke. This product has been classified according to its physical structure and properties as needle coke, sponge coke and shot coke (Ellis, 1998). Needle coke is obtained from carbonization of high aromatic content asphaltene-free feedstocks (i.e. FCC decanted oils), it is the premier coke, and it is used in graphite electrode manufacture (Ellis, 1998). On the other hand, sponge coke and shot coke are formed, typically as a mixture, when processing vacuum residues. Usually, the sponge coke content increases when the asphaltene and the heteroatom content in the vacuum residue decrease. Sponge coke that meets strict property specifications is considered anode grade coke; otherwise it is used as fuel. Moreover, if the feedstock used has a high content of asphaltenes and heteroatoms, shot coke can be present in high proportions (50 wt% or more).

Figure 1.2: Samples of different cokes obtained from vacuum residue processing. Left: shot coke. Right: sponge coke (Elliot, 2001).

Figure 1.2 shows samples of shot coke and sponge coke. Shot coke comprises dense low porosity spherical clusters with 2 – 10 mm diameters, frequently present as agglomerates up to the size of basketballs. These large agglomerates are fragile and can be broken easily; however, the small spheres are very hard (these small particles give the shot coke the high hardness characteristic). Sponge coke, is a friable solid material with pores on the surface, and internal cavities connecting the pores.

Shot Coke in Delayed Coking Units

Ellis and Bacha (1996) illustrate the appearance of shot coke in delayed coking units, and show the meaning of unit operating conditions (flow, temperature and pressure) in shot coke formation. Moreover, these examples illustrate the existence of a narrow range in operating variables where the appearance of shot coke can be promoted or suppressed.

When high asphaltene feedstocks are processed, shot coke production has a big impact on delayed coking drum operation. Typical situations include hot spots in the coke bed and coke bed collapse when the bottom head is opened (Elliot, 2001). These situations impact the unit performance and profit, and present safety hazards.

For example, hot spots in the coke bed are created because the cooling water introduced in the drum cannot penetrate the big coke clusters. This water is introduced in the drum after it has completed the filling period and has been steam striped to remove light ends. Thus, the water in the drum has a preferential flow and the coke is not cooled homogeneously, causing deformation of the drum when cooling water is pumped at high flow (called the “banana” effect), or eruptions arise in the drum when the cutting water impacts these hot spots (big pieces of coke are expelled from the top of the drum).

Likewise, the coke bed formed in the drum can collapse. Consequently, when the drum bottom head is opened to complete water drainage and start the coke-cutting step, the coke bed can collapse over the structure platform due to its instability, creating a dangerous situation for personnel in that area. This coke has a temperature over 373 K and must be removed, creating a delay in the unit operation.

Elliot (2001) and Malik (2000) have proposed new designs and changes in operational procedures in delayed coking units to deal more effectively with shot coke production. In design, the proposals are oriented to improve safety and operational reliability with modifications focused on how to deal with and handle shot coke. In operational procedures, authors agree that shot coke formation can be reduced by using highly aromatic feedstocks mixed with the vacuum residue, increasing the operating pressure and / or the recycle ratio, and reducing the heater outlet temperature (Ellis & Bacha, 1998; Elliot, 2001).

However, incorporating the alternatives indicated above does not guarantee that the problems related to shot coke can be solved (Coker Discussion, 1999). Besides, the unit profit diminishes because the incorporation of new designs represents additional investment in existing units and increases the cost of new units; the incorporation of other feedstocks reduces the vacuum residue processing capacity; and changes in operating variables (pressure, recycle ratio and temperature) increases the coke yield.

Motivation

As light petroleum resources have become increasingly scarce and reserves of heavy oil remain available (according to Martinez, Benito & Callejas (1997a) around 40 trillion barrels of heavy oil are available), the oil industry has been forced to increase the amount of low quality heavy feedstocks processed in delayed coking units to meet market demands for fuels. Consequently, the production of shot coke in delayed coking units has increased affecting the safety and profitability of refineries. Although new designs and changes in operational procedures have been implemented to deal more effectively with shot coke production (Elliot, 2001; Malik, 2000), the application of these alternatives do not guarantee a reduction in its formation (Coker discussion, 1999); moreover, the knowledge of how effective they can be is uncertain, due the lack of information about shot coke formation when low quality feedstocks are processed.

A Link Between Phase Behaviour and Coke Formation

Abedi, Seyfaie & Shaw (1998) observed a link between coke formation and phase behaviour. The system evaluated was a mixture of Athabasca Bitumen Vacuum Bottoms, Dodecane and hydrogen. They found that working with this mixture at 655 K and 6.3 MPa, a third condensed phase identified as asphaltenic in nature appears (from L_1L_2V to DL_1L_2V). This phase transition is not reversible and the phase formed persists even at room temperature. However, if the same mixture with the same composition was heated to 700 K at a lower pressure (3.8 MPa) so that the trajectory remains within the L_1V region, no evidence of dispersed phase formation arises. This result suggests that the origin of the transition is related to phase behaviour and not to reaction kinetics since higher reactivity is expected at higher temperatures.

Furthermore, the literature review shows that the coking mechanism, although based on kinetic phenomena comprises a phase separation prior to coke formation; moreover, the “quality” of the liquid phase where the condensation and polymerization reactions are taking place affects the different types of coke formed, and the production of the various coke forms is very sensitive to pressure even when other process variables are held constant. Zou (2002) has evaluated the phase equilibrium behaviour for mixtures of ABVB and n-C_{12} at constant temperature and different compositions and pressures. The diagram obtained at 613 K shows SLV behaviour at pressures far below the bubble point for any composition of ABVB. When the operating pressure reaches the mixture bubble pressure, the appearance of more than one liquid phase is evident at ABVB wt. fractions lower than 0.75. Considering the role of phase behaviour in coke formation and the importance of phase “quality” in shot coke formation, a study aimed at establishing a link between the system operating conditions (affecting the phase behaviour) and the type of coke formed is justified.

Objectives and Scope

The principal objectives of this study are to establish a relationship between the phase behaviour of feedstocks for coking processes and the production of sponge and shot coke which can be used to minimize shot coke formation. The specific objectives are to:

1. Build a laboratory scale unit for the production of coke from heavy oil vacuum residues;
2. Investigate the impact of operating conditions, principally pressure, on the extent of shot coke and sponge coke formation. Special attention will be focused on the importance of operating conditions near the feedstock bubble point on the type of coke formed;
3. Identify critical steps in the coke formation mechanism and their relationship with the phase behaviour of the system where coking reactions are taking place.

Importance

Understanding shot coke formation phenomenon will help to improve operational performance of delayed coking units when low quality feed stocks are processed, leading to safer operation and higher profits. Furthermore, the identification of critical steps in the coking mechanism and their relationship with phase behaviour gives a different perspective to study and understand the coking process in heavy oils and their vacuum bottoms.

Organization of Thesis

This document is divided into seven chapters. Chapter 1 comprises the introduction. Chapter 2 contains background material on shot coke formation and phase diagrams required to understand this thesis, as well as the fundamentals of the delayed coking models used to design the laboratory apparatus. Chapter 3 presents the feedstock properties, the apparatus design criteria, the apparatus description, the methodology and the selection of the operating conditions. Chapter 4 contains the experimental matrix and the evaluation criteria for the products and the data gathered. Chapter 5 presents experimental results and their discussion. Finally, chapters 6 and 7 comprise the conclusions, recommendations and suggestions for future work in this area.

Chapter 2 – Literature Review

This chapter contains four sections. The first section presents the main variables that impact the structure of the coke formed in the drums of the delayed coking process. The second section reviews the existing works about shot coke formation, highlights the shortage of these investigations and the need for the present project. The third section deals with phase equilibrium and the development of phase diagrams to explain and understand the phase behaviour of chemical mixtures and their application, and to explain the appearance of solid phases in hydrocarbon mixtures. The fourth section is dedicated to delayed coking models, their use and the variables that characterize them.

Variables Affecting Shot Coke Formation

According to Ellis & Bacha (1996) and Elliot (2001), the variables which impact coke structure are the quality of the feedstock and the operating variables including pressure, temperature, vapor velocity and recycle ratio.

Feedstock Quality

Different authors (Marsh et al., 1985; Ellis & Bacha, 1996; and Rodriguez et al., 1998) agree that the feedstock properties associated with the production of shot coke are asphaltene content and Conradson carbon residue content.

The asphaltene content can be measured as the toluene soluble fraction that precipitates from the sample when it is mixed with an excess of n-pentane or n-heptane. If the solvent used is n-heptane, the amount of precipitated material is lower than the amount of precipitated material when the solvent used is n-pentane. It is worth noting that the cited works based their conclusions on n-heptane insoluble asphaltene content.

On the other hand, the Conradson Carbon Residue is a destructive analysis that measures the tendency of a sample to produce coke by heating it under nitrogen atmosphere at 773 K during 15 minutes. Nowadays, the Microcarbon Residue Method (ASTM-D4530) is the method used to measure carbon residue. No difference exists between Microcarbon

Residue and Conradson Carbon residue Method (ASTM Standards, 1998) other than precision.

These researchers claim that the tendency to produce shot coke increases when the ratio between the asphaltene content and the Conradson carbon residue content approaches 0.5. Moreover, the characterization of vacuum residues from different heavy oil sources show that this ratio (asphaltene content / Conradson carbon content) is equal to or higher than 0.5; therefore, if the operating conditions are favourable, the formation of shot coke is likely when these feedstocks are processed.

Another fact that shows that the feedstock quality has an important impact on the coke structure is the use of decanted oil mixed with vacuum residue. Decanted oil is the residual product from the Fluid Catalytic Cracking (FCC) process. This hydrocarbon stream is highly aromatic (more than 70% aromatics) and its incorporation into the coker with the feedstock (between 15% and 20% of the total feedstock) suppresses shot coke formation. This suppressing action can be related to the solubility effect of the aromatics on the asphaltenes (Elliot, 2001), although, this has not been shown experimentally.

Operating Variables

Operating variables refer to the pressure, temperature, vapor velocity and recycle ratio within the coker.

Pressure: the reduction of the coker pressure favours the formation of shot coke. Ellis & Bacha (1996) illustrate this fact with examples where narrow variations of this variable (around 34 kPa) have a marked impact on the coke structure formed. Moreover, the operating pressure in delayed coking commercial units, where these heavy feedstocks are processed, is as low as 240 kPa and new designs are expected to operate at 205 kPa. Therefore, the risk of shot coke formation in new delayed cokers is significant.

Temperature: higher temperatures favour shot coke formation and temperature changes of 5 K or less can either suppress or promote shot coke formation (Ellis & Bacha, 1996). In a commercial delayed coking unit, the heater outlet temperature varies between 763 and 773 K. However, scaling down of these units is reached by operating the small-scale units at lower temperatures, which may vary between 690 and 723 K (Velutini & Guerrero, 1996; Ali, 1998).

Vapor Velocity: the feedstock flow is not an important variable affecting product yields in the delayed coking technology but according to Marsh et al. (1985) and Ellis & Bacha (1998), this variable is an important parameter for shot coke formation because it impacts the vapor superficial velocity that is thought to give the spherical shape to shot coke particles. The vapor superficial velocities in commercial delayed coking units are between 0.12 and 0.21 m/s (PDVSA-Intevep, 1999). These velocities are too high to be achieved in laboratory scale units. Instead, the vapor velocity in such cokers can be selected from delayed coking pilot plants that produce shot coke with vapor velocities between 0.015 – 0.018 m/s (Velutini & Guerrero, 1996; Ali, 1998).

Recycle Ratio: it is calculated with the following expression:

$$RR = \frac{HF}{FF} \tag{2.1}$$

HF is the heater flow. It is measured at the inlet of the heater after the recycling stream has been mixed with the fresh feed at the bottom of the main fractionator (see Figure 1.1). FF is the fresh feed flow. It is measured before the processed feedstock has been pumped to the main fractionator (Figure 1.1). Both flows are measured in barrels per day.

The recycle ratio in delayed coking units varies from 1.03 to 1.30. The highest values are used in commercial units where needle coke is produced while the lowest values are typical values in delayed coking units where the coke yield is to be minimized, e.g.: the delayed coking units where vacuum residues from heavy oils are processed. Moreover, the reduction in the recycle ratio favours shot coke formation because the concentration of asphaltenes in the reacting mixture is greater (Elliot, 2001).

It is worth noting that delayed coking units dedicated to process vacuum residues from heavy oils are designed to work at operating conditions that maximize the yield of distillates and minimize coke production. These operating conditions are lower pressures, higher temperatures and lower recycle ratios. Thus, considering that such feedstocks have high asphaltene content, the production of shot coke, particularly in newer units is likely.

Coking Mechanism

It is well known that thermal treatment of hydrocarbons follows a free radical mechanism where cracking reactions take place in the initiation step, and condensation and polymerization reactions comprise the final step. The reactions in the final step explain the formation of heavy fractions and products like coke.

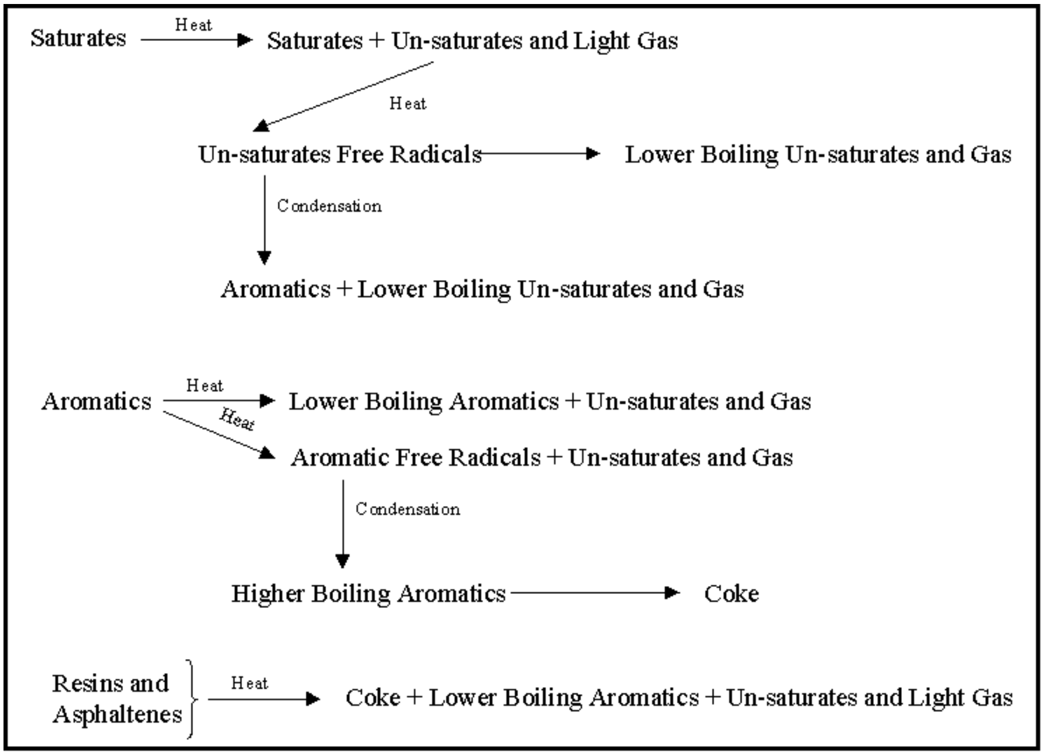

Figure 2.1: Coke products from petroleum fractions (Speight, 1998)

The complexity of the mixtures that represent petroleum and their vacuum residues makes the identification of the reaction pathway of each hydrocarbon compound a very difficult task. Instead, reaction pathways of different fractions are expressed - Figure 2.1 (Speight, 1998).

As indicated in Chapter 1, the mixtures to be evaluated in this thesis are mixtures of vacuum residues with n-dodecane. According to Figure 2.1, the incorporation of this saturate compound will produce hydrocarbons that will form part of the distillate and gas products.

Although the model in Figure 2.1 is purely kinetic, Wiehe (1993) reformulated this mechanism by introducing the existence of liquid-liquid separation between reacted asphaltenes and lighter compounds before coke formation; and later, Abedi et al. (1998) suggested a link between coke formation and phase behaviour. These works provide a link between coking kinetics and phase separation during thermal treatment of hydrocarbons. However, no one has studied the influence of both phenomena on the type of coke formed (i.e. needle, sponge or shot coke).

Most of the research on coke formation (Marsh et al., 1985; Ellis & Bacha, 1996 and Rodriguez et al., 1998) has only been related to needle coke and sponge coke. The shot coke formation mechanism has been included in these works because the content of this material in those special cokes affects their final physical properties and prices. In these studies, they processed high quality feedstocks obtained from light crude oils but did not evaluate the impact of lower quality feedstocks (i.e. vacuum residues from heavy crude oils) with the asphaltene content / Conradson carbon ratio over 0.5. Indeed, while these studies represent the main source of information about shot coke formation, their conclusions do not necessarily apply when lower quality feedstock are processed.

Marsh et al. (1985) reported the mechanism currently accepted for shot coke formation. This mechanism establishes, among the main steps, that high velocities in the reactor are required to create the spherical particulates that comprise shot coke. Based on these results and considering that a highly turbulent medium is required for the formation of spherically shaped precursors that form shot coke, Ellis and Paul (1998) considers it a difficult task to produce shot coke under laboratory conditions because superficial velocities are too low. However, shot coke has been obtained during the evaluation of vacuum residues from heavy feedstocks in PDVSA-Intevep's delayed coking pilot plant with superficial vapor velocities one order of magnitude lower than those found in commercial delayed coking units (Velutini & Guerrero, 1996; Ali, 1998). This fact suggests that when lower quality feedstocks are processed, the mechanism of shot coke formation follows a pathway different from that proposed for shot coke formation when processing high quality feedstocks.

The increasing interest in the upgrading of heavy crude oils has led researchers to try to understand the behaviour of these feedstocks and their fractions. Therefore, other explanations and mechanisms of coke formation have been based on the works of Marsh et al. (1985) and Wiehe (1993), but related to the processing and upgrading of heavy feedstocks. Menéndez et al. (1997) and Rahimi et al. (1998, 1999) have studied the impact of different fractions of vacuum residues from heavy oils in the coke formation process. Although their main interest is not related to shot coke formation, they describe the formation of this material. Three contributions of these studies are: first, that the coke formation process, although characterized by a kinetic regime, comprises certain phenomena that can be related to phase behaviour; second, that a difference in phase "quality" explains differences in the type of coke formed and that difference in phase quality is related to the formation of a high viscosity medium where the mesophase cannot grow and coalesce to form coke having optical textures of fine grained mosaics like shot coke can arise; and third, that the appearance of shot coke particles under laboratory conditions is possible when processing samples from low quality heavy oils. However, the fact that these studies have been carried out on fractions of vacuum residues and not on the whole residue suggests a lack of information about the synergistic effects of all these fractions together on the coke formation process.

Phase Behaviour

According to the previous sections in this chapter, two parameters have a significant influence on the final structure and the reaction pathway of the coke formed in reactors; first, the operating conditions that are defined by temperature and pressure; and second, the properties and composition of the liquid phase where the coking reactions are taking place. The study and explanation of these phenomena are not easy tasks and the selection of a specific chemical engineering science to accomplish it, is not straightforward. However, considering the importance of the parameters indicated above, it seems that thermodynamics provides a suitable physics to help understand and explain these phenomena. More specifically, phase diagrams and the evolution of phase diagrams as reactions progress may provide key insights into the production of the various coke forms.

Therefore, this section deals with phase diagrams. It starts with basic concepts and fundamentals which are required for their understanding, followed by a description of the different phase diagrams that cover the experimentally observed phase behaviours; and finally, the application of phase diagrams and phase behaviour to solid deposition.

Phase Diagrams

Phase diagrams are graphical representations of the effect of pressure (P), temperature (T) and composition (x) in the number and the types of phases in equilibrium. These representations illustrate interrelationships between all of the variables, and facilitate interpolation and extrapolation. Common representations are P-T, P-x and T-x in bi-dimensional diagrams and P-T-x in tri-dimensional diagrams.

The Phase Rule

The physical state of a system is established when the temperature, the pressure, the volume and the compositions of all phases are fixed; however, at equilibrium, these variables are not independent and fixing some of them establishes values for the others. The number of independent variables is obtained with the Gibbs phase rule.

For a system with N chemical species presented at equilibrium in π phases, the variables are temperature, pressure and N-1 mole fractions in each phase. Thus, the number of variables is $2 + (N-1)*\pi$.

The equations or constraints that connect these variables are:

1. The condition for equilibrium:

$$\mu_i^1 = \mu_i^2 = \mu_i^3 \ldots = \mu_i^\pi \tag{2.2}$$

Where μ_i is the chemical potential of i^{th} component. The chemical potential is defined as the change in total Gibbs energy when dn_i moles of component "i" are added to the system at constant temperature, pressure, and moles of the other components.

$$\mu_i = \left(\frac{\partial G}{\partial n_i} \right)_{T,P,n_{j \neq i}} \tag{2.3}$$

The Combination of equations 2.2 and 2.3 produces (π -1)*N equations.

2. In the case of equilibrium with R independent chemical reactions, for each independent reaction:

$$\sum_{i=1}^{N} \mu_i \times dn_i = 0 \tag{2.4}$$

3. The existence of C critical phenomena represents equal number of constraints.

Thus, the total number of constraints is (π -1)*N + R + C.

The number of independent variables or degrees of freedom of a system (F) is the difference between the number of variables and the number of constraints. This equation is known as the Gibbs phase rule:

$$F = 2 + N - \pi - R - C \tag{2.5}$$

Some examples are listed in Table 2.1, where the number of initial phases, C, and the number of reactions are set to zero. The cited examples concern key features of phase diagrams and projections. That is to say that the application of the Gibbs phase rule determines the geometrical features of the phase diagram that represents each particular case. In this Table, S, L and V represent solid phase, liquid phase and vapor phase, respectively.

Table 2.1: Degrees of freedom and features

F	Geometrical Feature	Example
0	Point	N = 1; π = 3. SLV point
1	Line	N = 2; π = 3. SLV
2	Surface	N = 1; π = 1. S L V
3	Volume	N = 2; π = 1. S L V

Behaviour Classification Scheme of Scott and van Konyneburg

This classification scheme of Scott and van Konyneburg (1980), was developed for binary mixtures; however, many of the features of the phase diagrams for multi-component mixtures are identical to those found in the phase diagrams of binary mixtures. Therefore, this classification scheme is useful to understand phase diagrams for multi-component organic systems. It represents all but one of the experimentally observed phase behaviours for binary systems.

Before starting with the identification of the different types of phase diagrams, it is convenient to define some related terms:

- Lower Critical Solution Temperature (LCST): temperature at which two liquids become critical as the temperature is isobarically lowered.
- Upper Critical Solution Temperature (UCST): temperature at which two liquids become critical as the system temperature is raised.
- Lower Critical End Point (LCEP): occurs at the intersection of the lowest temperature of a three phase curve and the critical mixture curve.
- Upper Critical End Point (UCEP): is the intersection on the UCST and a three phase curve where two phases (liquid – liquid or liquid – vapor) critically merge to form a single phase in the presence of a non-critical phase (vapor or liquid).
- K-point: the point where one liquid phase and one vapor phase become critical in the presence of a liquid phase ($L_1 = V + L_2$).

- L-point: the point where two liquid phases become critical in the presence of a vapor phase ($L_1 = L_2 + V$).

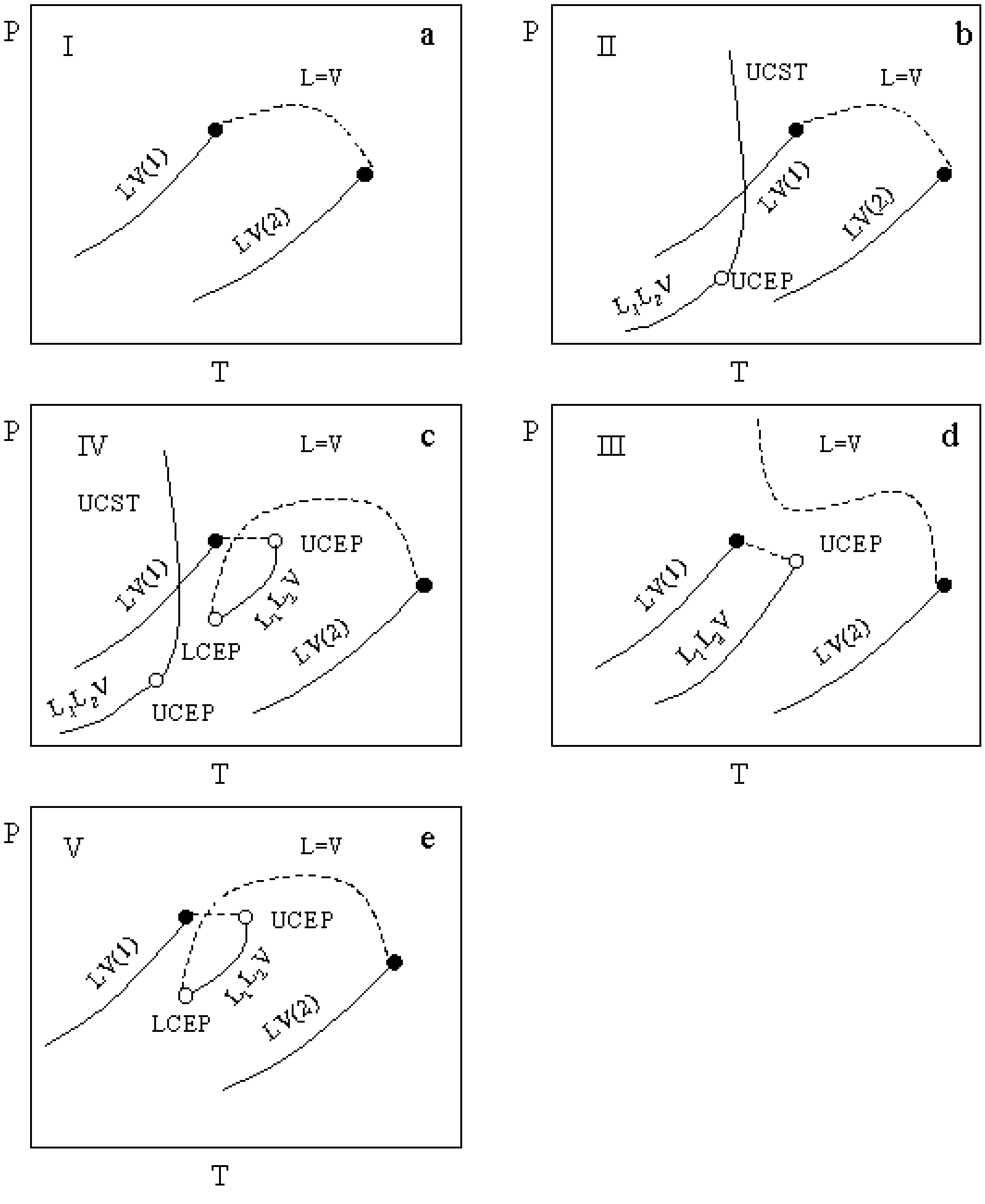

Figure 2.2: Pressure – Temperature projections illustrating the classification of the phase behaviour of binary mixtures.

Figure 2.2 shows the five types of diagrams in the classification of Scott and van Konyneburg. These diagrams are represented with continuous and broken lines and black and white circles. The continuous lines can represent any of the following three different features; first, the vapor pressure lines which are denoted as LV(1) for the light component and LV(2) for the heavy component; second, the three-phase line that is denoted as L_1L_2V; and third, other phenomena like LCST or UCST. The broken lines represent critical phenomena such as L = V loci. The black circles represent the critical points for the components. Finally, the white circles indicate the presence of UCEP and LCEP. The following is a description of each type of diagram.

Type I: this is the simplest possible phase behaviour for a binary mixture. In this phase behaviour (Figure 2.2a) there is a single liquid phase. The critical mixture curve connects the critical points of both components. This phase behaviour usually occurs when the components in the mixture are of similar molecular size and structure (e.g. benzene + toluene).

Type II: this diagram is shown in Figure 2.2b. Like Type I phase diagrams, a continuous critical locus links the critical points of the pure components; additionally, two liquid phases appear at low temperatures in the P-T projection (L_1L_2V). This three-phase line finishes in a UCEP that is also an L-point where both liquids become critical in the presence of a vapor ($L_2 = L_1 + V$). From this point, the UCST line that represents the critical region $L_1 = L_2$ extends to high pressures. This phase behaviour is observed in hydrocarbon mixtures when the components differ in molecular size and structure.

Type IV: this projection is presented before the Type III projection because it arises from the Type II projection as the differences between the two components becomes greater. In this phase behaviour (Figure 2.2c), two three-phase lines, L_1L_2V, occur. The first line is at temperatures below the UCST line (similar to that existing in type II diagrams) and ends in the UCEP (L-point). The second L_1L_2V line is close to the critical point of the lighter component and connects the two branches of the critical locus that starts at the critical point of each component. The first branch of the critical locus starts at the critical point of the more volatile component and connects the second L_1L_2V line at the UCEP under high pressure and temperature. This UCEP is also a K-point where a liquid phase and a vapor phase become critical in the presence of a second liquid phase ($V = L_1 + L_2$).

The second branch of the critical locus goes from the critical point of the less volatile component to the LCEP of the second L_1L_2V line. This LCEP is also a L-point ($L_1 = L_2 + V$). The occurrence of this type of phase behaviour is observed when the species in the mixture differ considerably in the strength of their intermolecular potential. For example, ethane – ethanol (Mc Hugh and Krukonis, 1993).

Type III: this projection is represented in Figure 2.2d. This projection has two critical loci segments. The first branch connects the critical point of the more volatile compound to the UCEP (also a K-point), which is the end of the three-phase line (L_1L_2V). The second branch of the critical line is connected to the critical point of the less volatile compound and extends to the lower region temperature but never intersects the L_1L_2V three-phase line; instead, it extends sharply to high pressures. This behaviour is expected in mixtures where the differences in size, structure or strength of the intermolecular forces is very large. For example water – alkane mixtures (Alwani and Schneider, 1963).

Type V: this phase behaviour is similar to type IV without the three phase line at low temperatures (Figure 2.2e). This behaviour is not well documented. Methane and hexane mixtures are examples of type V phase behaviour. Also, this behaviour has been identified in mixtures of hydrocarbons and either methanol (Brunner, 1985a) or pyridine (Brunner, 1985b).

Solid Interference

A solid phase appears in phase behaviour when temperatures below the melting temperature of the less volatile compound are considered. Two of many possible examples are illustrated in Figures 2.3 & 2.4.

Figure 2.3 shows a P-T projection with solid interference. In this case, the critical liquid – vapor line goes from the critical point of the more volatile component to the critical point of the less volatile component without discontinuity. Also, the solid – liquid – vapor line goes from the melting point of the less volatile component to lower temperatures as the pressure is raised.

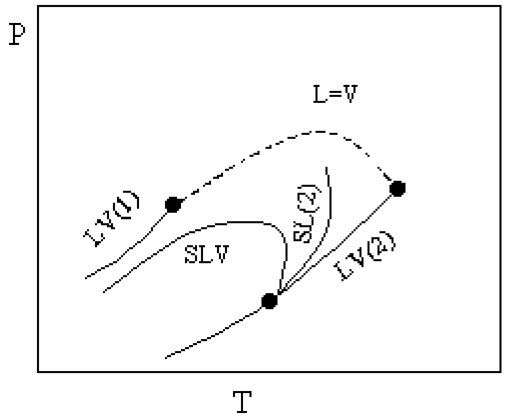

Figure 2.3: solid interference with a continuous critical line.

A more complex phase behaviour with solid interference is derived from the Type III phase diagram - (Figure 2.4). In this projection, the SLV three phase line and the critical curve are not continuous and both curves show two branches. One branch of the critical curve starts at the critical point of the more volatile component and ends at the intersection with the first branch of the SLV three phase curve. At this point ($S + L_1 = V$) a liquid phase and a vapor phase become critical in the presence of a solid phase. The other branch of the critical curve starts at the critical point of the less volatile component, extends at lower temperatures while the pressure is raised and connects the second branch of the SLV three phase curve at the UCEP. At this point the heavier liquid phase and a vapor phase become critical in the presence of a solid phase ($S + L_2 = V$). The second branch of the SLV curve starts at the melting point of the heavier component. It rises steeply with pressure and finishes at the UCEP.

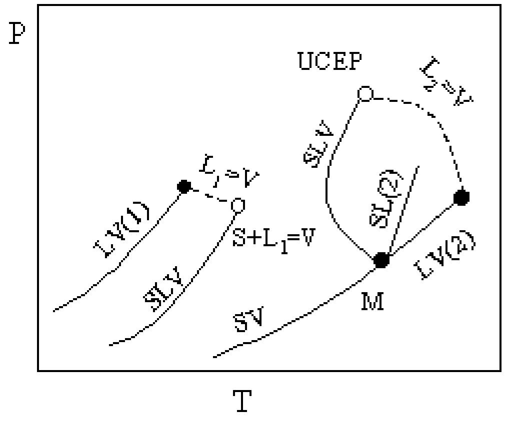

Figure 2.4: solid interference diagram derived from a type III diagram.

Phase Diagrams for Multi-component Systems:

Heavy oils and their vacuum residues are multi-component systems whose phase diagrams have more degrees of freedom than phase diagrams of binary systems; however, the development and interpretation of multi-component phase diagrams is based on binary analogues. Moreover, the classification of Scott and van Konynenburg (1980) is often used to interpret heavy oil mixtures.

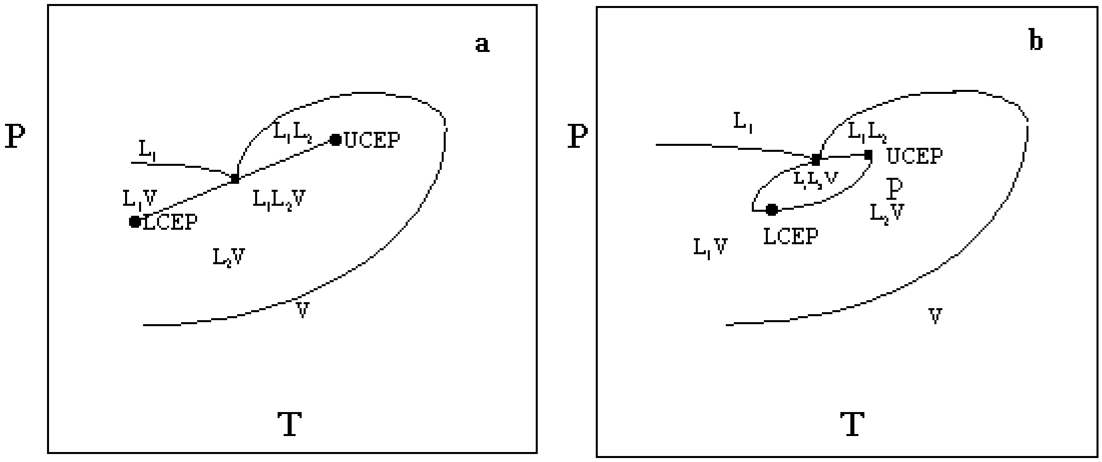

Figure 2.5: P-T phase diagram for Type V phase behaviour. Expansion from binary to ternary system.

Gregorowicz et al. (1992, 1993) and Shaw et al. (1993, 1997) expanded phase diagrams of binary systems to represent the phase behaviour of ternary systems. Figure 2.5a shows a P-T phase diagram at fixed composition of a Type V (see Figure 2.2e) binary system. The three-phase curve starts at the LCEP and finishes at the UCEP. The addition of a third component increases the degrees of freedom by one and expands the L_1L_2V phase behaviour from a curve to a region (Figure 2.5b).

Figure 2.6 shows P-T diagrams of the binary mixture of n-decylbenzene + ethane with the addition of carbon dioxide. This case illustrates the change in the three phase behaviour from a line to a region. Furthermore, the three-phase region shifts to higher pressures and lower temperatures as more carbon dioxide is added to the system.

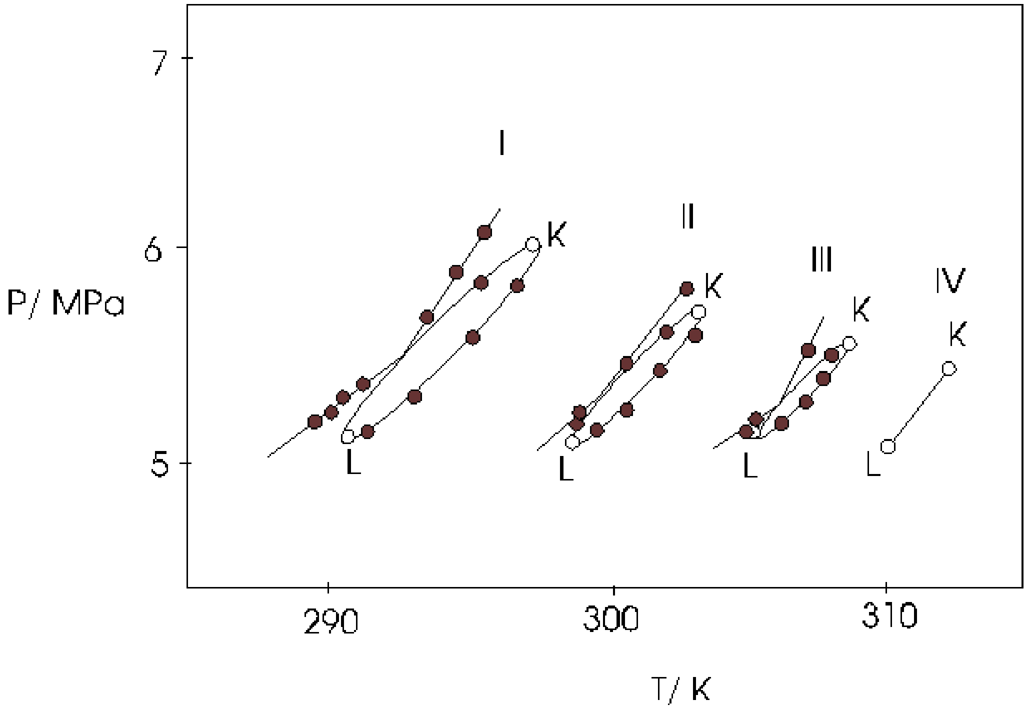

Figure 2.6: P-T diagrams of n-decylbenzene + ethane + carbon dioxide I) 40 mole % carbon dioxide, II) 20 mole % carbon dioxide, III) 10 mole carbon dioxide and IV) n-decylbenzene + ethane.

It is worth noting, from the explanation above, that the existing theory for the phase behaviour of mixtures and the development of phase diagrams is associated with non-reacting systems. However, the identification of the special properties of supercritical fluids (SCF) to enhance chemical reacting systems (Mc Hugh & Krukonis, 1993) has driven the research in this area to improve the understanding of the phase behaviour of complex mixtures.

Regarding the understanding of heavy oil processing, the work of Abedi et al. (1998) raises the first explanation of coking and asphaltene precipitation in association with phase behaviour. They showed for example that coke yield was greater in L_1L_2V regions than in L_1V regions, even if the temperature and composition were fixed, and that the onset of coke formation arose at lower temperatures in L_1L_2V zones than in L_1V zones. Furthermore, the aims of this thesis are to use phase behaviour and phase diagram theory to identify critical pathways in the coking process, and to explain the relationship between the liquid phase where the coking reactions are taking place and the coke structures formed.

Delayed coking Models

One of the objectives of this thesis is to setup the laboratory apparatus to carry out the experiments required to study the effect of phase behaviour on the structure of coke formed. The setup of this apparatus is accomplished in three steps: first, the design and specification of main equipment; second, the assembly of this equipment to make the final apparatus; and finally, the development of appropriate procedures. To accomplish the first step, calculation of the flows and properties of the different streams and products were required to complete general and specific mass and heat balances. These calculations are not straightforward because the processing of petroleum fractions at temperatures above 623 K (350 ºC) leads to cracking and condensation reactions. For this reason, the use of a predictor model is required. For the purpose of this thesis, the most adequate predictor model is one related to delayed coking technology.

Delayed coking models are used to predict product yields and qualities as functions of feedstock properties and operating conditions of a unit. These models are frequently used as integrated files in existing refinery simulators oriented to plan and evaluate the performance of these chemical complexes. Examples of these refinery simulators are HYSYS, Aspen Orion, RefModL and PROSiE. These models are based on standard correlations that were developed with operational data from commercial delayed coking units or with robust cracking and condensation reaction models.

The main variables considered are the feedstock properties and the operating conditions. The feedstock properties are typically represented with Conradson carbon residue or Microcarbon residue, the specific gravity and the sulphur content. In some models, additional data such as distillation curves and asphaltene content are included. Table 2.2 shows standard correlations (PDVSA-Intevep, 1999) for delayed coking product yields based on the Conradson carbon content of the feedstock and do not consider the unit operating conditions (assumed to be developed for typical delayed coking operating conditions). The last column in this Table gives the feedstock API range of application for these correlations.

The results of these proprietary models can be simple or detailed. The simple results include product yields (gases, distillates and coke) with fixed cut points for the different liquid products (gasoline, naphtha and gas-oils) and limited or no product properties. On the other hand, the detailed results include composition of gas product, adjustment of the liquid products' cut points according to the users' requirements and properties of each product including the coke. Evaluation of the performance of the main equipment like the furnace, drums or reactors and fractionator are frequently included.

Table 2.2: Delayed coking product yields (wt%)

PRODUCT	CORRELATION	FEEDSTOCK API
Gas	$7.8 + 0.144 \times CCR$	0.16 – 11.9
Gasoline	$11.29 + 0.343 \times CCR$	0.36 – 20.5
Gas oil	$100 - Coke - Gasoline - gas$	2.30 – 21.8
Coke	$1.6 \times CCR$	1.78 – 45.8

For this thesis, two delayed coking models developed by PDVSA-Intevep were used to generate the design data, to crosscheck the results and to evaluate the performance of the new apparatus. These two models are: a detailed model called CCDCC (Cabrera, Sanoja, & Ali, 1997) and a general model called PCR-230 (Cabrera, Guerrero, & Ali, 1998). CCDCC was developed with operational data from a commercial delayed coking unit. This model generates product yield, detailed composition of gas product and specific gravity and distillation curve for each liquid product. The PCR-230 model was developed with experimental data from a delayed coking pilot plant. It calculates product yields.

Table 2.3 shows, for each model, the main variables and their application ranges. In this Table three issues are worth noting: first, the higher number of variables used in the CCDCC model; second, the fact that PCR-230 does not need the recycle ratio in the reaction module; and third, the difference in the reaction temperature and pressure application range.

The larger number of variables in the CCDCC model is related to the detailed information that this model generates in comparison with the PCR-230 model. The omission of the recycle ratio in the PCR-230 model is due to the fact that the recycle stream is not incorporated in delayed coking pilot plant units. Finally, the difference in the reaction temperature application range is because the CCDCC reaction temperature is measured at the heater outlet while the PCR-230 reaction temperature is measured inside and at the top of the coker. The heater outlet temperature is measured before the feed is introduced into the cokers. The vaporization and cracking reactions that take place in the coker consume energy and drop the coker internal temperature. In the CCDCC model a heater outlet temperature of 763 K corresponds to 698 K inside the coker. The pressures in commercial units vary more than in systems like pilot plants or laboratory units. These variations are related to operational procedures (for example steam stripping and cokers switching). Also, the accumulation of coke in the outlet lines, in commercial delayed coking units, affects the pressure readings. Thus, 300 kPa for the CCDCC model is equivalent to 240 kPa in the PCR-230 model. The CCDCC model was used to generate the detailed data required to design the unit. On the other hand, the general model (PCR-230) was used to crosscheck the design values as well as to evaluate the performance of the new apparatus.

Table 2.3: Variables in the delayed coking models used to design and evaluate the apparatus (Cabrera, Sanoja, & Ali, 1997 and Cabrera, Guerrero, & Ali, 1998).

	CCDCC	PCR-230
FEEDSTOCK		
API	4.0 – 9.0	0.78 – 9.9
CCR (wt%)	20.0 – 27.0	14.5 – 32.0
Sulphur (wt%)	2.3 – 7.0	---
N (ppmw)	4500 – 9650	---
REACTION		
Pressure (kPa)	270 – 340*** 210 – 280*	204 – 377
Temperature (K)	760 – 766**	693 – 760

	695 – 701*	
Recycle Ratio	1.04 – 1.10	---
FRACTIONATION		
Kero draw plate temperature (K)	466 – 489	---
LCGO draw plate temperature (K)	522 – 544	---
HCGO draw plate temperature (K)	616 – 638	---

*Effective equivalent condition into the coker.
**Pre-heater temperature.
***Coker pressure.

Summary

The operating conditions in the delayed coking units (especially temperature and pressure) and the quality of the feedstock appear to have a strong influence on the formation of different coke structures, like shot coke. Moreover, the existing theory for the coking mechanism and shot coke formation suggests that both kinetic and phase behaviour participate in the coke formation mechanism when vacuum residues from heavy oils are processed. Therefore, the use of thermodynamic concepts associated to phase behaviour and phase diagrams is an important tool in explaining these issues; however, they have yet to be applied to coking. Key questions remain unresolved:

1. The impact of phase behaviour on the type of coke produced has not been investigated in the open literature.
2. There is conflicting evidence as to whether hydrodynamics play a role in shot coke formation.
3. Coke formation mechanistic studies have focussed on “high quality” coker feeds. It is not clear whether these results are applicable to heavy oil vacuum bottoms.

Some of these issues are addressed with the laboratory scale coker constructed as part of this thesis.

Chapter 3 – Materials, Apparatus and Methodology

This chapter presents, in three sections, the materials and the laboratory apparatus used to complete the experiments. The first section shows the properties of the different vacuum residue samples and n-dodecane; the second section is dedicated to the laboratory apparatus. It includes the basis for the design of the apparatus, the apparatus description and the methodology used to carry out each experiment; finally, the last section is dedicated to the selection of the operating conditions.

Feedstocks

The feedstocks used to carry out the experimental matrix were vacuum residues that were processed alone or mixed with n-dodecane (n-C_{12}). These vacuum residues are Athabasca Bitumen Vacuum Bottom (ABVB), Heater feedstock and Cerro Negro both from Venezuela. The properties of these feedstocks are shown in Table 3.1.

Table 3.1: Properties of different vacuum residue samples and n-dodecane.

	ABVB	Heater Feedstock	Cerro Negro	n-C_{12}
Specific gravity	1.043**	1.0442	1.0520	0.749
Conradson carbon (wt%)	21.4	22.6	23.3	0
Sulphur (wt%)	6.87	4.09	4.35	0
Viscosity (cSt)		774.2	53360	
Viscosity temperature (K)		408	373	
MW	1700	957		
Saturate (wt%)	6.8	11.0	5.6	100
Aromatic (wt%)	41.99	52.0	48.5	0
Resin (wt%)	19.04	18.4	31.4	0
Asphaltene (wt%)	32.18	18.6	14.5	0
V (ppm)	344	1136	678	0
Ni (ppm)	137	121	145	0

For ABVB, the specific gravity was measured at 293 K. This property and the molecular weight have been published before (Cai, Shaw & Chung, 2000) and the saturate, aromatic, resin and asphaltene analyses were performed in Core Lab^{TM} Petroleum Services laboratories (2002). Analyses for the other two residues were carried out in PDVSA-Intevep laboratories (Morin, 2002).

It is worth noting, in Table 3.1, that the asphaltene content / Conradson carbon content ratio for all the residues is higher than 0.5; therefore, if the operating conditions are favourable, the formation of shot coke is likely when these feedstocks are processed.

Laboratory Apparatus

This section includes the basic considerations for the design of the experimental apparatus, the apparatus description, and the experimental methodology. The premises that support the apparatus design are discussed; following this, the apparatus description that identifies main equipment components and depicts the process flow for the feedstock and products; finally, this section closes with the description of a methodology used to complete each experiment.

Laboratory Unit Design Premises

The laboratory unit design premises are based on the literature review and prior experience. They are oriented to simulate the delayed coking technology at bench scale and facilitate the formation of different coke structures (shot and sponge coke). These premises are:

1. Process the least quantity of sample per test.
2. Guarantee a vapor velocity between 0.015 and 0.018 m/s, when vacuum residue from heavy oil crude is processed at 240 kPa and 797 K.
3. According to previous works (Menéndez et al., 1997; Rahimi et al., 1998, 1999), the mesophase "quality" has an important effect on the coke formed. Rahimi (1999) showed that the mesophase induction period, for Athabasca vacuum bottoms, were found to be 26 – 30 minutes after the desired temperature was reached (these were batch experiments). Thus, the pumping period is set between 30 – 45 minutes to allow for mesophase and coke formation.

4. Coker dimensions allow easy coke removal and the possibility to place this device inside an electric furnace. For easy coke removal the coker internal diameter should be as large as possible.

In order to design this apparatus the compositions and properties of main streams had to be estimated. This task was relatively easy for equipment before the coker because the fluid in this section was specified as ABVB. However, the equipment downstream of the coker had to be designed to handle the light hydrocarbon products obtained from the thermal cracking of ABVB; therefore, a delayed coking model was used to estimate the compositions and properties of expected coker effluents, distillates and non-condensable products. Appendix A comprises the calculations with the delayed coking models used to establish the range of flowrate and product properties.

Apparatus Description

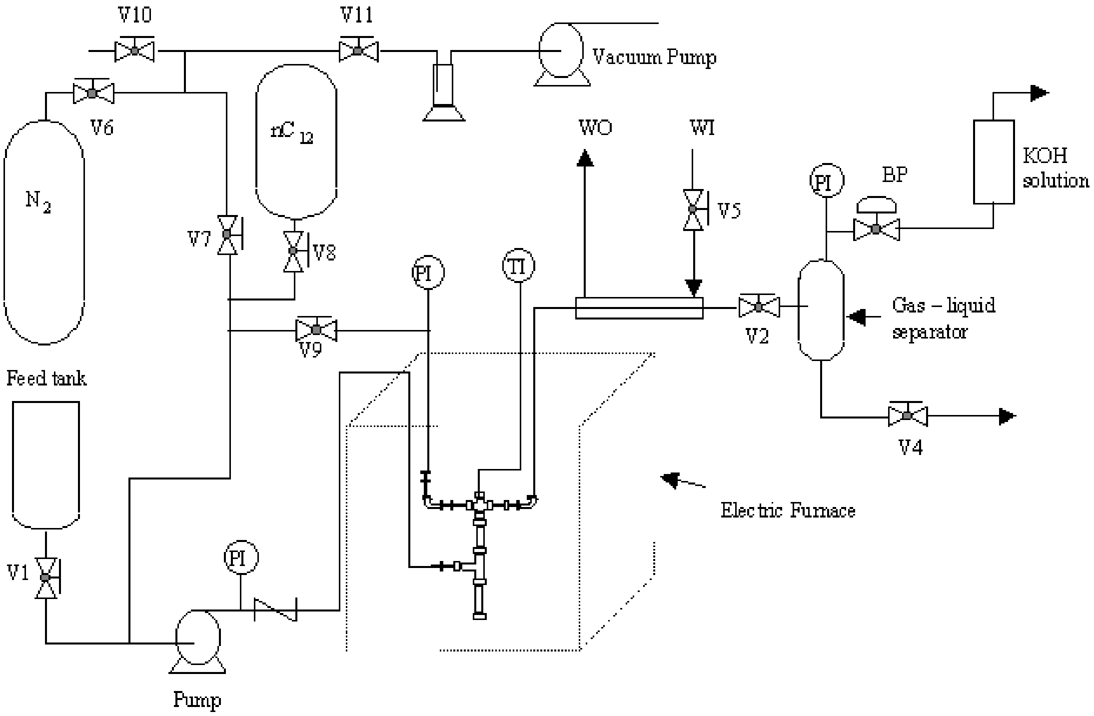

Figure 3.1: Apparatus schematic.

Figure 3.1 shows a schematic of the laboratory apparatus. The apparatus has three main sections; the feed section that comprises the feed tank reservoir, the feed pump, the nitrogen cylinder, the n-C_{12} vessel and the vacuum pump; the reaction section that includes the coker and the electric furnace; and the light product handling section with the condenser, the gas-liquid separator and the H_2S scrubber. Detailed descriptions of main equipment are presented in Appendix B.

The feedstock is pumped from the feed tank to the coker, in the reaction section, at the desired flowrate (the pump calibration comprises Appendix C). Lines connecting the different equipment (feed tank to pump and pump to coker) are heated using heating tapes and insulation in order to avoid plugging of the lines due to the high viscosity of the fluid. The temperature in these lines is maintained between 423 K – 473 K.

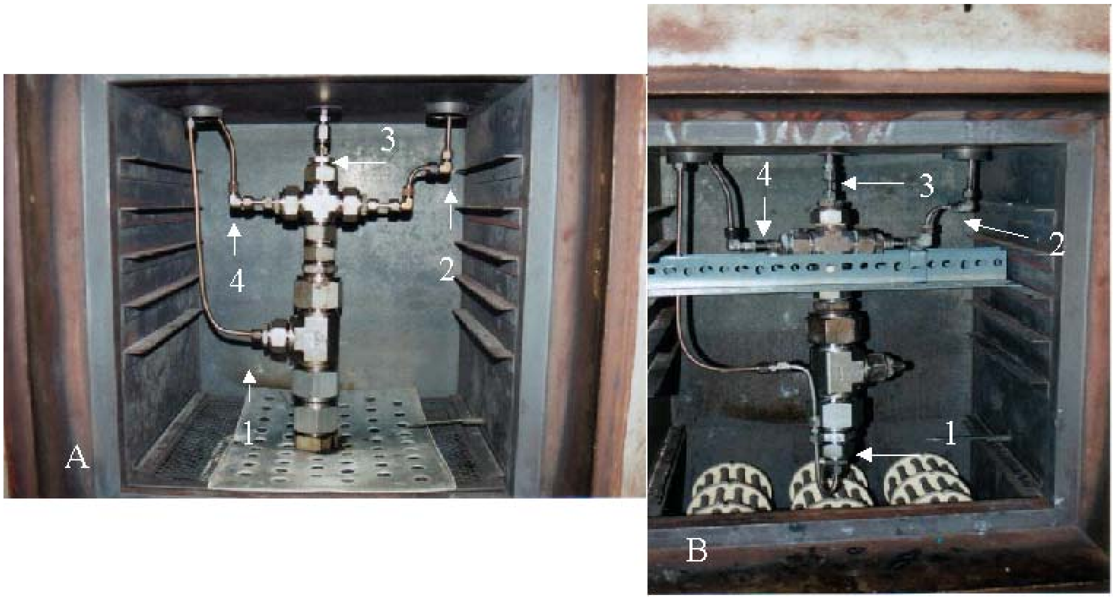

Figure 3.2**:** Coker design versions. A: lateral inlet version. B: bottom inlet version. 1: feedstock inlet; 2: vapor outlet; 3: thermocouple connection; 4: pressure transducer connection.

The coker was designed in two versions, Figure 3.2, that differ in the location of feedstock inlet: the bottom inlet version and the lateral inlet version. The bottom inlet version resembles the coker in the delayed coking technology, where the feedstock inlet is on the bottom and the accumulated material is always exposed to the feed going into the coker. However, the coker used to carry out the bulk of the experimental matrix was the lateral inlet version because there is less perturbation of the coking material by incoming feedstock. It is worth noting that the connections for the feedstock inlet, the products outlet, the thermocouple and the pressure transducer are the same.

In the coker, the feedstock temperature increases to the target value; consequently, cracking, polymerization and condensation reactions take place to produce light hydrocarbons and coke. The light hydrocarbons exit the reaction system as vapor. This vapor is cooled with water using a counterflow heat exchanger (the design of this equipment is shown in Appendix D). After cooling, this stream is separated using the gas liquid separator where the liquid products are collected in the bottom and the non-condensable products escape through the top. The gas stream is used to control the system pressure with a backpressure valve (BP) and the H_2S content is removed in the H_2S scrubber before it is discharged to the exhaust system. The heavy fractions remaining in the coker form coke.

The variables measured to monitor unit performance during each experiment are pressure and temperature. Pressure is measured at three different points of the apparatus: the feed pump discharge, the coker and the gas - liquid separator; meanwhile, temperature is measured at five different points: the feed vessel discharge, the feed pump discharge, the coker, and the condenser inlet and outlet. Moreover, the unit works with a data acquisition system (Intel 100), which records the coker pressure and all the temperatures. Detailed information about the connection of sensors to the apparatus and its setup can be found in appendix E.

Ancillary equipment include a nitrogen gas cylinder and associated plumbing used for three main steps in each experiment: to pressure test the unit before each experiment; to create an inert atmosphere in the gas-liquid separator at the experiment operating pressure; and to clean the lines “in situ” at the end of each experiment in order to avoid plugging. The vacuum pump is used before starting each experiment to remove nitrogen gas from the coker. N-dodecane from the n-C_{12} vessel is used at the beginning of each experiment to increase the pressure in the coker to the desired value. This step creates an “n-dodecane saturated atmosphere” in the coker before the feed is introduced, and avoids rapid vaporization of n-dodecane in mixtures with the vacuum residue at the beginning of experiments.

Methodology

The development of the operational procedures was an iterative process that helped to identify apparatus modifications in order to guarantee its safe operation, minimize variation of the coker operational variables and facilitate collection of all materials and products to successfully complete the mass balances. Detailed descriptions of the experimental procedures (apparatus preparation, start-up, shut down and maintenance) are presented in Appendix F. This section summarizes the procedure used to complete the experiments and presents the “learned” steps in the procedure development process.

The procedure used to complete the experiments is summarized as follows: First, the feedstock (vacuum residue alone or mixture of vacuum residue and n-dodecane) and the chemicals required to carry out the experiment (antifoaming, n-dodecane and KOH solution) were loaded to their corresponding vessels. Next, the furnace, the heating tapes and the heating plate were turned on; the gas-liquid separator was pressurized with nitrogen up to the pressure set-point and the coker was evacuated using the vacuum pump. After the temperature in the coker reached the set-point, n-dodecane was used to increase the coker pressure up to the pressure set-point. The next step is to feed the feedstock into the coker during the 45 minutes feed period. When the feeding period is completed, the pump is turned off and the material inside the coker is kept at the temperature and pressure set points for a 120 minutes coking period. Finally, the heating systems are turned off, the apparatus cooled down and the products collected to complete the mass balance and the required analyses.

As indicated above, the development of the methodology and procedures to complete each experiment was an iterative process. Following the steps included in the final procedure that impacted the performance of the apparatus:

- The time required for the electric furnace to reach the temperature set point is between 2 – 3 hours. Moreover, the adjustment of the furnace temperature set point, at the end of the feeding period, is required to avoid temperature increase in the coker during the coking period. During the feed period a furnace temperature between 710 – 720 K yields a coker temperature between 693 – 698 K. During the coking period the furnace temperature must be between 5 – 10 K lower than during the feed period.

- When the apparatus is working at low pressure (239 kPa), at the end of the feed period the pressure in the coker increases indicating that heavy material (asphaltenes and coke) plug the coker outlet. This situation happens because the evolution of vapor in the reacting mixture generates a foam front that raises the heavy hydrocarbon to the coker outlet. In order to avoid foam formation, the use of antifoaming Si-based polymer was implemented. This polymer is used in commercial delayed coking units for the same purpose. The amount of antifoaming used in these experiments was between 0.2 and 0.4 wt% mixed with the feedstock.

- The pressurization of the gas – liquid separator with nitrogen avoids big changes in the coker pressure at the beginning of the feeding period. These pressure variations cause the evacuation of the material in the coker (risk of outlet line plugging) and the operation under unstable conditions.

- If large quantities of n-dodecane are used in the experiment (working at higher pressure or processing diluted mixtures), the liquid stored in the gas – liquid separator can go back to the coker during the cooling down process. Therefore, to avoid this situation the valve between the gas – liquid separator and the heat exchanger must be closed at the end of experiments.

- The use of nitrogen straightaway the experiment has finished is not recommended because the unconverted feedstock in the lines before the coker can be displaced to the coker. Additionally, heavy hydrocarbons and coke that are initially in the coker can plug the coker outlet line.

- The cleaning of the coker outlet line is required to avoid accumulation of heavy hydrocarbons that form coke and to remove the remaining material that has to be considered as product in the mass balance.

- The cleaning of the lines between the coker and the feed tank and recovery of materials improves the present mass balance.

Operating Conditions

As indicated in chapter 2, the main operating variables in a delayed coking unit which impact coke structure and yield are temperature, recycle ratio, vapor velocity (this variable is not considered important with respect to the coke yield) and pressure; therefore, the values and range of variation of these variables, in the laboratory apparatus, were selected based on previous pilot plant units (Velutini & Guerrero, 1996; Ali, 1998); and on the desire to evaluate the feedstock close to its bubble point.

The temperature in pilot plant delayed coking units (Velutini & Guerrero, 1996; Ali, 1998) varies between 690 and 723 K. Therefore, the coker temperature was fixed at 698 K for these evaluations; however, some experiments were conducted at higher and lower temperatures (718 K and 687 K, respectively).

The incorporation of recycle streams in laboratory apparatus is complicated because it requires fractionation of the collected liquid products and pumping of the heavy fraction back into the coker and was not found to be practical. This is justified because delayed coking units, when used to process residues from heavy oil, work with low recycle ratio (1.03 – 1.05); and the production of shot coke is likely with low or no recycle (Elliot, 2001).

The vapor velocity in the coking coker can be selected from other delayed coking pilot plants that produce shot coke with vapor velocities between 0.015 – 0.018 m/s (Velutini & Guerrero, 1996; Ali, 1998). According to the design (see Appendix B) the feedstock flowrate to carry out the experiments is 5 mL/min. At this flowrate the vapor velocity in the coker when the unit processes vacuum residue alone is 0.016 m/s; however, this variable has higher values when the unit is processing mixtures of vacuum residue and n-dodecane.

As indicated in the objectives of this thesis, the bubble point of the feedstock defined the operating conditions in the apparatus. Since the coker temperature was fixed at 698 K, the coker pressure range was fixed to evaluate the feedstock above, below and close to the bubble point. Thus, the feedstock bubble pressure at different compositions was calculated using the Computer Modelling Group's phase property program (CMG Prop). In these simulations, two approaches were used: first, ABVB was considered as one component; and second, ABVB was divided into two pseudo-components.

One component ABVB model

The Athabasca Bitumen Vacuum Bottom's (ABVB) properties used for these calculations were specific gravity, mean molecular weight and the average boiling temperature (1217 K). The former two properties are those reported in Table 3.1; and the average boiling temperature was calculated using the equation 3.1 (Speight, 1998).

$$T_{boiling}(^{\circ}F)=\left\{\left[\frac{(MW-140)\times(SG)^{2.5}}{3.40}\right]\times 10^{7}\right\}^{1/3} \tag{3.1}$$

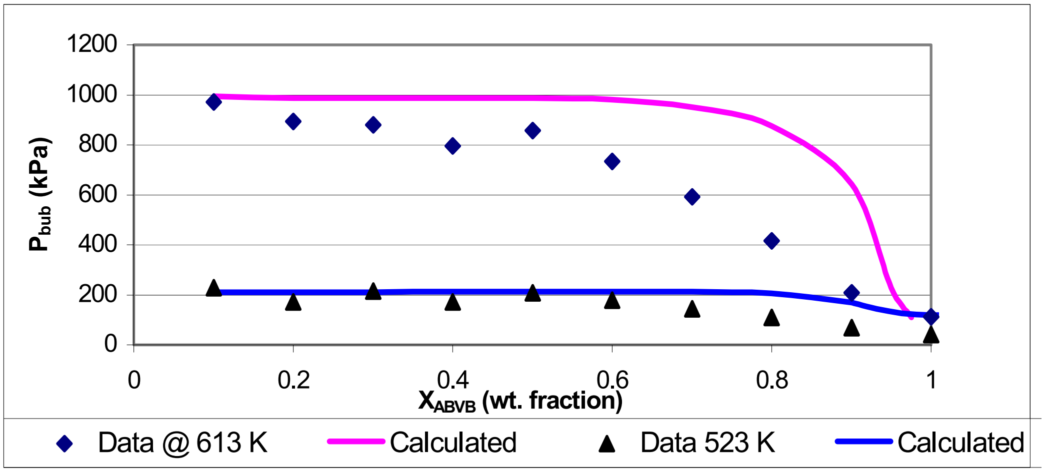

Figure 3.3: Comparison of bubble pressure data and calculations where ABVB is considered as one component for mixtures of ABVB and n-C_{12} at 523 K and 613 K (250 °C and 340 °C).

Figure 3.3 shows the bubble pressure for experimental data (Zou, 2002) and calculations using Computer Modelling Group's phase property program for mixtures of ABVB + n-dodecane at 523 K and 613 K. In all the cases the calculations show higher values than the experimental data.

Two pseudo-component ABVB model

The properties of these pseudo-components were simulated with the HYSIM OIL characterization routine (Shaw, 1997). These properties are shown in Table 3.2.

Table 3.2: Physical and critical properties of the ABVB pseudo-components

Component	Wt%	MW	Density (Kg/m^3)	P_c (kPa)	T_c (K)	V_c (m^3/Kmol)	w
Heavy	33.64	3710.6	1103.9	774.5	1122.4	3.70	1.370
Light	66.36	680.7	1009.3	1487.0	915.4	1.57	0.914

Figure 3.4 shows the bubble pressure for experimental data (Zou, 2002) and calculations for mixtures of ABVB + n-dodecane at 523 K and 613 K. Here the calculated values do not differ significantly from the experimental values.

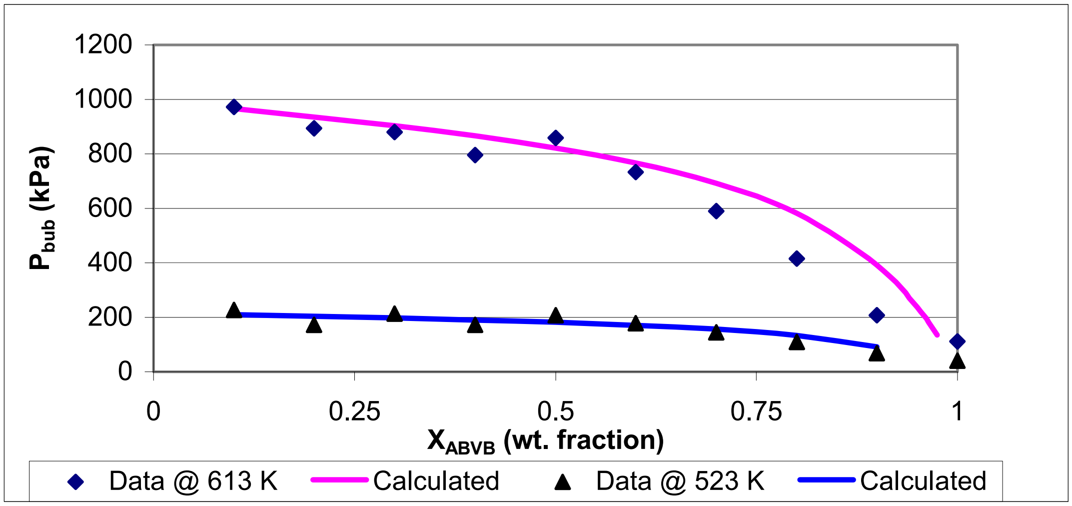

Figure 3.4: Comparison of bubble pressure data and calculations for mixtures of ABVB and n-C_{12} at 523 K and 613 K (250 °C and 340 °C) where ABVB is considered as two pseudo-components.

Although the two psedo-component model fits the data better, there is no proof that either model represents the bubble pressure at 698 K. Therefore, both models are considered valid and the experimental matrix was designed to carry out experiments at pressures below 2000 kPa and above 6000 kPa (Figure 3.5 and Table 3.3), the anticipated range of the bubble pressure at 698 K.

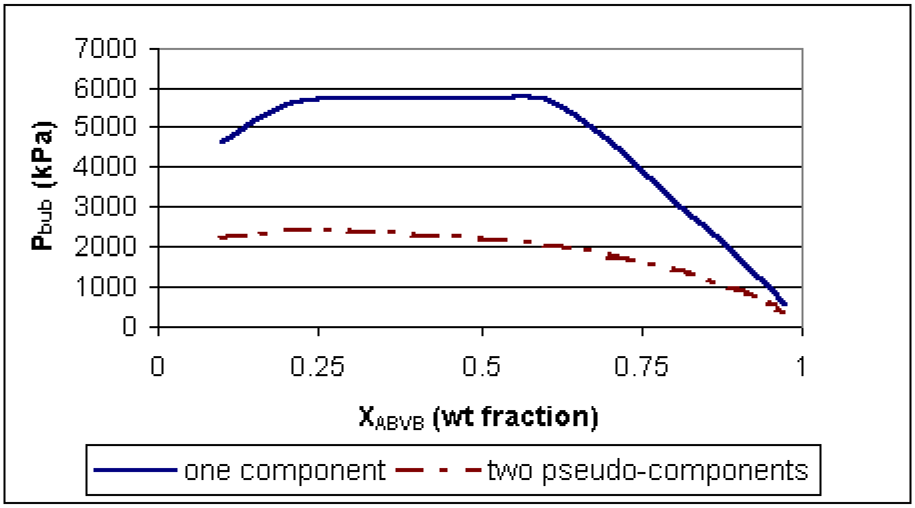

Figure 3.5: Calculated bubble pressures for mixtures of ABVB and n-dodecane at 698 K.

Table 3.3: Bubble pressure, for mixtures of ABVB and n-dodecane at 698 K, calculated with two different models.

X_{ABVB} (wt fraction)	One component (kPa)	Two pseudo-components (kPa)
0.1	4621	2161
0.2	5559	2376
0.3	5746	2360
0.4	5746	2280
0.5	5746	2165
0.6	5746	2009
0.7	4656	1795
0.8	3125	1480
0.9	1780	975
0.95	1028	593
0.975	566	350

It is worth noting (see Figure 3.5) that both models predict a reduction of the bubble pressure at low concentrations of ABVB (less than 20 wt%). This behaviour is common for asymmetric mixtures. Critical points are also expected at temperatures higher than the critical temperature of n-dodecane and at low ABVB concentrations.

Summary

Three vacuum residues (ABVB, Cerro Negro and Heater Feedstock) alone or mixed with n-dodecane were used to carry out the experiments in this thesis. These experiments were completed in a new laboratory apparatus designed and set-up to simulate delayed coking technology, at low pressure, but capable of operating over a broad range of pressures. The temperature range is 687 – 720 K and pressure range from 100 to 6100 kPa.

In this new apparatus, the feedstock is conveyed from the feedstock vessel to the coker where cracking and condensation reactions produce light and heavy hydrocarbons. The light hydrocarbons leave the coker as vapor, are cooled in a heat exchanger and split into liquid and gas. The liquid product is collected in the gas – liquid separator and the gas product is used to control the pressure in the apparatus before being exhausted. The heavy hydrocarbons remain in the coker to produce coke.

Each experiment is completed in two stages: the first stage is the pumping of feedstock into the coker during 45 minutes (feeding period); and in the second stage the material inside the coker is kept at the operating conditions for 120 minutes (coking period). The operating conditions in the apparatus were selected to process feedstocks above or below their bubble point.

The efficacy of the apparatus design and operating procedures along with other experimental issues is addressed in chapter 4.

Chapter 4 – Experimental

This chapter has three sections: the experimental matrix, an evaluation of experimental and product analysis techniques, and an equipment performance evaluation. The experimental matrix section describes all the experiments performed in this thesis in terms of feedstock composition and operating conditions. The evaluation of experimental and product analysis techniques section illustrates the quality of the results obtained and the utility of product characterization. The last section summarizes equipment performance.

Experimental Matrix

As indicated in chapter 3, three vacuum residues alone or mixed with different proportions of n-dodecane were evaluated in these experiments. The full experimental matrix was completed for ABVB while the other two vacuum residues were only evaluated at certain levels. The independent variables considered were composition and pressure.

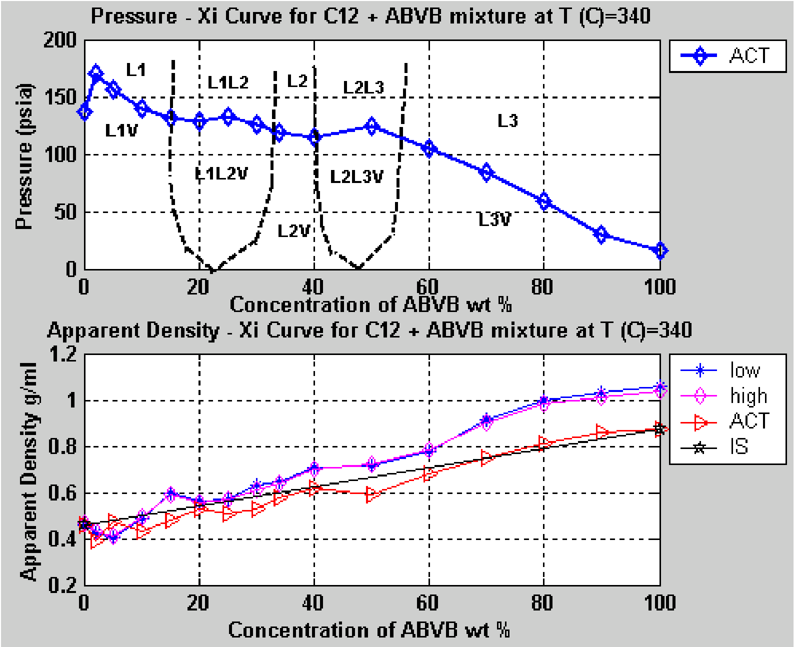

Figure 4.1: Phases diagram at 613 K (340 ºC) for mixtures of n-C_{12} + ABVB (Zou, 2002).

According to the work of Zou (2002), the appearance of more than one liquid phase is evident at ABVB wt. fractions less than 0.60; moreover, complex and dense liquid phases appear when the mixture processed has between 40 wt% and 60 wt% ABVB (see Figure 4.1). In addition, preliminary results indicated that evaluation at concentrations below 40 wt% ABVB was required. As the phase behaviour at lower temperatures cannot be extrapolated with certainty to higher temperature, six ABVB weight fractions were selected for these experiments. These weight fractions are: $X_1 = 0.3$, $X_2 = 0.4$, $X_3 = 0.45$, $X_4 = 0.5$, $X_5 = 0.6$ and $X_6 = 0.8$.

Based on the estimated bubble pressures at 698 K and the selected weight fractions of ABVB used in these experiments (Figure 3.5 and Table 3.3), the following five operating pressures above and below the anticipated feedstock bubble pressure were chosen: $P_1 =$ 239 kPa, $P_2 =$ 791 kPa, $P_3 =$ 2240 kPa, $P_4 =$ 3550 kPa and $P_5 =$ 6101 kPa.

Furthermore, replications were performed at three test points in order to determine the reproducibility of the results. Table 4.1 shows the experimental matrix. The subscript numbers indicate the experiment number identification.

Table 4.1: Experimental matrix for evaluation of mixtures of ABVB and n-Dodecane.

	ABVB wt fraction					
Pressure (kPa)	X_1 (0.3)	X_2 (0.4)	X_3 (0.45)	X_4 (0.5)	X_5 (0.6)	X_6 (0.8)
P_1 (239)	E_{41}			E_{34} / E_{35}*		
P_2 (791)			E_{32}	E_{33} / E_{31}⁺	E_{09}	E_{11}
P_3 (2240)				E_{38}		
P_4 (3550)	E_{42}	E_{14} / E_{22}	E_{28}	E_{30}	E_{12} / E_{20}	E_{15}
P_5 (6101)	E_{40}	E_{21}	E_{27}	E_{29}	E_{19}	E_{43}

*The experiment was performed with the inlet at the bottom of the coker.

⁺The experiment was performed at lower temperature (687 K instead of 698 K).

As indicated above, additional experiments were completed with two other vacuum residue samples. These experiments were selected to evaluate the apparatus when processing feedstocks that are known as shot coke producers at both commercial and pilot plant scales. The purpose of this evaluation was to determine the performance of this apparatus when processing 100 wt% vacuum residue under delayed coking conditions which favour shot coke formation and to provide a basis for testing the accuracy of the coke formation models.

Table 4.2: Experimental matrix for evaluation of other vacuum residues. Composition is related to ABVB content (wt fraction) on the mixture and pressure in kPa.

Vacuum residue	Cerro Negro	Heater feedstock	Heater feedstock	Heater feedstock
Experiment ID	E_{24}	E_{25}	E_{26}	E_{36}
Wt. fraction	0.6	1.0	1.0	1.0
Pressure (kPa)	240	240	240	180
Temperature (K)	698	698	718	720
Coker	Lateral feed	Lateral feed	Lateral feed	Bottom feed

According to previous work (Ellis & Bacha, 1996; Elliot, 2001), the pressure, the vapor velocity and the temperature in the cokers all have an important impact on shot coke formation. Reductions in coker pressure and / or increases in vapor velocity and / or increases in coker temperature favour the formation of shot coke. Therefore, the experiments with Cerro Negro and Heater Feedstock were conducted at low pressure (between 180 kPa and 240 kPa), high temperature (between 698 K and 720 K) and in some cases; the coker was modified to increase the vapor velocity through the coke bed. The operating conditions for these experiments are shown in Table 4.2.

Evaluation of Experimental and Product Analysis Techniques

Three objectives were proposed in this thesis; first, to set-up an apparatus to simulate the delayed coking process; second, to identify critical steps in the coke formation mechanism and their relationship with the phase behaviour of the system where coking reactions are taking place; and third, to determine the impact of operating conditions on the nature of the coke formed. Therefore, the analyses conducted on the operational data and coke products were selected to evaluate these goals.

Data Acquisition and Mass Balances

The evaluation of the laboratory apparatus and the identification of critical steps in the coking mechanism were completed using the operational data and the mass balances for each experiment.

The operational data were acquired and stored using a Data Acquisition System. As indicated in chapter 3, the variables monitored were pressure and temperature. Pressure was measured at three different points in the apparatus: the feed pump discharge, the coker and the gas - liquid separator. From these measurements, the only data acquired and stored on a routine basis was the coker pressure. Temperature was measured and stored at five different points: the feed vessel discharge, the feed pump discharge, the coker, and the condenser inlet and outlet. Although all of these variables are important to monitor the apparatus and determine its performance, the key variables that define the operating conditions of each experiment are the temperature and pressure in the coker.

The mass balance was obtained by weighing the feed mixture (vacuum residue and n-dodecane), the n-dodecane added to the n- C_{12} vessel and the KOH solution before and after each experiment; and weighing the liquid products and the coke collected at the end of each experiment. The non-condensed hydrocarbons (the gaseous products) were determined by difference. The results presented include, for each experiment, a general mass balance and a petroleum residue mass balances.

Table 4.3 shows the equations used to complete the mass balances. The descriptions of the variables included in this Table are indicated below:

LP: weight of the liquid products (g) collected at the end of the experiment.

FV_1: weight of the feed vessel (g) before the experiment starts.

FV_2: weight of the feed vessel (g) at the end of the experiment.

LR: weight of feedstock accumulated in lines before the coker.

SS_1: weight of KOH solution (g) charged to the hydrogen sulphide scrubber before starting the experiment.

SS_2: weight of material (g) in the hydrogen sulfide scrubber after the experiment has finished.

$nC_{12}V_1$: Weight of n-dodecane (g) added to the n-C_{12} vessel before starting the experiment.

$nC_{12}V_2$: Weight of n-dodecane (g) remaining in the n-C_{12} vessel after the experiment has finished.

Coke: weight of coke (g) collected at the end of the experiment.

$X_{Residue}$: weight fraction of residue in the feedstock.

$X_{n\text{-}dodecane}$: weight fraction of n-dodecane in the feedstock.

Table 4.3: Mass balance equations.

General Mass Balance	
Mass Balance (MB)	$\frac{(LP+Coke+SS_2-SS_1)}{(FV_1+nC_{12}V_1-FV_2-nC_{12}V_2-LR)}\times 100$
Distillate yield (GDY)	$\frac{LP}{(FV_1+nC_{12}V_1-FV_2-nC_{12}V_2-LR)}\times 100$
H_2S yield (GSY)	$\frac{(SS_2-SS_1)}{(FV_1+nC_{12}V_1-FV_2-nC_{12}V_2-LR)}\times 100$
Coke yield (GCY)	$\frac{Coke}{(FV_1+nC_{12}V_1-FV_2-nC_{12}V_2-LR)}\times 100$
Gases and losses (GG)	$100-GDY-GSY-GCY$
Petroleum Residue Mass Balance	
H_2S yield (SY)	$\frac{(SS_2-SS_1)}{[(FV_1-FV_2-LR)\times X_{\mathrm{Re}\,sidue}]}\times 100$
Distillate yield (DY)	$\frac{(LP-(nC_{12}V_1-nC_{12}V_2)-(FV_1-FV_2-LR)\times X_{n-dodecane})}{[(FV_1-FV_2-LR)\times X_{\mathrm{Re}\,sidue}]}\times 100$

Coke yield (CY)	$\dfrac{Coke}{[(FV_1 - FV_2 - LR)\times X_{\mathrm{Re}\,sidue}]}\times 100$
Gases & losses (G)	$100 - SY - DY - CY$

Table 4.4 shows an example mass balance calculation for experiment 33. Appendix H comprises mass balances for all of the experiments.

Table 4.4: Mass balance calculation for experiment 33.

Experiment Identification Vacuum residue Feedstock composition	E_{33} ABVB ABVB 50 wt%; n-C_{12} 50 wt%	
X_{Residue}	0.5	
$X_{\mathrm{n\text{-}dodecane}}$	0.5	
Data gathered	Before the experiment	After the experiment
KOH Solution (g)	$SS_1 = 56.00$	$SS_2 = 56.86$
Feedstock vessel (g)	$FV_1 = 722.04$	$FV_2 = 524.03$
n-C_{12} vessel (g)	$nC_{12}V_1 = 57.14$	$nC_{12}V_2 = 17.4$
Lines before the coker (g)		LR = 5.92
Liquid products (g)		LP = 169.92
Coke product (g)		Coke = 39.64
General Mass Balance		
MB (wt%)	$\dfrac{(169.92+39.64+56.86-56.00)}{(722.04+57.14-524.03-17.4-5.92)}\times 100 = 90.76$	
GDY (wt%)	$\dfrac{169.92}{(722.04+57.14-524.03-17.4-5.92)}\times 100 = 73.31$	
GSY (wt%)	$\dfrac{(56.86-56.00)}{(722.04+57.14-524.03-17.4-5.92)}\times 100 = 0.37$	
GCY (wt%)	$\dfrac{39.64}{(722.04+57.14-524.03-17.4-5.92)}\times 100 = 17.10$	
GG (wt%)	$G\,\&\,L = 100 - 73.30 - 0.37 - 17.1 = 9.24$	
Petroleum Residue Mass Balance		

SY (wt%)	$\frac{(56.86-56.00)}{[(722.04-524.03-5.92)\times 0.5]}\times 100=0.9$
DY (wt%)	$\frac{[169.92-(57.14-17.4)-(722.04-524.03)*0.5]}{[(722.04-524.03-5.92)\times 0.5]}\times 100=35.54$
CY (wt%)	$\frac{39.64}{[(722.04-524.03-5.92)\times 0.5]}\times 100=41.27$
G	$100-0.9-41.27-35.54=22.29$

Coke Type Evaluation

The evaluation of the structure of the coke produced in these experiments was defined based on the differences between shot coke and sponge coke as reported in the literature. Density and elemental composition for sponge and shot coke are similar. See Table 4.5 (Ellis & Bacha, 1996).

Table 4.5: Properties of samples of shot and sponge coke gathered from the same source (Ellis & Bacha, 1996).

	Shot coke	Sponge coke
Raw coke volatile material (w%)	9.6	10.2
Apparent density (g/cc)	1.83	1.79
Pore volume (mm^3/g)		
100 – 15 μm	7	19
15 – 0.1 μm	26	48
0.1 – 0.014 μm	10	16
100 – 0.014 μm	43	83
Sulphur (w%)	1.9	2.0
Iron (ppmw)	470	410
Silicon (ppmw)	60	60
Vanadium (ppmw)	540	530
Nickel (ppmw)	200	190
Calcium (ppmw)	130	100
Sodium (ppmw)	120	100
Hardness	27	70

Regarding their appearance, the authors (Ellis & Bacha, 1996; Elliot, 2001) both agree that shot coke comprises individual spherical clusters whereas sponge coke is a solid material with pores on the surface and internal cavities connecting the pores. The differences in physical properties are reflected in the material porosity and the coke hardness. Table 4.5 shows properties of shot coke and sponge coke samples gathered from the same coke pile in a commercial delayed coking unit (Ellis & Bacha, 1996). The pore size distribution differs somewhat. On the other hand, the coke hardness, measured with the Hardgrove Grindability Index (HGI) (ASTM-D5003-95) a standard method used to measure coke hardness, differs significantly. According to Ellis and Bacha (1996), the HGI is around 70 for good non-calcined sponge coke and as low as 27 for shot coke (the lower the value, the harder the coke). Therefore, both physical appearance and hardness differences were selected to determine coke type.

The purpose of the direct observation of coke samples was to identify differences in the structure of coke particles that allow classification of these materials into shot coke and sponge coke. The samples analyzed were raw samples and polished samples. The raw samples were not subject to further treatment after being gathered from the coker. These samples were used to identify superficial differences among coke samples. The polished and sectioned samples were used to detect differences, within the coke sample, related to formation of different structures in the coke matrix

These observations were performed with three different microscopes: an electronic microscope Intel Play QX3+^{TM}, a Scanning Electron Microscope (SEM) model S – 4500 and a polarized light microscope Reichert – Jung MeF3. The first microscope was used for observation of raw coke samples from most of the experiments. The SEM was used to observe raw and polished coke samples from one of the experiments carried out in this study and a raw shot coke sample produced in a different pilot scale apparatus. The polarized light microscope was used to observe the same polished coke sample processed with the SEM.

Ellis and Bacha (1996) published pictures of shot coke particles from a commercial delayed coking unit. Those shot coke particles are like those in Figure 4.2; however, to identify the shot coke particles produced in the new apparatus, it is required to know the appearance of shot coke particles produced in a small scale delayed coking apparatus. Figure 4.3 shows a picture of these particles. The shot coke from the pilot plant has a smooth surface like the commercial shot coke particles, is more porous and the particles are spheres or ovals instead of spheres only. These differences can be related to the differences in vapor velocities inside the coker.

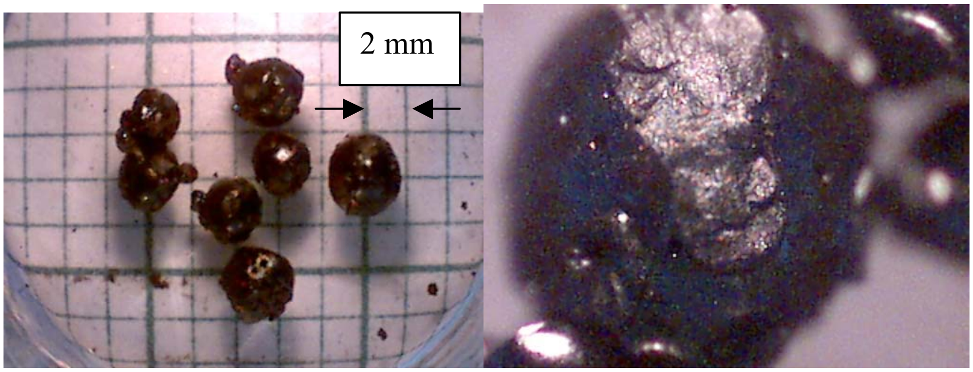

Figure 4.2: Shot coke particles produced in a commercial delayed coking unit. Feedstock: Heater Feedstock (Morin, 2002).

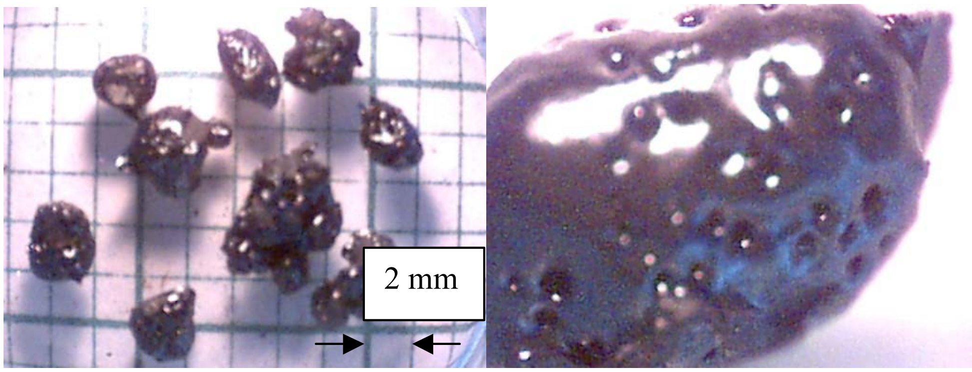

Figure 4.3: Shot coke particles produced in a delayed coking pilot plant. Feedstock: Heater Feedstock (Morin, 2002).

Figure 4.4 shows pictures of shot coke and sponge coke produced in a delayed coking pilot plant when processing Heater Feedstock (Morin, 2002). The shot coke particle is a sphere with smooth and bright surface while the sponge coke particle has a random form with sharp edges, opaque rough surface that is indicative that this particle is not an individual cluster in the coke bulk.

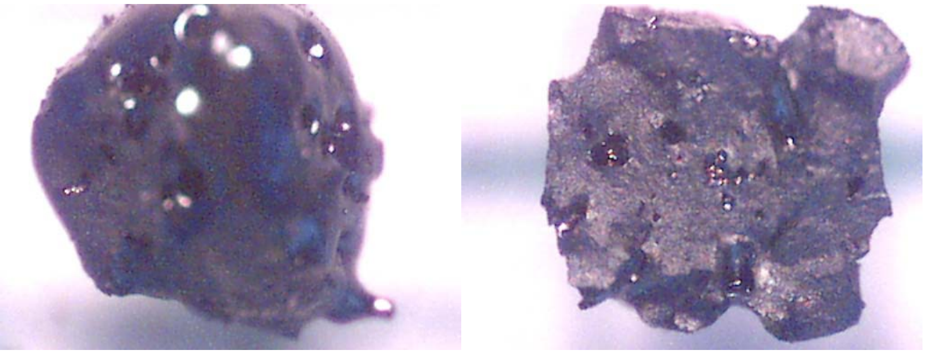

Figure 4.4: Shot coke (left) and sponge coke (right) produced in a delayed coking pilot plant. Feedstock: Heater Feedstock (Morin, 2002).

Thus, the target for the microscope identification of shot coke particles in the coke samples produced in this study is based on the following characteristics: Spherical or oval individual particles with smooth surfaces. The porosity of the surface is not a determinant characteristic because the shot coke particles produced in pilot apparatus can be as porous as sponge coke.

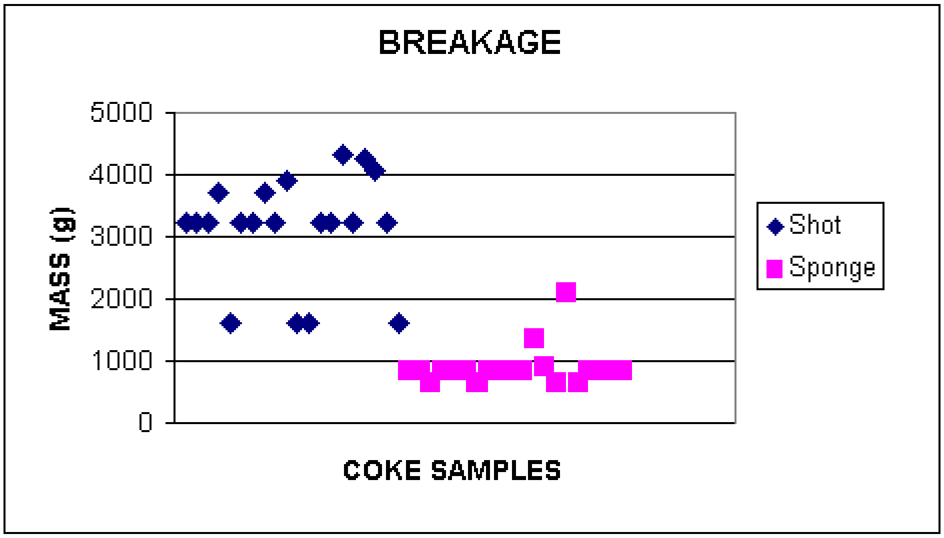

Figure 4.5: Breakage mass for shot coke and sponge coke particles.

Coke hardness could not be measured with the ASTM standard method, (ASTM-D409-97), because the amount of sample required was too large (1000 g). The coke sample produced in each experiment is between 20 g and 70 g. Thus, a method was developed to evaluate hardness. This method consists of subjecting a coke particle to increasing weights until it is broken. According to the calibration and set up of this method (see

Appendix I), shot coke particles can resist over 1500 g, typically more than 3000 g, and sponge coke particles do not support more than 1000 g (Figure 4.5). This difference provides a clear and objective measure for discriminating between shot coke and sponge coke.

Equipment Performance Evaluation

Coker Operating Conditions

The control of the temperature and pressure in the coker were determined by the effectiveness of both the electric furnace temperature control and the backpressure valve, respectively. Table 4.6 shows the average, minimum and maximum standard deviations obtained for both variables from all the experiments. It is worth noting that the standard deviation at different temperature set points did not differ while the standard deviation for the coker pressure varied according to the pressure set point.

Table 4.6: Standard deviations for temperature and pressure in the coker.

	Temperature (K)	Pressure (kPa)				
	687-698-720	240	791	2240	3550	6100
St. Deviation	σ (K)	σ (kPa)	σ (kPa)	σ (kPa)	σ (kPa)	σ (kPa)
Mean	1.03	4	8	8	21	22
Maximum	1.61	6	11	8	31	36
Minimum	0.60	3	7	8	13	9

Figure 4.6 shows pressure and temperature in the coker for experiment 43. Temperature and pressure in the coker for all the experiments are shown in Appendix G. According to the data presented in Table 4.6 and Figure 4.6, the control of the operating variables in the coker was excellent. The 95% confidence limit for temperature variation was ± 3 K. The 95% confidence limit for pressure variation is related to the pressure. At low pressure (239 kPa or lower) the limit is ± 11 kPa, at intermediate pressure (791 - 2240 kPa) ± 22 kPa and at high pressure (3550 – 6101 kPa) ± 72 kPa.

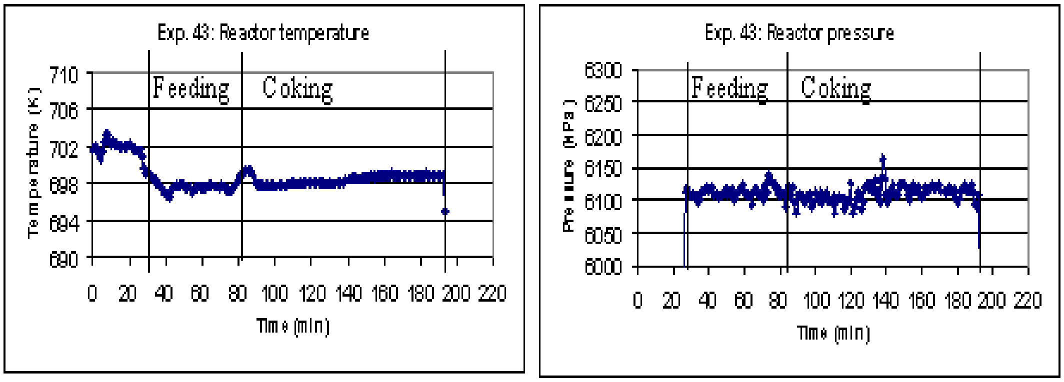

Figure 4.6: Coker variables (temperature and pressure) for experiment 43.

Performance of the feed pump

The feed pump was selected to provide feedstock superficial velocities similar to other pilot plant units. This section summarizes the performance of this device. Figure 4.7 shows the deviation for all the experiments completed in this study as function of the content of vacuum residue in the sample conveyed. The deviation is defined as:

$$Deviation = \frac{(ActualFlow - ExpectedFlow)}{(ActualFlow)} \times 100 \tag{4.1}$$

According to the calibration of the feed pump (see Appendix C), the deviation is around ±5%. For most of the experiments performed with mixtures of n-dodecane and vacuum residue the vapor velocity in the coker was within 10% of the design value. However, in the three experiments performed with vacuum residue alone, the pump conveyed the material but the flow rates were low compared to the design values. The deviations exceeded 35%. Clearly, if the apparatus is to be used to process 100 wt% vacuum residue, modification of the pump suction system is required to achieve design flow rates.

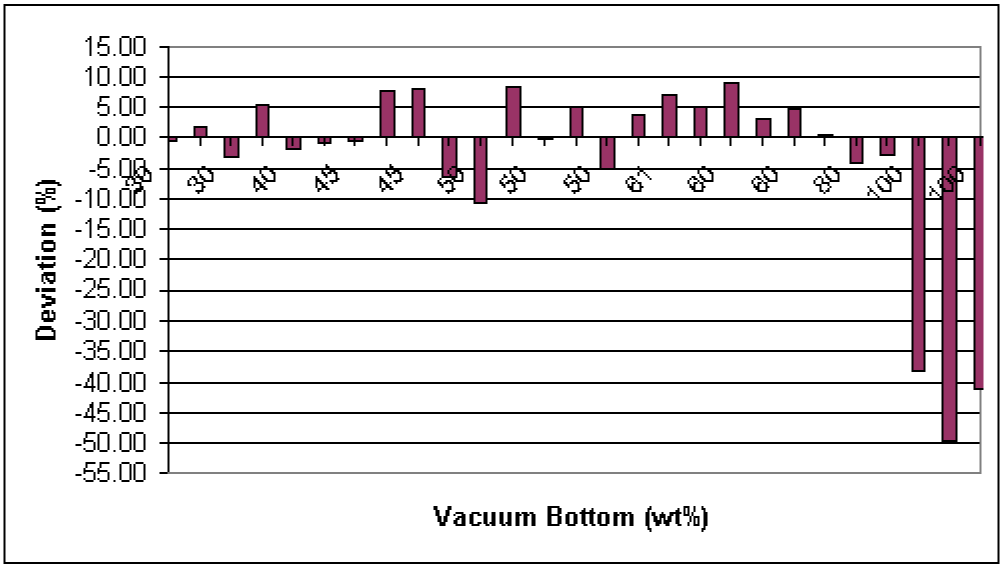

Figure 4.7: Feed pump. Flow rate error represents the difference between the actual flow and the expected flow.

Performance of the Coker effluent condenser

The effluent condenser was designed to guarantee a maximum of 303 K at the outlet. Figure 4.8 shows the inlet and outlet temperature of this equipment during the course of experiment 41, which was carried out at the most extreme conditions for this equipment: low pressure (240 kPa) and high fraction of n-dodecane in the feedstock (70 wt%). In this case, although the condenser inlet temperature reached 700 K the outlet temperature was below 303 K. Thus, this equipment worked according to design and ensured that all condensable products were recovered in the gas – liquid separator.

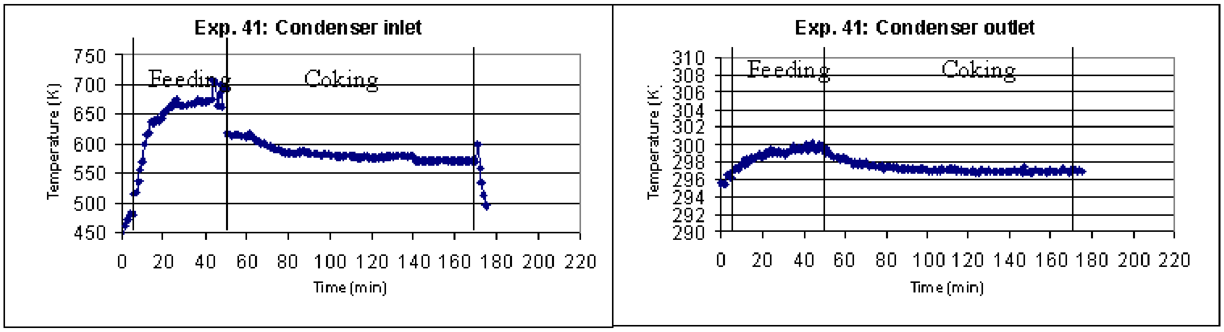

Figure 4.8: Experiment 41: condenser inlet and outlet temperatures.

Summary

The experimental work in this thesis was accomplished in two steps: first, the development and evolution of the experimental matrix; and second, the analyses of operational data, mass balance calculations and coke structure analysis.

In the development of the experimental matrix, the feedstock composition, the coker temperature and the coker pressure were the variables that defined the experiments carried out. The feedstock composition was adjusted, for ABVB, at six different weight fractions of the vacuum bottom ($X_1 = 0.3$, $X_2 = 0.4$, $X_3 = 0.45$, $X_4 = 0.5$, $X_5 = 0.6$ and $X_6 = 0.8$) while the other vacuum bottoms were evaluated at 0.6 wt fraction (Cerro Negro) and 1.0 wt fraction (heater feedstock). The coker temperature set point value was 698 K with additional experiments completed at 687 K and 720 K. The coker pressure was the variable adjusted to process the sample above or below its bubble point. In the experimental work, five pressure levels were evaluated ($P_1 = 239$ kPa, $P_2 = 791$ kPa, $P_3 = 2240$ kPa, $P_4 = 3550$ kPa and $P_5 = 6101$ kPa

The analyses of the operational data and the mass balance of each experiment were the basic material to evaluate the performance of the new apparatus and to identify critical steps in the coke formation process. On the other hand, the analyses of the structure of the coke samples produced were carried out with microscopic observation of raw and polished samples, as well as hardness tests, in order to detect different coke structures.

Regarding the performance of main equipment, the only limitation found was that the feed pump could not maintain design flow rates with highly viscous materials like 100 wt% vacuum residue. All other equipment components performed according to specifications.

Chapter 5 – Results and Discussion

As indicated in chapter 1, there are three objectives of this thesis: first, setup a laboratory apparatus to simulate the delayed coking process; second, evaluate the impact of operating conditions on the structure of the coke formed; and third, identify critical steps in the coking process and their relationships with the phase behaviour of the reacting mixture. This chapter is divided into three sections that cover the goals of the thesis. The performance of the new apparatus is evaluated in the first section where the product yields are compared with the design specifications. The structure of the coke samples is addressed in the second section. In the third section, a phase diagram that reflects the variation of coke yield with feedstock composition and pressure, and identifies phase boundaries that indicate changes in the mixture phase behaviour associated with changes in the coke yield is presented.

Evaluation of the Laboratory Apparatus

Reproducibility of Mass Balances

As indicated in chapter 4, two types of mass balances were calculated for each experiment: the General Mass Balance and the Petroleum Residue Mass Balance. The reproducibility of these results and their usefulness is addressed here.

Table 5.1 shows three examples of both mass balances for experiments performed under the same operating conditions (feedstock composition, coker temperature and coker pressure). According to these data, small variations in the general mass balance have a significant impact on the petroleum residue mass balance. The differences are particularly noticeable for the hydrogen sulphide, gas and distillate yields. The impact on coke yield is small.

The difference in the hydrogen sulphide yield is related to the fact that the quantity produced is low (2.51 g per 225 g of vacuum bottom) and small losses during the collection of the liquid products have a huge impact on the calculated values.

Table 5.1: Reproducibility of General and Petroleum Mass Balances.

Experiment Identification	E_{12}	E_{20}	E_{14}	E_{22}	E_{34}	E_{35}
Nominal ABVB (wt%)	60.02	59.68	39.98	40.05	50.00	50.00
Pressure (kPa)	3562	3553	3559	3556	238	239
Temperature (K)	697	697	698	699	699	699
GENERAL MASS BALANCE (wt%)						
H_2S	0.09	0.00	0.16	0.01	0.28	0.45
Gas & losses	10.16	9.97	15.21	9.77	7.51	9.27
Distillates	71.03	71.59	75.99	81.98	78.76	77.45
Coke	18.73	18.44	8.64	9.30	13.45	12.84
PETROLEUM BASED MASS BALANCE (wt%)						
H_2S	0.23	0.01	0.67	0.06	0.66	1.15
Gas & losses	26.93	25.80	63.69	34.21	17.73	23.86
Distillates	23.18	26.48	-0.51	29.19	49.88	41.95
Coke	49.65	47.71	36.15	36.54	31.73	33.04

The differences in the gas and distillate yields are related to how these values are obtained. As indicated in chapter 2, the processing of hydrocarbon compounds at temperatures above 620 K favours cracking and condensation reactions that produce lighter products (non-condensable and distillate) and heavier compounds (asphaltene and coke). The reaction pattern of each compound in a complex mixture like those prepared in this work is difficult to determine; instead, the reaction tendencies of different hydrocarbon groups (for example the saturate, resin, aromatic and asphaltene fractions) have been determined (Speight, 1998). According to these previous studies, n-dodecane reacts to produce olefins and lighter saturates compounds that form part of the gas and distillate products. The fraction of n-dodecane that remains in the distillate products and leaves the system as non-condensable is unknown; however, the gas and distillates yields are calculated assuming n-dodecane is a non-reactive material. Moreover, the higher gas yields are justified because the losses are considered as part of these results. This makes the distillate and gas yields, based on the petroleum residue processed, inaccurate.

For these reasons, hydrogen sulphide, distillate and gas yields are not included in the result analyses. On the other hand, coke yields are reliable because the only source of this material is the vacuum residue processed in the apparatus. The 95% confidence limit for coke yield is ± 1.72 wt%. This compromise in apparatus and procedure design reflects the focus of this work: coke structure and yield.

Comparison of Product Yields with Delayed Coking Models

The delayed coking models used to accomplish this evaluation were the CCDCC and the PCR-230 models (see chapter 2 and appendix A for more details).

Table 5.2: Comparison of product yields obtained in the new apparatus and the expected values according to the delayed coking models.

API	4.01								
CCR	22.6								
Sulphur (wt%)	4.09								
Experiment ID	E_{25} [1]			E_{26} [2]			E_{36} [3]		
Case	This work	CCDCC	PCR-230	This work	CCDCC	PCR-230	This work	CCDCC	PCR-230
Pressure (kPa)	240	240	240	240	240	240	178	178	178
Temperature (K)	698	698	698	718	718	718	720	720	720
Yields (wt%)									
H_2S	0.76	1.10	---	0.87	1.15	---	0.67	1.11	---
Gas	13.38	7.83	7.62	10.71	7.38	8.57	14.70	7.03	8.10
Distillates	53.25	58.20	59.09	58.17	67.54	59.63	59.53	71.91	62.33
Coke	32.61	32.87	33.28	30.26	23.93	31.80	25.11	19.95	29.57

1. Within range of application of both the CCDCC & PCR-230 models.
2. Just outside the range of application of the CCDCC model.
3. Just outside the range of application of both models.

Experiments 25, 26 and 36 (Table 5.2) were performed using 100 wt% heater feedstock (a commercial delayed coker feedstock) under operating conditions close to the operating conditions of commercial delayed coking units. Thus, results obtained from these experiments should coincide with values obtained from the coker models that are fit to industrial data. At the reference condition E_{25} the data and the models agree. At higher temperatures the data and models disagree. The CCDCC model diverges more rapidly than the PCR-230 model. The coking models clearly cannot be used outside their narrow range of application. At the reference condition (within the range of application of both models), it is clear that the experimental hydrogen sulphide and the distillate yields are lower and the gas yields are higher than the calculated values. The experimental coke yields are well predicted by the models.

Other data useful for evaluating the performance of the new apparatus are those obtained when mixtures of ABVB and n-dodecane are processed at low pressures, providing that n-dodecane vaporizes and does not affect coking reactions. Figure 5.1 shows that at low pressures coke yield is independent of composition.

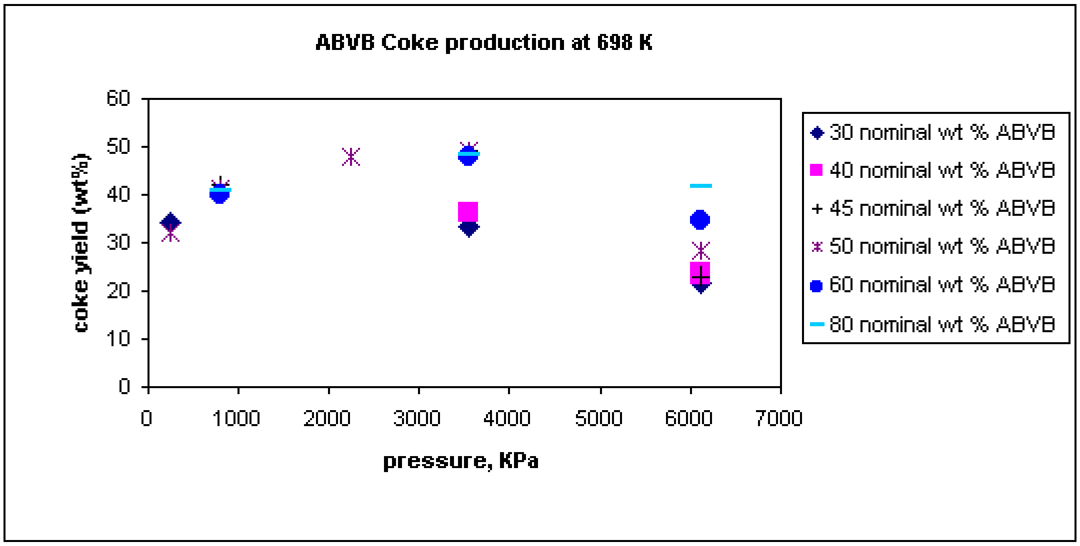

Figure 5.1: Coke yield as function of pressure for different mixtures of ABVB + n-dodecane.

If solution effects are ignored, product yields at low pressure can be compared with predicted values under similar conditions. Figure 5.2 shows the coke yields from experiments carried out with mixtures of n-dodecane and ABVB at 698 K & 240 kPa and the values predicted with the delayed coking models. The error bars reflect 95% confidence limits for the experimental data. Again, predicted and experimental coke yields agree within the accuracy of the data and models.

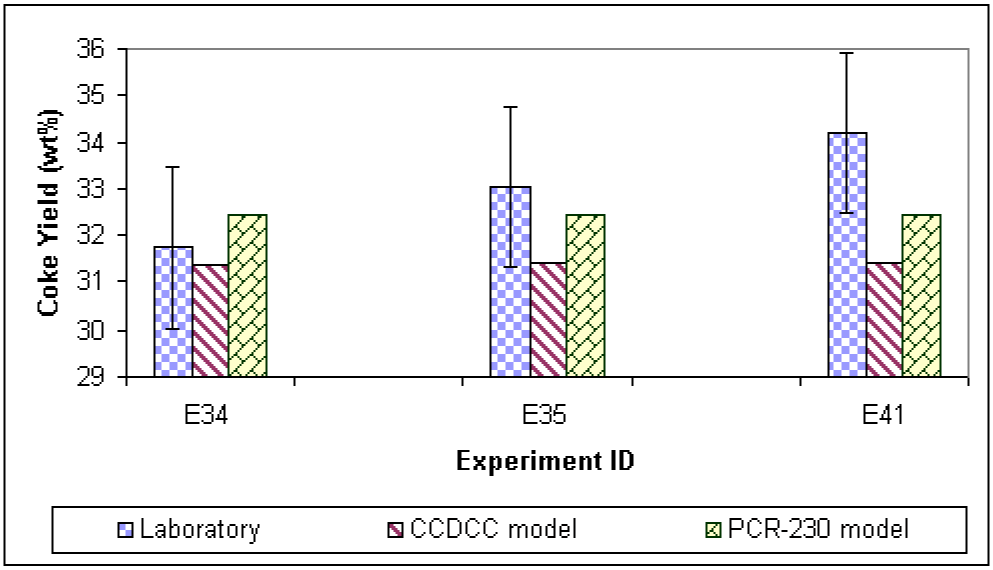

Figure 5.2: Experiments with mixtures of ABVB and n-dodecane at low pressure. Coke yields based on the residue processed (E_{34}: ABVB 50 wt%, P=238 kPa, T=699 K; E_{35}: ABVB 50 wt%, P=239 kPa, T=699 K; E_{41}: ABVB 30 wt%, P=239 kPa, T=699 K).

From the cases presented in Table 5.2 and Figure 5.2, the experimental coke yields agree closely with values predicted by delayed coking models over the range of application of coking models. Therefore, the new laboratory coker simulates delayed coking units, in at least this respect.

Coke Type Evaluation

Surface Morphology and Particle Breakage Test Results

Coke structure was evaluated with three different microscopes and the application of a hardness test. Appendix J contains images of microscopic observations and the results of hardness tests for most of the experiments completed (the experiments indicated in Table 4.1). This section highlights specific experiments that are considered the key to identifying the formation of different types of coke.

The experiments were selected based on the phase behaviour of ABVB + n-dodecane mixtures reported by Zou (2002) and Abedi et al (1998), and the impact of operating conditions on coke yield. As indicated in chapter 4, multiple phase behaviour for ABVB + n-dodecane appears at ABVB concentrations between 20 – 60 wt% over a broad range of temperatures and Abedi et al (1998) showed that at 25 wt% ABVB in n-dodecane large LLV zones were present at temperatures up to at least 680 K. Besides, the data in Figure 5.1 shows an important impact of the mixture composition on the coke yield at high pressure (3500 – 6100 kPa). Thus, the key experiments are: E_{19}, E_{20}, E_{21}, E_{22}, E_{27}, E_{28}, E_{29}, E_{30}, E_{38}. Figures 5.3 to 5.11 show photomicrographs of these coke samples. While not specified, the scale for each image is approximately 2 mm x 4 mm.

The microscopic identification of shot coke particles in the coke samples is based on the following characteristics: Spherical or oval individual particles that are easy to separate from the coke bulk and possess a smooth surface. The porosity of the surface is not a determinant characteristic because shot coke particles produced in laboratory apparatus can have as many pores as sponge coke (Figure 4.3).

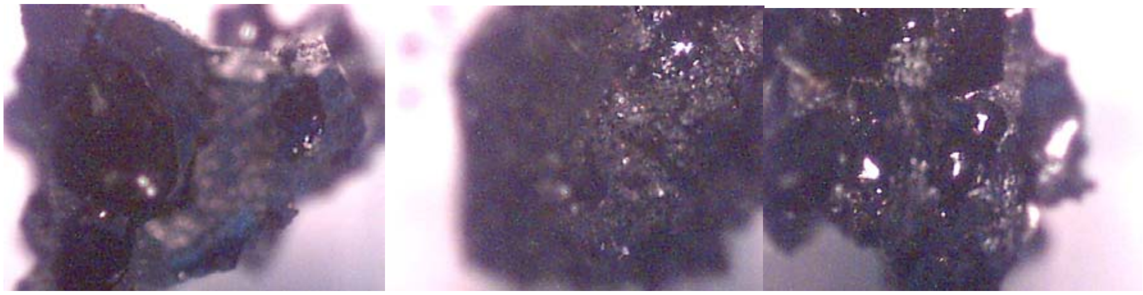

Figure 5.3: E_{19} (ABVB: 60 wt%; 6100 kPa): photomicrographs of coke samples.

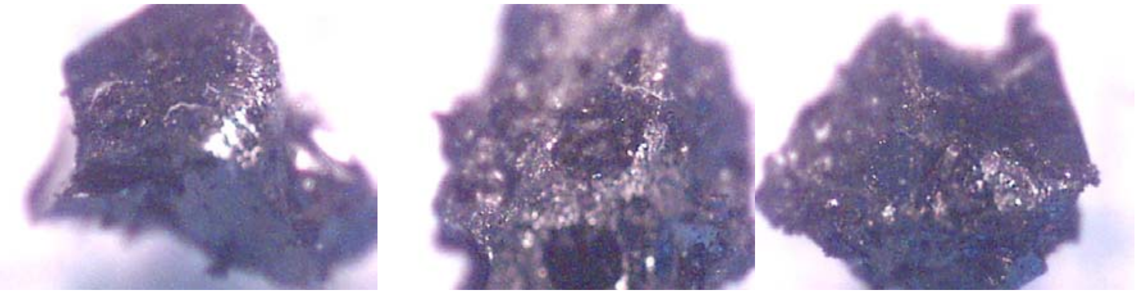

Figure 5.4: E_{20} (ABVB: 60 wt%; 3550 kPa): photomicrographs of coke samples.

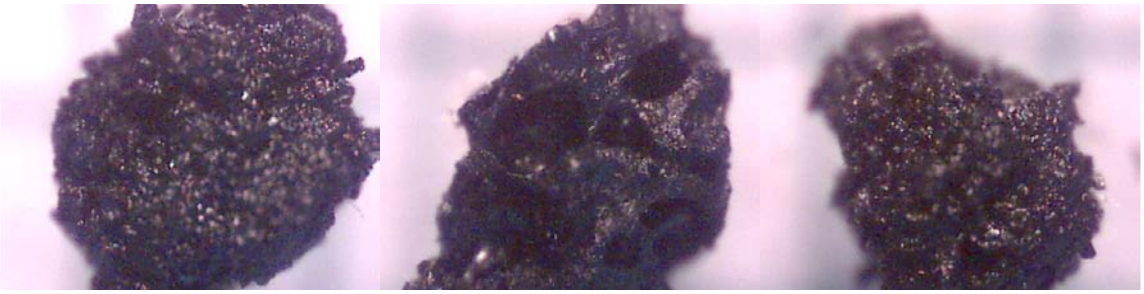

Figure 5.5: E_{21} (ABVB: 40 wt%; 6100 kPa): photomicrographs of coke samples.

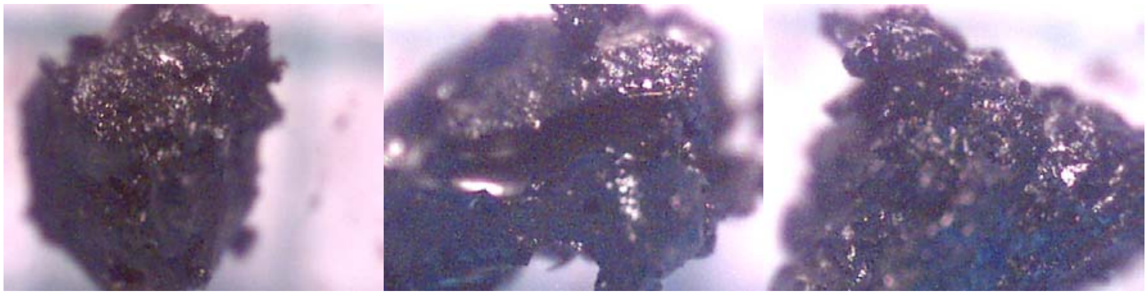

Figure 5.6: E_{22} (ABVB: 40 wt%; 3550 kPa): photomicrographs of coke samples.

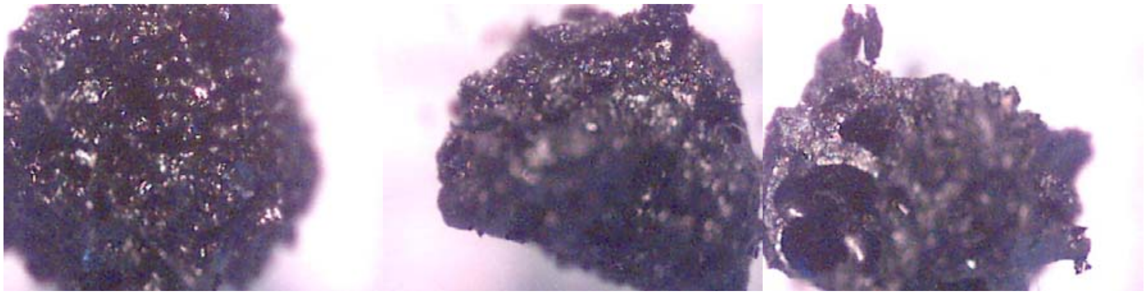

Figure 5.7: E_{27} (ABVB: 45 wt%; 6100 kPa): photomicrographs of coke samples.

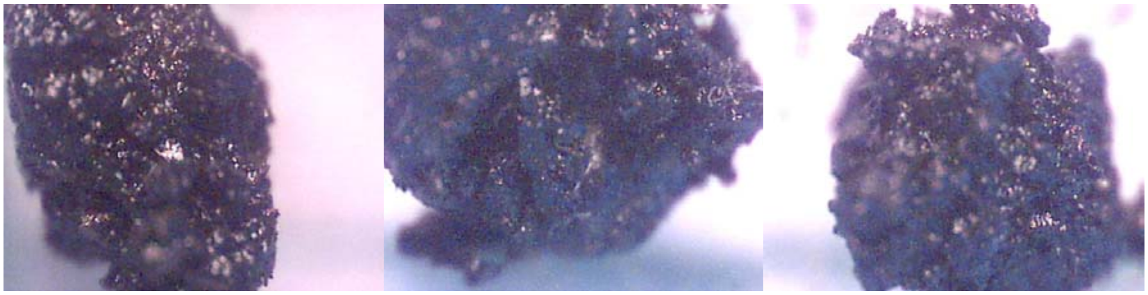

Figure 5.8: E_{28} (ABVB: 45 wt%; 6100 kPa): photomicrographs of coke samples.

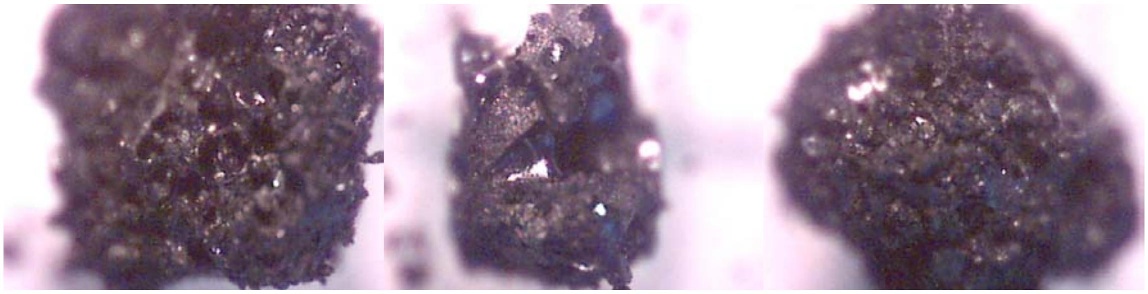

Figure 5.9: E_{29} (ABVB: 50 wt%; 6100 kPa): photomicrographs of coke samples.

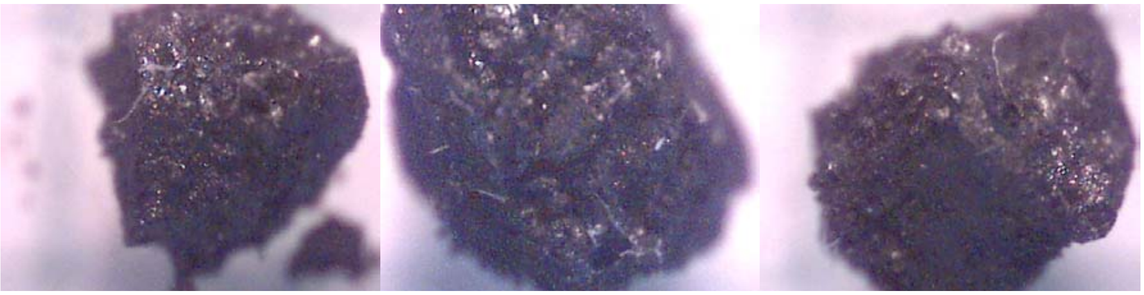

Figure 5.10: E_{30} (ABVB: 50 wt%; 3550 kPa): photomicrographs of coke samples.

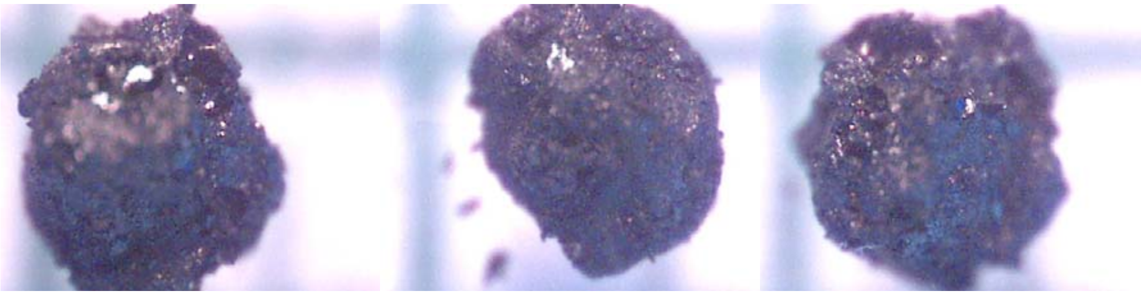

Figure 5.11: E_{38} (ABVB: 50 wt%; 2240 kPa): photomicrographs of coke samples.

The images shown above (Figures 5.3 to 5.11) were selected as representative of the coke samples produced because they are typical specimens obtained when particles with dimensions between 2 – 8 mm are separated from the coke bulk and in most of the cases their forms are the closest to spheres or ovals. Although in some cases the particles are spheres, these particles were not individual clusters in the coke bulk and their surfaces were not smooth surfaces like those shown in chapter 4 (Figures 4.2, 4.3 and 4.4).

Figure 5.12 shows the average results of the hardness tests for the coke samples produced from mixtures of ABVB and n-dodecane. The graphic includes the average breakage mass for the coke samples produced in this evaluation (see Appendix J for details) and the average breakage mass for shot coke particles and sponge coke particles produced in a delayed coking pilot plant (see Appendix I). These data show that the breakage mass for the coke samples produced in these experiments is below 1000 grams and comparable to the values expected for sponge coke samples.

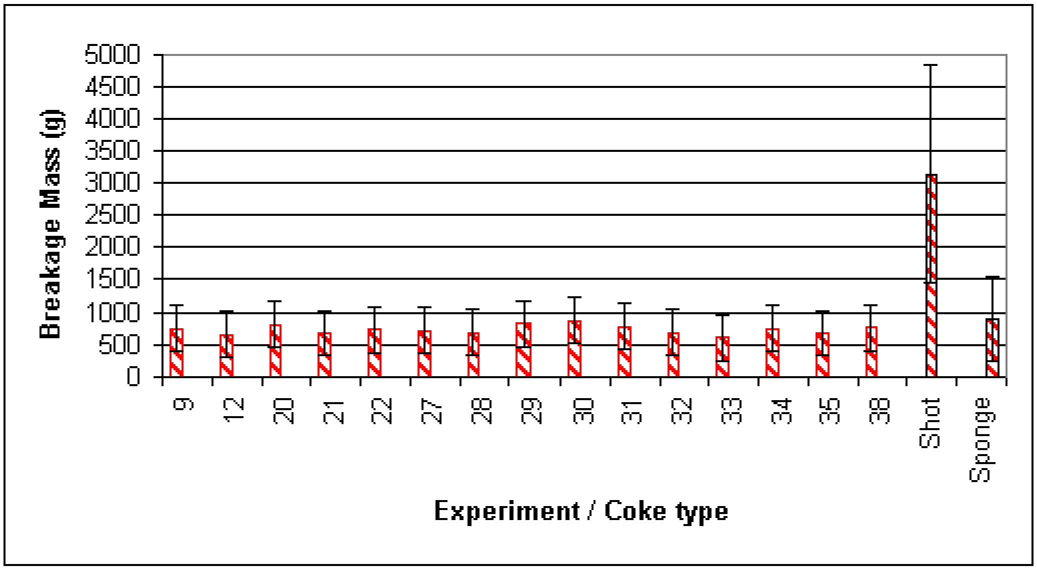

Figure 5.12: Breakage mass average values for coke samples produced in different experiments and reference values for shot coke and sponge coke. Error bars represent the 95% confidence limits.

Therefore, the microscopic inspection and the hardness evaluation indicate that only sponge coke particles were formed. However, to determine the impact of phase behaviour on the structure of the coke, it is mandatory to show that the new apparatus can produce shot coke when processing a shot coke forming feedstock under the appropriate operating conditions.

As indicated in chapter 2, shot coke is produced in delayed coking units when these plants are working at high temperatures and lower pressures. Thus, a known shot coke producing feedstock, Heater Feedstock, was processed in the new apparatus at operating conditions that facilitate the formation of shot coke. The experiments were E_{25}, E_{26} and E_{36}.

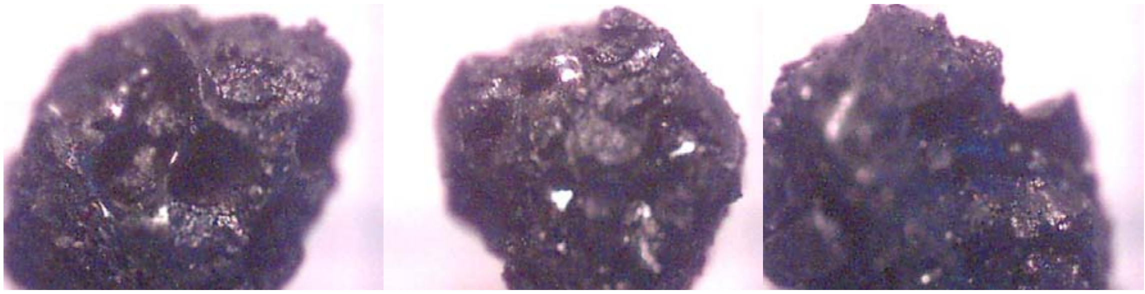

Figure 5.13: E_{25} (Heater Feedstock; 698 K; 240 kPa): photomicrographs of coke samples.

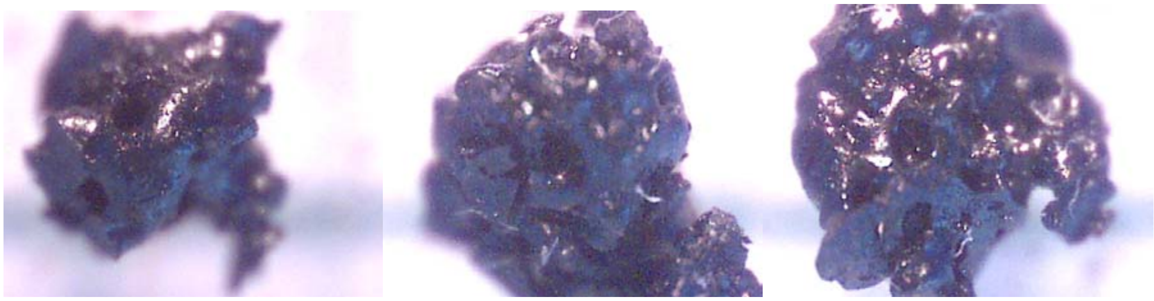

Figure 5.14: E_{26} (Heater Feedstock; 718 K; 240 kPa): photomicrographs of coke samples.

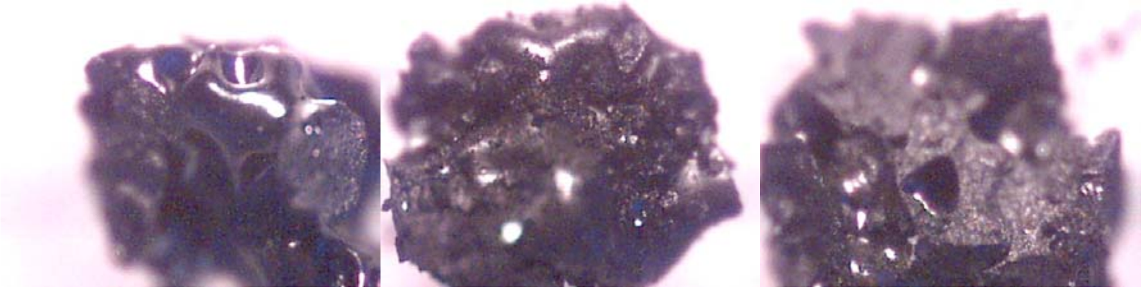

Figure 5.15: E_{36} (Heater Feedstock; 720 K; 178 kPa): photomicrographs of coke samples.

The photo micrographs (Figures 5.13 to 5.15) show that these coke samples have random forms; and in comparison with the coke samples for ABVB + n-dodecane at higher pressures (Figures 5.3 to 5.11), these coke particles have more pores and brighter surfaces. Furthermore, The hardness tests indicate that these particles are only as hard as sponge coke particles (see Table 5.3).

In the data reported in Table 5.3 the breakage weight for Experiment 36 stands out. Although it is not as high as the values expected for shot coke, the breakage mass is the highest average value for the coke samples obtained in the new apparatus. This result is expected because the operating conditions (the highest temperature and the lowest pressure in the coker) reduce the volatile material in the coke produced and increase its hardness. One can say with more than 99 % confidence that this material is not shot coke.

Table 5.3: Breakage weights average values for experiments carried out with Heater Feedstock.

Experiment / Coke Type	Breakage mass (g)	σ (g)
Sponge Coke	892	322
Shot Coke	3137	850
Experiment 25	772	118
Experiment 26	807	228
Experiment 36	1093	363

Microscopic Examination of Particle Sections

According to previous studies about coke formation mechanisms cited in chapter 2, the formation of spheres of mesophase produces shot coke or sponge coke. Shot coke is characterized by the formation of small mesophase spheres in a more dense medium while more ordered coke structures like sponge coke are formed in a less viscous medium where the mesophase spheres can grow and coalesce. Thus, the identification of different structures at this level is helpful to determine whether or not shot coke formed in the new apparatus.

This evaluation was carried out on coke samples from Experiment 36. The electronic microscope QX3+^{TM} could not be used for this study. The Scanning Electron Microscope (SEM) Model S – 4500 and a polarized light microscope Reichert – Jung MeF3 are more appropriate, and were used instead.

Figures 5.16 and 5.17 show SEM and polarized light microscope pictures of shot coke particles from a delayed coking pilot plant and the coke sample from Experiment 36.

In Figure 5.16, the superficial differences between the two coke samples are evident. The shot coke sample comprises individual spherical particles fitted together to form the bulk coke (A); on the other hand, the coke sample from experiment 36 is one piece where no individual particles can be distinguished (C). Moreover, higher magnification of these two samples highlights more noticeable differences on the coke surfaces (B and D). The shot coke sample has a smooth surface while the other coke sample has an irregular surface with abrupt changes and variable orifice sizes.

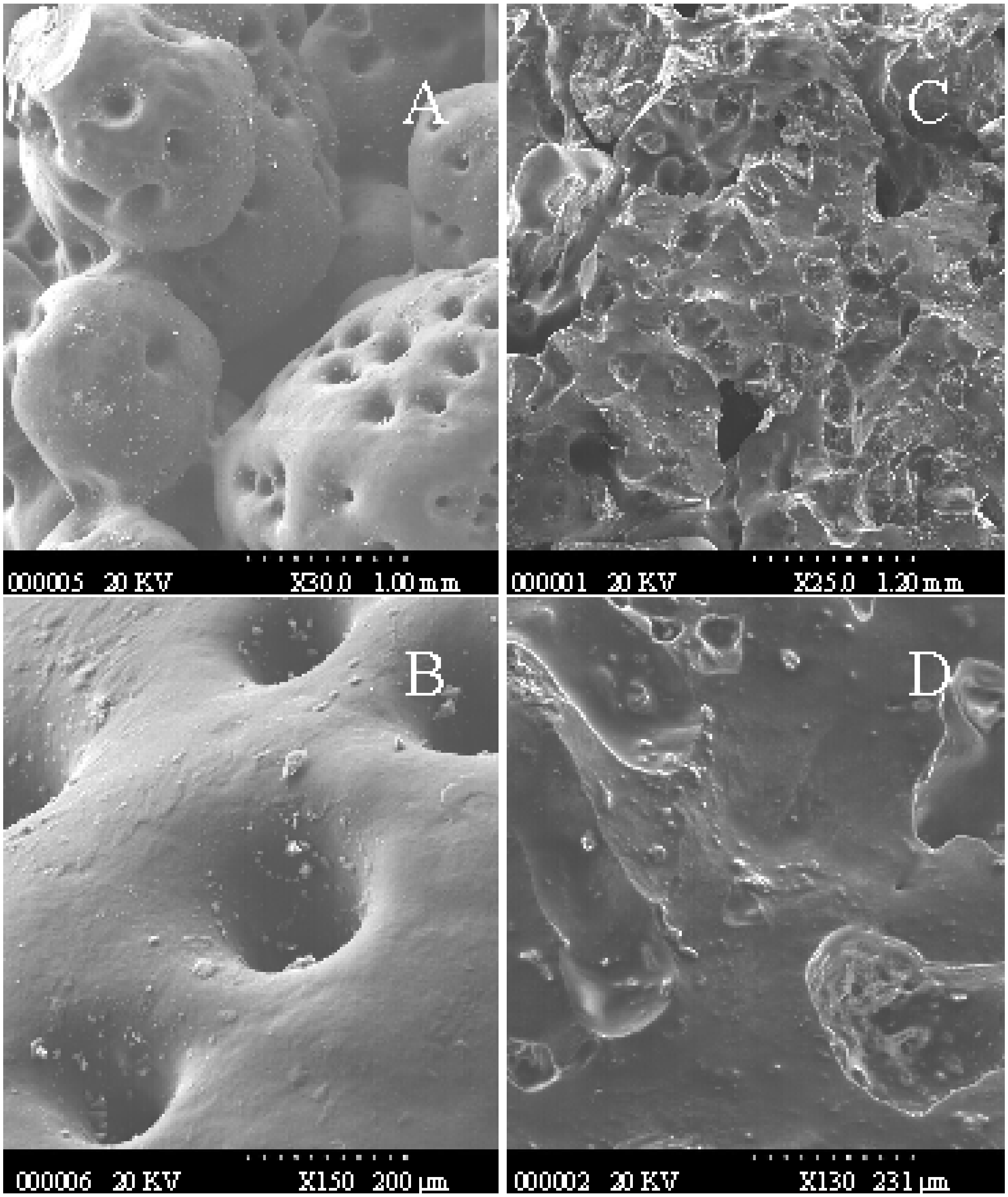

Figure 5.16: SEM. A, B: shot coke produced in a delayed coking pilot plant. C, D: coke sample produced in experiment 36.

Figure 5.17 shows pictures of polished coke samples for experiment 36 under non-polarized light and polarized light. In the low magnification pictures (A, B), the coke sample comprises the material inside the black border. The black dots are pores. The high magnification pictures (C, D) present a smaller zone of the coke sample shown in pictures A and B. Under polarized light the sample does not show the appearance of different structures indicative of the simultaneous formation of different coke types. Based on these results, it is evident that the processing of low quality shot coke producing feedstocks in the new apparatus does not lead to shot coke formation, even when this unit is used to process these feedstocks under more severe conditions (higher internal temperatures and lower pressures in the coker) than other delayed coking pilot plants, with shot coke producing feeds. Therefore, other parameters, that have not been indicated before and were not considered in the design of this apparatus and the experiments performed, are affecting the formation of different coke structures.

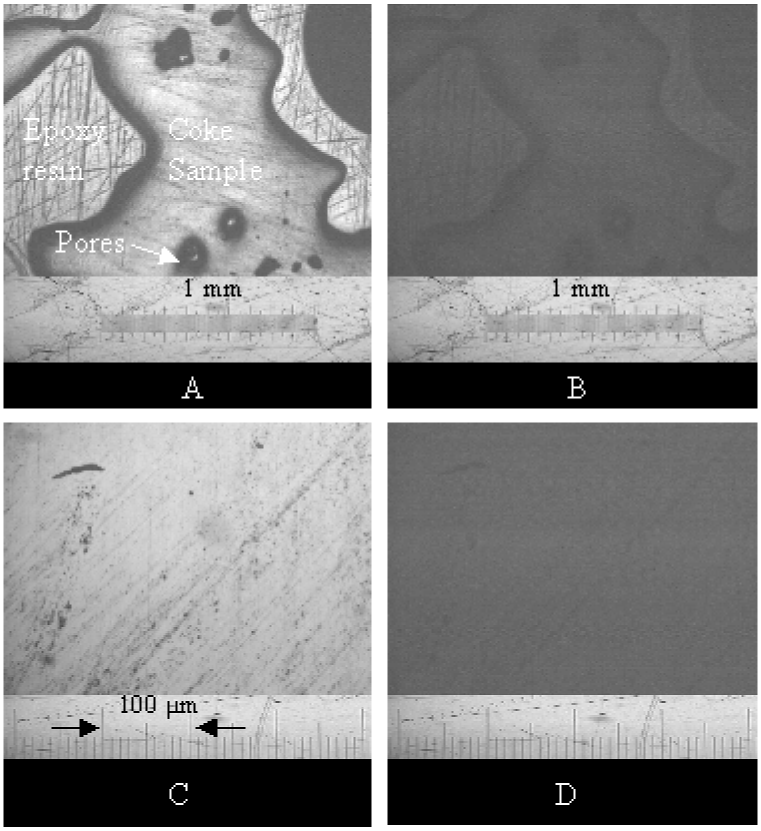

Figure 5.17: Polarized Light Microscope. Pictures A and C: non-polarized light. Pictures B and D: polarized light. Sample from experiment 36.

A comparison of the operating parameters, that could affect the formation of shot coke and sponge coke, between the new apparatus and other delayed coking pilot suggests two main differences: the feeding period and the difference between the internal temperature and the heating device temperature.

The feeding periods in other delayed coking pilot plants where shot coke has been produced are between 2 and 3 hours while in the new apparatus this time was 45 minutes. However, it is worth noting that the feeding periods in those delayed coking pilot plants are very small in comparison with commercial delayed coking units (as indicated in chapter 1, this period is between 11 and 24 hours). These differences do not avoid the formation of different coke structures. For this reason, the length of the feeding period, although it must be considered for future experiments, is not considered to be an important parameter affecting the formation of different coke types.

Regarding the difference between the internal temperature and the heating device temperature, it is important to mention that in other delayed coking pilot plants the heating devices temperatures are as high as 773 K for coker temperatures around 698 K, while the heater outlet temperatures, in commercial delayed coking units, are between 760 and 780 K (see chapter 1). On the other hand, in the new apparatus the heating device temperature was between 710 and 720 K for internal temperatures of 698 K; furthermore, the experiments carried out at 720 K required a heating device temperature around 740 K. High surface temperatures in the other delayed coking pilot plants and commercial units generate hot spots in the processed feedstocks that may have a significant impact on the different types of coke produced.

These issues will be addressed in future work. At this time no direct link has been established between coke type formed and phase behaviour.

Coke Formation and Phase Behaviour

Other researchers (Speight, 1998) have speculated on the impact of phase behaviour on coke formation but research to relate them has not been conducted before. The goal of this section is to identify critical steps in the coke formation mechanism, expressed as the changes in the coke yields, which are related to the phase behaviour of the feedstock.

Variation of Coke Yield with Pressure

Figure 5.18 shows the change of coke yield (obtained from the petroleum residue mass balance) with feedstock composition, for experiments conducted at the same operating temperature and pressure.

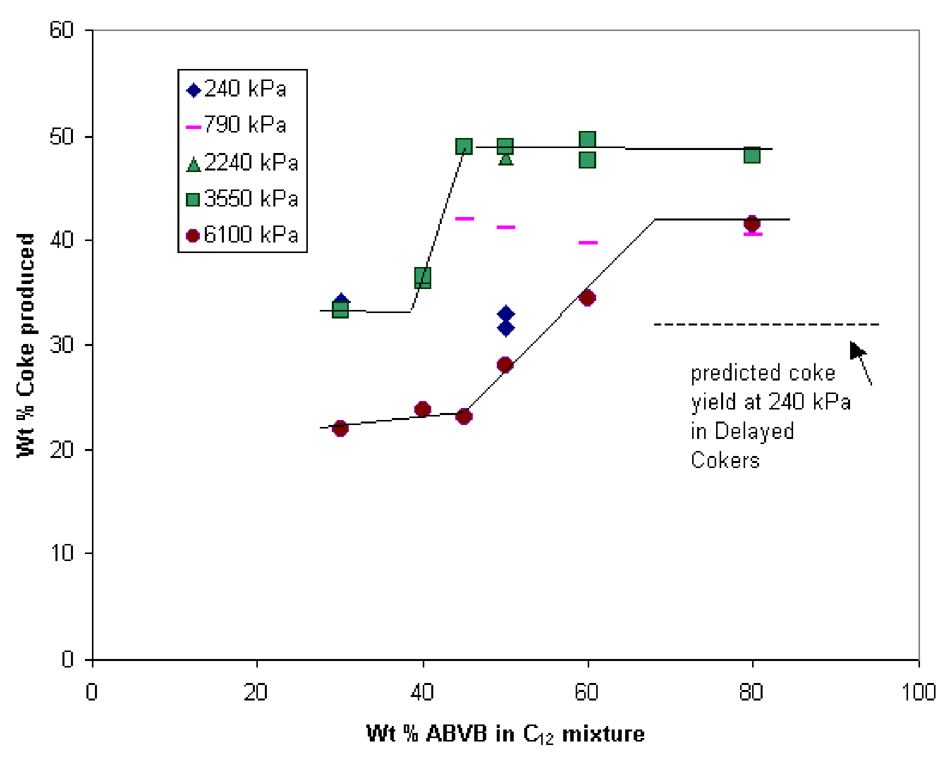

Figure 5.18: Coke yield from ABVB in ABVB + n-dodecane mixtures at 698 K.

As shown in Figures 5.1 and 5.18, the coke yield increases with pressure up to a maximum that is registered at 3550 kPa. This increase in coke yield follows the observed tendency in commercial and pilot plant delayed coking cokers (PDVSA-Intevep, 1999). Pressure increases in these cokers forces more hydrocarbons to remain in these devices, where condensation reactions produce more heavy material that finish as additional coke. Commercial delayed cokers work at pressures between 240 and 1200 kPa, which are values inside the pressure range of the increasing coke yields indicated above. However, this theory is not applicable to the results obtained at higher pressures (6100 kPa) that show a significant reduction of the coke yield in comparison with the experiments carried out at 3550 kPa.

This reduction of coke yield at 6100 kPa has not been reported before. From the data in Figure 5.18, it is evident that above 3550 kPa n-dodecane influences the reacting system as an asphaltene-diluting compound and as a terminal chain reacting compound. As asphaltene-diluting compound, n-dodecane influences the reacting liquid phase and creates a medium where asphaltenes remain diluted. The dilution of asphaltenes and inhibition of the coke formation reactions has been reported before. According to Wiehe (1993), the coke induction period is the capacity of the heptane soluble fraction to keep the asphaltene fraction in suspension and inhibit the formation of coke. The heptane soluble fraction comprises polar aromatic compounds different from n-dodecane. However, the experiments conducted by Wiehe (1993) were at 673 K and lower pressures (maximum 1200 kPa) than those used in this thesis. At such conditions, the saturate compounds, like n-dodecane, vaporize. Moreover, the incorporation of a saturate compound, at the high concentration levels used in this thesis, was not studied in the cited work.

The induction period, prior to coke formation, is lengthened when the heptane soluble fraction is high enough to keep the asphaltenes in suspension. After this period, asphaltenes start to precipitate and an asphaltene rich phase, where coking reactions take place rapidly, is formed. Wiehe (1998) did not report the impact of the induction period on the coke yield; however, the results reported in this thesis indicate that the incorporation of n-dodecane, at certain operating conditions, impacts coke yield. Thus, the action of n-dodecane is not limited only to the effect on coke induction period; it also inhibits coke formation reactions and favours the terminal reactions that increase distillate yields.

This selective behaviour of n-dodecane can be related to the reaction pathway of saturates compounds, as indicated in chapter 2. For example, compounds like n-dodecane are not coke precursor compounds; instead, they react to produce saturate compounds, un-saturates compounds and free radicals. The production of un-saturate compounds follows the liberation of hydrogen molecules that at pressures higher than 4000 kPa (Speight, 1998) can promote hydrogenation reactions. The free radicals can react with other large molecules in a termination reaction that prevents condensation.

Variation of Coke Yield with Feedstock Composition

In Figure 5.18, the experiments performed at 3550 and 6100 kPa show three levels of coke yield that depend on the ABVB concentration in the feedstock. For the purpose of this thesis, these three levels are identified as Low Coke Yield, Transition and High Coke Yield. The Low Coke Yield occurs at low ABVB concentrations: at 3550 kPa the limit value is around 35 – 40 wt % while at 6100 kPa this value is around 45 wt %. The Transition is a range where the coke yield increases with ABVB concentration up to the value of the High Coke Yield: at 3550 kPa this range is between 40 wt % and 45 wt % while at 6100 kPa this value is between 45 wt % and around 70 wt % (or maybe the coke yield continues increasing with ABVB concentration). Finally, the High Coke Yield region occurs beyond the Transition region.

These data were used to construct a coke yield model as a function of feedstock composition and operating conditions at 698 K (Figure 5.19). In this diagram, three sets of lines are presented.

The dashed line represents the bubble pressure curve for the mixture. It is notional because, due to reactions occurring, it cannot be measured or estimated with certainty. From the calculations in chapter 3 only minimum values (in the absence of chemical reaction) can be determined (see Figure 3.5).

The continuous line delimits the Low Coke Yield and the High Coke Yield regions according to the cusps obtained in the coke yield data in Figure 5.18 (the cusps identified experimentally are represented as black dots in the diagram).

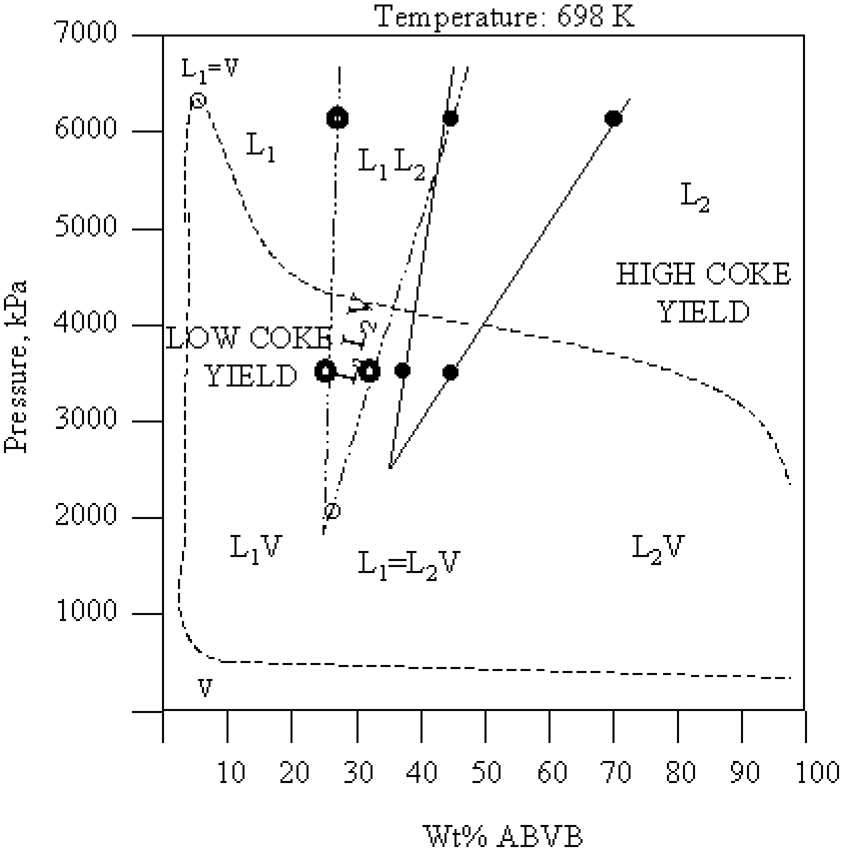

Figure 5.19: Phase diagram represents a coke yield model as function of feedstock composition and pressure.

The third set of lines, dot dashed, requires some explanation. In order to operate the coker at fixed pressure, n-dodecane was injected prior to the feed period. The higher the initial pressure in the apparatus, the greater the mass of n-dodecane required. Consequently, the influent composition fed to the coker shifted with respect to the origin and this must be accounted for if one is to compare the coking results with the known phase behaviour of ABVB + n-dodecane system (Zou, 2002; Abedi et al 1998). This material is displaced during the feeding period. From the mass balances the cusps move from ABVB 70 wt % at 6100 kPa to ABVB 45 wt % at 6100 kPa, from ABVB 45 wt % at 3550 kPa to ABVB 33 wt % at 3550 kPa, from ABVB 45 wt % at 6100 kPa to ABVB 29 wt % at 6100 kPa and from ABVB 38 wt % at 3550 kPa to ABVB 27 wt % at 3550 kPa. This is the maximum translation and ignores displacement by the influent. This adjustment does not alter the qualitative argument raised by the diagram, that is to say that low coke yields are expected at L_1, L_1V region zones, intermediate coke yields in L_1L_2, L_1L_2V zones and high coke yields in L_2, L_2V zones. The resulting phase behaviour boundaries are also consistent with prior work.

In addition, the L point ($L_1 = L_2 + V$) at more than 25 wt % ABVB must be present according to the work of Abedi (1998). So the L_1L_2V region and hence the transitional coke formation region does not extend to the dew curve.

Coke Yield and the Impact of n-Dodecane

The main objective in the processing of heavy oils and bitumen is the production of high value light liquid products with reduction in the yields of low value residual materials like coke. Therefore, the main objective of delayed cokers and other vacuum residue processing technologies (for example fluidcoking and flexicoking) is minimizing coke yield while maximizing the production of distillates. When ABVB is processed in delayed cokers that work under the most favourable conditions to maximize distillate yields (in a pilot plant this condition is 240 kPa and 698 K), the coke yield is expected to be between 31 wt % and 34 wt %. However, when ABVB is processed diluted with n-dodecane (30 – 45 wt % ABVB) at 6100 kPa and 698 K, the coke yield diminishes to 22-24 wt %. A reduction in coke yield of this magnitude has a favourable impact on the cost of heavy oil processing. Therefore, this result opens a line of inquiry for research and development of alternatives to existing processes for heavy oils that reduce in coke yields.

Summary

The performance of the new apparatus indicates that it simulates industrial delayed coking processes in terms of product yields. The yields of H_2S, gas and distillate are least certain because of the product recovery method and the use of n-dodecane as a solvent. However, the coke yields are accurate to within ± 1.7 wt% (95% confidence limits).

Microscopic evaluation of the coke samples and strength test results indicate that shot coke was not produced in the new coker apparatus. An additional parameter, overheating of feed, which has not been reported before and was not considered in the design of the new apparatus, appears to be very important with respect to the formation of this type of coke. Other aspects of the design and operation of the new coker are equivalent to delayed coking pilot plants where shot coke is produced with the same feeds. Consequently, the influence of phase behaviour on shot coke versus sponge coke could not be assessed, at this time.

Although the impact of phase behaviour on coke type formation could not be determined with these experiments, the results obtained allow for the study of the impact of n-dodecane on the coke formation mechanism. Dodecane can possess two functions: as an asphaltene-diluting agent that inhibits coke formation reactions and as a selective reagent that favours terminal reactions versus condensation reactions. The net effect of this action is the reduction of coke yield when the coker pressure is increased at fixed composition above 3550 kPa. The impact of dilution is clear from the results for coke yield in Figure 5.18. At 3550 kPa coke yield is reduced from ~50 wt % in the L_2 phase to ~33 wt % in the L_1 phase as the ABVB concentration goes from 45 wt % to ~38 wt %. As pressure is increased from 3550 kPa to 6100 kPa for 80 wt% ABVB in the L_2 phase, coke yield drops from ~50% to 42% suggesting a link with reaction only, as one expects that the mixture is at or above the bubble pressure at 3550 kPa.

The impact of n-dodecane in the feedstock highlights the need for the development of generalized coke yield models that account for phase behaviour. Further, these results indicate a clear direction for future research and development that could lead to new and economically viable processes for heavy oil upgrading with substantially reduced coke yields.

Chapter 6 – Summary and Conclusions

The processing of vacuum residues in delayed coking units produces two different types of coke: sponge coke and shot coke. While the former is the desired product, the latter one is undesired because it causes operational problems that affect the safety and profit of the units. The formation of these different cokes is associated with two main factors: the properties of the feedstock and the operating conditions in the reactor (pressure, temperature and recycle ratio). Regarding the feedstocks quality, high asphaltene content is the main characteristic of shot coke producing feedstocks; therefore, the vacuum residues from heavy oils are likely sources of this material. On the other hand, the adjustment of operating conditions in the reactor promotes or suppresses shot coke formation. Given that coke precursor compounds react in a liquid phase with properties (composition, viscosity and density) determined by these operating conditions, it is evident that the coke formation process is not only related to the reaction rate of the system but also to the phase behaviour of the liquid phase where coking is taking place.

Moreover, Wiehe (1993) expressed in a kinetic model the influence of the liquid phase on the coking rate (induction period). Afterwards, Rodríguez et al. (1998), Menéndez et al. (1997) and Rahimi et al. (1998, 1999) claimed that the quality of the liquid phase, specifically related to its viscosity, determines the structure of the coke formed. Thus, the relationship between phase behaviour and coke formation is broadly recognized. However, the application of phase behaviour to the understanding of heavy oil processes and coke formation is rare (Abedi et al., 1998). Furthermore, the aim of this thesis is to use phase behaviour and phase diagram theory to identify critical pathways in the coking process; and to explain the relationship between the liquid phase, where the coking reactions are taking place, and the coke structures formed.

From the results of this thesis, the following specific conclusions are drawn:

1. Given the similarity of experimental product yields and values predicted by standard coking models (where applicable), the new apparatus simulates delayed coking technology at low pressures. Furthermore, this new apparatus is

capable of operating over a broad range of temperatures and pressures. The temperature range is 687 – 720 K and the pressure range is 100 - 6100 kPa.

2. The production of different coke structures in the new apparatus was not possible because parameters, other than those considered in the design of the new apparatus and not reported in the literature, affect the formation of these products. Superheating of heat-exchange surfaces, for example, appears to be an uncontrolled variable in prior studies. Consequently, the impact of phase behaviour per se of the reacting system on the structure of the coke formed remains unresolved.

3. Phase behaviour has a dramatic effect on coke yield. With small changes in composition at fixed temperature and pressure, coke yields can be halved or doubled. For example, at 698 K and 3550 kPa the coke yield goes from 33 % to 50 % as ABVB concentration in n-dodecane goes from 38 wt % to less than 45 wt %. At 6100 kPa and the same temperature, coke yield goes from 23 % to 42 % as ABVB concentration goes from 45 wt % to less than 80 wt %.

4. n-Dodecane can exert two effects on coking kinetics: as an asphaltene-diluting agent that inhibits coke formation reactions and as a reagent that favours terminal reactions over condensation reactions. Both pathways are active. However, the dramatic changes in coke yield with small changes in composition at fixed temperature and pressure highlight the impact and dominance of phase related phenomena.

5. Coke yields for n-dodecane + ABVB mixtures at 698 K allow for the identification of low coke yield and high coke yield regions as function of concentration and pressure. These regions link with the known phase behaviour of ABVB + dodecane mixtures. The L_1V region is associated with low coke yield, the L_1L_2V region with intermediate coke yield and the L_2 or L_2V region with high coke yield. This information is presented in a coking diagram that highlights conditions for further experimental evaluation, and will be used to develop more robust coke formation models.

6. The dramatic differences in coke yield within the various regions present an enormous economic incentive for further research in this area.

Chapter 7 – Recommendations for Future Work

1. Coking experiments with vacuum residue alone at low pressure (240 kPa) and temperatures above 760 K is required to determine whether or not overheating of the feedstock is an important parameter in shot coke formation.

2. After determining the appropriate operating conditions that produce shot coke in the new apparatus, the impact of phase behaviour on coke structure should be evaluated.

3. From the experimental data and the coke yield tendency reported in Figure 5.18, the following systems are recommended for further evaluation:

    a. Comparison of ABVB 40 wt% and 45 wt% at 698 K and 3550 kPa.

    b. Comparison of ABVB 45 wt% and 50 - 60 wt% at 698 K and 6100 kPa.

    c. ABVB composition: 20 – 30 wt% at 698 K and Pressure: 800 – 2000 kPa.

    The evaluation of these systems will facilitate to determine differences that justify the cusps in coke yield. Detailed analysis of the liquid products is recommended: SARA (saturate, aromatic, resin and asphaltene), NMR (nuclear magnetic resonance), and HPLC (high performance liquid chromatography). Complimentary studies of these reacting systems using SAXS is also recommended as this technique allows one to determine the structure of asphaltenes prior to and during reaction by phase.

4. The new apparatus works adequately when processing mixtures of vacuum residues and n-dodecane; however, if it would be used to process vacuum residues alone and the flow rate is a key parameter in this evaluation, it requires the modification of the feed pump suction system. Modifications to this system must be designed; however. One option is to pressurize the feed vessel with an inert gas (nitrogen), to help the feedstock flow to the pump inlet.

5. The significant reduction in coke yield when ABVB is processed in mixtures with n-dodecane (ABVB content between 30 – 45 wt%), in comparison with typical delayed cokers, opens a line of inquiry for future research in this area. Some issues for future work include:

    a. The working pressure in the design and manufacture of equipment is critical. According to the results of this thesis, the lowest coke yields were achieved at 6100 kPa; however, the optimum minimum pressure (between 3550 an 6100 kPa) to reach the desired coke yield has not been determined.

    b. The evaluation of other solvents like heavier saturates, mixtures of different compounds and even the inclusion of aromatic compounds can improve the process (for example reduction in the working pressure, reduction in the solvent – residue ratio and reduction in the coke yield).

    c. A critical step in this development is the impact of the high severity conditions on the solvent used. Do we need a make up or the solvent has to be replaced completely?

    d. Evaluation of the impact on the quality of liquid products produced.

Nomenclature

Variables

CCR	Conradson carbon residue
Coke	Weight of coke (g) collected at the end of the experiment.
Cp	Heat capacity
CY	Coke yield. Petroleum residue mass balance
D	Diameter; D_I, outlet tubing diameter; D_e, external diameter; D_0, inside diameter
DY	Distillate yield. Petroleum residue mass balance
F	Number of degrees of freedom
f	pump discharge flow
FF	Fresh feed flow (MBD)
FV_1	Weight of the feed vessel (g) before the experiment starts
FV_2	Weight of the feed vessel (g) at the end of the experiment.
$F_{\nu1;\, \nu2;\, \alpha}$	Parameter from F-Tables
g	Acceleration due to gravity
G	Gibbs energy; Petroleum residue gas and losses; mass velocity
GCY	Coke yield. General mass balance
GDY	Distillate yield. General mass balance
GG	Gases and losses. General mass balance
GSY	H_2S yield. General mass balance
h	Heat transfer coefficient
HF	Heater flow (MBD)
H_R	Heat of reaction
k	thermal conductivity
Kw	Watson characterization factor
L	Length
LP	Weight of the liquid products (g) collected at the end of the experiment
LR	Weight of feedstock accumulated in lines before the reactor.
m	mass flow
MB	Mass balance
MW	Molecular weight
N	Number of components; number of data; number of observations
n	Number of moles
$nC_{12}V_1$	Weight of n-dodecane (g) added to the n-C_{12} vessel before starting the experiment.
$nC_{12}V_2$	Weight of n-dodecane (g) remaining in the n-C_{12} vessel after the experiment has finished.
p	number of estimated coefficients
P	Pressure; P_c, critical pressure; P_r, reduced pressure; P_α, confidence limit.
Q	Heat transferred

R	Independent chemical reactions
r	Number of runs in the number of runs; multiple correlation coefficient
RR	Recycle ratio
S	Pump stroke
SG	Specific gravity
SS_1	Weight of KOH solution (g) charged to the hydrogen sulphide scrubber before starting the experiment.
SS_2	Weight of material (g) in the hydrogen sulfide scrubber after the experiment has finished.
SY	H_2S yield. Petroleum residue mass balance
T	temperature; T_c, critical temperature; T_b, normal boiling point; T_r, reduced temperature; T_{c1}, cold temperature in; T_{c2}, cold temperature out; T_{h1}, hot temperature in; T_{h2}, hot temperature out
U	Overall heat transfer coefficient
V	Molar volume; V_c, critical molar volume
W_F	Total rate of vapor condensation
x	Mole fraction or liquid phase mole fraction
X	Weight fraction
Y	Statistical value; Y_c, measured; Y_{est}, estimated; $\hat{Y}_c$, average
α	level of significance
ΔH_f	Heat of formation
μ	Chemical potential; viscosity
π	Number of phases
λ	Latent heat of vaporization
ρ	Density
σ	Standard deviation
ω	Acentric factor

Subscripts

0	surface
b	bulk
boiling	Boiling
c	Critical
est	Estimated
i	Component i
j	Component j
l	Liquid
M	mixture
pc	Pseudo-critical
ss	Stainless steel
v	Vapor

Superscripts

π	π phase

Acronyms

ABVB	Athabasca Bitumen Vacuum Bottoms
ACT	Actual density
API	American Petroleum Institute
ASTM	American Standard for Testing and Materials
BP	Backpressure valve
CMG	Computer Modelling Group
D	Condensed asphaltenic phase
E	Experiment
FCC	Fluid Catalytic Cracking
Gz	Graetz number
HCGO	Heavy coker gas-oil
HGI	Hardgrove Grindability index
IS	Ideal Solution density
KERO	Kerosene
L	Liquid phase
L_1	Low density liquid phase
L_2	High density liquid phase
LCEP	Lower critical endpoint
LCGO	Light coker gas-oil
LCST	Lower critical solution temperature
LPG	Liquid petroleum gas
PDVSA	Petróleos de Venezuela, Sociedad Anónima.
Pr	Prandtl number
P-T	Pressure-temperature phase diagram (const. x)
P-T-x	Tri-dimensional diagram
P-x	Pressure-composition phase diagram (const. T)
Re	Reynolds number
S	Solid phase
SCF	Supercritical fluids
SEM	Scanning electron microscope
TBP	True boiling point
T-x	Temperature-composition phase diagram (const. P)
UCEP	Upper critical endpoint
UCST	Upper critical solution temperature
V	Vapor Phase
WI	Water inlet
WO	Water Outlet

References

Abedi S.J., Seyfaie S., and Shaw J. M, "Unusual retrograde condensation and asphaltene precipitation in a model heavy oil system", Petroleum Science and Technology 16(3&4) (1998): 209-226.

Ali, V., "Evaluación de aditivos desarrollados por el ICP como agentes reductores del rendimiento de coque en Coquificación Retardada", Technical report INT-4653. Caracas, Venezuela: Petróleos de Venezuela-Intevep, S.A. (1998).

Alwani, Z.; Schneider, G.; Ber. Bunsenges. Phys. Chem; 71 (1963) 78 – 84.

American Lewa®, "Modular Metering Pumps, Process Diaphragm Pumps, Metering and Blending Systems", Lewa® Operating Handbook, February 1998.

ASTM Standards: 1998 Annual Book, "Designation D409-97. Standard Test Method for Grindability of Coal by the Hardgrove-Machine Method", Section 5: Petroleum Products, Lubricants and Fossil Fuels. Volume 05.05: Gaseous, Coal and Coke, 180 - 187.

ASTM Standards: 1998 Annual Book, "Designation D4530-93. Standard Test Method for Determination of Carbon Residue (Micro Method)", Section 5: Petroleum Products, Lubricants and Fossil Fuels. Volume 05.02: Petroleum Products and Lubricants (II): D2597 – D4629, 919 – 923.

ASTM Standards: 1998 Annual Book, "Designation D5003-95. Standard Test Method for the Hardgrove Grindability Index (HGI) of Petroleum Coke", Section 5: Petroleum products, lubricants and Fossil Fuels. Volume 05.03: Petroleum Products and Lubricants (III): D-4636 – latest; catalyst, 268 - 269.

Benito, Ana M.; Callejas, Maria A.; and Martinez, Maria T., "Kinetics of asphaltene hydroconversion. 2. Catalytic hydrocracking of a coal residue", Fuel 76 no.10 (1997c): 907 - 911.

Bird, Biron; Stewart, Warren; and Lightfoot, Edwin, Transport Phenomena, New York: John Wiley & sons, 1960.

Brunner E., J. Chem. Thermodynamics, 17 (1985a) 671 – 679.

Brunner E., J. Chem. Thermodynamics, 17 (1985b) 985 – 994.

Butz, Thorsten; and Oelert, Hans-henning, "Application of petroleum asphaltenes in cracking under hydrogen", Fuel 74 (1995): 1671 – 1676.

Cabrera L., Guerrero J., and Ali V., "PCR-230 correlation model", PDVSA-Intevep, Internal communication, 1998.

Cabrera L., Sanoja L., and Ali V., "CCDCC correlation model", PDVSA-Intevep. Internal communication, 1997.

Cai, H.Y.; Shaw, J.M.; and Chung, K.H., "Hydrogen solubility measurements in heavy oil and bitumen cuts", Fuel, revised 01-21-2000, accepted 11-03-2000.

Callejas, Maria A.; Martinez, Maria T., "Hydroprocessing of a Maya residue. I. Intrinsic kinetics of asphaltene removal reactions"; Energy & Fuels 14 (2000a): 1304 - 1308.

Callejas, Maria A.; Martinez, Maria T., "Hydroprocessing of a Maya residue. II. Intrinsic kinetics of the asphaltenic heteroatom and metal removal reactions", Energy & Fuels 14 (2000b): 1309 - 1313.

Chen, Yu-Wen; and Tsai, Ming-Chang, "Hydrotreating of residue oil over aluminium borate – supported Co-Mo and Ni-Mo catalysts", Catalysis Today 50 (1999): 57 – 61.

Coker Discussion. Previous, "How to not make shot coke?", 07/07/1999. http://www.coking.com/disc1_frm.htm (18 Feb. 2001).

Core Lab Petroleum services, "SARA and Elemental Analysis for University of Toronto ABVB", File number: 52137-2001-8275, Feb - 01, 2002, Calgary.

Dew, Ki L.; Wang, Lai Y.; and Seon, Ihl W., "Hydrotreatment of an atmospheric residual oil over the dispersed cobalt and molybdenum catalysts in a carbon expanded-bed reactor", Fuel 75 (1996): 1186-1192.

Elliot, John D. "Shot coke: design and operation". http://www.fwc.com/publications/tech_papers/index.cfm. (20 Feb. 2001).

Ellis, Paul E.; Paul, Christofer A., "Tutorial: delayed coking fundamentals". In the AICHE Spring National Meeting, paper 29ª, New Orleans, LA, USA, (1998).

Ellis, Paul; and Bacha, John, "Shot coke", Light Metals. The Minerals, Metals & Materials Society (1996): 477 – 484.

Fraser, D.A.S., Probability & Statistics. Theory and Application, Toronto, University of Toronto; 1991.

Gray, M. R. "Tutorial on Upgrading of Oilsands Bitumen". http://www.ualberta.ca/~gray/~Library/Tutorials/Upgrading/ (28 March 2002).

Gray, M. R., Upgrading Petroleum Residues and Heavy Oils, New York, Marcel Dekker, Inc, 1994.

Gray, M. R.; Zhao, Y.; and McKnight, C., "Coke and minerals removal from bitumen hydroconversion catalysts", Fuel 79 (2000): 285 – 294.

Gregorowicz, J., de Loos, Th. W. and Swann Arons, "Unusual retrograde condensation in ternary hydrocarbon systems", Fluid Phase Equilibria, 73 (1992): 109 – 115.

Gregorowicz, J., de Loos, Th.W. and de Swaan Arons, J., "Liquid-liquid-vapor phase equilibria in the system ethane + propane + eicosane: retrograde behaviour of the heavy liquid phase", Fluid Phase Equilibria, in press.

Malik, Tarik, "Containment system for coke drums", U.S patent 6.039.844, 03-21-2000.

Marsh, H.; Calvert, C.; and Bacha, J., "Structure and formation of shot coke – a microscopy study", Journal of Materials and Science 20 (1985): 289 – 302.

Martinez, Maria T.; Benito, Ana M.; and Callejas Maria A., "Kinetics of asphaltene hydroconversion. 1. Thermal hydrocracking of a coal residue", Fuel 76 no. 10 (1997b): 899 - 905.

Martinez, Maria T.; Benito, Ana M.; and Callejas Maria A., "Thermal cracking of coal residues: Kinetics of asphaltene decomposition", Fuel, 76, no. 9, (1997a): 871 - 877.

Mc Hugh, M.; Krukonis, V., Supercritical Fluid Extraction, Toronto, Butterworth – Heinemann, , 1993.

McGrath, Michael J and Houde, Edward, "Upgrading options for processing heavy crudes". Prepared for Presentation at AIChE Spring Meeting 14-18 March 1999. http://www.fwc.com/publications/tech_papers/index.cfm. (20 Feb. 2001).

Menéndez, R.; Granda, M.; and Bermejo, J., "Relationship between pitch composition and optical texture of cokes", Carbon 35 no. 4 (1997): 555 – 562.

Mirzayeva, L. M.; Akhiverdiyev, E. T.; and Alilev, A. D. et al, "Coke formation during the catalytic cracking of residual oil by oxide catalysts based on activated aluminium alloys", Petroleum Chemistry 4 (1995): 341 – 346.

Montgomery, Douglas C., Design and Analysis of Experiments, New York: John Wiley & sons, 1996.

Morín, J. C., Caracterización e Identificación de Residuos de Vacío y Muestras de Coque, Petróleos de Venezuela, S.A (PDVSA) Intevep, 2002.

Nuñez, Manuel; Pachon, Zarith; Kaparov, Viatcheslav; and Resasco, Daniel, "Deactivation of Ni-Mo / Al2O3 catalyst aged in a commercial reactor during the hydrotreating of de-asphalted vacuum residuum", Applied Catalyst A: General 199 (2000): 263 – 273.

Parker, R. J.; Hawkins, R. W.; D'agnone, K., "Coking of Athabasca bitumen in a laboratory coker", AIChE Interbational Conference on Refinery Processing, New Orleans, LA, USA, 2002.

Perry, Robert H.; Green, Don W.; and Maloney, James O. (Eds.). (1999). Perry's Chemical Engineers' Handbook Seventh Edition. U.S.A.: McGraw – Hill.

Petróleos de Venezuela, S.A (PDVSA) Intevep, Taller de Coquificación Retardada, December 1999.

Petróleos de Venezuela, S.A (PDVSA) Manufacturing & Marketing, Clasificación de crudos, March 2000.

Rahimi, P.; Gentzis, T.; Dawson, W. H.; Fairbridge, C.; Khulbe, C.; Chung, K.; Nowlan, V.; and DelBianco, A.; "Investigation of coking propensity of narrow cut fractions for Athabasca bitumen using hot-stage microscopy", Energy & Fuels 12, 1998: 1020 – 1030.

Rahimi, Parvis; Gentzis, Thomas; Kubo, Junichi; Fairbridge, Craig; and Khulbe, Chandra, "Coking propensity of Athabasca bitumen vacuum bottoms in the presence of H-donors – formation and dissolution of mesophase from a hydrotreated petroleum stream (H-donor)", Fuel Processing Technology 60 (1999): 157 – 170.

Rodríguez-Reinoso, F.; Santana, P.; Romero, E.; Diez, M. A.; and Marsh H., "Delayed coking: industrial and laboratory aspects", Carbon 36 no. 1 (1998): 105 –116.

Scott, R. L., van Konynenburg, P. H., "Critical lines and phase equilibria in binary van der Waals mixtures", Philos. Trans. R. Soc. London, 298, 495-540, (1980).

Shaw, J. M., de Loos, Th. W., and de Swaan Arons, J., "Prediction of unusual retrograde condensation in model reservoir fluids", Fluid Phase Equilibria, 84(1993), 251-266.

Shaw, J. M., de Loos, Th. W., de Swaan Arons, J., "An explanation for solid? Liquid? Liquid? Vapor phase behaviour in reservoir fluids", Petroleum Science and Technology 15(5&6) (1997) 503-521.

Speight J.G., Petroleum chemistry and refining, Wyoming, USA, Taylor & Francis, 1998.

Velutini, G.; Guerrero, J., "Homologación de la unidad de coquificación retardada de Amuay (CRAY) en la planta piloto PCR-230", Technical report. Caracas, Venezuela: Petróleos de Venezuela-Intevep, S.A. 1996.

Weinreb, Glen; McCabe, Etephen, InstruNet® User Manual. Manual Version 1.30.8, Omega Technology Company, 1996 – 1998.

Weissman, Jeffrey G., "Review of processes for down-hole of catalytic upgrading of heavy crude oil", Fuel Processing Technology 50 (1997):199 – 213.

Wiehe, Irwin A., "A phase-separation kinetic model for coke formation", Ind. Eng. Chem. Res., 32 (1993): 2447-2454.

Yang, Ming-Gang; Nakamura, Ikusei; and Fujimoto, Kaoru, "Hydro-thermal cracking of heavy oils and its model compounds", Catalysis Today 43 (1998): 273 - 280.

Zou X.Y., "Selective removal of inorganic fine solids, heavy metals and sulphur from heavy oils/bitumen", PhD diss., University of Toronto, 2002. (In Progress).

Appendix A: Product Yields and Properties

One of the objectives of this thesis is to setup the laboratory apparatus to carry out the experiments required to study the effect of phase behaviour on the structure of the coke formed. The setup of this apparatus is accomplished in three steps: first, the design and specification of main equipment; second, the assembly of these equipment to make the final apparatus; and finally, the development of the appropriate procedures. To accomplish the first step, the calculations of the flows and properties of the different streams and products are required to complete general and specific mass and heat balances. These calculations are not straightforward because the processing of petroleum fractions at temperatures above 623 K (350 ºC) causes both cracking and condensation reactions; for this reason, the use of a predictor model is required. For the purpose of this thesis, the most adequate predictor model is one related to the delayed coking technology. Therefore, this appendix presents the results obtained with delayed coking models.

Although the laboratory unit is used to process mixtures of heavy oil vacuum residues and n-C_{12}, the basic calculations were done assuming that the unit processes vacuum residue alone. The three main reasons that support this consideration are; first, shot coke is formed when vacuum residues are processed alone; second, the mathematical models used to estimate product yields are based on vacuum residue properties, so dilution of these feedstocks with n-Dodecane places the feedstock properties values out of the application range; and third, at low pressure the solvent flashes on entry leaving only vacuum residue.

Two delayed coking models developed by PDVSA-Intevep (Cabrera, Sanoja, & Ali, 1997; Cabrera, Guerrero, & Ali, 1998) were used in this thesis. These two models are: CCDCC and PCR-230. The CCDCC model was used to generate the detailed data required to design the unit. On the other hand, the general model (PCR-230) was used to crosscheck the design values.

The input parameters for each model are shown in Table A-1. The feedstock properties are those for ABVB in Table 3.1. The CCDCC model was developed with operational data from a commercial delayed coking unit using the heater outlet temperature (higher than the coker top temperature by 50 – 70 K) and the pressure at the top of the cokers as operational variables.

Table A-1: Input parameters in the delayed coking models: Ranges of application and values

	CCDCC		PCR-230	
FEEDSTOCK	Range	Value	Range	Value
API	4.0 – 9.0	3.51	0.78 – 9.9	3.51
CCR (wt%)	20.0 – 27.0	21.4	14.5 – 32.0	21.4
Sulphur (wt%)	2.3 – 7.0	6.87	---	---
Nitrogen (ppmw)	4500 – 9650		---	---
REACTION				
Pressure (kPa)	210 – 280* 270 – 340	240*	204 – 377	240
Temperature (K)	695 – 701* 760 – 766	698*	693 – 760	698
Recycle Ratio	1.04 – 1.10	1.07	---	---
FRACTIONATION				
Kero draw plate temperature (K)	466 – 489	476	---	---
LCGO draw plate temperature (K)	522 – 544	530	---	---
HCGO draw plate temperature (K)	616 – 638	626	---	---

*Effective equivalent condition.

So regarding temperature, the heater outlet temperature is measured before the feed is introduced into the cokers. The vaporization and cracking reactions that take place in the coker consume energy and drop the coker internal temperature. In the CCDCC model a heater outlet temperature of 763 K corresponds to 698 K inside the coker.

As for pressure, the commercial units present more variation than systems like pilot plants or laboratory units. These variations are related to operational procedures (for example steam stripping and cokers switching). Also, the accumulation of coke in the outlet lines, in commercial delayed coking units, affects the pressure readings. Thus, 300 kPa for the CCDCC model is equivalent to 240 kPa in the PCR-230 model.

On the other hand, the PCR-230 model was developed with experimental data from a delayed coking pilot plant. In this case, the reaction temperature was set to the required temperature in the new apparatus and the reaction pressure, although the unit will be designed to run at pressures as high as 6100 kPa, was set to 240 kPa because this is the typical pressure in delayed coking units.

Table A-2 shows product yields calculated with the two Delayed Coking models property of PDVSA-Intevep. According to these results, the gas yield for the PCR-230 model is noticeably lower than the gas yield from the CCDCC model (7.62 vs. 8.93). The reason for this difference is because the PCR-230 model does not estimate the hydrogen sulphide content in the gaseous stream. This difference is reflected in the yields of C_1 – C_2, distillate and coke. In spite of this, the results obtained with both models are similar.

Table A-2: Product yields (wt%) calculated with the delayed coking models at the reference condition.

	CCDCC	PCR-230
$C_1 - C_2$	3.98	4.45
LPG	3.83	3.17
H_2S	1.12	---
Total Gas	8.93	7.62
Distillates	59.72	59.87
Coke	31.35	32.51

Table A-3 shows the yields and properties of gaseous and liquid products generated with the CCDCC model. Individual component properties, like MW, critical properties (T_c, V_c and P_c) and the acentric factor (w), were obtained from the Chemical Engineers' Handbook (Perry et al., 1999); on the other hand, for the liquid products (gasoline, naphtha, LCGO and HCGO), that represent complex mixtures of hydrocarbons, the MW

T_c, V_c and P_c were calculated with the correlations of Twu and the acentric factors (w) were calculated with the equation of Edmister (Gray, 1994).

Table A-3: Detailed information about products yields and properties

	Mass (wt%)	MW	T_c (K)	V_c (m^3/kmol)	P_c (kPa)	Kw	w
H_2	0.04	2	33	0.0640	1320.0		-0.2150
H_2S	1.12	34.08	374	0.0990	9000.0		0.0960
CO_2	0.03	44.01	304	0.0950	7390.0		0.2240
CO	0.04	28.01	133	0.0950	3490.0		0.0480
C_1	1.77	16.04	191	0.0990	4590.0		0.0110
C_2	1.84	30.07	305	0.1460	4850.0		0.0980
C_2=	0.18	28.05	282	0.1320	5030.0		0.0860
C_3	1.44	44.09	370	0.2000	4210.0		0.1490
C_3=	0.46	42.08	366	0.1880	4630.0		0.1370
NC_4	0.92	58.12	425	0.2550	3770.0		0.1970
IC_4	0.30	58.12	425	0.2550	3770.0		0.1970
C_4=	0.71	56.1	420	0.2410	4040.0		0.1900
NC_5	0.02	72.15	470	0.3150	3360.0		0.2510
IC_5	0.06	72.15	470	0.3150	3360.0		0.2510
GASOLINE	3.24	85	503	0.3618	3074.2	12.79	0.2964
NAPHTHA	8.17	115.2	588	0.4553	2764.0	11.863	0.3369
KERO	12.56	181.3	713	0.6986	2049.9	11.648	0.5083
LCGO	10.67	242.7	798	0.9106	1672.9	11.589	0.6602
HCGO	25.08	327.5	896	1.1352	1411.0	11.439	0.8486
COQUE	31.35						
	Gasoline	Naphtha	Kero	LCGO	HCGO		
SG	0.662095	0.757007	0.839618	0.888954	0.948002		
TBP (K)							
0	310	336	388	438	512		
10	320	372	480	574	640		
20	325	374	501	602	701		
30	330	386	512	610	716		
50	341	410	535	627	746		

70	352	433	554	646	786		
80	357	444	563	655	806		
90	363	455	577	679	839		
100	384	489	605	734	931		
Boiling point (K)	**337**	**402**	**519**	**607**	**708**		

The data included in Table A-3 were used to complete the design of main equipment that comprise the apparatus. The equipment and design calculations are presented in appendixes B, C and D.

Appendix B: Laboratory Unit Design

This section presents a description of main equipment starting with the electric furnace, which is an existing equipment used to keep the reaction temperature during each experiment and its internal dimensions defined the coker size; next, the coker structure and final dimensions, and finally, the design mass balance. Once the design mass balance was fixed, the rest of equipment could be specified; therefore, following the mass balance, the feed tank, the feed pump, the heat exchanger, the gas-liquid separator and the H_2S scrubber are described and specified.

Electric Furnace:

Figure B-1 includes two pictures of the electric furnace showing a general view of this equipment with the main sections (picture A), and a close-up of the heating camera with the tubing to connect the coker (picture B).

Figure B-1: Pictures showing the electric furnace. A: general view. B: detail of the heating camera with the tubing to connect the coker.

In this equipment can be identified two sections. First, the heating camera that corresponds to the free space in the furnace where the object to be heated is placed; and second, the temperature control console that can be identified in Figure B-1-A as a small black box attached laterally to the furnace.

The heating camera dimensions are 0.41 m in height, 0.375 m in depth, 0.41 m in width. Inside the heating camera the following parts can be observed (figure B-1-B):

1. Electric resistance: a coiled metallic wire located on the bottom of the camera and supported with three ceramic pieces. It is used to supply the energy required to reach the desired internal temperature.

2. Metallic screen: protective piece located above the electric resistance. It separates such heating device from falling objects when placing in to heat them or to complete maintenance works. It also protects the heated objects from being exposed to high temperatures due to direct contact.

3. Thermocouple: instrument located above the metallic screen and extended from the wall where the temperature control console is attached. This thermocouple senses the internal temperature in the camera and gives the reference value for the action of the temperature control system.

4. Fins: extended surfaces on the lateral walls of the furnace. Each wall has five (5) fins; each fin is 0.0254 m depth. The function of these extended surfaces is increase the internal surface area available on the walls to increase the heat transferred from the wall to the heated body.

The heating camera has three holes on the upper wall. One hole, located on the centre of this wall, is typically used to pass through a lamp wire connection; and the other two orifices, with 0.038 m internal diameters and equidistant from the centred hole, are used in this equipment to allow hot air to escape the heating camera and avoid overpressure.

Regarding the set up of the experimental apparatus, the centre hole is used to pass through the coker thermocouple; likewise, the lateral holes are used to pass through the tubing to connect the pump discharge to the coker, the coker pressure transducer and the coker outlet to the condenser. These tubing are shown in Figure B-1-B. The tubing located on the left side is used to connect the pump discharge to the coker (lower tubing) and the pressure transducer (upper tubing); meanwhile, the tubing in the right side is used to connect the coker outlet to the light product condenser.

The temperature control console, located in the small black box, has a display to show the internal temperature of the heating camera. Also, this display shows the temperature control set point value when the adjusting set point buttons, located below the display, are manipulated.

Coker:

The internal dimensions of the furnace heating camera and the available commercial tubing and fittings determined the selection of the final dimensions of the coker. Moreover, the coker internal diameter has to be the largest possible for the easy removal of the coke formed. The available furnace internal dimensions are 0.41 m in height and 0.359 m in width approximately (the last dimension considers the presence of internal fins in the horizontal walls). Thus, the available commercial Swagelok tubing and fittings are 0.0381 m in outside diameter (1.5 inches in outside diameter).

The coker was designed and built with stainless steel Swagelok tubing and fittings in two versions: lateral inlet and bottom inlet.

For the lateral inlet version (see figure B-2), once the feedstock goes into the coker, separation of light and heavy components originally present in the feedstock or formed due to the beginning of cracking reactions occurs. The light components leave the coker through the top. The heavy components go to the bottom of the coker and never contact new components going into the coker. The heavy components in the bottom of the coker crack and condense to produce gas, distillates and coke. The vaporized products leave the coker through the top and the coke is accumulated in the bottom.

The longest coker dimensions are 0.306 m in width and 0.3902 m in height. Thus, it can be fixed inside the furnace. In this design, the distance between the bottom of the coker and the feed inlet port is 0.14 m approximately.

For the bottom inlet version (Figure B-3), the heavy components are accumulated in the bottom of the coker and they are always exposed to the new light and heavy components entering in the coker. Likewise, the light components leave the rector through the top and the heavy components remain reacting to produce gas, distillates and coke.

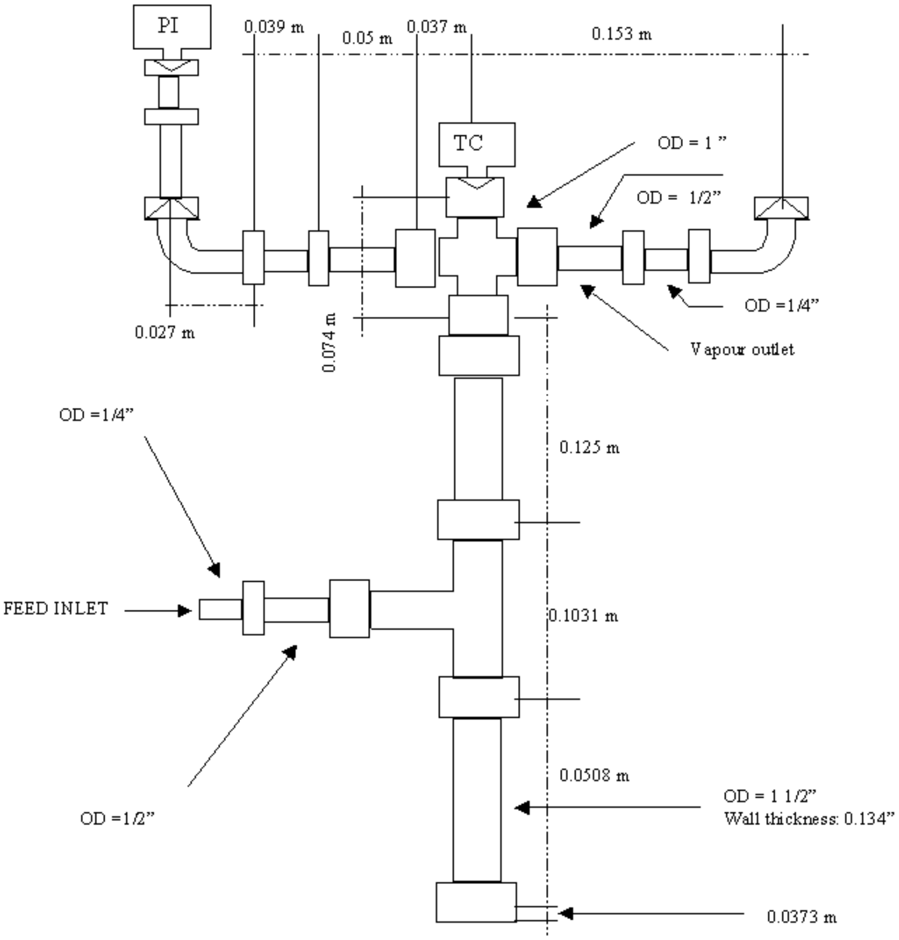

Figure B-2: Drawing of the coker lateral inlet version showing approximate dimensions.

According to the data shown in Figure B-3, the dimensions of the coker bottom inlet version do not differ considerably from those of the coker lateral inlet version.

The bottom inlet version resembles the coker in the delayed coking technology, where the feedstock inlet is on the bottom and the accumulated material is always exposed to the feed going into the coker. However, the coker used to carry out the experimental matrix was the lateral inlet version because least perturbation of the coking material by incoming feedstock is likely to happen in this model; therefore, more importance is associated to operating conditions (pressure and temperature) than to vapor velocity in the coke formation process.

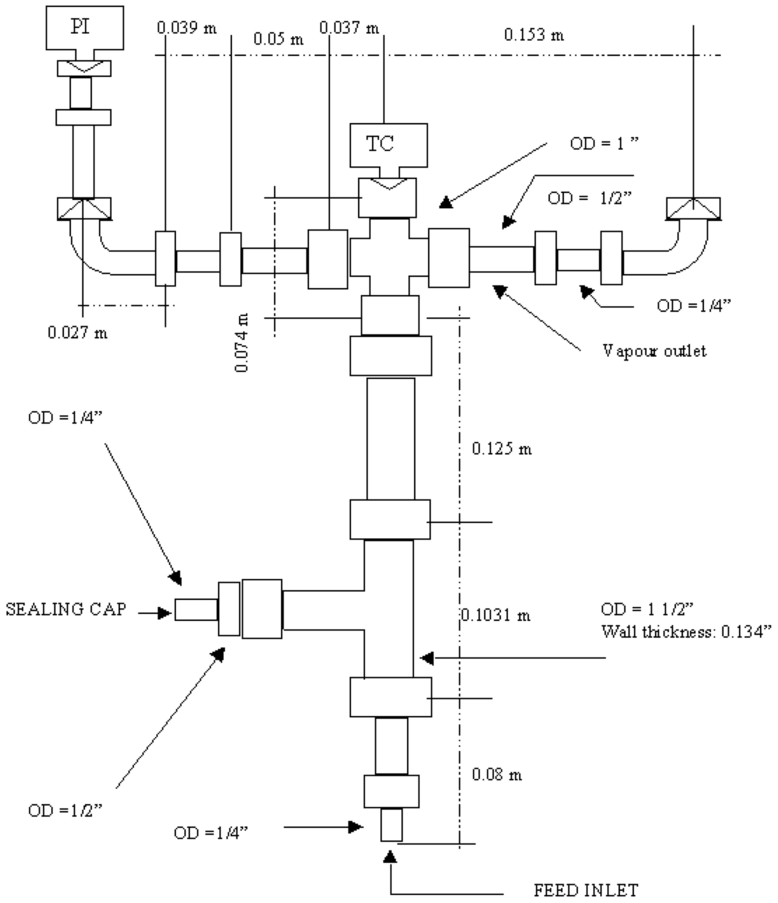

Figure B-3: Drawing of the coker bottom inlet version showing approximate dimensions.

In these two versions, Swagelok tubing and fittings were used to make these units. Although different fittings from Swagelok or any other company could be used to make these cokers, the identification of the different fittings used in this work would save time if a fitting has to be replaced. Therefore, the description and identification of these tubing and fittings are included.

Figure B-4 shows a picture of the lateral inlet version coker installed in the heating camera. In the picture, the different parts of the coker are identified with a number that corresponds to the item number in Table B-1.

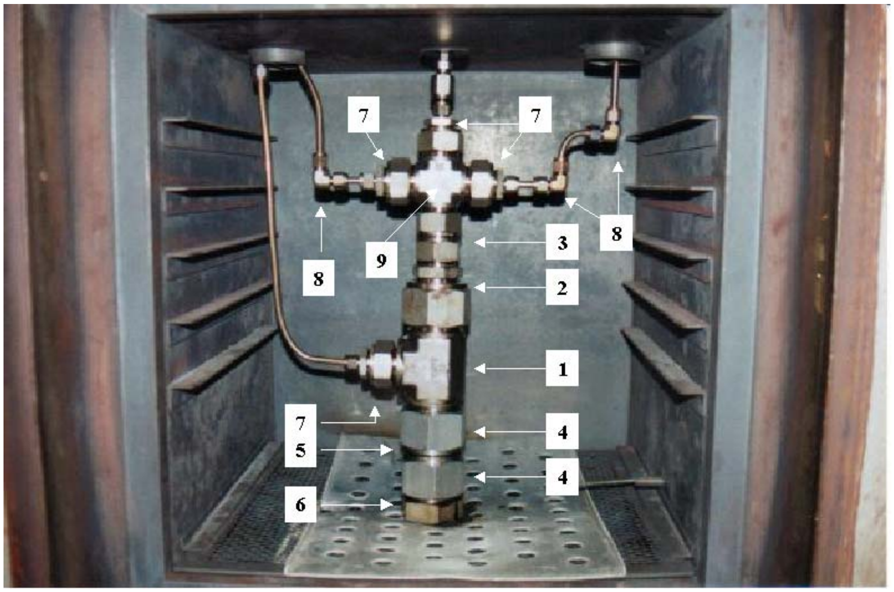

Figure B-4: Lateral inlet version coker.

Figure B-5 shows a picture of the bottom inlet version coker installed in the furnace. In this case, the numbers identify the fittings changed in the lateral inlet version to set up the bottom inlet version. These changes include substituting the 1.5 inches stainless steel tubing on the bottom for two reductions and plugging the lateral inlet connection. Likewise, these fittings are identified in Table B-1.

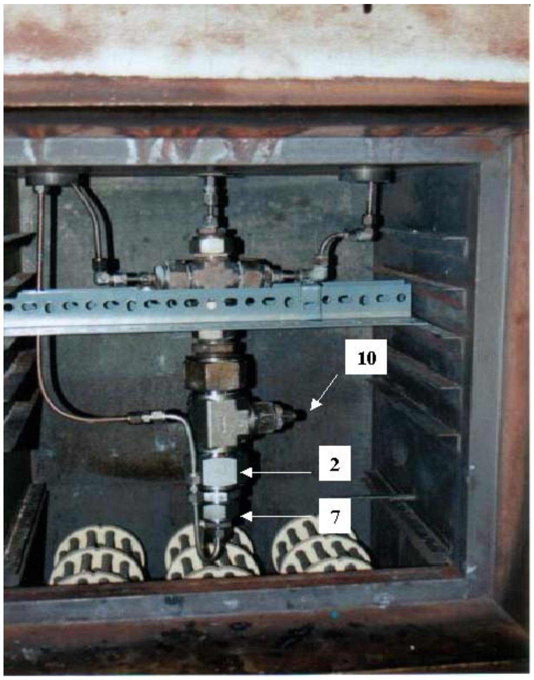

Figure B-5: Bottom inlet version coker.

Table B-1 contains the basic ordering numbers and the descriptions for tubing and fittings used to set up the coker in both versions. The codes and descriptions included in this table are the same as used by Swagelok to identify these pieces. The item number column was included to relate such information with Figures B-4 and B-5.

Table B-1: Swagelok identification of tubing and fittings for Coker set up.

Item number	Basic Ordering Number	Description
1	SS-2400-3-24-16	Reducing union tee. Connects fractional tubes 1” x 1 ½” x 1 ½”.
2	SS-1610-R-24	Reducer. Connects fractional tube to fractional swagelok port 1” x 1 ½”.
3	SS-1611-PC	Port connector. Connects two fractional swagelok ports 1” x 1”.
4	SS-2402-1 SS-2403-1 SS-2404-1	Nut 1 ½” (6). Front ferrule 1 ½” (6). Back ferrule 1 ½” (6).
5	T-24W-134	1 ½” OD tubing.
6	SS-2400-C	Cap ends of fractional tube 1 ½”.
7	SS-400-R-16	Reducer. Connects fractional tube to fractional swagelok port 1” x ¼”.
8	SS-400-9	Union elbow. Connects fractional tubes ¼” x ¼”.
9	SS-1610-4	Union cross. Connects fractional tubes 1”.
10	SS-400-P	Plug ends of fractional swagelok port ¼”.

Mass Balance:

After selecting the final coker’s dimensions, the feedstock flow was fixed to ensure a vapor velocity inside the coker between the range indicated in the Operating Conditions and in the Design Premises (0.015 – 0.018 m/s) sections.

Table B-2 shows the main parameters associated to the unit mass balance. The molecular weight for vapor coming out of the coker was calculated from the data reported in Table A-2. The vapor velocity is 0,01606 m/s with the feedstock flow set point in 5 g/min. The pumping time is 45 minutes and the total amount of sample per test is 0.225 kg. During these experiments H_2S is formed in the system. Thus, provisions must be taken to prevent this compound from being vented to the atmosphere.

Table B-2: Variables for laboratory plant equipment specification.

Coker O.D (inch)	1.5		
Coker wall thickness (inch)	0.134		
Vapor velocity (m/s)	**0.01606**		
Pressure (kPa)	138		
Temperature (K)	797		
Coke density (Kg/m^3)	876.5		
Vapor MW	112.3		
Vapor vol. Flow (m^3/s)	1.235e-5		
Vapor mol flow (mol/min)	0.031		
Vapor mass flow (g/min)	3.43		
Total feed flow (g/min)	5.00		
Total time (min)	45		
Total sample (kg)	0.225		
	(g/min)	Total (g)	
H_2S	0.0558	2.51	
	(L/min)	Total (g)	Litres
Gas @ 101 kPa, 293 K	0.336	17.58	13.45
	(g/min)	Total (g)	
Distillates	2.984	134.27	
Coke		70.48	
Coke volume (cm^3)	8.041e-5		

Feed Vessel:

Figure B-6 shows a drawing of the feedstock storage vessel. It is a stainless steel cylindrical container with 0.089 m internal diameter and 0.085 m in height. The total volume capacity is approximately 0.52 L, which is enough to store the total feedstock sample of 0.225 kg. It is equipped with an aluminium lid to protect the feedstock from contaminants. This vessel works at atmospheric pressure and the feedstock is discharged through a 0.00635 m (1/4 inch) diameter orifice located in the bottom.

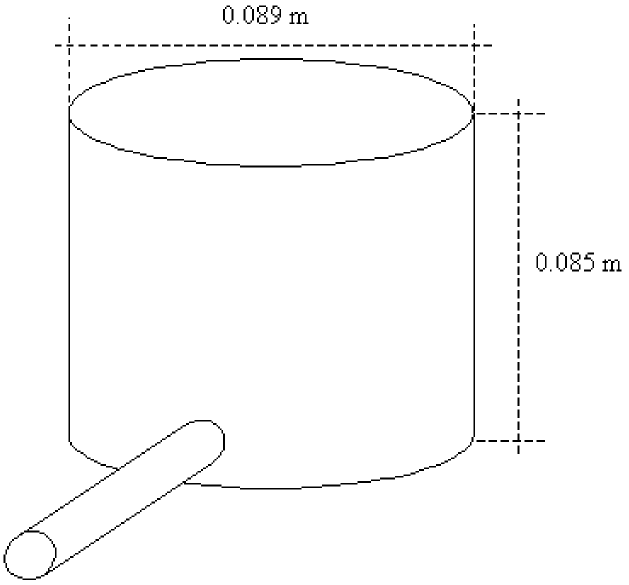

Figure B-6: Feedstock vessel draw showing main dimensions.

Furthermore, the feed vessel has a magnetic stirrer that is 0.027 m in length. It is used to mix the components in the feedstock (residue and n-C_{12}) before the experiment is started.

Pump:

Figure B-7 shows a drawing of the feed pump. This unit is a positive displacement pump that produces a volumetric flow when a stroke volume, determined by the plunger area and the stroke length, is periodically displaced. In this pump three main sections can be identified: the driver, the drive element, and the pump head.

The driver is a 0.33 hp electric motor that works at 3450 RPM and 150 V. It supplies the required power to raise the fluid conveyed from suction to discharge pressure. This motor is equipped with a switch that turns the unit “ON” and “OFF”.

The pump drive element converts the rotation of the electric motor into an oscillating movement. The hand wheel is used to change the stroke length. It has a scale indicating the stroke length variation ranging from 0 to 10 mm with 0.1 mm precision. It can be manipulated with the pump running or stopped; moreover, clockwise rotation reduces the stroke length.

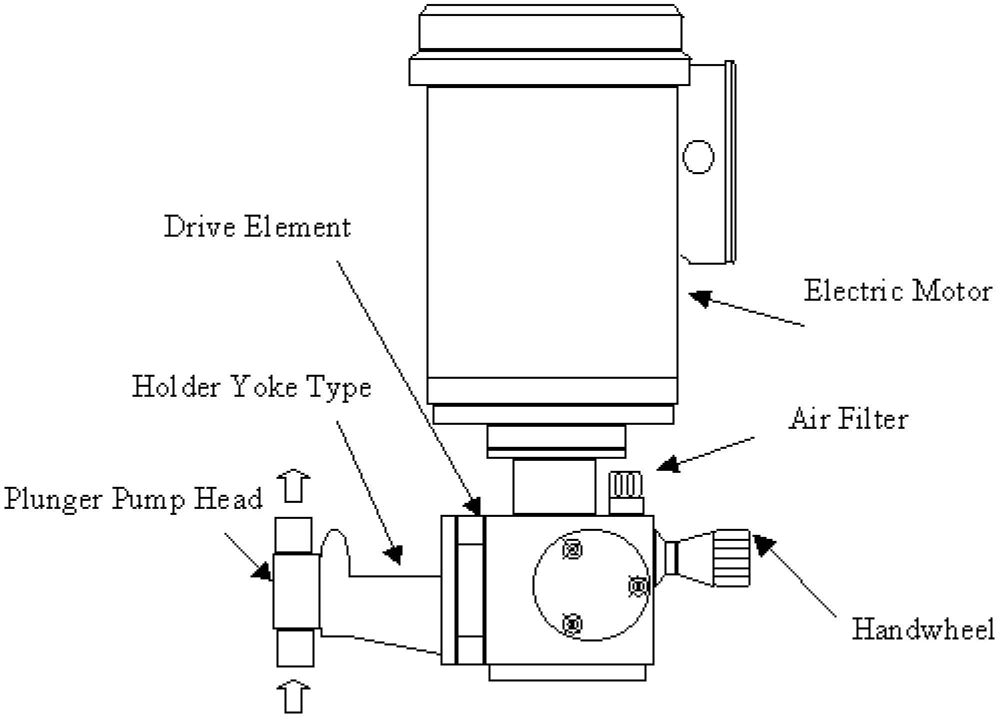

Figure B-7: Diagram of the feed pump indicating main parts.

The pump head is the section of the pump where the transported fluid is handled. This particular unit is designed as plunger pump head. The plunger pump head is attached to the drive element via a Yoke type pump head holder that completely separates the drive element lubricant from the pumped fluid. The direction of flow is from bottom to top. The suction and delivery pipes have check ball valves that prevent backflow and improper delivery.

Table B-3 shows the process design data. The technical data sheet of this pump and detailed information about safety, installation, operation, servicing maintenance and spare parts can be found in the Operating Manual (American Lewa, 1998).

Table B-3: Feed pump process design data

Fluid temperature (K) min/max	423.15 / 473.15
Specific gravity (Kg/m^3)	1040
Viscosity (cP) min / max	16 / 616
Discharge Operating pressure (kPa) min / max	137.95 / 6207.79
Suction operating pressure (kPa)	Flooded

As mentioned before, the feed flow of vacuum residue is kept at 5 g/min; therefore, previous to the development of the experimental matrix, the calibration of the feed pump was carried out. Detailed information of such calibration procedure is shown in Appendix C. It is worth mentioning that the feed pump is a reciprocating unit that handles a fixed volumetric flow as function of the stroke length and the mass flow is a function of the fluid gravity at the operating temperature. Moreover, the vacuum residue gravity at the specified design operating temperature is around 1000 Kg/m^3. Consequently, the feeding flow during these experiments is 5 mL/min.

The following mathematical model is the result of the calibration procedure. This equation is used to predict the pumping flow as a function of the stroke length and the discharge pressure.

$$f = -0.36465119 + 1.34938111 * S - 0.0011065 * P \tag{B.1}$$

Where:

f: flow (mL/min).

S: pump stroke (mm).

P: pump discharge pressure (psig).

Coker Effluents Condenser:

The coker's effluent will be vapor hydrocarbons at elevated temperature (around 673 K) that should be cooled to condense the heavy fractions (fraction C_5^+) and facilitate their separation from the incondensable. To accomplish this step, a counterflow shell and tube heat exchanger with water at 293 K as the cooling fluid is used. The criteria, procedure and correlations used to design this equipment are presented in appendix D.

Figure B-8 shows a drawing of the coker effluent condenser indicating process temperatures for both the hydrocarbon and cooling water streams and the dimensions of this equipment. The tubing used for both the shell and tube sides of this device are stainless steel 316.

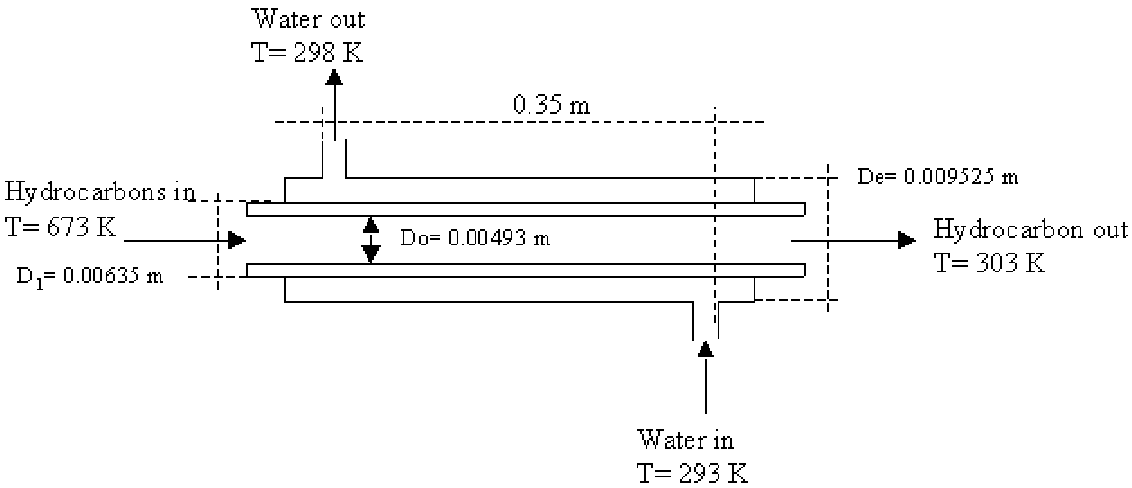

Figure B-8: Hydrocarbon condenser schematic showing main dimensions and streams temperatures.

H_2S Scrubber:

The thermal processing of bitumen causes the production of hydrogen sulphide. This compound will evolve as part of the gas stream and its release into the atmosphere can generate hazardous situations. For this reason, the gas stream is scrubbed with a saturated KOH solution previous to being discharged into the atmosphere.

Table B-4: Heats of Formation, ΔH_f in Kcal/mole @ 298 K

$H_2S_{(g)}$	-19.96
$KOH_{(aq)}$	-480.99
$K_2S_{(aq)}$	-463.38
$H_2O_{(l)}$	-285.85

The reaction that takes place in the scrubber is:

$$H_2S_{(g)} + 2KOH_{(aq)} \rightarrow K_2S_{(aq)} + 2H_2O_{(l)} \tag{B.2}$$

Table B-4 shows the heat of formation for these substances at 298 K (Perry et al., 1999) and the heat of reaction ($\mathrm{H_R}$), calculated in equation 3.3, indicates that this reaction is exothermic.

$$H_R = -(-19.96 + 2 \times (-480.99)) + (-463.38 + 2 \times (-285.85)) = -53.14 kJ/mole \tag{B.3}$$

According to the design data, the total amount of H_2S produced is 2.51 g (see Table B-2) and based on the reaction that takes place in the scrubber (equation B.2), the minimum amount of KOH required is 8.27 g. The KOH concentration in the solution used in these experiments is 20 wt% and the minimum amount of such solution per test (to ensure enough KOH in the system to neutralize the H_2S produced) is 41.36 g.

Appendix C: Feed Pump Calibration

As mentioned in chapter 3, the feed flow was fixed at 5.0 mL/min; consequently, the feed pump was calibrated before the experiments. The product of this calibration process is a model, developed using the Least Square method (Montgomery, 1996), to predict the adjustment required in the pump stroke to obtain the required flow at the apparatus's working pressure. The system used to complete this calibration; the data analysis and the final model along with its validation are presented in this section.

System:

The system is based on volume measurements of the pump discharge. The schematic, Figure C-1, shows that the pump suction was connected to the feed tank and the discharge was lined up to a graduated cylinder with two valves before the cylinder to increase the pump discharge pressure up to the desired values.

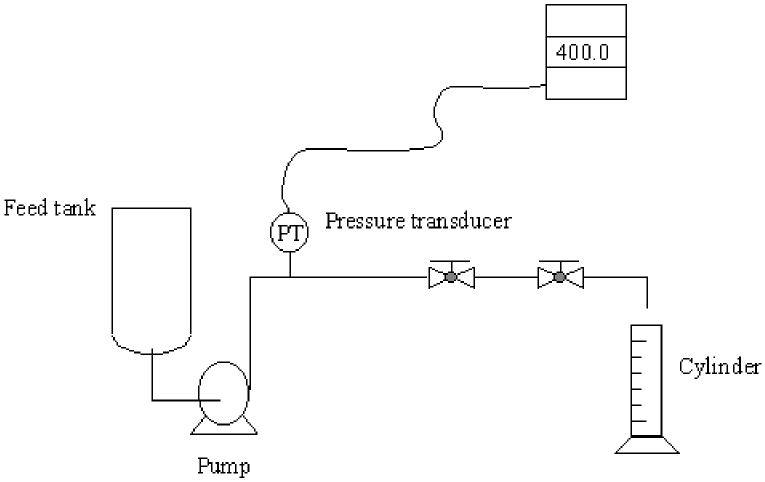

Figure C-1: Schematic representing the system used to calibrate the feed pump.

Hydrocarbon oil, with the properties indicated in Table C-1, was used to perform the calibration.

According to the pump design data sheet, to avoid damage to seals and internal parts, the operating temperature must be below 473 K. For this reason, the pumping temperature for the vacuum residue during the experimental evaluation was set at 433 K. At this temperature, the vacuum residue viscosity is expected to be around 270 cP. Thus, the calibration test was carried out at a temperature between 303 and 313 K, with the hydrocarbon oil viscosity between 285 and 220 cP.

Table C-1: Properties of the hydrocarbon oil used to calibrate the feed pump.

Flash Point (K)	486
Fire Point (K)	517
Viscosity @ 310 K (cP)	248
Viscosity @ 327 K (cP)	151
Viscosity @ 373 K (cP)	51

Data Acquisition and Analysis:

Table C-2 shows the measurements taken during the pump calibration tests. The minimum and maximum values for the pump stroke are 3.0 mm and 8.0 mm; for the pump discharge pressure, these values are 43 psi and 949 psi.

Table C-2: Data measured during the pump calibration process.

Meas. ID	Stroke (mm)	P. Average (psig)	Time (min:s)	Volume (cc)	Flow (cc/min)	Flow sequence
1	5.0	350	2:34	13.0	5.06	-
2	5.0	800	2:04	10.0	4.84	-
3	4.5	45	2:22	13.6	5.75	-
4	4.5	100	3:11	18.0	5.65	-
5	4.0	89	3:25	17.2	5.03	-
6	4.0	204	3:47	19.2	5.07	-
7	4.5	304	2:33	14.2	5.57	-
8	5.0	425	2:40	16.0	6.00	-
9	5.5	213	2:27	17.0	6.94	-
10	5.5	52	2:23	17.0	7.13	+
11	6.0	51	2:19	17.4	7.51	+
12	6.0	100	2:17	17.4	7.62	+
13	6.0	200	2:19	17.4	7.51	+

14	6.0	800	2:18	17.4	7.57	+
15	6.0	100	2:20	17.2	7.37	+
16	6.0	855	2:18	15.4	6.70	-
17	5.0	740	2:59	16.2	5.43	-
18	5.0	800	3:01	16.4	5.44	-
19	5.0	50	2:27	15.8	6.45	-
20	5.0	50	2:30	15.8	6.32	-
21	5.5	52	2:24	17.0	7.08	+
22	5.5	82	2:28	17.2	6.97	-
23	5.5	100	2:28	17.2	6.97	-
24	5.5	125	2:30	17.4	6.96	-
25	4.5	108	3:10	17.8	5.62	-
26	4.5	253	3:11	17.2	5.40	-
27	4.5	310	3:12	17.2	5.38	-
28	4.5	575	3:14	16.2	5.01	-
29	5.5	223	2:27	17.0	6.94	-
30	5.5	180	2:29	17.0	6.85	-
31	7.0	240	2:13	19.4	8.75	+
32	4.0	130	3:37	17.2	4.76	-
33	4.0	625	3:49	16.0	4.19	-
34	6.5	613	2:18	17.4	7.57	+
35	6.5	282	2:23	19.4	8.14	+
36	8.0	885	1:51	17.2	9.30	+
37	3.5	529	3:55	14.2	3.63	-
38	3.5	183	3:55	15.4	3.93	-
39	7.0	410	2:02	17.8	8.75	+
40	7.0	748	2:02	16.8	8.26	+
41	3.5	520	3:55	14.4	3.68	-
42	4.0	695	3:37	15.0	4.15	-
43	4.5	930	3:13	14.8	4.60	-
44	6.0	700	2:44	18.4	6.73	-

45	6.5	893	2:32	19.4	7.66	+
46	7.0	455	2:03	17.4	8.49	+
47	7.5	102	2:01	18.4	9.12	+
48	8.0	600	2:00	19.4	9.70	+
49	8.0	290	1:47	18.2	10.21	+
50	6.5	280	2:13	18.0	8.12	+
51	3.5	128	3:57	16.8	4.25	-
52	4.0	750	3:45	15.0	4.00	-
53	7.5	755	2:01	18.0	8.93	+
54	7.5	102	2:01	19.2	9.52	+
55	7.0	99	2:02	18.6	9.15	+
56	3.5	949	3:59	13.4	3.36	-
57	6.5	68	2:20	19.0	8.14	+
58	4.0	43	3:45	18.2	4.85	-
59	7.5	420	2:01	18.4	9.12	+
60	8.0	449	2:04	20	9.68	+
61	8.0	159	2:06	21.2	10.10	+
62	3.5	45	4:00	17.2	4.30	-
63	7.5	79	2:03	19.4	9.46	+
64	7.5	825	2:08	18.6	8.72	+
65	6.5	482	2:29	19.2	7.73	+
66	3.5	368	3:58	15.6	3.93	-
67	7.0	907	2:01	16.8	8.33	+
68	8.0	52	0:56	10.2	10.93	+
69	6.5	635	2:15	17.2	7.64	+
70	4.5	475	3:24	17.6	5.18	-
71	7.0	54	2:05	19	9.12	+
72	7.5	155	2:02	19.6	9.64	+
73	3.5	100	3:55	16.5	4.21	-
74	8.0	585	2:02	19.8	9.74	+
75	6.0	480	2:19	17	7.34	+

76	4.0	87	3:43	18.4	4.95	-
77	6.5	141	2:31	20.8	8.26	+
78	7.0	501	2:02	17.4	8.56	+
79	4.0	275	3:43	17.8	4.79	-
80	8.0	548	2:00	19.6	9.80	+
81	7.5	265	2:02	19.2	9.44	+
82	3.5	753	3:54	14.8	3.79	-
83	6.5	235	2:12	17.8	8.09	+
84	6.0	233	2:14	17	7.61	+
85	5.5	485	2:27	16	6.53	-
86	8.0	765	1:58	19	9.66	+
87	4.5	605	3:29	18.2	5.22	-
88	8.0	460	1:59	19.6	9.88	+
89	3.5	44	3:59	17.8	4.47	-
90	7.0	850	2:16	18.8	8.29	+
91	4.0	139	3:46	18.6	4.94	-
92	7.5	558	2:00	18.6	9.30	+
93	5.0	612	2:31	14.8	5.88	-
94	7.0	157	2:15	20	8.89	+
95	5.5	790	2:42	17.2	6.37	-
96	6.0	885	2:18	16.2	7.04	+
97	5.0	101	2:30	16	6.40	-
98	7.5	150	2:02	19.8	9.74	+
99	5.0	49	2:33	16.6	6.51	-
100	6.5	468	2:17	18.2	7.97	+

The mathematical model was developed using classical regression analysis, which requires that the dependent variable (in this case the flow) must be statistically independent. The Run Test method (Fraser, 1991) was used to determine the statistical independence of these data.

Table C-3 shows the parameters needed to evaluate the statistically independence of the data gathered. The average flow is 6.98 and these data comprise 100 observations (N). In Table C-2, observations above the average are identified as positive (+) and below the average are identified as negative (-). Thus, a sequence of identical observations (positive or negatives) followed and preceded by a different observation is called run. The number of runs, which occur in a sequence of observations, gives an indication as to whether or not results are independent random observations. Specifically, if a sequence of N observations is an independent observation of the same random variable, that is, the probability of a (+) or a (-) result does not change from one observation to the next, then the sampling distribution in the number of runs in the sequence is a random variable "$\check{r}$" with a mean value and variance.

Table C-3: Random Measurements: Parameters for the Evaluation.

	Flow
Average	6.98
N	100
$\check{r}$	48
n	50

Let it be hypothesized that there is no trend by assuming that the sequence of N observations are independent observations of the same random variable. The hypothesis can be tested at any desired level of significance α by comparing the observed runs to the interval between $\check{r}_{n;1-\alpha/2}$ and $\check{r}_{n;\alpha/2}$ where n=N/2. If the observed runs fall outside the interval; the hypothesis would be rejected at the α level of significance. Otherwise, the hypothesis would be accepted. The values for $\check{r}_{n;1-\alpha/2}$ and $\check{r}_{n;\alpha/2}$ can be obtained from Table C-4.

In this case, it is hypothesized that there is not trend between the 100 observations. The acceptance region for the hypothesis is $\breve{r}_{50;1-\alpha/2} < \breve{r} < \breve{r}_{50;\alpha 0;}$ provided that $P_\alpha = 1 - \alpha$ is sufficiently small.

Regarding the flow measurements, for $\alpha = 0.10$, $\breve{r}_{50;0.95} = 42$ and $\breve{r}_{50;0.05} = 59$ (see Table C-4), $\breve{r} = 48$ falls well between the previously indicated values. This means that the maximum confidence level at which the hypothesis can be rejected is significantly less than 90% ($P_\alpha = 1 - \alpha = 1 - 0.1 = 0.9$). For this reason, the hypothesis is accepted. There is no underlying trend in these data.

Table C-4: Percentage points of run distribution (values of $r_{n;\alpha/2}$ such that Prob [r_n > $r_{n;\alpha}$]=α, where n=N_1=N_2=N/2)

	α					
	1- α/2			α /2		
n=N/2	0.99	0.975	0.95	0.05	0.025	0.01
5	2	2	3	8	9	9
10	5	6	6	15	15	16
20	13	14	15	26	27	28
30	21	22	24	37	39	40
40	30	31	33	48	50	51
50	38	40	42	59	61	63
60	47	49	51	70	72	74
70	56	58	60	81	83	85
80	65	68	70	91	93	96
90	74	77	79	102	104	107
100	84	86	88	113	115	117

Model Development:

The Least Square method (Montgomery, 1996) was used to establish a functional relationship between the flow (dependent variable), the pump stroke and the pump discharge pressure (independent variables). The final model is shown below:

$$f = -0.36465119 + 1.34938111 * S - 0.0011065 * P \tag{C.1}$$

Where:

f: pump discharge flow (cc/min)

S: pump stroke (mm)

P: pump discharge pressure (psig)

Model Evaluation:

The model is assessed statistically in order to determine its usefulness. This evaluation comprises the significance test on the Multiple Correlation Coefficient “r”.

The Multiple Correlation Coefficient “r” is defined as:

$$r^2 = \frac{\sum_{i=1}^{i=100} (Y_{est} - \hat{Y}_c)^2{}_i}{[\sum_{i=1}^{i=100} (Y_{est} - \hat{Y}_c)^2{}_i + \sum_{i=1}^{i=100} (Y_{est} - Y_c)^2{}_i]} \tag{C.2}$$

Where:

Y_c: measured dependent variable. In the pump calibration procedure, this variable is the flow.

Y_{est}: estimated value for each point in the measured data. It is calculated using the model and each particular calibration value (pump stroke and pressure).

$\hat{Y}_c$: the average measured value. $\hat{Y}c = \frac{\sum_{i=1}^{i=100} Y_{ci}}{N}$ (C.3)

The Null Hypothesis, r = 0, can be evaluated at some confidence level $P_\alpha = 1 - \alpha$, in terms of “r_α ”. Therefore, if $r > r_\alpha$ at a confidence level that is sufficiently large (higher than 90%), the hypothesis can be rejected and “r” can be considered statistically significant. The parameter “r_α ” is defined as:

$$|r_\alpha| = \sqrt{\frac{\nu_1 * F_{\nu_1;\nu_2;\alpha}}{(\nu_2 + \nu_1 * F_{\nu_1;\nu_2;\alpha})}} \tag{C.4}$$

$$\nu_1 = p - 1 \tag{C.5}$$

$$\nu_2 = N - p \tag{C.6}$$

Where:

p: number of estimated coefficients. It is equal to the number of variables (dependent and independent). In this particular case: $p = 3$.

N: number of data. N=100.

$F_{\nu1;\nu2;\alpha}$: parameter obtained from F-Tables for any given p, N and α (Montgomery, 1996).

Table C-5 shows the results of the evaluation of the model as a whole. In this case, $r = 0.99469 > r_\alpha = 0.71157$ for Pα = 99%. Consequently, r ≠ 0 and it is statistically significant. This means that the model is adequate.

Table C-5: Statistical analysis of the model. Multiple Correlation Coefficient, "r"

N	100
P	3
ν_1	2
ν_2	97
$F_{2;97;0.01}$	99.49
r^2	0.98941
r	0.99469
r_α	0.71157

Figure C-2 shows the monogram used to adjust the feed pump stroke length as a function of the system working pressure.

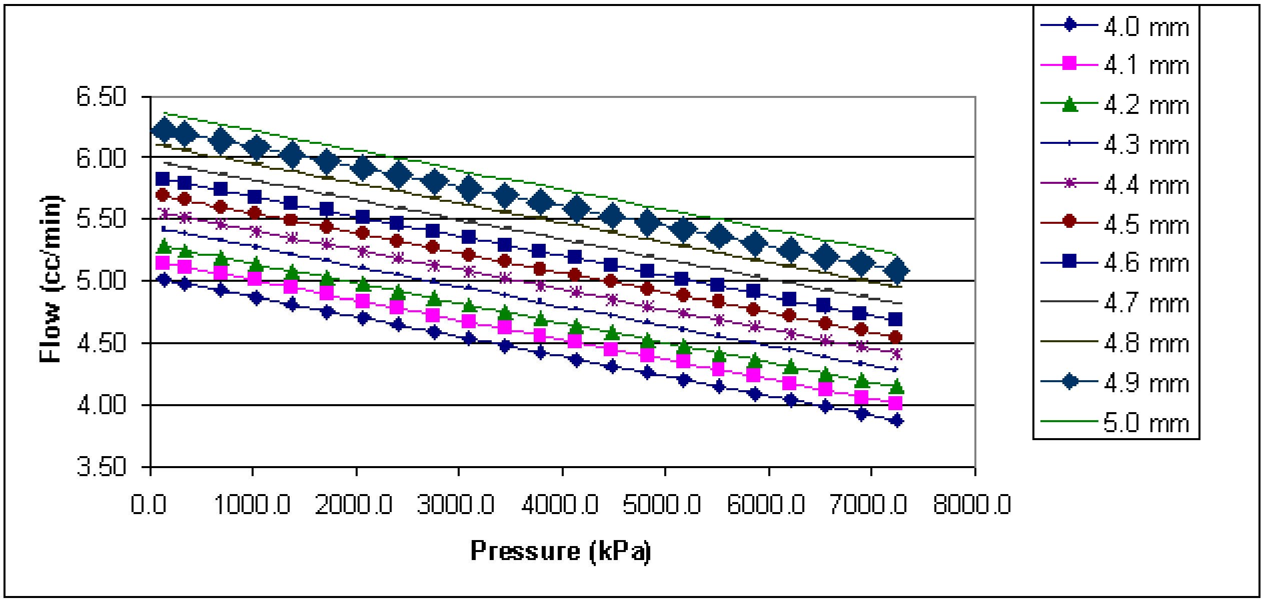

Figure C-2: Flow as function of pressure for different feed pump stroke length.

Moreover, the model was used to predict the required adjustments in the pump stroke to keep the flow around 5.0 mL/min at specific operating pressures. These conditions were evaluated experimentally and the results, which are shown in Table C-6, possess errors less than 5%.

Table C-6: Model evaluation. Predicted and experimental values.

Stroke (mm)	P. Av. (psig)	Time (min:s)	Volume (cc)	Flow (cc/min)	Predicted (cc/min)	Diff (cc/min)	Error (%)
4.0	37	4:30	22.6	5.02	4.99	0.03	0.603
4.7	850	4:30	23.4	5.20	5.04	0.16	3.136
4.3	470	4:30	22.8	5.07	4.92	0.15	2.941
4.5	633	4:30	23.8	5.29	5.01	0.28	5.327
4.1	154	4:30	23.2	5.16	5.00	0.16	3.067
4.6	760	4:30	23.4	5.20	5.00	0.20	3.816
4.2	273	4:30	23.0	5.11	5.00	0.11	2.161

Appendix D: Coker Effluent Condenser

This appendix presents detailed information for the design of the coker effluent condenser. Figure D-1 shows a diagram with the main variables considered.

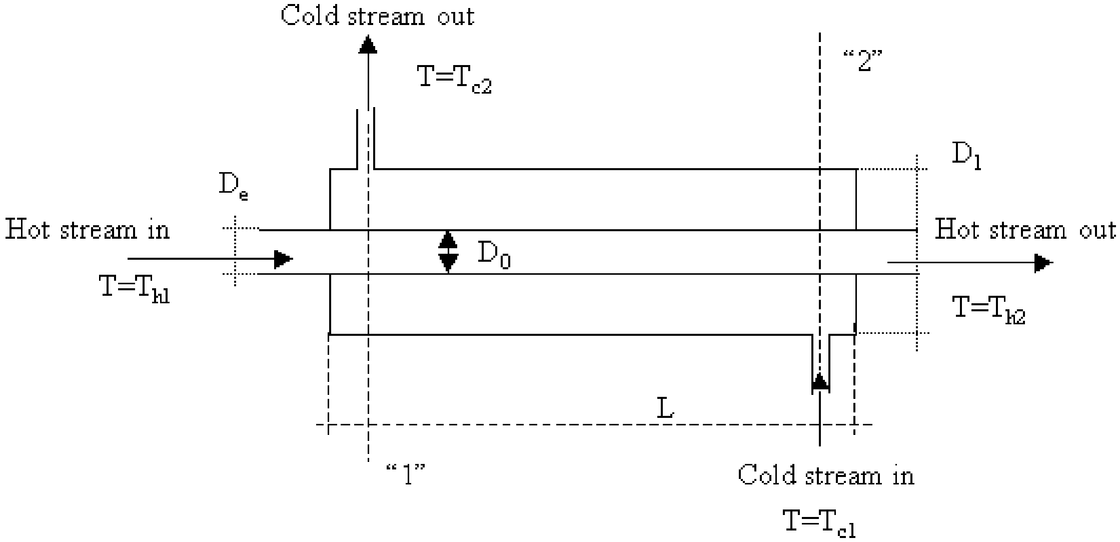

Figure D-1: Schematic of the counterflow shell and tube heat exchanger.

Three main steps were required to design this equipment; first, the selection of the product temperature at the condenser outlet and the calculation of the heat of condensation; second, the specification of operating conditions; and third, the calculation of the condenser length required to remove the heat.

The selection of the outlet temperature and the calculation of the heat of condensation of the coker effluent were accomplished using the CMG phase property program to calculate the following information at different temperatures during the cooling process: the number of phases, each phase composition and each phases' properties. These results are shown in Table D-1 and D-2 with the temperature varying from 673 K to 303 K at 241 kPa of constant pressure. According to these results, the liquid phase first appears at 650 K; and most of the liquid products (gasoline, naphtha, KERO, LCGO and HCGO) are in the liquid phase at 303 K; therefore, 303 K is considered the final hydrocarbon product temperature. Moreover, the heat of condensation of the coker effluent was calculated to be ~63 W.

Table D-1: Phases composition for coker effluents during cooling

P (kPa) 241

T (K)	673	651	650		643		543		443		343		303	
Component (mole %)	Vapor	Vapor	Liquid	Vapor	Liquid	Vapor	Liquid	Vapor	Liquid	Vapor	Liquid	Vapor	Liquid	Vapor
H_2	3.45	3.45	0.02	3.45	0.02	3.55	0.02	4.38	0.02	5.25	0.01	6.59	0.01	7.30
H_2S	5.36	5.36	0.07	5.36	0.08	5.51	0.11	6.78	0.20	8.06	0.62	9.69	1.20	10.02
CO_2	0.13	0.13	0.00	0.13	0.00	0.13	0.00	0.16	0.00	0.20	0.00	0.25	0.01	0.27
CO	0.23	0.23	0.00	0.23	0.00	0.24	0.00	0.29	0.00	0.35	0.00	0.44	0.00	0.49
C_1	18.07	18.07	0.13	18.08	0.13	18.59	0.14	22.92	0.17	27.44	0.27	34.34	0.36	37.93
C_2	10.02	10.02	0.11	10.03	0.11	10.30	0.14	12.69	0.23	15.15	0.58	18.64	1.03	20.10
C_2=	1.05	1.05	0.01	1.05	0.01	1.08	0.01	1.33	0.02	1.59	0.04	1.97	0.07	2.14
C_3	5.35	5.35	0.08	5.35	0.08	5.50	0.12	6.76	0.24	8.02	0.85	9.46	1.74	9.40
C_3=	1.77	1.77	0.02	1.77	0.03	1.82	0.04	2.24	0.07	2.66	0.25	3.16	0.49	3.20
NC_4	2.6	2.6	0.05	2.60	0.06	2.67	0.10	3.28	0.23	3.84	1.04	4.03	2.09	3.18
IC_4	0.86	0.86	0.02	0.86	0.02	0.88	0.03	1.08	0.07	1.28	0.27	1.40	0.56	1.20
C_4=	2.06	2.06	0.04	2.06	0.04	2.12	0.07	2.60	0.17	3.05	0.72	3.28	1.48	2.70
IC_5	0.05	0.05	0.00	0.05	0.00	0.05	0.00	0.06	0.01	0.07	0.04	0.06	0.06	0.04
NC_5	0.13	0.13	0.00	0.13	0.00	0.13	0.01	0.16	0.02	0.19	0.11	0.15	0.18	0.08
GASOLINE	6.24	6.24	0.22	6.24	0.23	6.41	0.51	7.79	1.71	8.61	7.79	4.83	10.32	1.67
NAPHTHA	11.6	11.6	0.84	11.61	0.90	11.91	2.51	14.06	10.14	12.37	22.43	1.70	21.69	0.28
KERO	11.33	11.33	3.32	11.34	3.66	11.55	14.49	10.48	29.53	1.80	23.71	0.02	21.43	0.00
LCGO	7.19	7.19	7.71	7.19	8.60	7.15	24.30	2.56	20.78	0.07	15.06	0.00	13.60	0.00
HCGO	12.51	12.51	87.36	12.46	86.04	10.40	57.41	0.37	36.39	0.00	26.20	0.00		

Table D-2: Change of stream properties during cooling and heat of condensation for coker effluents

P (kPa)	241													
T (K)	673	651	650		643		543		443		343		303	
	Vapor	Vapor	Liquid	Vapor	Liquid	Vapor	Liquid	Vapor	Liquid	Vapor	Liquid	Vapor	Liquid	Vapor
Z-factor	0.9808	0.9782	0.022	0.9782	0.022	0.9797	0.0219	0.9862	0.022	0.9873	0.0231	0.9868	0.0242	0.9854
Molar vol. (m^3/kmol)	22.74892	21.94016	0.4938	21.92109	0.48852	21.71087	0.41068	18.4558	0.33639	15.07518	0.27322	11.66731	0.25256	10.29278
MW	112.25	112.25	312.18	112.13	310.73	106.55	276.87	67.75	236.88	46.99	200	32.08	187.46	27.93
Enthalpy (kJ/kmol)	115291.91	108450.0	218763.4	108166.4	211059.1	100978.2	110920.8	48741.42	36178.72	24927.02	-12152.30	12763.50	-25399.75	9934.82
Cp (kJ/kmol/K)	311.47	304.84	954.75	304.33	943.52	286.98	756.79	160.57	567.09	93.06	402.67	50.02	347.04	39.44
Density (Kg/m^3)	4.94	5.12	632.76	5.12	636.63	4.91	674.77	3.67	704.81	3.12	732.67	2.75	742.92	2.72
Viscosity (Kg/s/m)	1.40E-05	1.30E-05	9.00E-05	1.30E-05	9.20E-05	1.30E-05	1.25E-04	1.30E-05	1.77E-04	1.20E-05	2.56E-04	1.10E-05	2.98E-04	1.00E-05
Phase (volume %)			0.0014	99.9986	0.0646	99.9354	0.5979	99.4021	1.1551	98.8449	2.0949	97.9051	2.3633	97.6367
Phase (mole %)			0.0624	99.9376	2.7913	97.2087	21.2803	78.7197	34.3706	65.6294	47.7463	52.2537	50.2846	49.7154
Flow (kg/s)	5.7167E-5													
DQ (W)		3.49	0.11		2.13		21.45		16.91		14.24		4.90	
Q (W)	63.23													

The water outlet temperature was calculated with equation (D.1).

$$Q_{water} = m \times Cp \times (T_{c1} - T_{c2}) = Q_{hydrocarbons} \tag{D.1}$$

Table D-3 shows the design parameters of this equipment. Figure D-1 can be used as a reference to identify the variables indicated in this Table.

Table D-3: Condenser design parameters.

D_o (m)	0.00493
D_e (m)	0.00635
D_1 (m)	0.009525
T_{h1} (K)	673
T_{h2} (K)	303
T_{c1} (K)	298
T_{c2} (K)	293
Hydrocarbon mixture (Kg/s)	5.71667E-05
Water (L/s)	0.00333

The minimum heat exchanger length was calculated with the following procedure:

1. Assume condenser length.
2. Calculate the heat transfer coefficients and the overall heat transfer coefficients in points 1 and 2 (see Figure D-1).
3. Calculate the heat transferred.
4. If the heat transferred is lower or higher than the heat of condensation, the condenser length is increased or decreased respectively. Afterwards, steps 2 and 3 are repeated until the heat transferred is equal to or slightly higher than the heat of condensation.

The heat transferred in the condenser is calculated with the following equation (Perry et al. 1999) that considers the overall heat transfer coefficient varying linearly with the temperature in the streams. This precaution is taken because when the fluids are in laminar flow regime, the variation of U_0 with position may be large (Bird, Stewart & Lightfot, 1960).

$$Q = \pi \times D_e \times L \times \frac{(U_{01} \times \Delta T_1 - U_{02} \times \Delta T_2)}{Ln\left(\dfrac{U_{01} \times \Delta T_1}{U_{02} \times \Delta T_2}\right)} \tag{D.2}$$

Where:

$$\Delta T_1 = T_{h1} - T_{c1} \tag{D.3}$$

$$\Delta T_2 = T_{h2} - T_{c2} \tag{D.4}$$

The overall heat transfer coefficient was calculated with the following equation (Bird et al., 1960):

$$U_0 = D_0^{-1} \times \left(\frac{1}{D_0 \times h_0} + \frac{Ln(D_e / D_0)}{2 \times k_{ss}} + \frac{1}{D_e \times h_1} \right)^{-1} \tag{D-5}$$

Following the detailed information about the correlations used to calculate the heat transfer coefficients and fluid properties (coker effluent and cooling water).

The heat transfer coefficients of the coker effluents at the inlet and the outlet of the condenser were calculated with different correlations because of the different state of this stream in these points. At the inlet, the coker effluent is as vapor; and at the outlet, this hydrocarbon stream is a mixture of both condensate liquid and non-condensable.

At the inlet of the condenser, the heat transfer coefficient of the coker effluents was calculated with the following generalized Sieder-Tate relationship (Perry et al., 1999).

$$\frac{h \times D}{k_b} = 1.86 \times (Gz)^{1/3} \times (\mu_b / \mu_0)^{0.14} + 0.87 \times \left(1 + 0.015 \times Gz^{1/3}\right) \tag{D-6}$$

Where:

$$\mathrm{Gz} = \frac{\mathrm{Re_b} \times \mathrm{Pr_b} \times \mathrm{D}}{\mathrm{L}} \tag{D-7}$$

$$\mathrm{Re_b} = \frac{D \times G}{\mu_b} \tag{D-8}$$

$$\mathrm{Pr_b} = \frac{Cp_b \times \mu_b}{k_b} \tag{D-9}$$

The vapor viscosity at the condenser's wall temperature (μ_o) was calculated with the following expression (Perry et al., 1999):

$$\mu_o = 4.6 \times 10^{-4} \times 0.0034 \times T_r^{0.94} \times \frac{MW^{1/2} \times P_c^{2/3}}{T_c^{1/6}} \tag{D-10}$$

Where:

$$\mathrm{T}_r = \frac{\mathrm{T}}{\mathrm{T_c}} \tag{D-11}$$

The critical temperature (T_c) was calculated with the following mixing rule:

$$T_c = \sum_{j=1}^{n} \frac{x_j \times Vc_j}{\sum_{i=1}^{n} x_i \times Vc_i} \times Tc_j \tag{D-12}$$

The critical pressure (P_c) was calculated with the following mixing rule:

$$P_c = P_{pc} + P_{pc} \times \left[5.808 + 4.93 \times \left(\sum_{i=1}^{n} x_i \times \omega_i \right) \right] \times \left[\frac{T_c - T_{pc}}{T_{pc}} \right] \tag{D-13}$$

With:

$$T_{pc} = \sum_{i=1}^{n} x_i \times Tc_i \tag{D-14}$$

$$P_{pc} = \sum_{i=1}^{n} x_i \times Pc_i \tag{D-15}$$

At the outlet of such equipment, the heat transfer coefficient of the coker effluents was calculated with the Kern's modification of the Nusselt equation, which is valid for horizontal in-tube condensation at low flow rates (Perry et al., 1999).

$$h = 0.761 \times \left[\frac{L \times k_l^3 \times \rho_l \times (\rho_l - \rho_v) \times g}{W_F \times \mu_l} \right]^{1/3} \tag{D-16}$$

The heat transfer coefficients for the cooling water at the inlet and the outlet of the condenser were calculated with the slug flow annuli equation from Trefethen (Perry et al., 1999).

$$\frac{h \times D_{eq}}{k} = \frac{8 \times (m-1) \times (m^2 - 1)^2}{4 \times m^4 \times \ln(m) - 3 \times m^4 + 4 \times m^2 - 1} \tag{D-17}$$

Where:

$$\mathrm{m} = \frac{\mathrm{D_1}}{\mathrm{D_e}} \tag{D-18}$$

For the hydrocarbon side, the diameter D is simply the tube inlet diameter; however, for the cooling-water side this variable cannot be considered as the whole tube diameter because this fluid is moving between two concentric tubes. In this case, the diameter $\mathrm{D_{eq}}$ is calculated as a characteristic length.

$$\mathrm{D_{eq}} = D_1 \times \left(1 - \frac{D_e}{D_1} \right) \tag{D-19}$$

The thermal conductivity of the coker effluent at the inlet of the condenser (hydrocarbons as vapor) was calculated with the following equation (Perry et al., 1999)

$$k_g = 4.45 \times 10^{-7} \times T_r \times \frac{Cp}{\lambda} \tag{D-20}$$

Where:

$$\lambda = T_c^{1/6} \times MW^{1/2} \times \left(\frac{101.325}{P_c} \right)^{2/3} \tag{D-21}$$

Moreover, Tr, T_c and P_c are calculated with equations (D-11), (D-12) and (D-13), respectively.

The thermal conductivity of the hydrocarbon liquid phase at the outlet of the condenser was calculated with the following expression (Perry et al. 1999):

$$k_l = 4.407 \times 10^{-4} \times \rho_M \times MW^{0.7717} \times \left[\frac{3 + 20 \times (1 - T_r)^{2/3}}{3 + 20 \times \left(1 - \frac{293.15}{T_c} \right)^{2/3}} \right] \tag{D-22}$$

Where T_r and T_c are calculated with equations (D-11) and (D-12) respectively.

The thermal conductivity of the stainless steel tubing (k_{ss}) was calculated at the temperatures in points 1 and 2 (the subscripts 1 and 2 refer to the planes shown in figure D-1) from values reported by Perry et al. (1999). The temperatures in points 1 and 2 were calculated as the average between the cooling water and the coker effluent temperatures.

According to the data in Table D-4, the heat transferred is 64 W when the condenser length is 0.35 m. This value is higher than the heat that should be removed from the coker effluent stream (63 W). If the condenser length is 0.01 m smaller than the value indicated above, the heat transferred is lower than 63.23 W; therefore, the condenser length reported in Table D-4 (0.35 m) is the minimum length of this equipment to achieve the desired final temperature for the coker effluent. The length selected was 0.36 m.

Table D-4: Fluid properties and Condenser length calculation.

	Cooling water		Coker effluents		
Temperature (K)	293	298	673	303	
Viscosity (Kg*s^{-1}*m^{-1})	1.00E-03	8.91E-04	1.40E-05	2.98E-04	
Cp (J*Kg^{-1}*K^{-1})	4181.7	4179.5	2774.8	1851.3	
k (W*m^{-1}*K^{-1})	5.98E-01	6.06E-01	1.14E-01	9.8E-02	
Condenser length (m)					**0.35**
h_{water1} (W*m^{-2}*K^{-1})		1151.09			
h_{water2} (W*m^{-2}*K^{-1})	1165.71				
h_{hc1} (W*m^{-2}*K^{-1})			22.04		
h_{hc2} (W*m^{-2}*K^{-1})				3731.975	
k_{ss1} (W*m^{-1}*K^{-1})					17.4
k_{ss2} (W*m^{-1}*K^{-1})					14.9
U_{01} (W*m^{-2}*K^{-1})					21.7041
U_{02} (W*m^{-2}*K^{-1})					1025.0379
Q (W)					63.91

Appendix E: Data Acquisition System Configuration

This section describes the data acquisition system and presents information about the hardware and software configurations for the data acquisition system. The hardware configuration deals with wiring of sensors (pressure transducers and thermocouples) while the software configuration explains the settings for data recording. Moreover, additional information can be found in the user's guide (Weinreb and McCabe, 1196-98).

Data Acquisition System:

The system installed to acquire the operating data is InstruNet® model 100 by Omega. It is a hardware and software device that facilitates the interface of common laboratory and industrial equipment with computers for data acquisition and control.

Figure E-1 shows the configuration of the data acquisition system. It comprises two main devices: the controller and the network. The controller is an electronic board that installs into a computer and utilizes a 32-bit microprocessor to control all aspects of data acquisition related to its network. The network device is a small box where the sensors (thermocouples and pressure transducers) are connected. It provides 16 voltage input channels with screw terminal access that work at different ranges (± 5 V, ± 0.6V, ± 80 mV and ± 8 mV), 8 voltage output channels, and 8 bi-directional digital channels (Input / Output). The network device is connected to the controller with a DB-25 cable.

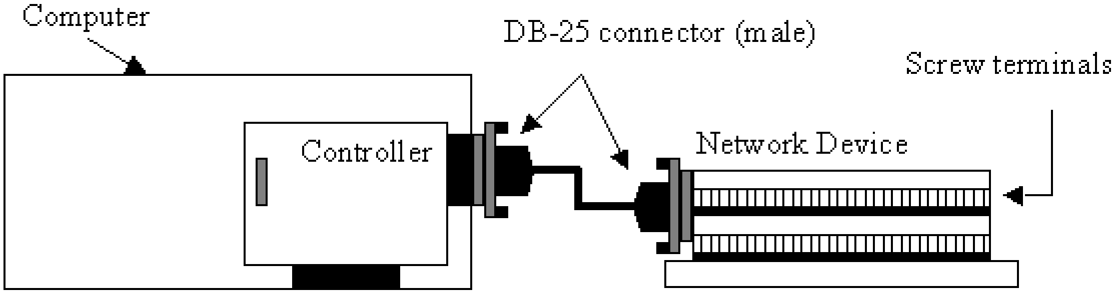

Figure E-1: Data Acquisition System. Main components and configuration.

Additionally, the data acquisition system includes software called "InstruNet World". This software allows one to set up and probe the network, record waveforms and data, save them to disk, load them from disk and view them post acquisition. It was programmed to record data at 10-second intervals during experiments.

More information about the data acquisition system, how to install InstruNet® hardware and software and how to verify their proper operation can be found in the user's guide (Weinreb and McCabe, 1196-98).

Hardware Configuration:

Pressure Transducer:

The pressure transducer used is model PX-213 by Omega. The wiring to the network device is shown in figure E-2.

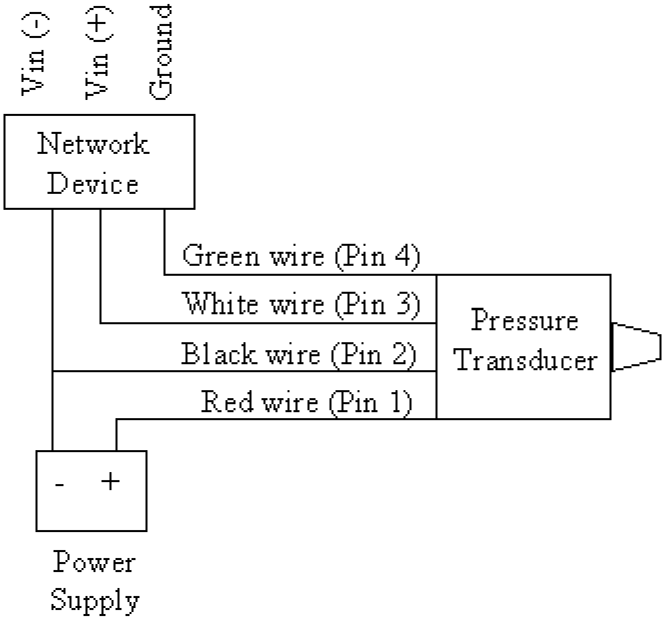

Figure E-2: Pressure transducer wiring.

A power supply of 24 Vdc at 15 mA is required to excite the sensor. The pressure transducer has four terminals or pins inside the connector. The appropriate wiring of these pins is as follow:

- Pin 1 connected to the power supply's positive pole

- Pin 2 connected to the power supply's negative pole, and both terminals (pin 2 and the negative pole) are wired to the network device's negative voltage input
- Pin 3 connected to the network device's positive voltage input; and
- Pin 4 connected to ground in the network device.

Thermocouple:

All the thermocouples installed in this apparatus are K thermocouples. The coker thermocouple is a 0.003175 m (1/8 ") outside diameter probe that is inside the coker; and the other thermocouples are self-adhesive thermocouples installed on the metal surface of vessels and tubing.

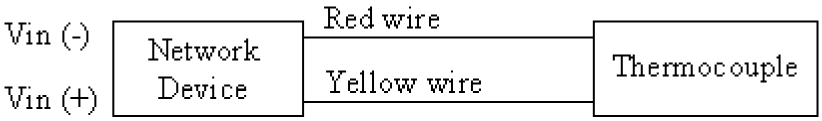

Figure E-3: Coker thermocouple wiring.

Figure E-3 shows the wiring for the coker thermocouple. This thermocouple is grounded; therefore, the wiring is connected to the network voltage inputs. The yellow wire or probe positive connection is wired to the positive voltage input and the red wire or K connection is wired to the negative voltage input.

Figure E-4 shows the wiring of the self-adhesive thermocouples. In these cases, the red wires were connected to the ground and the yellow wires were connected to the positive voltage input.

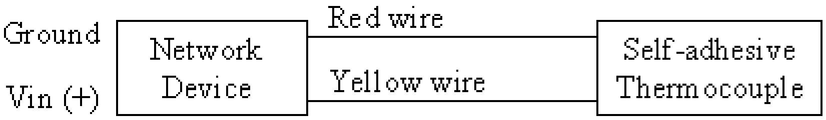

Figure E-4: Self-adhesive thermocouple wiring.

Software Configuration:

The “InstruNet World” software is installed after the hardware (controller and device). The instructions to complete its installation successfully are clearly explained in the user’s guide (Weinreb and McCabe, 1196-98). After installation, the software creates three different pages: the network page, the record page and the test page.

The network page is used to view and set parameters within an InstruNet network. It provides a spreadsheet format to scroll vertically through sensors and horizontally through the settings for each sensor. In this page, the user can define the type of sensor that is connected to the input and set the range of a voltage input. The record page is used to start, stop and view in real time waveforms. These waveforms, as well as data sheets in text format can be save to a disk. Also in this page, the sample rate and number of points digitalized per sensor can be specified. The test page is used to determine what InstruNet hardware is attached to the computer and to test all InstruNet hardware and software.

The installation of InstruNet World creates a default configuration that does not necessarily match with the requirements of sensor and data acquisition features; therefore, modifications of some of the options were required. These modifications are noted below:

Thermocouples:

The thermocouples installed in this apparatus are type K probes sensing temperatures that could be above 563 K (290 ºC) in some points like the coker internal and outlet temperatures and the light product condenser inlet. To measure temperatures above this value, the sensor’s range must be higher than 10 mV, which is the default value after the software “InstruNet World” has been installed. To change this configuration, select the “Network page” and in the “Hardware settings” set the “Range” field to ±80 mV.

Pressure Transducer:

InstruNet uses Volt, Amps and ºC as default units; therefore, the pressure transducer voltage output signal has to be modified to obtain a pressure equivalent value. This modification can be done in InstruNet because it supports calibration and conversion to different scales through the Mapping option.

Table E-1: Values for mapping of the coker pressure transducer

Internal (Volts)	External (psig)
0.475	0
5.475	1000

The Mapping setting area is available on the Network page. It defines the relationship between the "internal units" and the "external units". The "internal units" are InstruNet's default units (volts for the pressure transducer); the "external units" are what the user sees in the Network and Record pages (psig for the pressure transducer). To complete the mapping procedure two points are required to define a line on the Internal units vs. External units dimensional coordinate axis plane. Table E-1 shows the calibration points used to complete the pressure transducer mapping.

Record Setup:

The record setup dialog, available on the Record page, is used to set the base sample rate, the number of points to be acquired per scan, the number of scans, the recording mode, the storage mode and the display mode. Following, the meaning of the different fields and the values adjusted in this case:

1. Sample rate fields: specifies the number of points digitalized per second per channel. It was adjusted to 0.1

2. Points per scan field: specifies the number of points (4 bites per point) that are digitalized for each scan. This value was set to $1x10^6$.

3. Number of scans: represents the number of scans digitalized when the star button is pressed. Its value is 2147483647.

4. Scan mode: InstruNet supports two modes: Oscilloscope and Strip Chart. The Oscilloscope digitalizes individual scans whereas the Strip Chart links a set of scans together (the user does not notice the individual scans). The Oscilloscope

mode acquires and store scans of data in a buffer for processing. It has two variations: the Oscilloscope and the Oscillo Queued. In the first variation, the most recent scan of data will be returned for processing (first in, last out) while in the second variation, the Oscillo Queued, the data are get back in sequence (first in, first out). The scan mode adjusted in this case was Oscillo Queued.

5. Digitalize into: defines the option to storage the data. For this project, the option selected was “to ram buffer”.
6. File type: defines the file type where the data is stored. The option selected was “Text Merge”. It creates a text file that can be transformed to a excel archive for data processing purposes.

Appendix F: Operating Procedure

This section includes the procedures to prepare, start up and shut down the apparatus. Furthermore, it includes procedures and suggestions to complete the mass balance and to clean the apparatus before re-starting a new experiment. Use Figure F-1 to identify components.

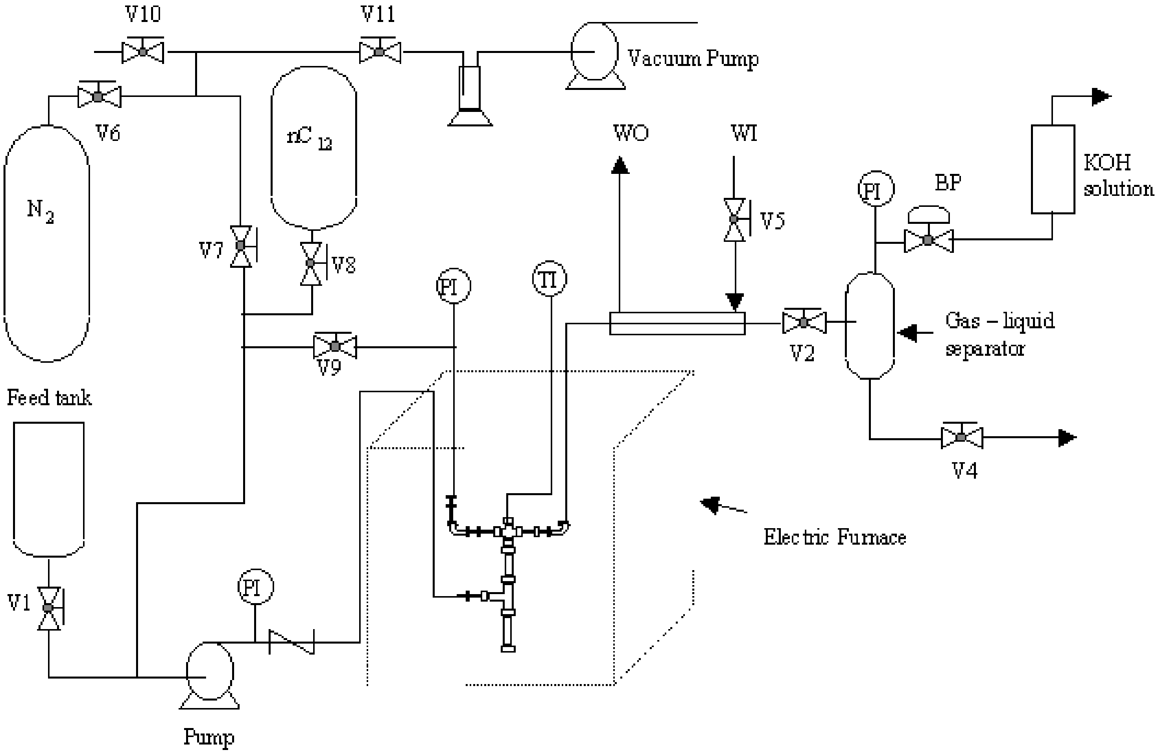

Figure F-1: Apparatus schematic.

Pressure Test:

1. Check that the BP valve, the gas–liquid separator bottom valve (V4), the n-Dodecane vessel bottom valve (V8), the purge valve (V10), the vacuum pump suction valve (V11) and the feed vessel discharge valve (V1) are closed; and the condenser outlet valve (V2) is opened.

2. Admit nitrogen to the system. First, completely open the cylinder head valve and valve V6. Finally, open valve V7 carefully to slowly increase the pressure in the apparatus.

3. Once the desired pressure has been reached (read the coker pressure transducer), close valve V6 and valve V7. This is an opportunity to check the system for leaks (the pressure must be kept at the target value for, at least, 5 minutes). Use the liquid leak detector on the connections between lines, vessels, pump and valves to check the system for leaks.

Unit Preparation:

4. Weigh and register the initial amounts of KOH solution, n-C_{12} for the n-C_{12} vessel, n-C_{12} for the feed vessel and vacuum residue. Fill the KOH solution vessel, the n-Dodecane vessel and the feed vessel with the corresponding materials.

5. If the apparatus is to operate at low pressure (239 kPa or less) add antifoaming agent to the feed vessel. The amount of antifoaming agent required is between 0.2 and 0.4 wt%.

6. Disconnect the feed vessel, weigh the feed vessel with the total amount of feed and register this value. Re-connect the feed vessel.

7. The feed mixture is prepared in the feed vessel; thus, turn on the heating plate to reduce the bitumen viscosity. When the vacuum residue becomes fluid, turn on the magnetic stirrer to enhance mixing between ABVB and n-Dodecane. Keep the agitation for 10 – 15 minutes before starting the experiments. The temperature in this vessel should be kept between 403 K and 473 K (130 °C and 200 °C) to facilitate pumping the fluid.

8. Turn on the electric furnace and select the temperature set point value. During the feeding period, the temperature set point value is between 710 and 720 K for a coker internal temperature between 693 and 698 K.

9. Turn on the heating tapes. During the warming up process, check the system for leakages and suspend this procedure if required. Also, open the BP valve regularly to avoid over-pressure in the apparatus due to nitrogen expansion. Once

the temperature in the coker has reached the desired value, adjust the apparatus pressure to the desired value.

10. Close the valve V2 to isolate the gas-liquid separation system. This section will be kept at the working pressure with nitrogen.
11. Open valve V5 to admit cooling water to the heat exchanger.
12. Reduce the pressure in the apparatus (excluding the gas-liquid separation system) to atmospheric pressure. To complete this step, close the cylinder head valve and valve V6; and open valves V9, V7 and V10.
13. Once the pressure in the reaction system has been reduced to atmospheric pressure or the close to atmospheric pressure, the system is ready to evacuate the remaining nitrogen. This action is completed with the following five steps: first, open valve V11 to align the apparatus and the vacuum pump; second, turn on the vacuum pump; third, close valve V10; fourth, when the indication of the pressure transducer becomes stationary, close valves V9, V7 and V11; and fifth, turn off the vacuum pump.
14. Check that the data acquisition system is ready and recording and verify that the pump stroke is adjusted to the desired value.

Unit Start-up:

Once the coker temperature has reached the required value, the gas-liquid separator system is pressurized and the rest of the apparatus is under vacuum pressure; the system is ready to start up the experiment.

15. Open the n-Dodecane vessel bottom valve (V8) to fill the coker with this compound and increase the pressure by vaporization. Wait until the pressure is stable. If the final pressure is lower than the required value, turn on the feed pump otherwise, open valve V2 to relief the system and adjust the pressure to the target value. Once the pressure adjustment process has finished, turn off the feed pump (if it was turned on) and close valve V8.

16. Open valve V1. Wait one minute until the feedstock fills the pump suction line; and turn on the feed pump to start pumping the feedstock to the coker system.

17. The pressure in the system will tend to rise. Therefore, open valve V2 slowly until it is opened completely.

18. The pressure will still be increasing with the valve V2 completely open. Consequently, the BP valve should be opened and used to control the pressure in the system.

19. After 45 minutes pumping the feed into the reaction system, the unit will be prepared to start the coking period. Close the BP valve and immediately turn off the feed pump. The pressure in the system will fluctuate. Therefore, both valves BP and V2 can be manipulated to keep this variable as close to the target as possible. At this time, the coking period starts.

20. Typically, when the pump is turned off, the temperature in the coker tends to rise. For this reason, the electric furnace temperature set point has to be diminished to keep the coker temperature within the desired range. The new furnace temperature set point varies for each experiment; however, an approximate value is between 5 and 10 K lower than the furnace temperature set point during the pumping period.

21. Close valve V1 to isolate the feedstock vessel.

22. Turn off the heating plate and the heating tape for the pump and the lines before the coker.

Unit Shut Down:

23. The coking period finishes after 120 minutes. Once it is finished, turn off the electric furnace and the rest of the heating tapes.

24. Completely close the BP to hold the apparatus pressurized during the cooling process. This procedure reduces the risk of plugging because it avoids the

stripping of heavy hydrocarbons and coke from the coker to the outlet line when such line is at high temperatures.

25. Close valve V2 to avoid backflow of distillates from the gas-liquid separator to the coker when the temperature in this equipment has diminished. This step is particularly important for those experiments at high pressures (3500 – 6000 kPa) and / or with low content of vacuum residue in the feedstock sample. This backflow happens because the large amount of n-C_{12} used to increase pressure or to prepare the feedstock sample increases the amount of liquid products in the gas – liquid separator to a level that could be above the inlet point.

26. Close valve V5 to interrupt the flow of cooling water through the condenser.

27. Once the coker is at room temperature, follow the next four steps to discharge the distillates from the gas – liquid separator without displacing heavy materials from the coker. First, close valve V2; second, slowly open valve V4 to discharge the liquid products in the selected collecting vessel; third, close V4 when no liquid is flowing through this line; fourth, slowly open valve V2 to equalize the pressure between the gas – liquid separator and the coker. Repeat these four steps until no liquid flows from the bottom of the gas – liquid separator.

28. Slowly open the BP valve to reduce the pressure in the apparatus to atmospheric pressure.

29. Open the Nitrogen cylinder head valve and valve V7. Afterwards, slowly open valve V8 to flush the apparatus with nitrogen and remove the remaining vapor into the gas –liquid separator system; moreover, the remaining hydrogen sulphide is absorbed in the scrubber.

30. Once the pressure in the apparatus has reached atmospheric pressure, the system is ready for maintenance.

Mass Balance and Maintenance:

The following aspects are important considerations to complete the mass balance, prepare the apparatus for the following experiments and reduce the risk of plugging.

31. Discharge the materials remaining in the H_2S scrubber and in the gas – liquid separator and weigh them. The difference between these values and the weight before the experiment started indicate the amount of H_2S produced and distillates gathered, respectively.

32. Discharge the material remaining in the n-Dodecane vessel and weigh it. The difference between the weight before the experiment started and this new value gives the amount of n-Dodecane used to increase the pressure in the apparatus.

33. Disconnect the feed vessel and weigh it. The difference between the initial weight and this new weight gives the amount of feedstock pumped in this experiment.

34. Disconnect the coker, disassembled it, remove the coke formed and weigh it.

35. Connect a temporary vessel (having a valve at the discharge orifice is likely) to the pump suction line.

36. To clean lines between the feed tank and the coker inlet, put solvent (toluene or THF are recommended) in the temporary vessel, open the valve and turn on the pump. Once the temporary vessel is empty turn off the pump and close valve V1. Repeat this procedure until the fluid coming out the lines is clear. Afterwards, the gathered material is vaporized and the remaining material is considered as non-processed feedstock.

37. To clean lines between the coker outlet and the gas – liquid separator, connect a temporary line between the coker inlet and outlet lines and repeat the procedure indicated in the step before. In this case, the remaining material is considered as part of the liquid products.

38. Once each experiment is finished, coke samples and distillates (condensed liquid products) are taken for analysis.

Appendix G: Operating Data

This appendix contains the operating data gathered for all of the experiments. Table G-1 presents the average values, maxima, minima and standard deviations for coker pressure and temperature measurements for all experiments. In this Table the experiment are identified with the experiment number, the vacuum residue processed and its weight percent in the mixture. Temperature and pressure traces for all experiments follow.

Table G-1: Summary of operating data for all the experiments carried out.

Exp. ID	Residue name	Wt%	Temperature (K)				Pressure (kPa)			
			Max	Mean	Min	σ	Max	Mean	Min	σ
E_{09}	ABVB	60	703	698	695	1.44	848	793	708	8.55
E_{11}	ABVB	80	702	697	695	1.22	848	794	758	6.76
E_{12}	ABVB	60	702	697	696	0.83	3749	3562	3500	15.73
E_{14}	ABVB	40	702	698	695	1.25	3702	3559	3493	22.90
E_{15}	ABVB	80	702	699	695	1.31	3681	3559	3474	23.18
E_{19}	ABVB	60	700	698	695	1.03	6333	6096	5982	36.01
E_{20}	ABVB	60	699	697	693	1.50	3656	3553	3433	26.49
E_{21}	ABVB	40	706	699	695	1.19	6290	6097	5992	32.35
E_{22}	ABVB	40	701	699	696	1.12	3663	3556	3392	30.69
E_{24}	Cerro Negro	60	699	698	696	0.84	259	238	195	3.66
E_{25}	Heater Feed.	100	699	698	696	0.60	269	240	200	4.55
E_{26}	Heater Feed.	100	719	718	716	0.68	253	240	232	2.90
E_{27}	ABVB	45	701	699	695	1.08	6176	6111	6039	19.59
E_{28}	ABVB	45	701	698	696	1.24	3632	3555	3409	22.14
E_{29}	ABVB	50	700	699	697	0.85	6277	6102	6017	25.11

E_{30}	ABVB	50	700	698	696	0.80	3625	3551	3454	19.04
E_{31}	ABVB	50	689	697	684	0.95	850	790	767	8.28
E_{32}	ABVB	45	701	699	697	1.02	815	786	757	11.04
E_{33}	ABVB	50	700	697	694	1.61	826	791	764	6.97
E_{34}	ABVB	50	700	699	696	0.47	288	238	210	4.48
E_{35}	ABVB	50	701	699	696	0.98	247	239	210	3.66
E_{36}	Heater Feed.	100	724	720	708	3.98	301	178	142	41.89
E_{38}	ABVB	50	702	699	697	0.74	2309	2241	2186	8.48
E_{40}	ABVB	30	703	698	697	1.31	6200	6107	6048	9.38
E_{41}	ABVB	30	702	699	696	1.27	296	239	203	5.52
E_{42}	ABVB	30	701	698	697	0.98	3619	3558	3455	13.31
E_{43}	ABVB	80	700	698	697	0.64	6163	6110	6070	10.97

Experiment 09 (E_{09}):

FEEDSTOCK	ABVB	n-dodecane
Wt%	59.95	40.05
PERIOD	FEEDING	COKING
Started (min)	21	66
Finished (min)	66	171

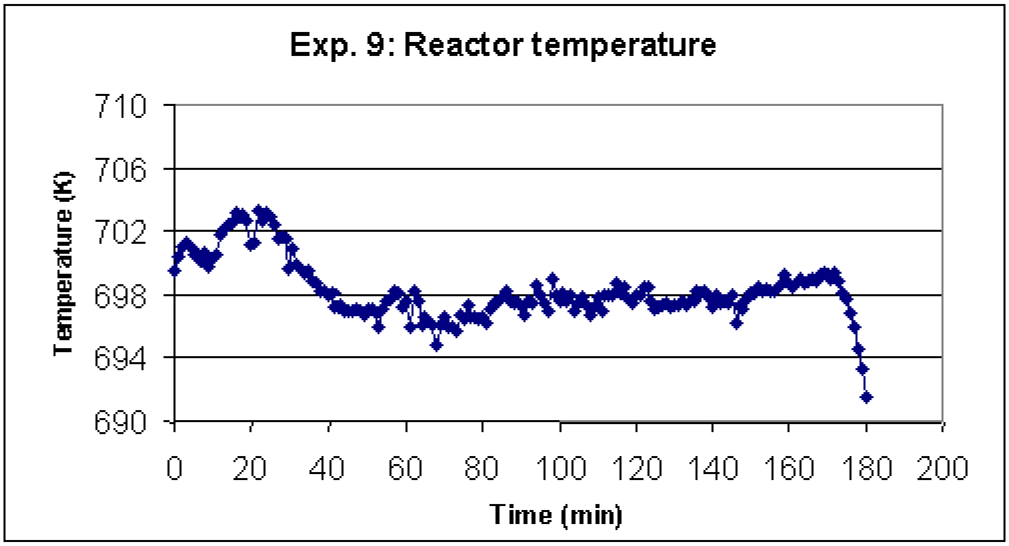

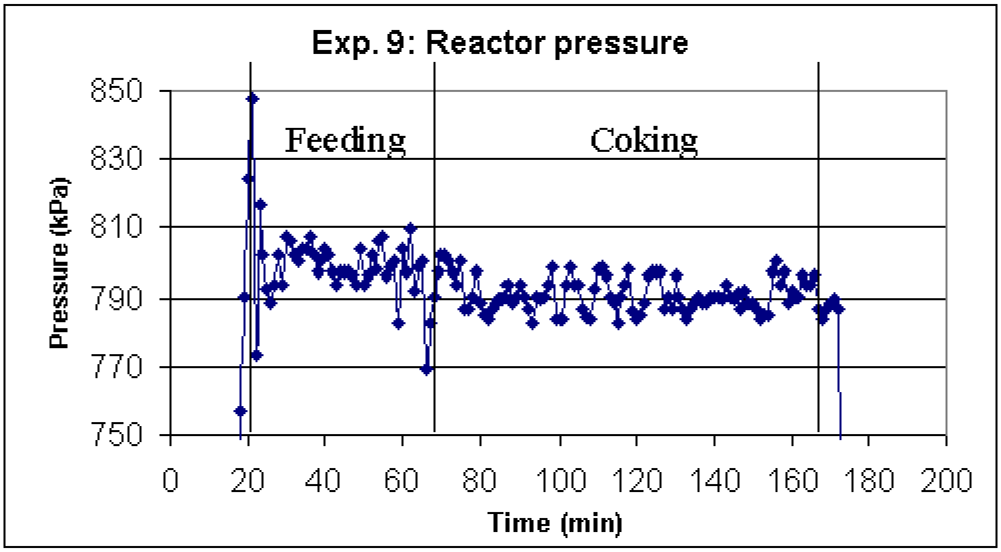

Experiment 11 (E_{11}):

FEEDSTOCK	ABVB	n-dodecane
Wt%	79.79	20.21
PERIOD	FEEDING	COKING
Started (min)	15	60
Finished (min)	60	180

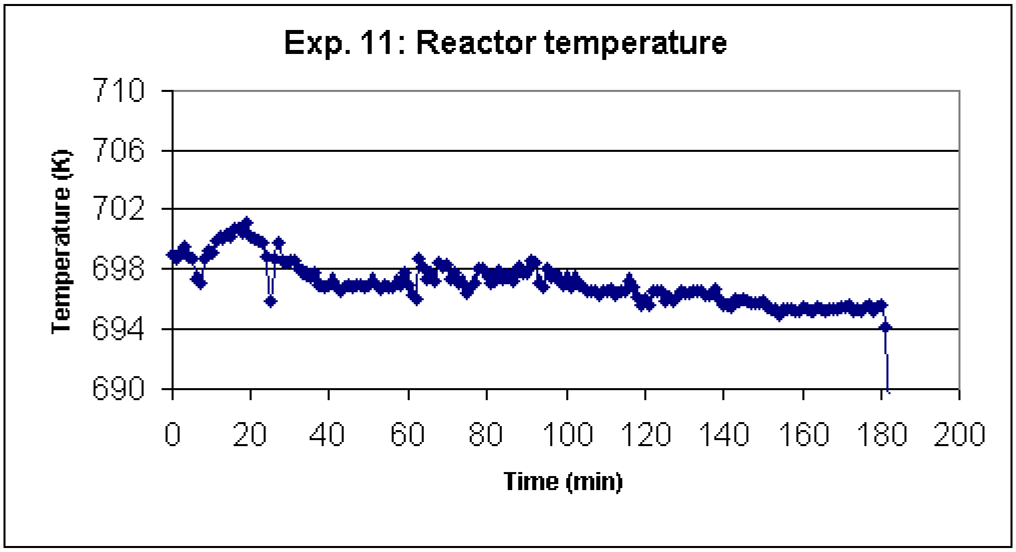

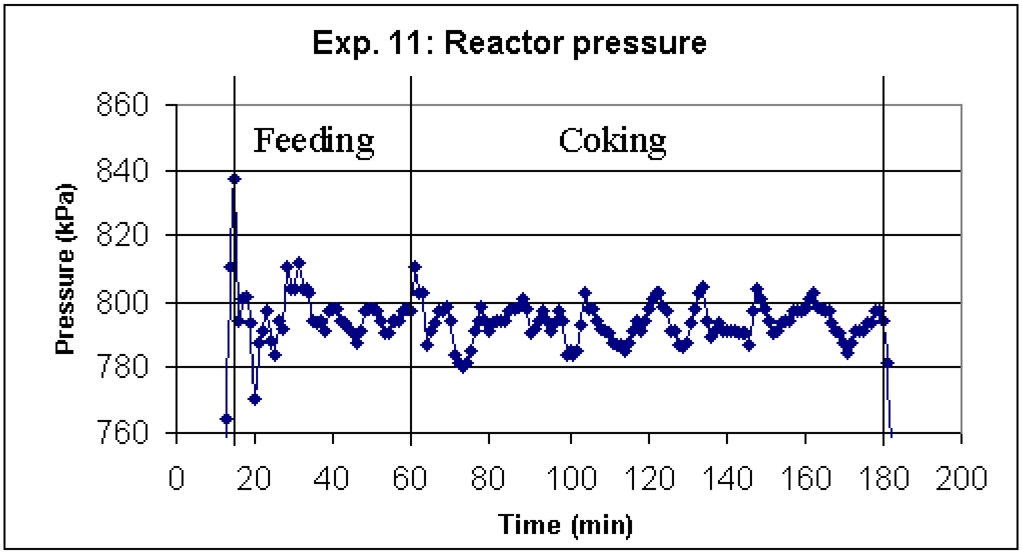

Experiment 12 (E_{12}):

FEEDSTOCK	ABVB	n-dodecane
Wt%	60.02	39.98
PERIOD	FEEDING	COKING
Started (min)	38	83
Finished (min)	83	203

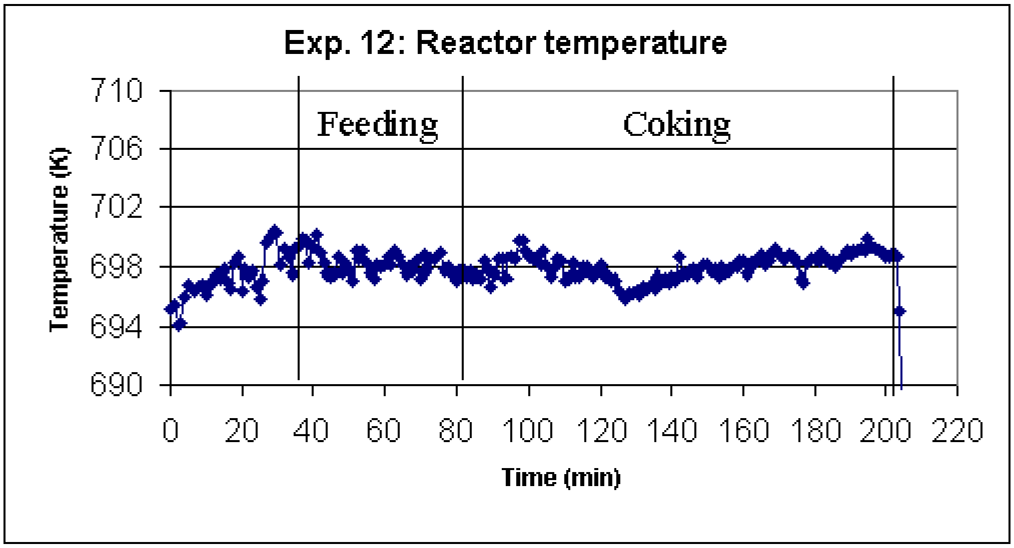

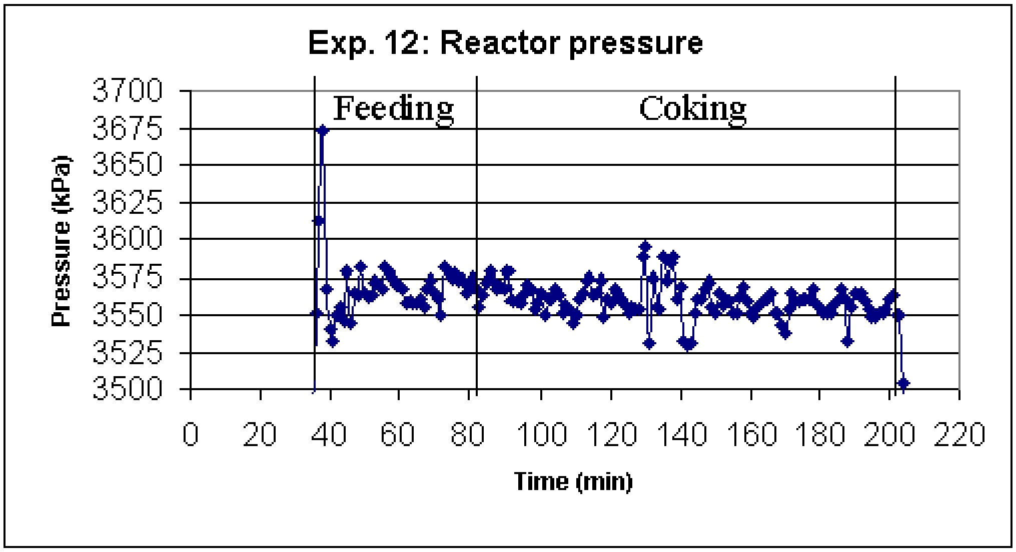

Experiment 14 (E_{14}):

FEEDSTOCK	ABVB	n-dodecane
Wt%	39.98	60.02
PERIOD	FEEDING	COKING
Started (min)	29	74
Finished (min)	74	194

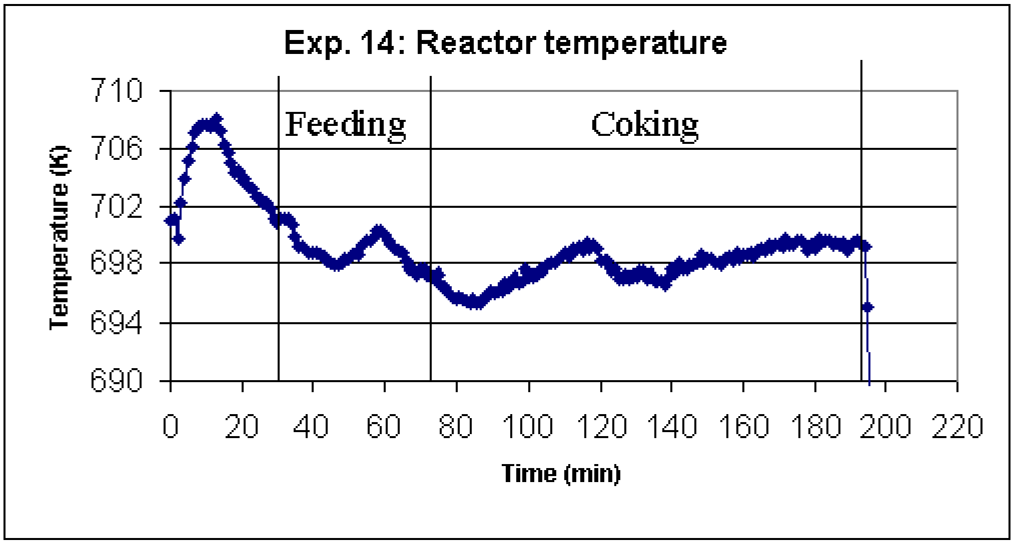

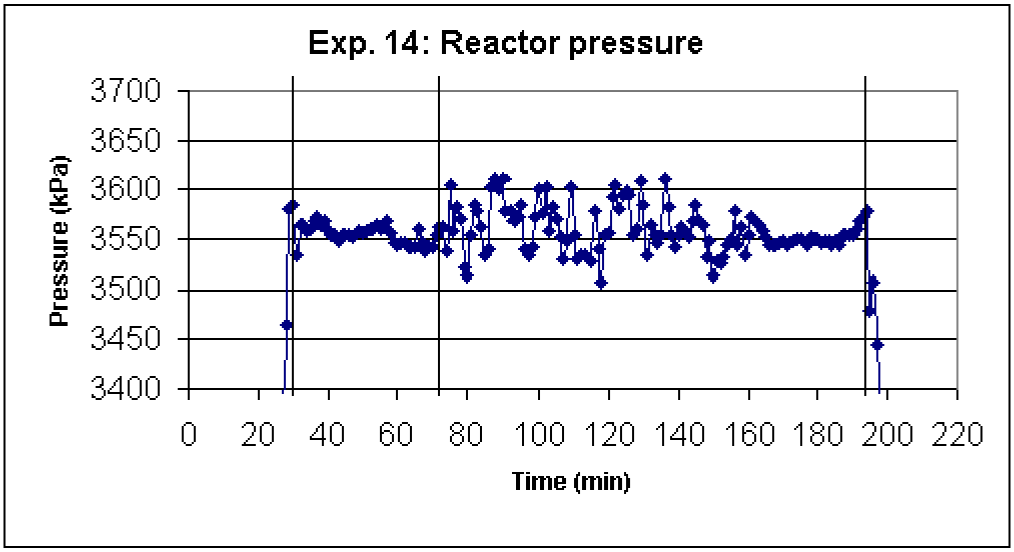

Experiment 15 (E_{15}):

FEEDSTOCK	ABVB	n-dodecane
Wt%	80.15	19.85
PERIOD	FEEDING	COKING
Started (min)	24	69
Finished (min)	69	179

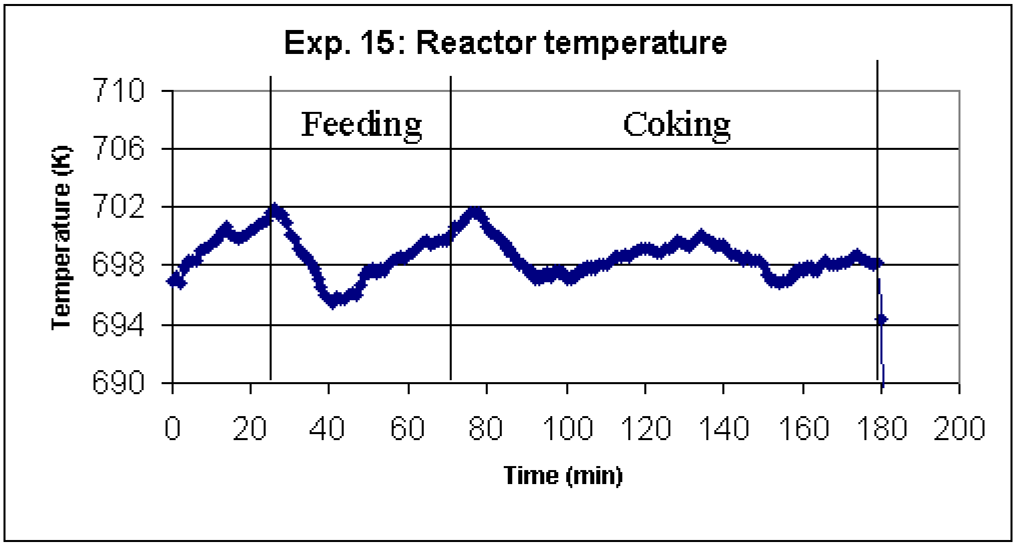

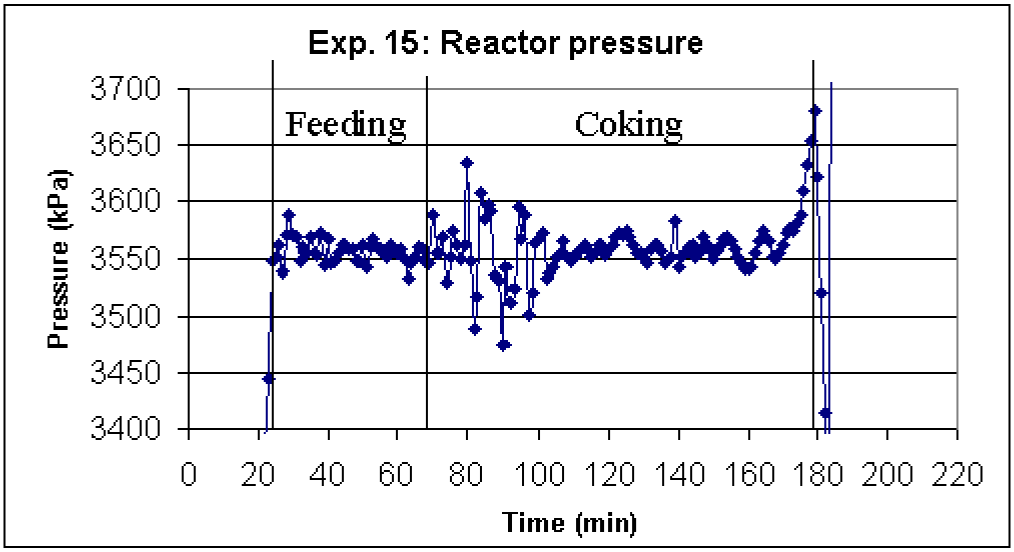

Experiment 19 (E_{19}):

FEEDSTOCK	ABVB	n-dodecane
Wt%	60.06	39.94
PERIOD	FEEDING	COKING
Started (min)	33	78
Finished (min)	78	198

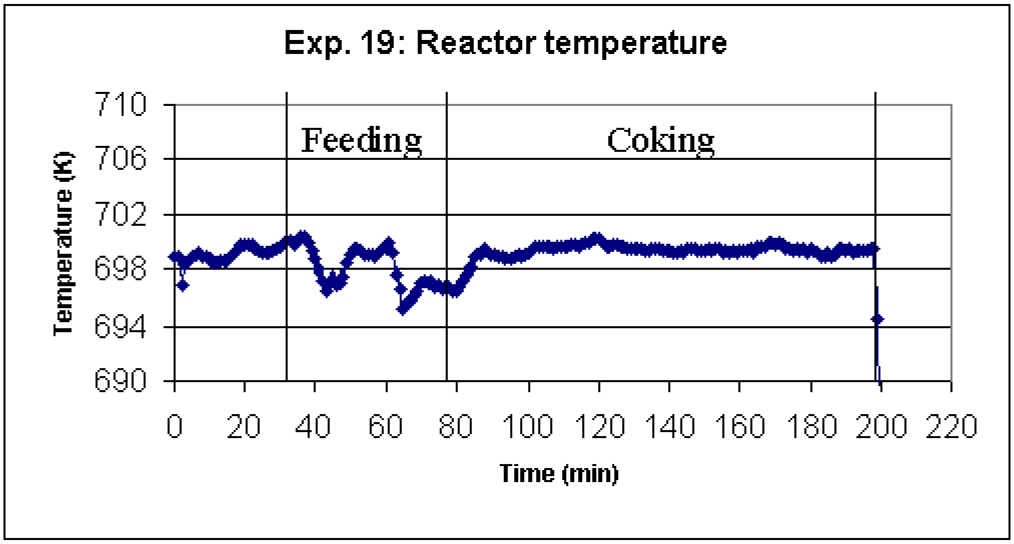

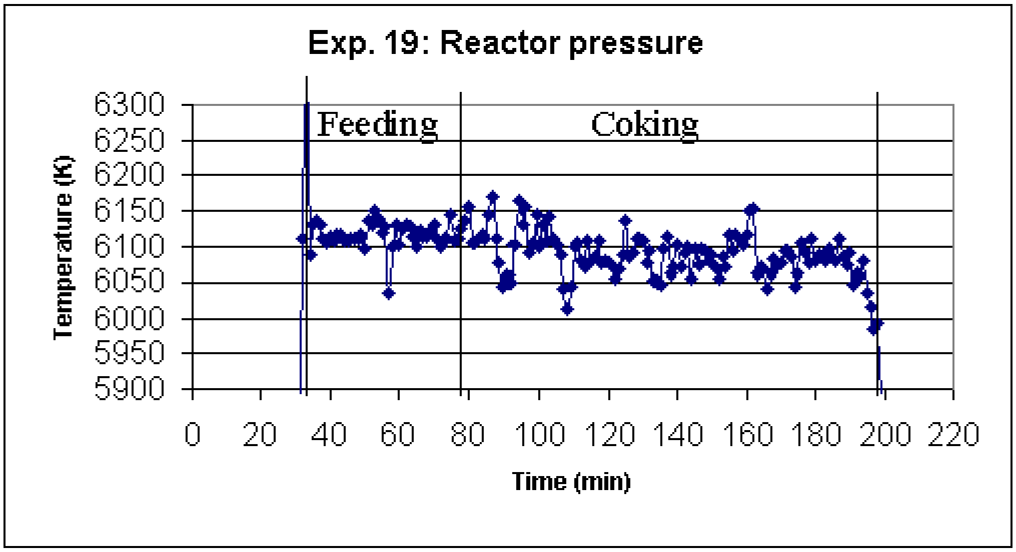

Experiment 20 (E_{20}):

FEEDSTOCK	ABVB	n-dodecane
Wt%	59.68	40.32
PERIOD	FEEDING	COKING
Started (min)	25	70
Finished (min)	70	190

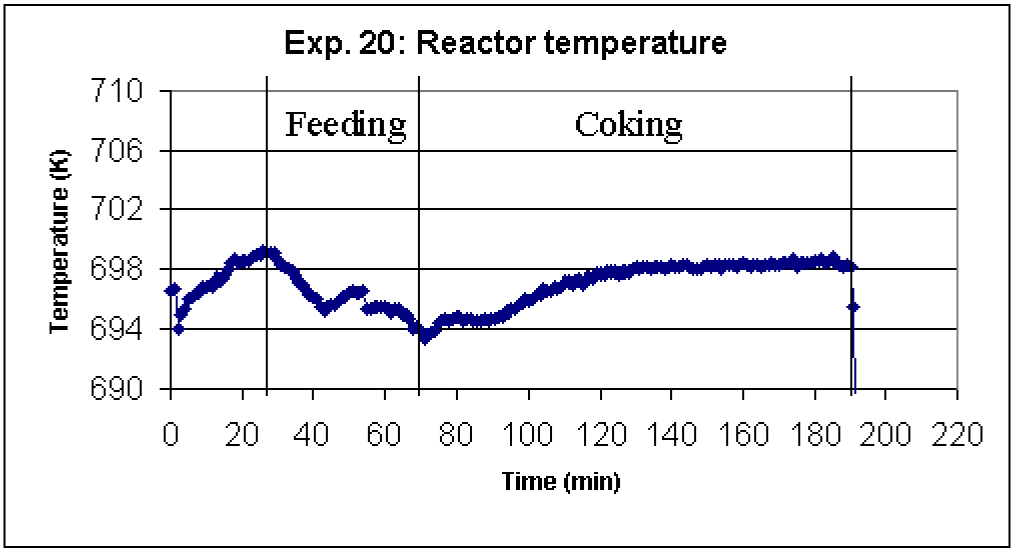

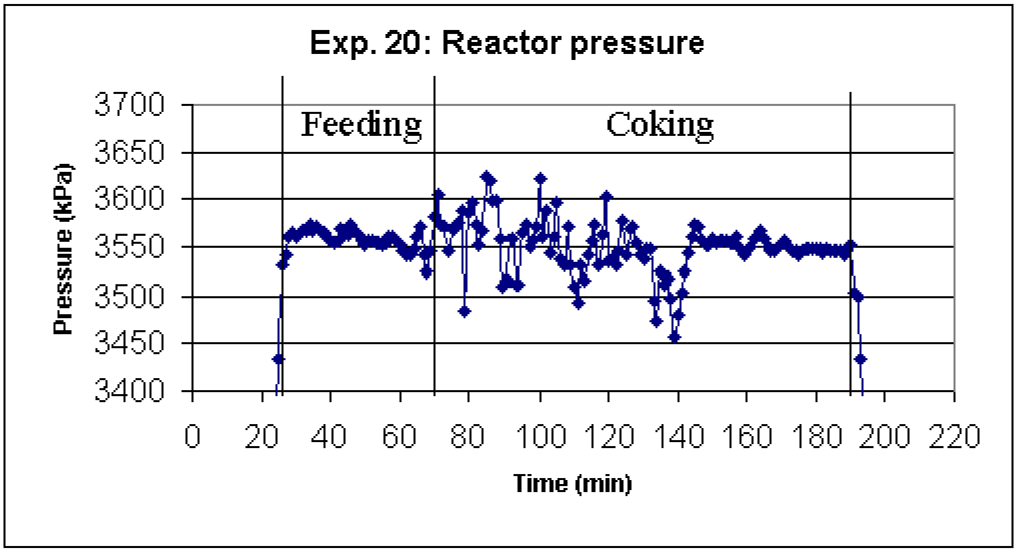

Experiment 21 (E_{21}):

FEEDSTOCK	ABVB	n-dodecane
Wt%	40.03	59.97
PERIOD	FEEDING	COKING
Started (min)	34	79
Finished (min)	79	199

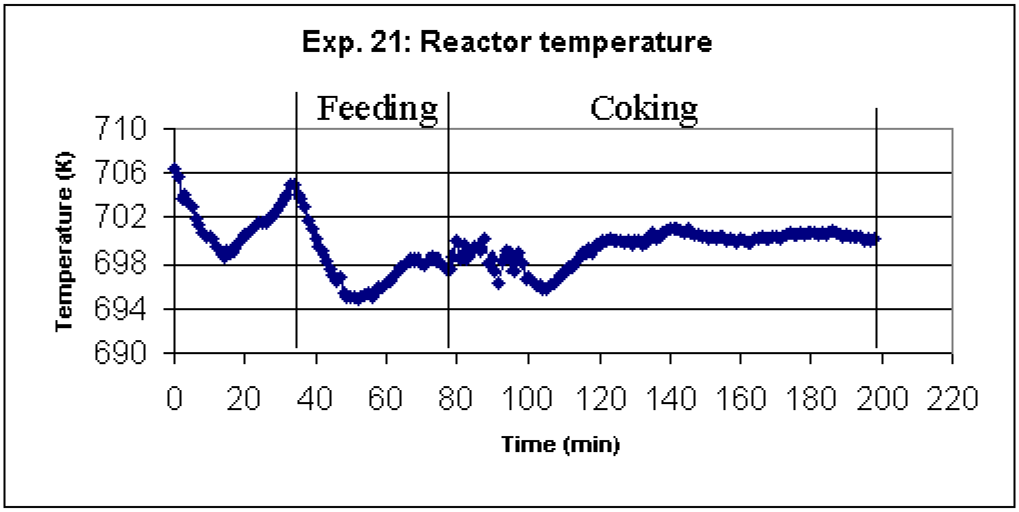

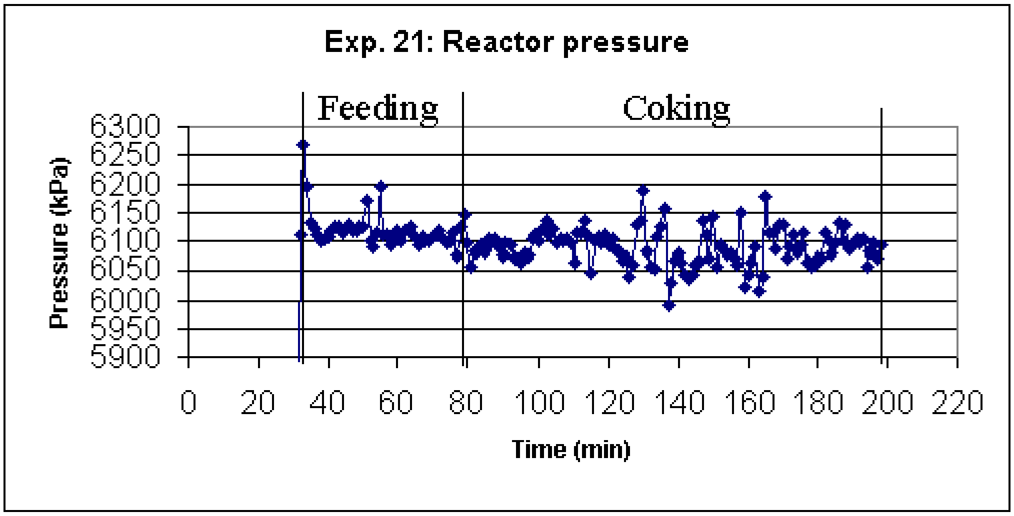

Experiment 22 (E_{22}):

FEEDSTOCK	ABVB	n-dodecane
Wt%	40.05	59.95
PERIOD	FEEDING	COKING
Started (min)	25	70
Finished (min)	70	190

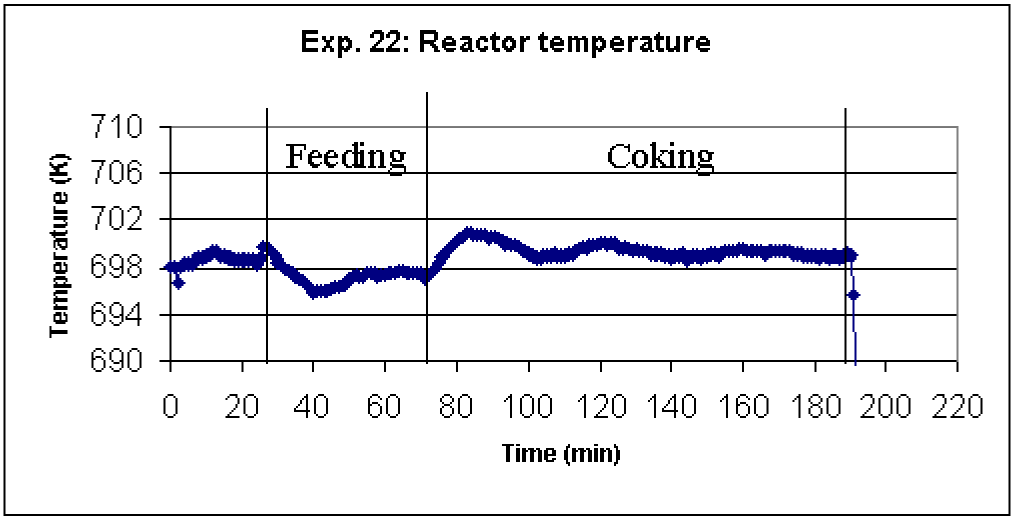

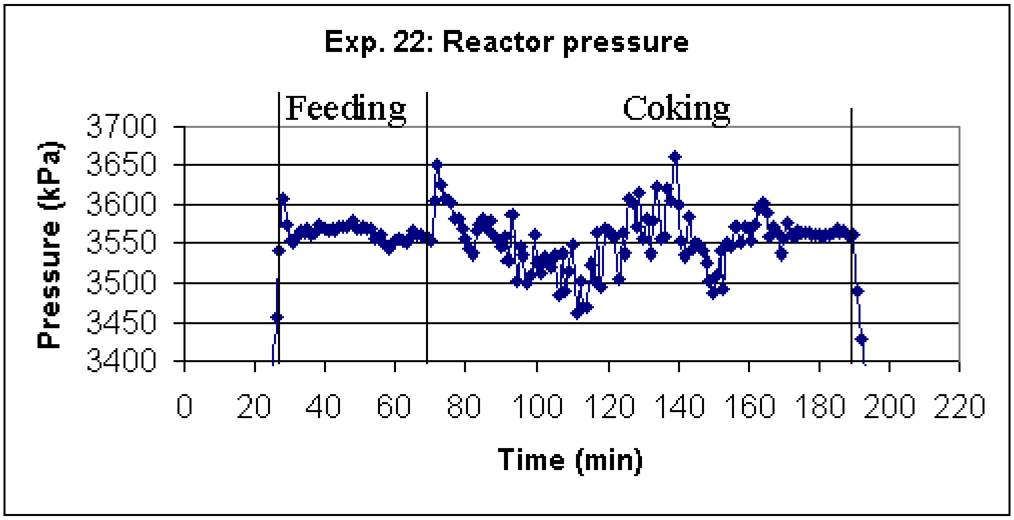

Experiment 24 (E_{24}):

FEEDSTOCK	Cerro Negro	n-dodecane
Wt%	61.22	38.78
PERIOD	FEEDING	COKING
Started (min)	04	49
Finished (min)	49	169

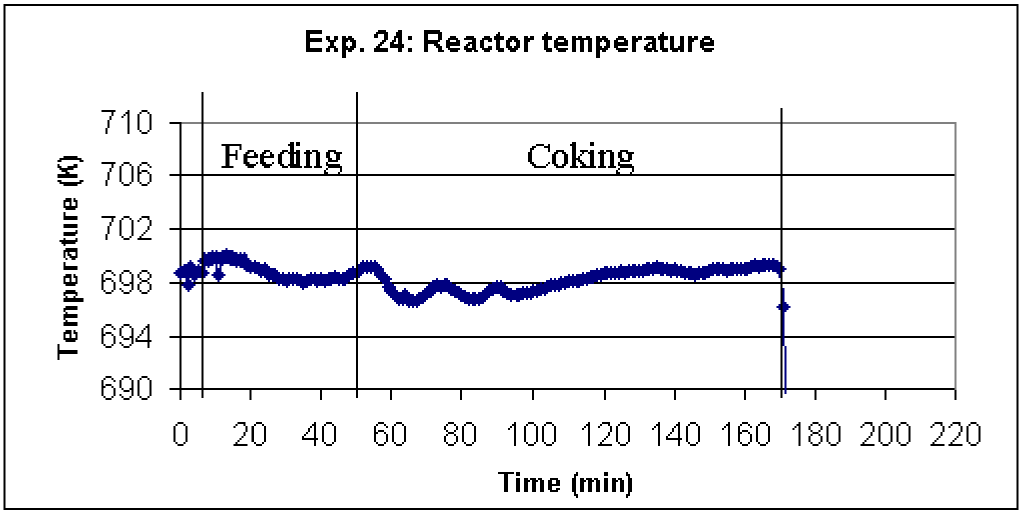

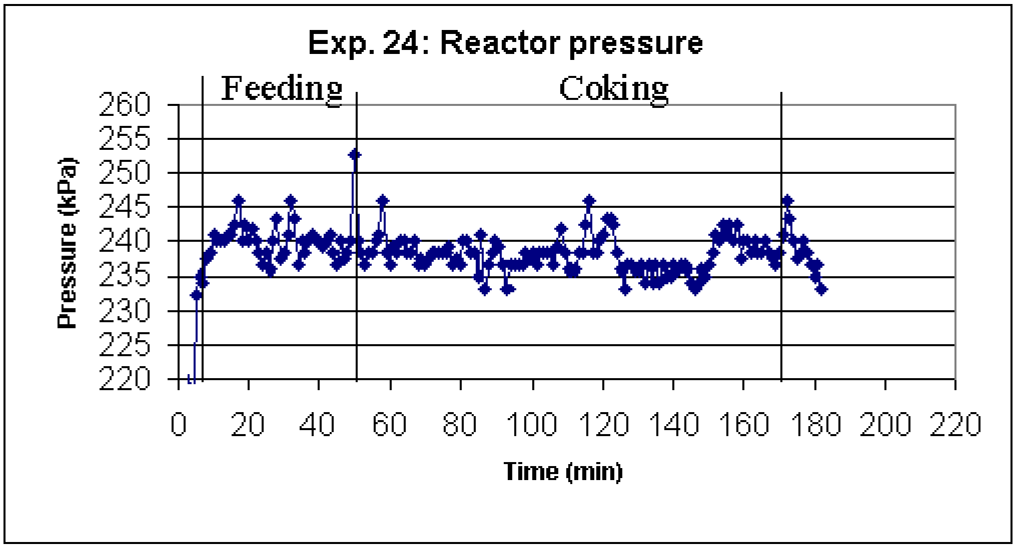

Experiment 25 (E_{25}):

FEEDSTOCK	Heater Feedstock	n-dodecane
Wt%	100.00	0.00
PERIOD	FEEDING	COKING
Started (min)	04	49
Finished (min)	49	169

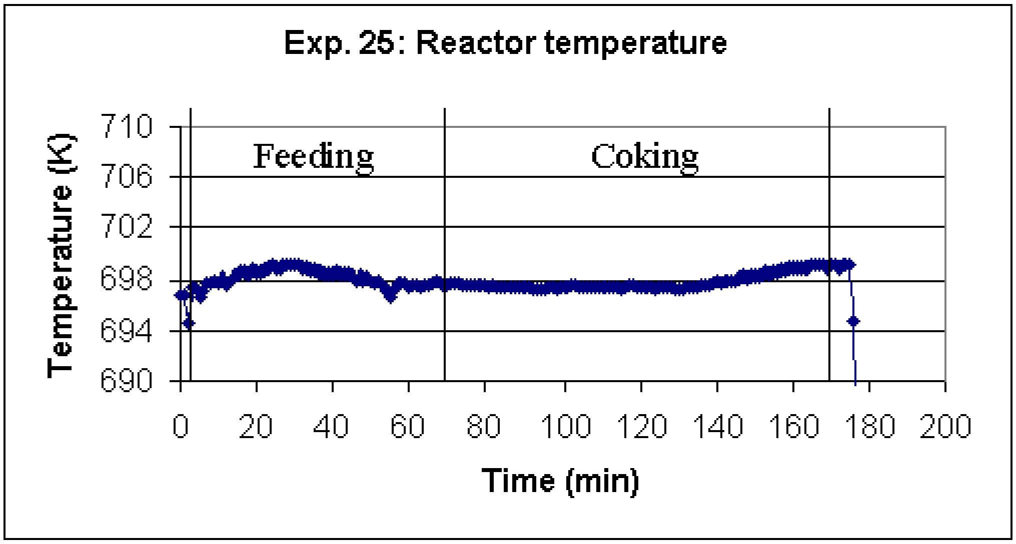

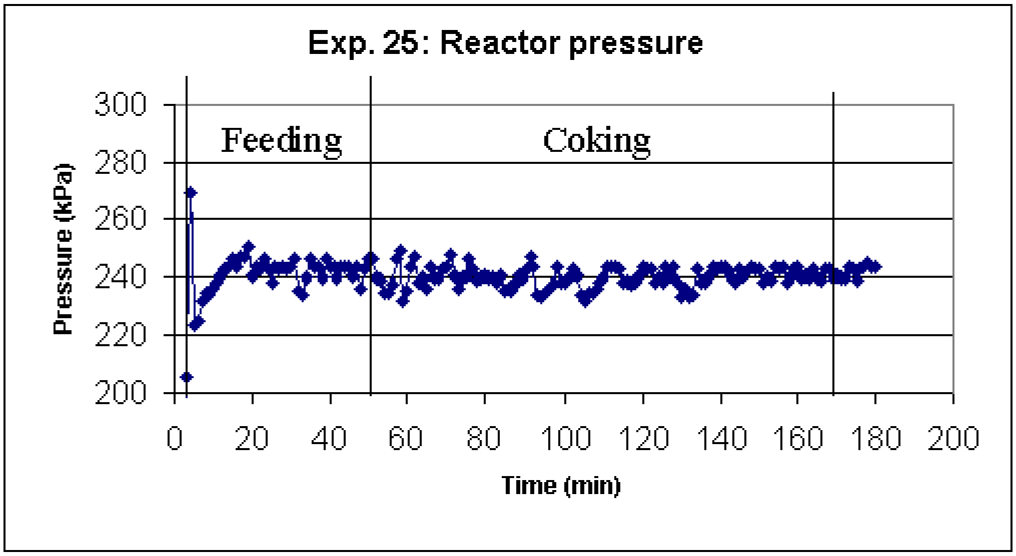

Experiment 26 (E_{26}):

FEEDSTOCK	Heater Feedstock	n-dodecane
Wt%	100.00	0.00
PERIOD	FEEDING	COKING
Started (min)	12	57
Finished (min)	57	177

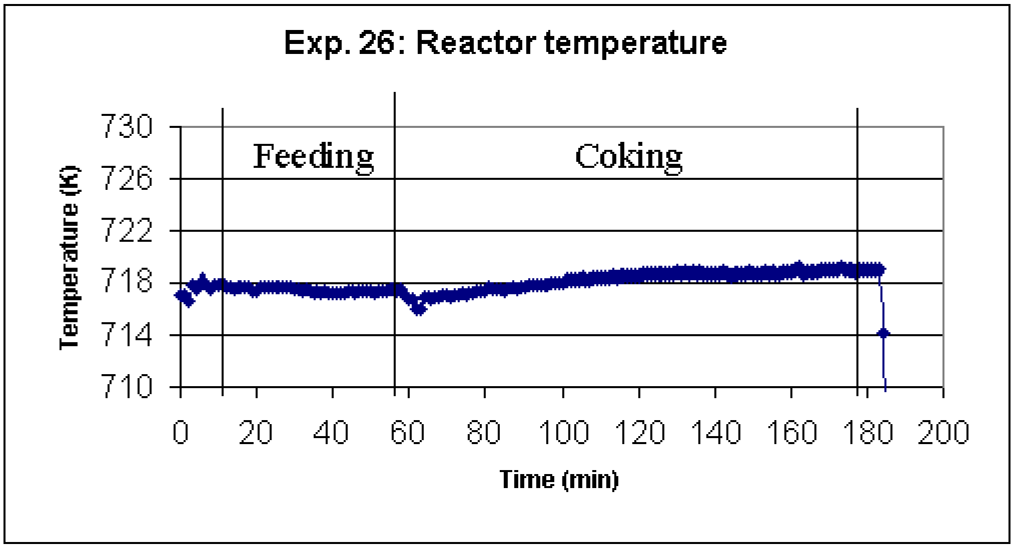

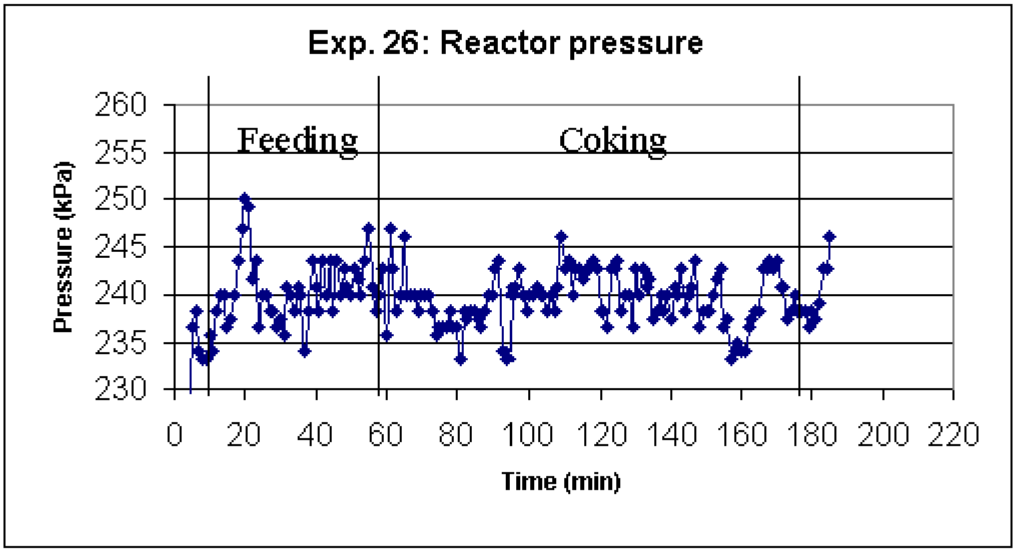

Experiment 27 (E_{27}):

FEEDSTOCK	ABVB	n-dodecane
Wt%	45.00	55.00
PERIOD	FEEDING	COKING
Started (min)	30	75
Finished (min)	75	195

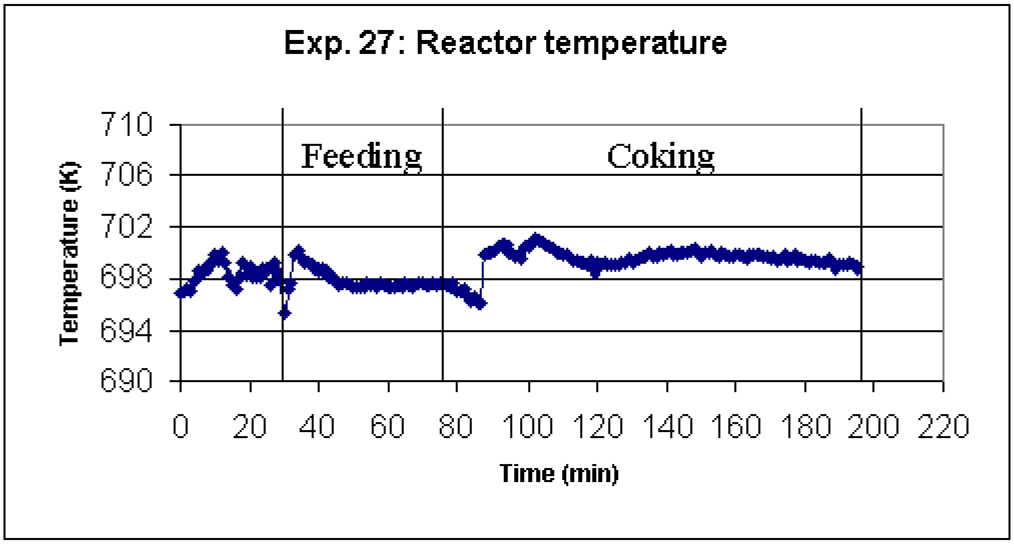

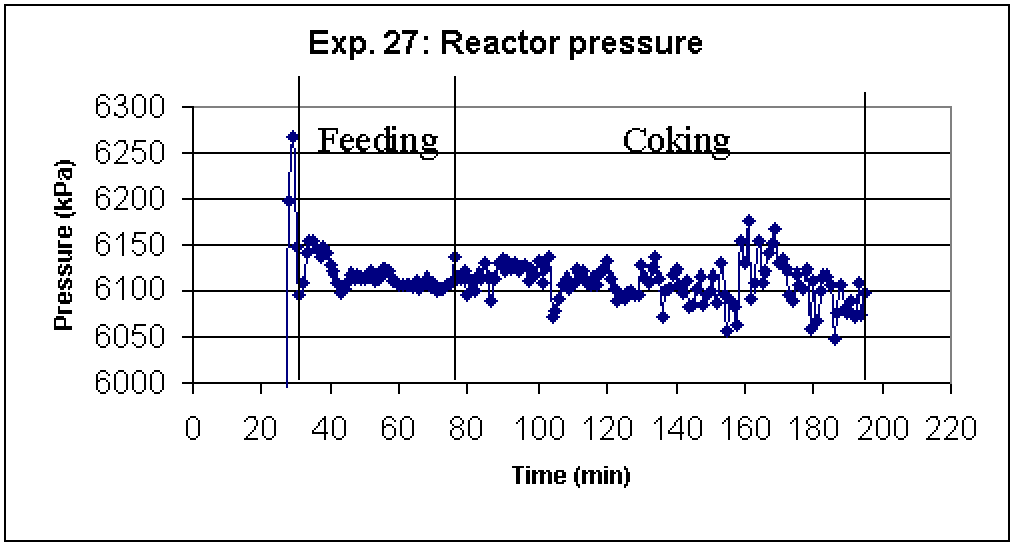

Experiment 28 (E_{28}):

FEEDSTOCK	ABVB	n-dodecane
Wt%	45.00	55.00
PERIOD	FEEDING	COKING
Started (min)	21	66
Finished (min)	66	186

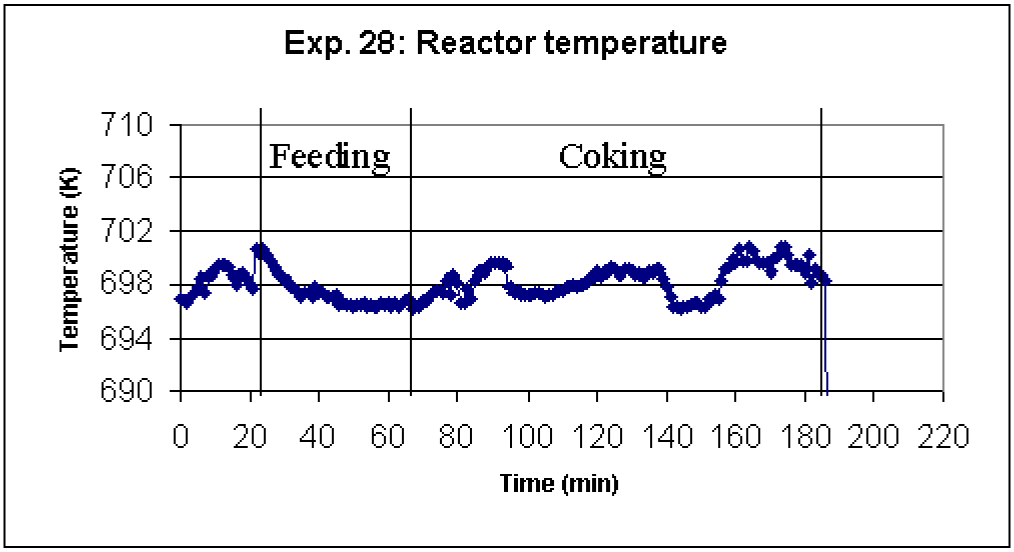

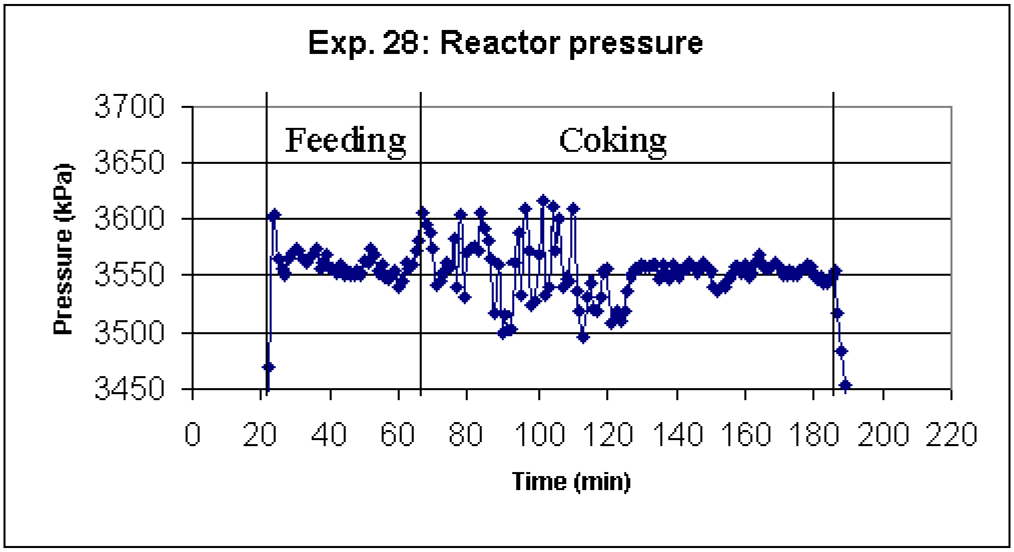

Experiment 29 (E_{29}):

FEEDSTOCK	ABVB	n-dodecane
Wt%	49.96	50.04
PERIOD	FEEDING	COKING
Started (min)	27	72
Finished (min)	72	192

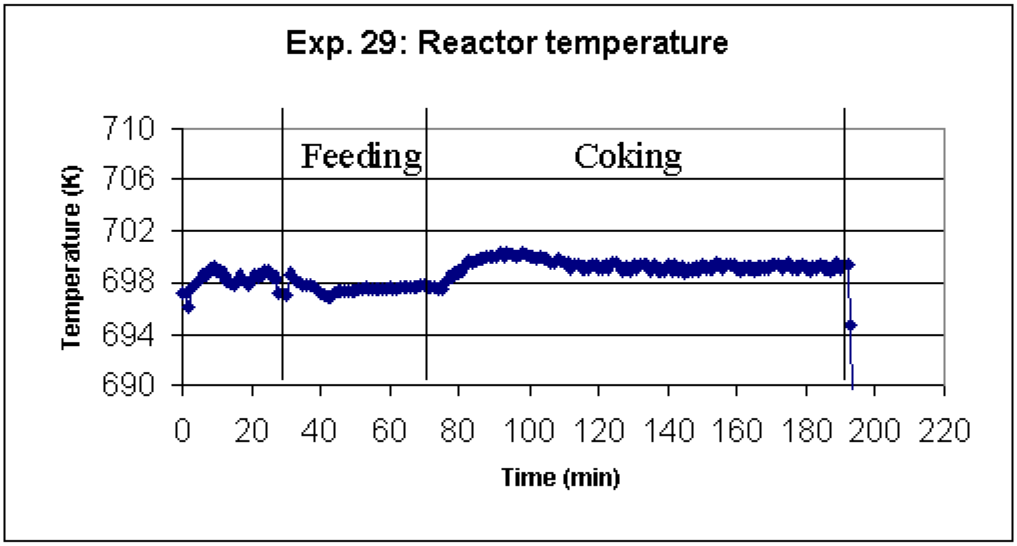

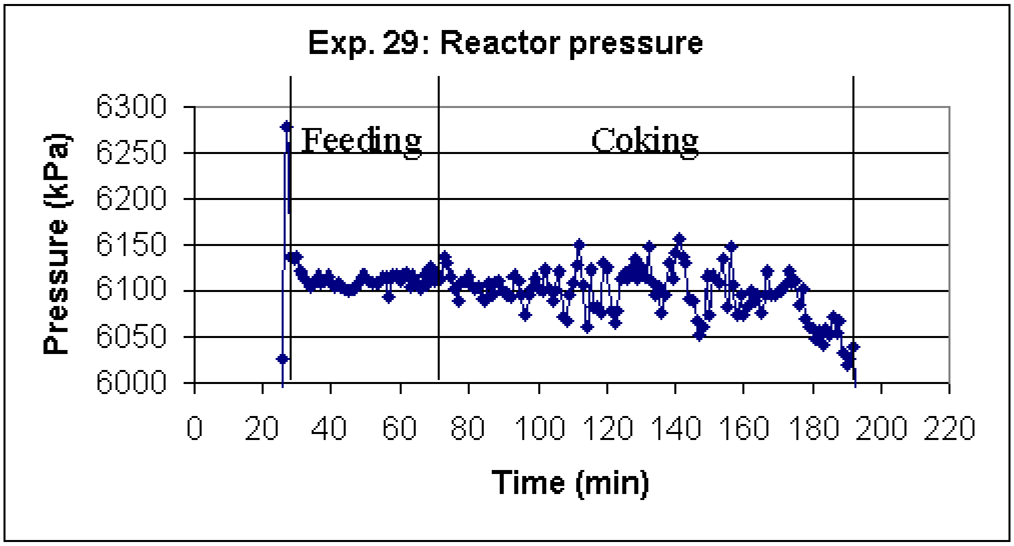

Experiment 30 (E_{30}):

FEEDSTOCK	ABVB	n-dodecane
Wt%	49.98	50.02
PERIOD	FEEDING	COKING
Started (min)	20	65
Finished (min)	65	185

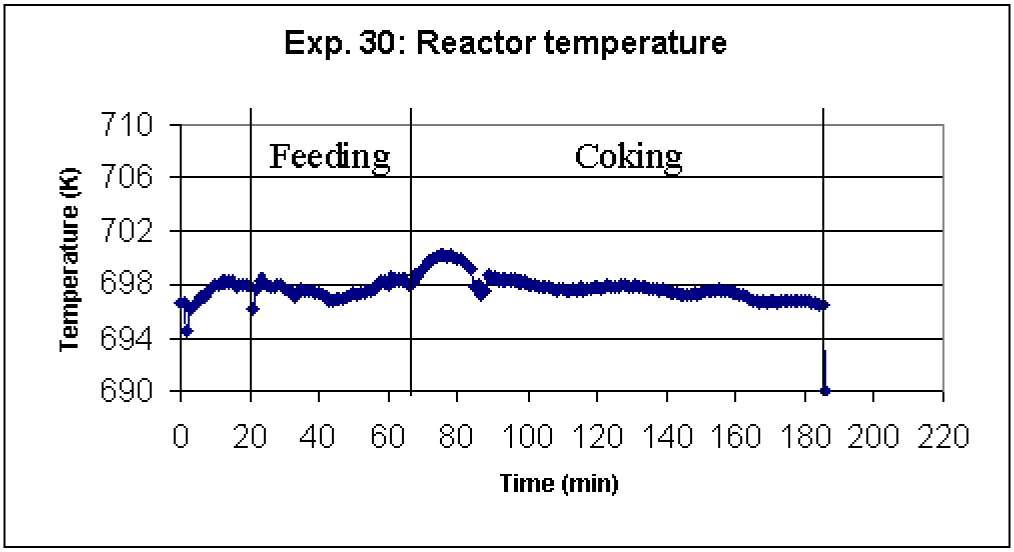

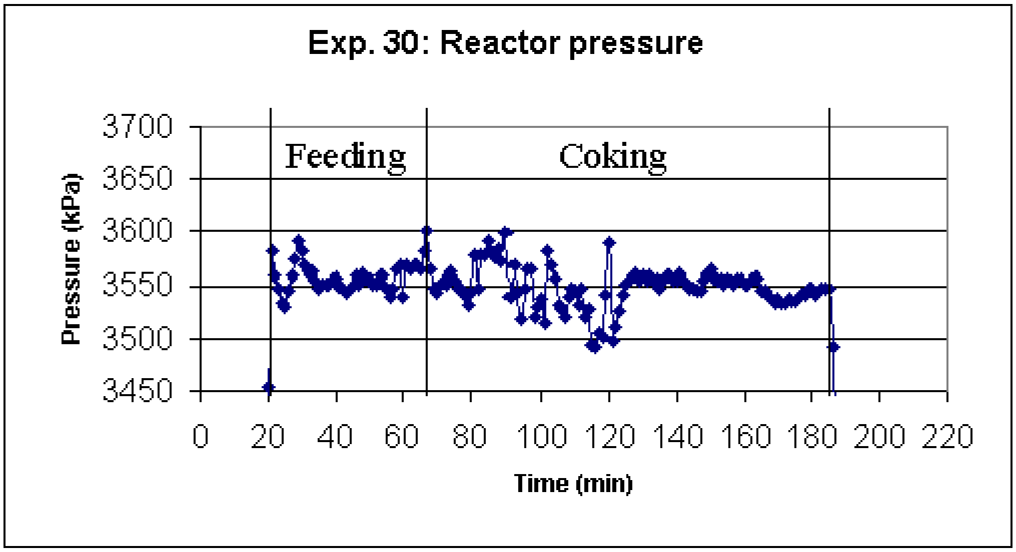

Experiment 31 (E_{31}):

FEEDSTOCK	ABVB	n-dodecane
Wt%	50.00	50.00
PERIOD	FEEDING	COKING
Started (min)	07	52
Finished (min)	52	172

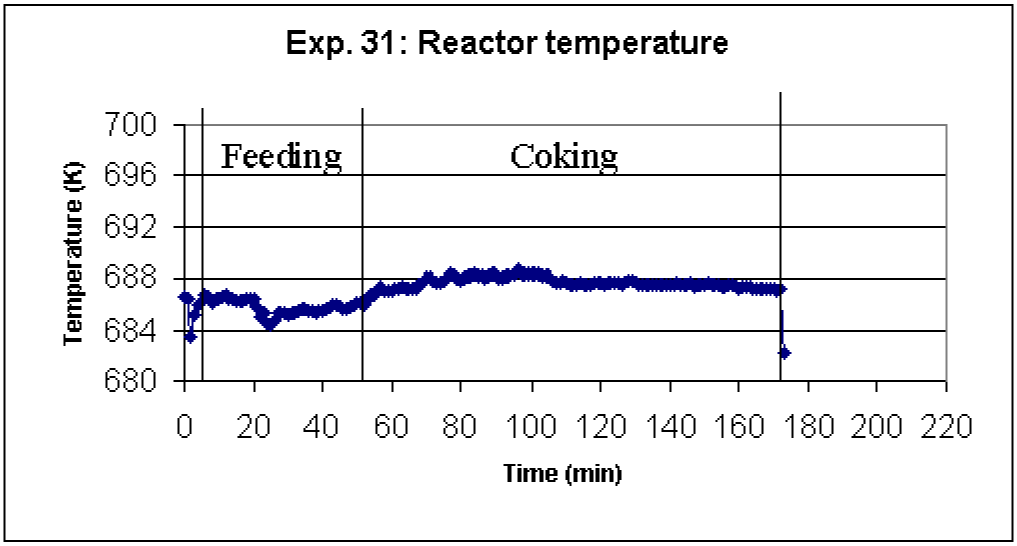

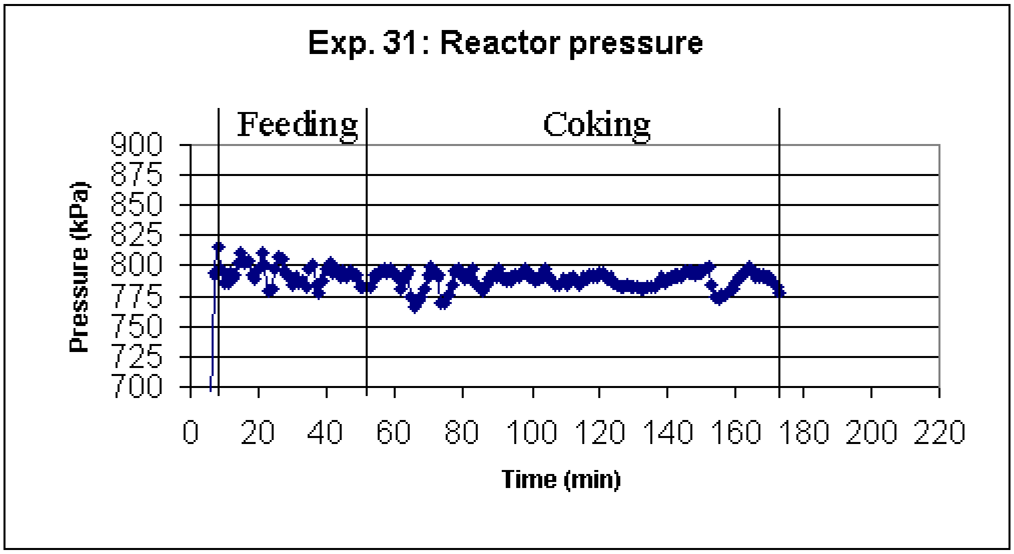

Experiment 32 (E_{32}):

FEEDSTOCK	ABVB	n-dodecane
Wt%	45.00	55.00
PERIOD	FEEDING	COKING
Started (min)	07	52
Finished (min)	52	172

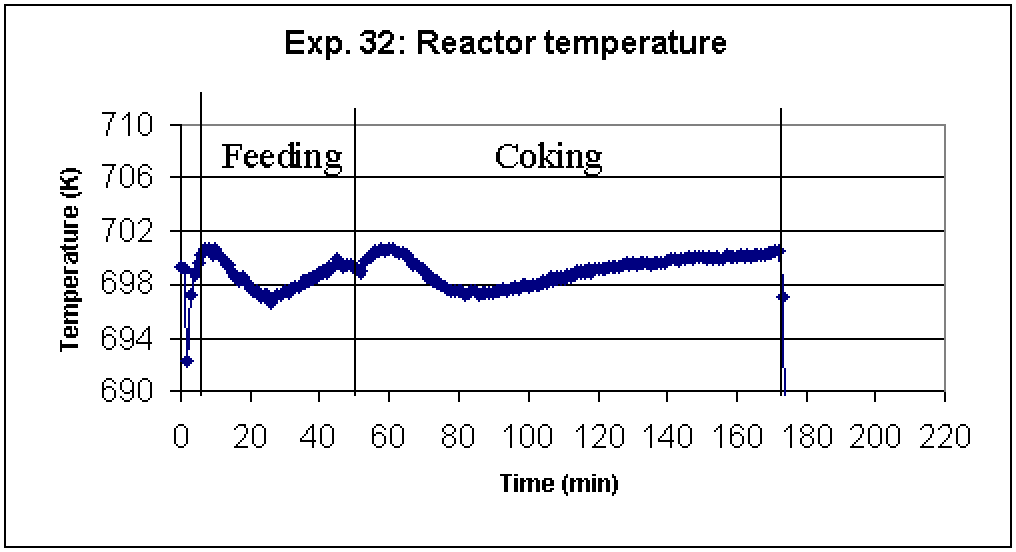

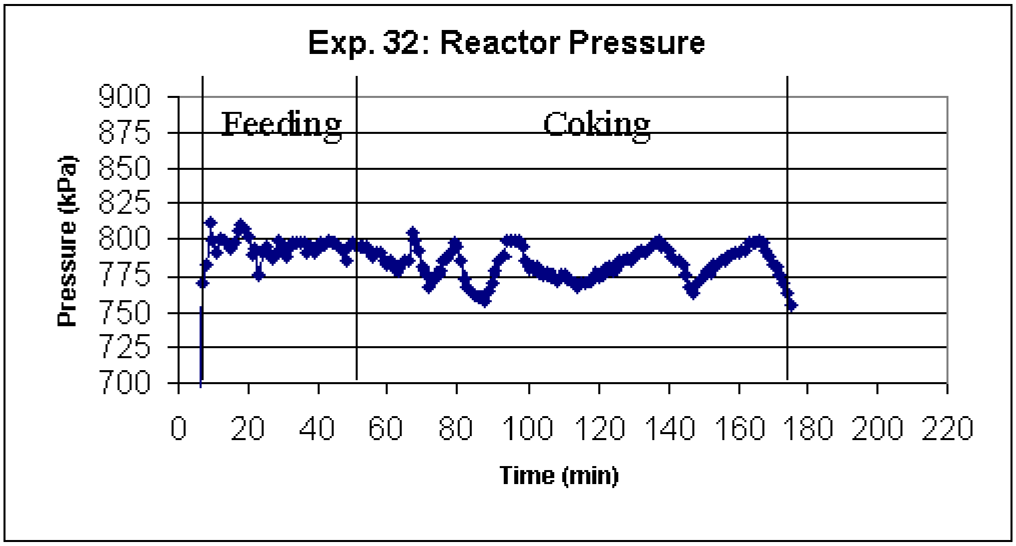

Experiment 33 (E_{33}):

FEEDSTOCK	ABVB	n-dodecane
Wt%	50.00	50.00
PERIOD	FEEDING	COKING
Started (min)	07	52
Finished (min)	52	172

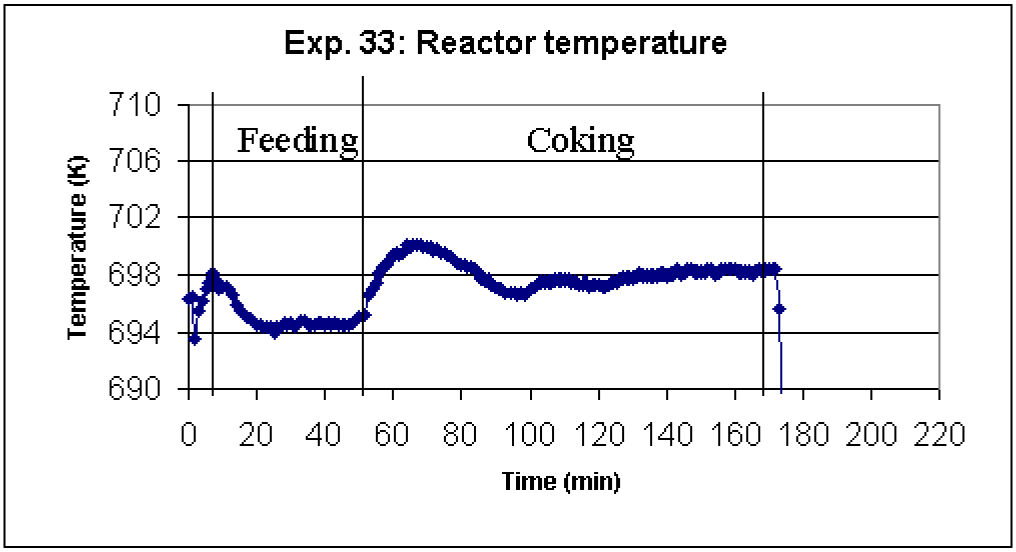

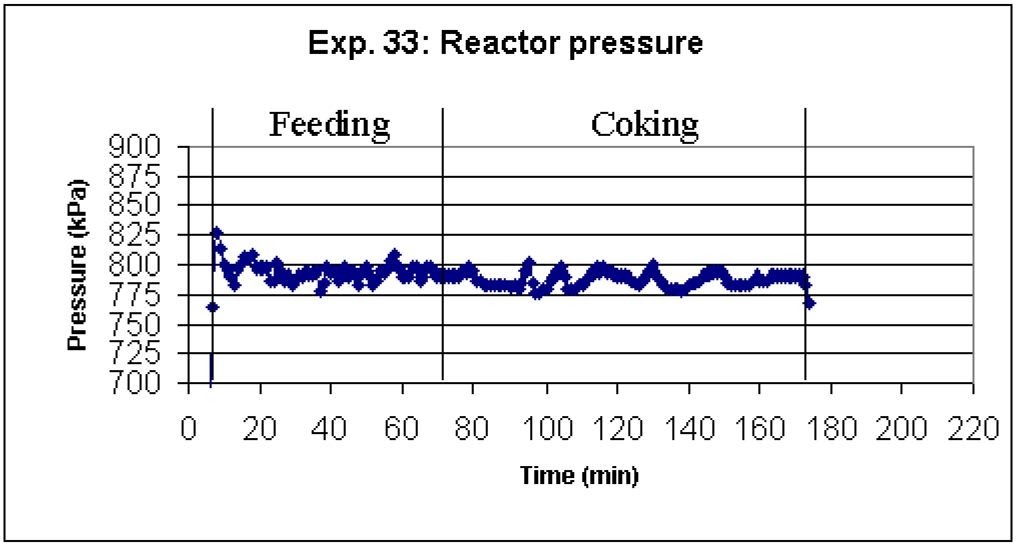

Experiment 34 (E_{34}):

FEEDSTOCK	ABVB	n-dodecane
Wt%	50.00	50.00
PERIOD	FEEDING	COKING
Started (min)	04	49
Finished (min)	49	169

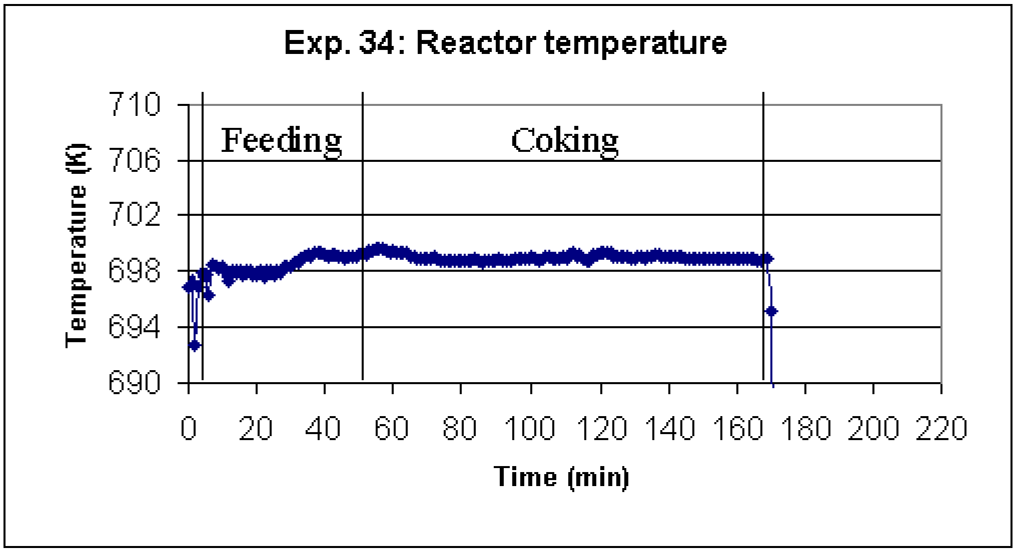

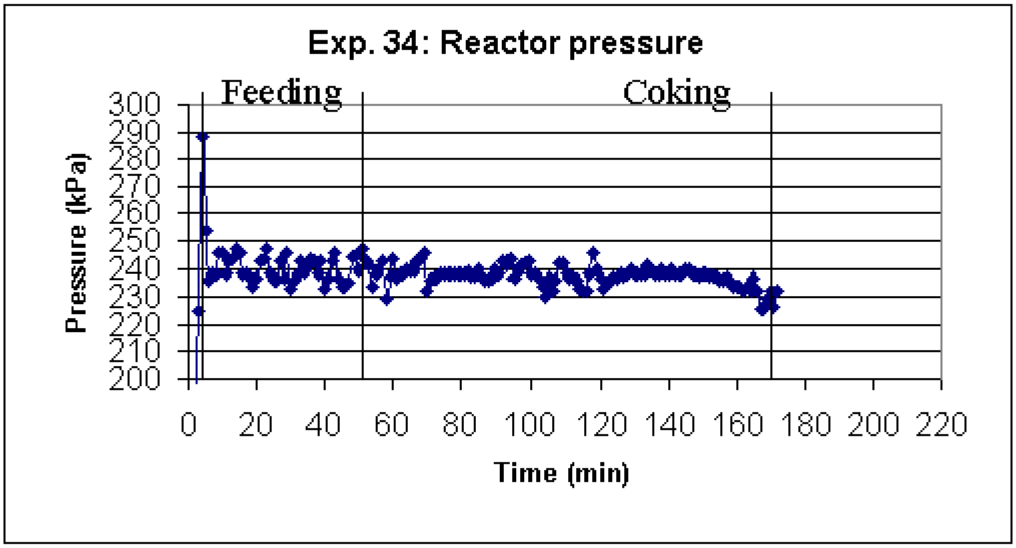

Experiment 35 (E_{35}):

FEEDSTOCK	ABVB	n-dodecane
Wt%	50.00	50.00
PERIOD	FEEDING	COKING
Started (min)	04	49
Finished (min)	49	169

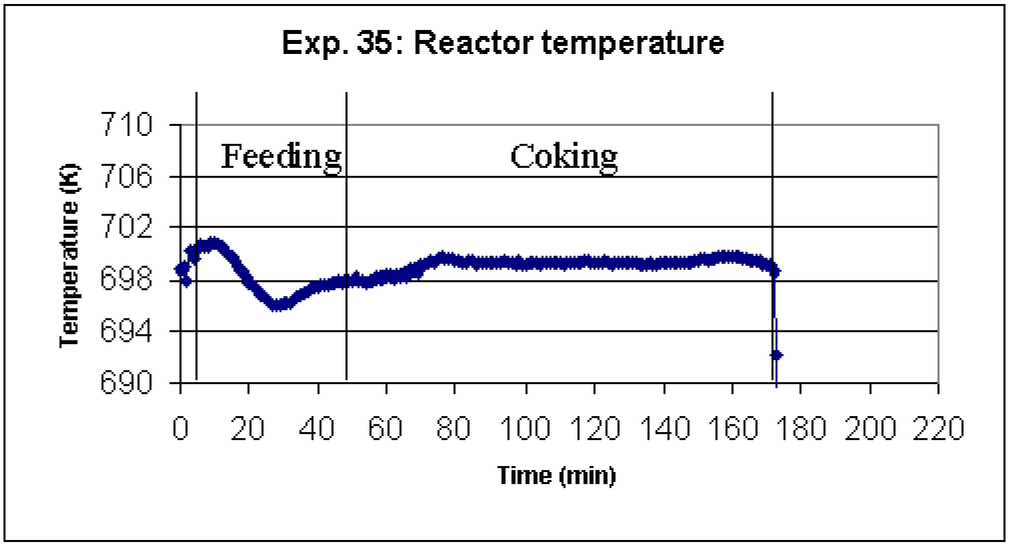

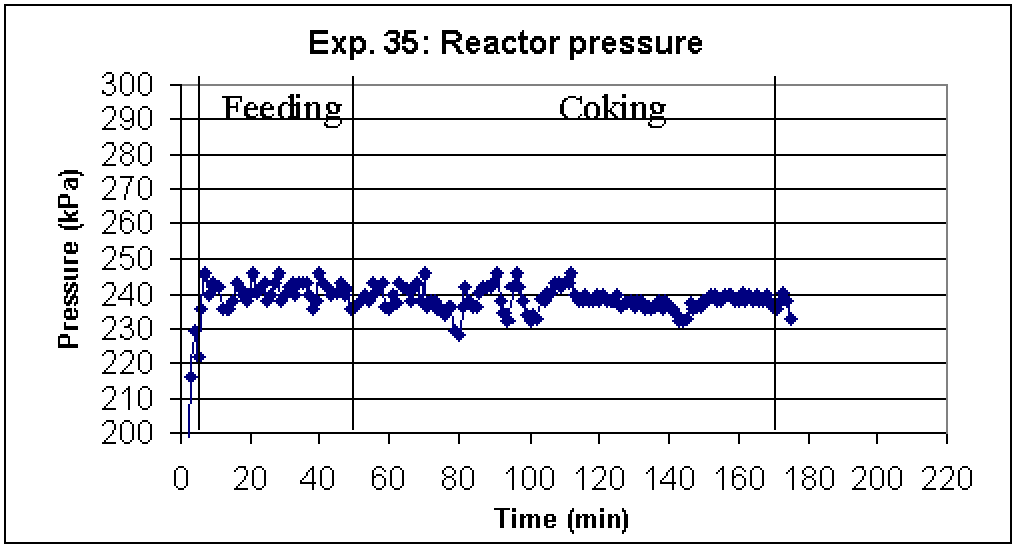

Experiment 36 (E_{36}):

FEEDSTOCK	Heater Feedstock	n-dodecane
Wt%	100.00	00.00
PERIOD	FEEDING	COKING
Started (min)	04	49
Finished (min)	49	169

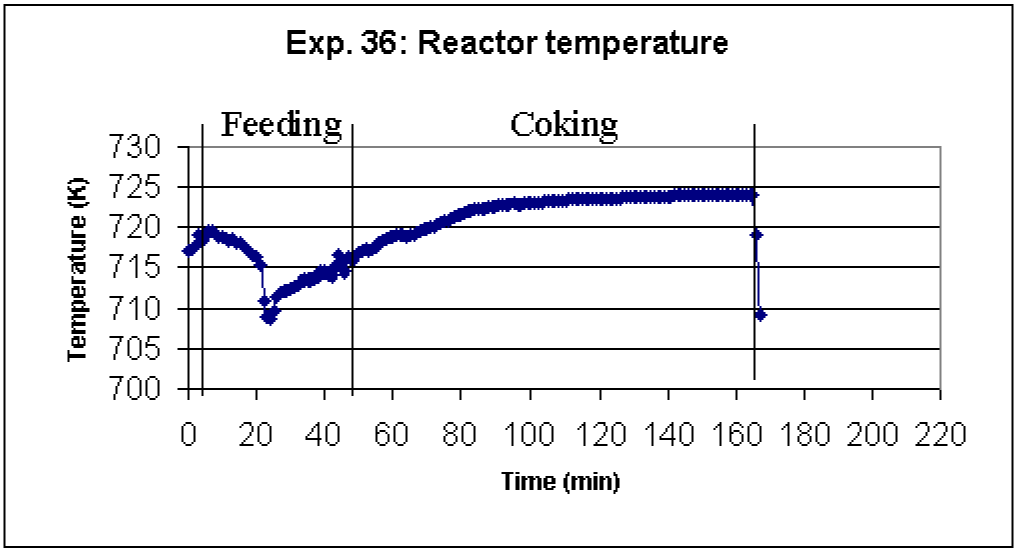

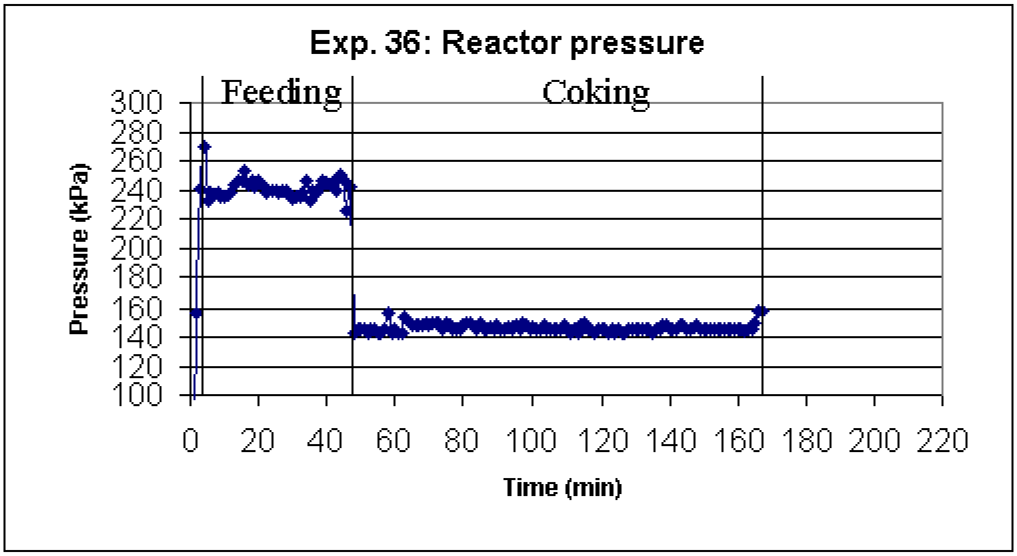

Experiment 38 (E_{38}):

FEEDSTOCK	ABVB	n-dodecane
Wt%	50.00	50.00
PERIOD	FEEDING	COKING
Started (min)	15	60
Finished (min)	60	180

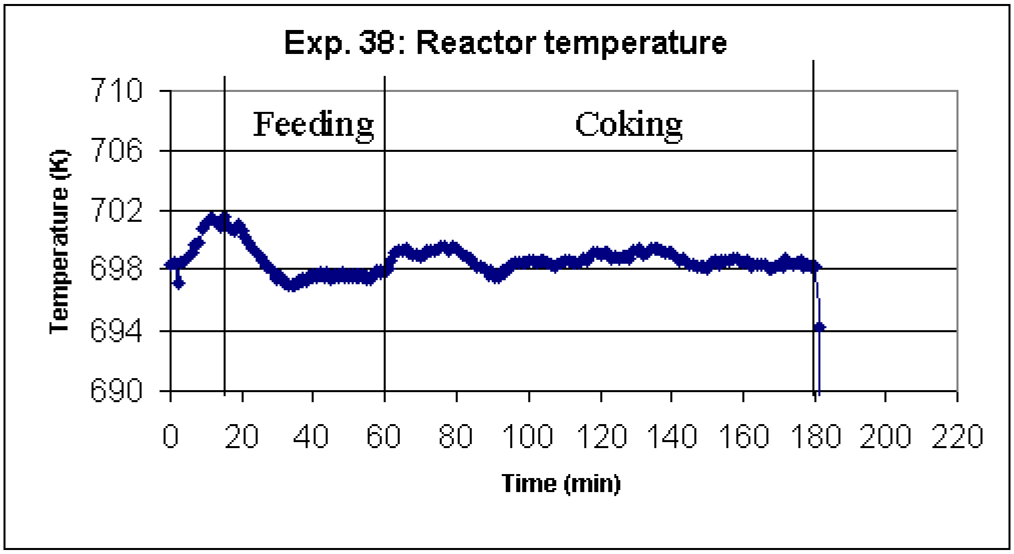

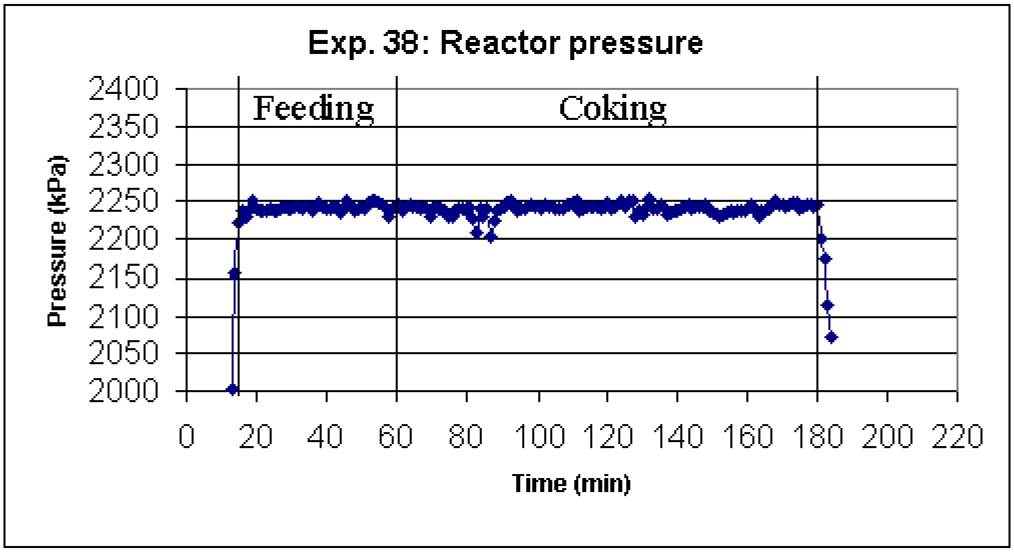

Experiment 40 (E_{40}):

FEEDSTOCK	ABVB	n-dodecane
Wt%	30.01	69.99
PERIOD	FEEDING	COKING
Started (min)	32	77
Finished (min)	77	197

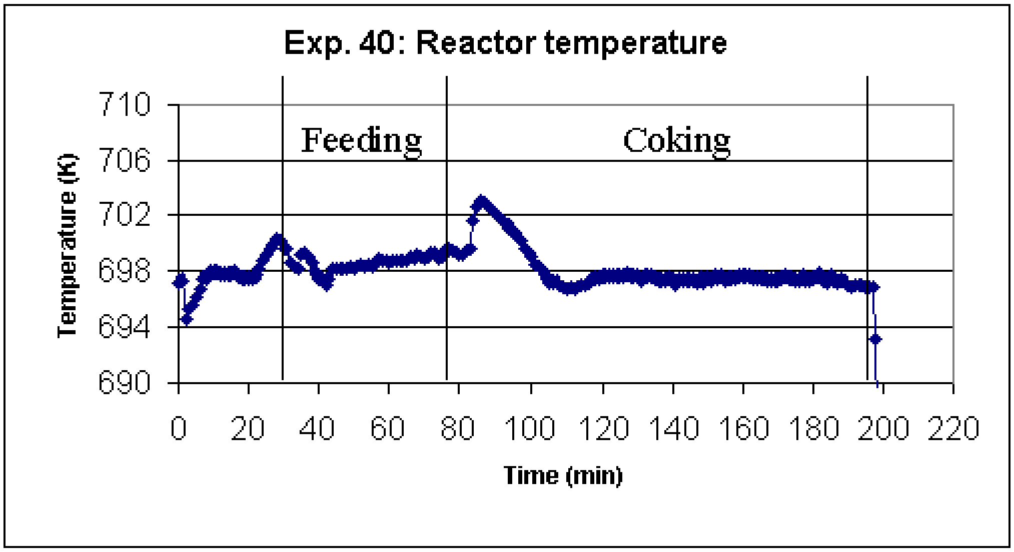

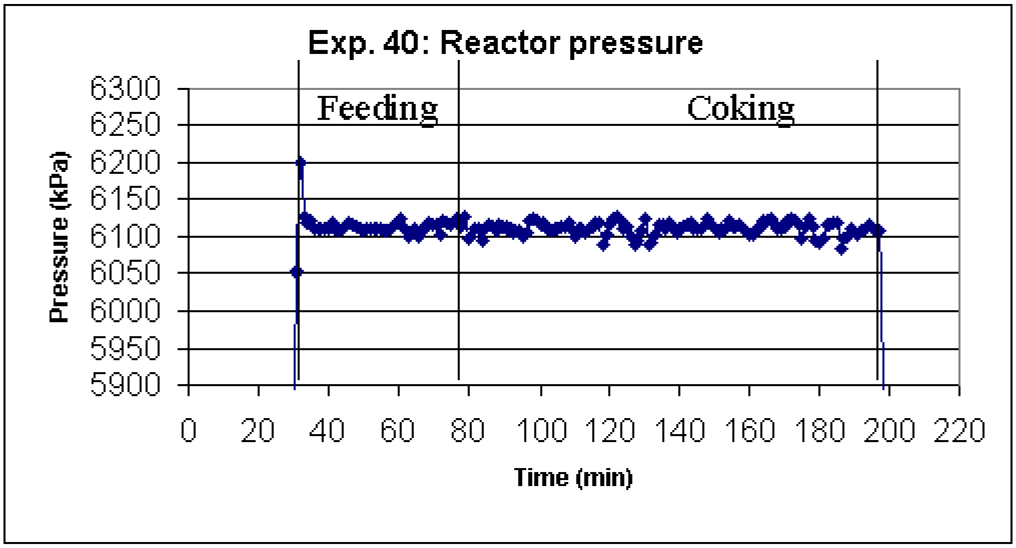

Experiment 41 (E_{41}):

FEEDSTOCK	ABVB	n-dodecane
Wt%	30.01	69.99
PERIOD	FEEDING	COKING
Started (min)	05	50
Finished (min)	50	170

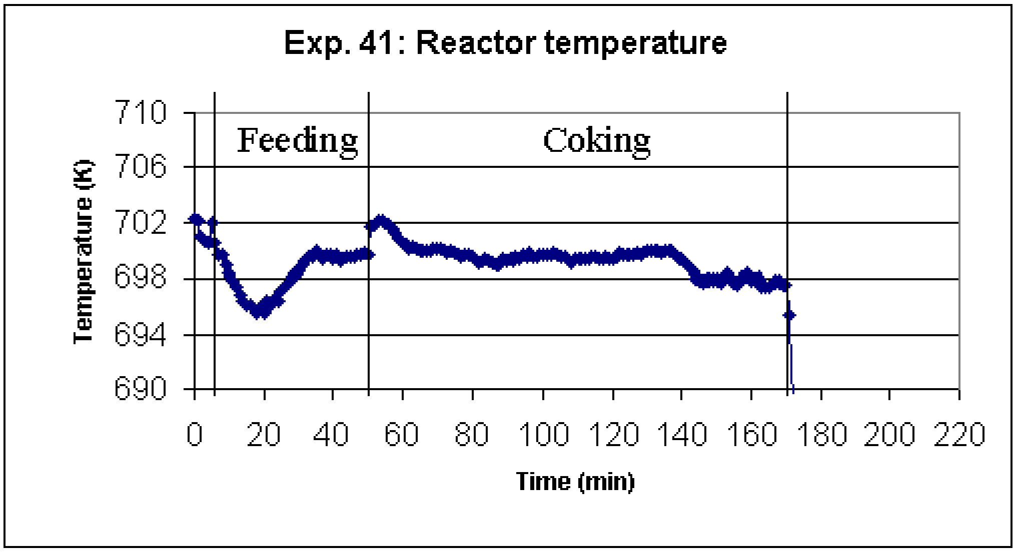

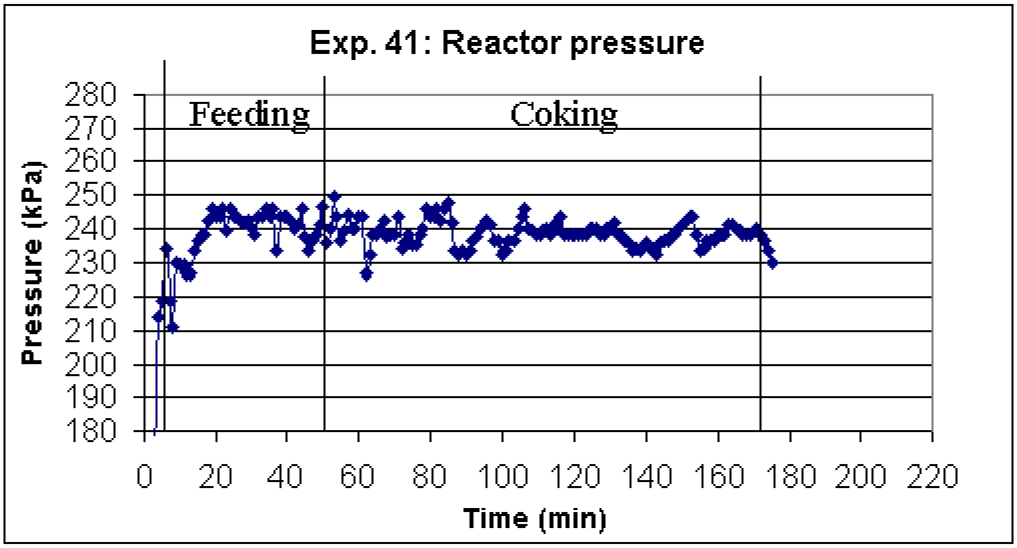

Experiment 42 (E_{42}):

FEEDSTOCK	ABVB	n-dodecane
Wt%	30.00	70.00
PERIOD	FEEDING	COKING
Started (min)	21	66
Finished (min)	66	186

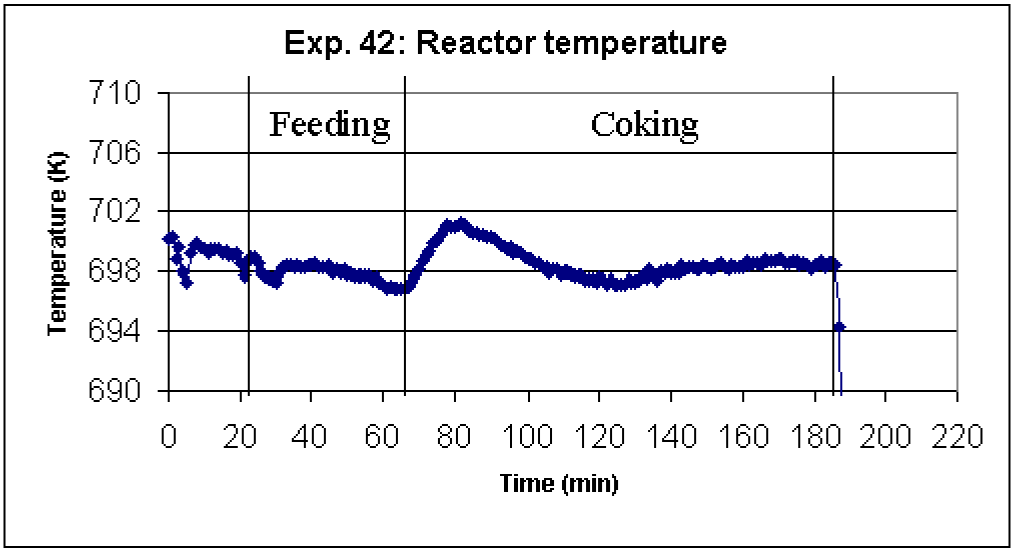

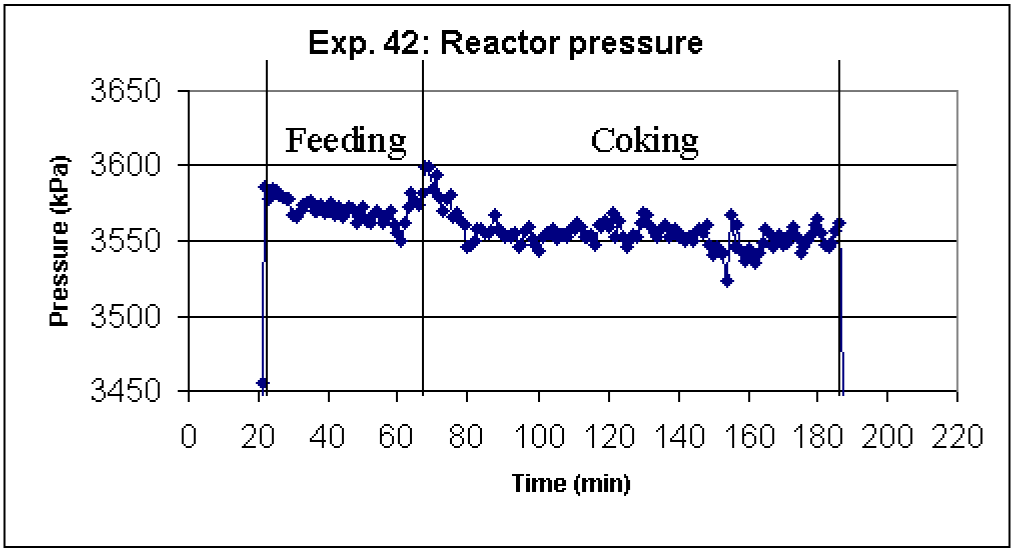

Experiment 43 (E_{43}):

FEEDSTOCK	ABVB	n-dodecane
Wt%	80.00	20.00
PERIOD	FEEDING	COKING
Started (min)	27	72
Finished (min)	72	192

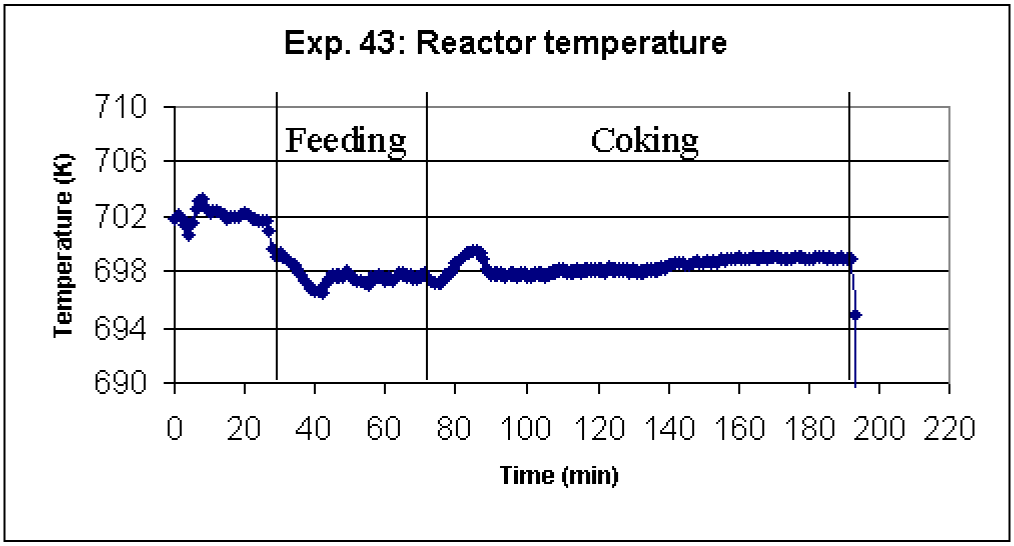

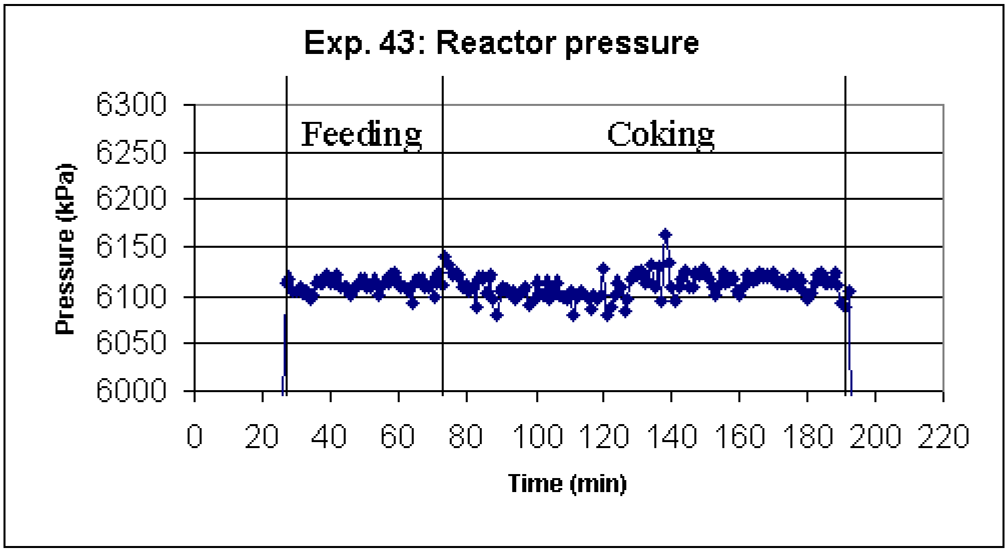

Appendix H: Mass Balances

This Appendix contains the information to complete the mass balance for each experiment. First the acronyms used in the mass balance data sheet are presented and explained. Table H-1 summarizes the mass balances (general mass balance and mass balance based on the vacuum residue processed) for each experiment. Finally, the detailed mass balance data sheet for each experiment is presented.

In Table H-1 and in each specific mass balance data sheet, the following variables and calculations are indicated:

LP: weight of the liquid products (g) collected at the end of the experiment.

FV_1: weight of the feed vessel (g) before the experiment starts.

FV_2: weight of the feed vessel (g) at the end of the experiment.

LR: weight of feedstock accumulated in lines before the reactor.

SS_1: weight of KOH solution (g) charged to the hydrogen sulphide scrubber before starting the experiment.

SS_2: weight of material (g) in the hydrogen sulfide scrubber after the experiment has finished.

$nC_{12}V_1$: Weight of n-dodecane (g) added to the n-C_{12} vessel before starting the experiment.

$nC_{12}V_2$: Weight of n-dodecane (g) remaining in the n-C_{12} vessel after the experiment has finished.

Coke: weight of coke (g) collected at the end of the experiment.

$X_{residue}$: weight fraction of residue in the feedstock.

$X_{n\text{-}dodecane}$: weight fraction of n-dodecane in the feedstock.

GCY: General coke yield.

GDY: General distillates yield.

GSY: General sulphur yield.

MB: General mass balance.

GG: gases and losses.

CY: sulphur yield based on the quantity of petroleum residue processed.

DY: distillate yield based on the petroleum residue processed.

SY: sulphur yield based on the petroleum residue processed.

G: gases and losses yield based on the petroleum residue processed.

Table H-1: Summary of Mass balances

Exp ID	General Mass Balance					Petroleum Mass Balance			
	GCY	GDY	GSY	MB	GGY	CY	DY	SY	GY
E_{09}	19.46	72.70	0.54	92.70	7.30	39.71	44.28	1.11	14.91
E_{11}	26.71	62.82	0.97	90.50	9.50	40.54	43.56	1.48	14.42
E_{12}	18.73	71.03	0.09	89.84	10.16	49.65	23.18	0.23	26.93
E_{14}	8.64	75.99	0.16	84.79	15.21	36.15	-0.51	0.67	63.69
E_{15}	25.62	57.86	0.19	83.67	16.33	48.18	20.74	0.37	30.71
E_{19}	11.65	80.80	0.02	92.46	7.54	34.47	43.17	0.05	22.31
E_{20}	18.44	71.59	0.00	90.03	9.97	47.71	26.48	0.01	25.80
E_{21}	5.16	85.03	0.04	90.23	9.77	23.70	31.22	0.21	44.88
E_{22}	9.30	81.98	0.01	91.29	8.71	36.54	29.19	0.06	34.21
E_{24}	19.08	74.85	0.50	94.43	5.57	35.81	52.79	0.93	10.46

E_{25}	23.48	66.34	0.55	90.37	9.63	32.61	53.25	0.76	13.38
E_{26}	23.08	68.09	0.66	91.83	8.17	30.26	58.17	0.87	10.71
E_{27}	5.83	82.94	0.03	88.80	11.20	23.01	32.65	0.11	44.23
E_{28}	14.60	76.12	0.14	90.86	9.14	49.18	19.58	0.48	30.77
E_{29}	7.99	81.79	0.05	89.83	10.17	27.94	36.37	0.16	35.54
E_{30}	15.75	73.86	0.15	89.76	10.24	49.12	18.48	0.47	31.92
E_{31}	19.45	69.53	0.29	89.27	10.73	47.87	25.00	0.47	26.42
E_{32}	15.35	72.12	0.28	87.76	12.24	41.94	23.86	0.78	33.42
E_{33}	17.10	73.30	0.37	90.76	9.24	41.27	35.54	0.90	22.29
E_{34}	13.45	78.76	0.28	92.49	7.51	31.73	49.88	0.66	17.73
E_{35}	12.84	77.45	0.45	90.73	9.27	33.04	41.95	1.15	23.86
E_{36}	21.22	65.78	0.56	87.57	12.43	25.11	59.53	0.67	14.70
E_{38}	17.54	73.97	0.06	91.56	8.44	47.90	28.91	0.15	23.03
E_{40}	3.51	86.80	0.01	90.32	9.68	22.13	16.75	0.07	61.06
E_{41}	8.49	83.67	0.26	92.42	7.58	34.19	34.24	1.05	30.52
E_{42}	6.00	86.04	0.00	92.04	7.96	33.27	22.58	-0.02	44.17
E_{43}	19.05	64.99	0.10	84.13	15.87	41.60	23.53	0.22	34.66

Date	11-16-2001			
Experiment ID	9			
Name	n-C12 40 w% 100 psig			
Vacuum residue ID	ABVB			
1.- KOH solution preparation:	Recipient filled	Recipient emptied	w%	
1.1.- KOH (g)				
1.2.- Water (g)	62.33	0.24		
SS_1	**TOTAL (g)**	**62.09**		
2.- Feed preparation	**FV_1**	**FV_2**	w%	
2.1.- n-Dodecane (g)	286.77	208.12	40.05	$X_{n-dodecane}$*100
2.2.- Vacuum residue (g)	429.27	311.54	59.95	$X_{Residue}$*100
	716.04	519.66		
	TOTAL (g)	**196.38**		
3.- Unit preparation	Recipient emptied	Recipient filled		
3.1.- n-Dodecane used to increase pressure (g)	60.77	0.28		
$nC_{12}V_1$	**TOTAL (g)**	**60.49**		
4.- Shutdown	Empty recipient	Recipient filled		
4.1.- n-Dodecane remaining in n-Dodecane vessel (g)	139.54	156.54		
$nC_{12}V_2$	**TOTAL (g)**	**17**		
4.2.- Flusing mixture collected (g)	139.53	141.52	Purge of pump and lines before reactor	
LR	**TOTAL (g)**	**1.99**		
4.3.- Liquid products (g)	139.53	312.47		
LP	**TOTAL (g)**	**172.94**		
4.4.- Coke collected (g)	138.72	**185**		
Coke	**TOTAL (g)**	**46.28**		
4.5.- KOH solution after the test (g)	77.1	140.48		
SS_2	**TOTAL (g)**	**63.38**		
5.- Mass Balance (g)				
5.1.- General				
Inlet (FV_1 + $nC_{12}V_1$-FV_2 - $nC_{12}V_2$ - LR)	**237.88**			
Outlet (LP+Coke+SS_2-SS_1)	**220.51**			
MB	**92.70**			
GSY: (SS_2 - SS_1)/(Inlet)*100	**0.54**			
GDY: (LP)/(Inlet)*100	**72.70**			
GCY: (Coke)/(Inlet)*100	**19.46**			
GG: (100 - H_2S - Distillates - Coke)	**7.30**			
5.2. Products (wt%): Assuming that n-Dodecane is in the distillates				
Feed (FV_1 -FV_2-LR)*$X_{Residue}$	**116.54**			
SY: [SS_2 - SS_1]/Feed*100	**1.11**			
DY: [(LP -($nC_{12}V_2$ - $nC_{12}V_1$) - Feed*$X_{n-dodecane}$]/Feed*100	**44.28**			
CY: (Coke/Feed*100)	**39.71**			
G: (100 - H_2S - Distillates - Coke)	**14.91**			
Pumping time (minutes)	**45**			
Flow (gr/min)	**4.36**			

Date	11-23-2001			
Experiment ID	11			
Name	n-C12 20 w% 100 psig			
Vacuum residue ID	ABVB			
1.- KOH solution preparation:	Recipient filled	Recipient emptied	w%	
1.1.- KOH (g)				
1.2.- Water (g)	62.41	0.13		
SS_1	**TOTAL (g)**	**62.28**		
2.- Feed preparation	**FV_1**	**FV_2**	w%	
2.1.- n-Dodecane (g)	146.06	105.31	20.21	$X_{n\text{-}dodecane}$*100
2.2.- Vacuum residue (g)	576.51	415.66	79.79	$X_{Residue}$*100
	722.57	520.97		
	TOTAL (g)	**201.60**		
3.- Unit preparation	Recipient emptied	Recipient filled		
3.1.- n-Dodecane used to increase pressure (g)	60.65	0.22		
$nC_{12}V_1$	**TOTAL (g)**	**60.43**		
4.- Shutdown	Empty recipient	Recipient filled		
4.1.- n-Dodecane remaining in n-Dodecane vessel (g)	78.35	97.24		
$nC_{12}V_2$	**TOTAL (g)**	**18.89**		
4.2.- Flusing mixture collected (g)	139.54	144.25	Purge of pump and lines before reactor	
LR	**TOTAL (g)**	**4.71**		
4.3.- Liquid products (g)	139.54	289.31		
LP	**TOTAL (g)**	**149.77**		
4.4.- Coke collected (g)	53.77	117.45		
Coke	**TOTAL (g)**	**63.68**		
4.5.- KOH solution after the test (g)	0	64.6		
SS_2	**TOTAL (g)**	**64.6**		
5.- Mass Balance (g)				
5.1.- General				
Inlet (FV_1 + $nC_{12}V_1$-FV_2 - $nC_{12}V_2$ - LR)	**238.43**			
Outlet (LP+Coke+SS_2-SS_1)	**215.77**			
MB	**90.50**			
GSY: (SS_2 - SS_1)/(Inlet)*100	**0.97**			
GDY: (LP)/(Inlet)*100	**62.82**			
GCY: (Coke)/(Inlet)*100	**26.71**			
GG: (100 - H_2S - Distillates - Coke)	**9.50**			
5.2. Products (wt%): Assuming that n-Dodecane is in the distillates				
Feed (FV_1 -FV_2-LR)*$X_{Residue}$	**157.09**			
SY: [SS_2 - SS_1]/Feed*100	**1.48**			
DY: [(LP -($nC_{12}V_2$ - $nC_{12}V_1$) - Feed*$X_{n\text{-}dodecane}$]/Feed*100	**43.56**			
CY: (Coke/Feed*100)	**40.54**			
G: (100 - H_2S - Distillates - Coke)	**14.42**			
Pumping time (minutes)	**45**			
Flow (gr/min)	**4.48**			

Date	11-28-01			
Experiment ID	12			
Name	n-C12 40 w% 500 psig			
Vacuum residue ID	ABVB			
1.- KOH solution preparation:	**FV$_1$**	**FV$_2$**	w%	
1.1.- KOH (g)				
1.2.- Water (g)	60.86	0.1		
SS$_1$	**TOTAL (g)**	**60.76**		
2.- Feed preparation	Recipient filled	Recipient emptied	w%	
2.1.- n-Dodecane (g)	285.43	209.50	39.98	$X_{n\text{-}dodecane}$*100
2.2.- Vacuum residue (g)	428.55	314.55	60.02	$X_{Residue}$*100
	713.98	524.05		
	TOTAL (g)	**189.93**		
3.- Unit preparation	Recipient emptied	Recipient filled		
3.1.- n-Dodecane used to increase pressure (g)	166.57	0.43		
nC$_{12}$V$_1$	**TOTAL (g)**	**166.14**		
4.- Shutdown	Empty recipient	Recipient filled		
4.1.- n-Dodecane remaining in n-Dodecane vessel (g)	139.54	196.13		
nC$_{12}$V$_2$	**TOTAL (g)**	**56.59**		
4.2.- Flusing mixture collected (g)	139.54	144.25	Purge of pump and lines before reactor	
LR	**TOTAL (g)**	**4.71**		
4.3.- Liquid products (g)	139.54	348.91		
LP	**TOTAL (g)**	**209.37**		
4.4.- Coke collected (g)	138.76	193.96		
Coke	**TOTAL (g)**	**55.2**		
4.5.- KOH solution after the test (g)	77.08	138.1		
SS$_2$	**TOTAL (g)**	**61.02**		
5.- Mass Balance (g)				
5.1.- General				
Inlet (FV$_1$ + nC$_{12}$V$_1$-FV$_2$ - nC$_{12}$V$_2$ - LR)	**294.77**			
Outlet (LP+Coke+SS$_2$-SS$_1$)	**264.83**			
MB	**89.84**			
GSY: (SS$_2$ - SS$_1$)/(Inlet)*100	**0.09**			
GDY: (LP)/(Inlet)*100	**71.03**			
GCY: (Coke)/(Inlet)*100	**18.73**			
GG: (100 - H$_2$S - Distillates - Coke)	**10.16**			
5.2. Products (wt%): Assuming that n-Dodecane is in the distillates				
Feed (FV$_1$ -FV$_2$-LR)*$X_{Residue}$	**111.17**			
SY: [SS$_2$ - SS$_1$]/Feed*100	**0.23**			
DY: [(LP -(nC$_{12}$V$_2$ - nC$_{12}$V$_1$) - Feed*$X_{n\text{-}dodecane}$]/Feed*100	**23.18**			
CY: (Coke/Feed*100)	**49.65**			
G: (100 - H$_2$S - Distillates - Coke)	**26.93**			
Pumping time (minutes)	**45**			
Flow (gr/min)	**4.22**			

Date	01/10/2002			
Experiment ID	14			
Name	n-C12 60 w% 500 psig			
Vacuum residue ID	ABVB			
1.- KOH solution preparation:	Recipient filled	Recipient emptied	w%	
1.1.- KOH (g)				
1.2.- Water (g)	54.98	0.13		
SS_1	**TOTAL (g)**	**54.85**		
2.- Feed preparation	**FV_1**	**FV_2**	w%	
2.1.- n-Dodecane (g)	435.36	334.01	60.02	$X_{n\text{-dodecane}}$*100
2.2.- Vacuum residue (g)	289.95	222.46	39.98	$X_{Residue}$*100
	725.31	556.47		
	TOTAL (g)	**168.84**		
3.- Unit preparation	Recipient emptied	Recipient filled		
3.1.- n-Dodecane used to increase pressure (g)	171.16	0.08		
$nC_{12}V_1$	**TOTAL (g)**	**171.08**		
4.- Shutdown	Empty recipient	Recipient filled		
4.1.- n-Dodecane remaining in n-Dodecane vessel (g)	0	57.58		
$nC_{12}V_2$	**TOTAL (g)**	**57.58**		
4.2.- Flusing mixture collected (g)	139.61	139.91	Purge of pump and lines before reactor	
LR	**TOTAL (g)**	**0.3**		
4.3.- Liquid products (g)	0	214.32		
LP	**TOTAL (g)**	**214.32**		
4.4.- Coke collected (g)	53.66	78.02		
Coke	**TOTAL (g)**	**24.36**		
4.5.- KOH solution after the test (g)	76.09	131.39		
SS_2	**TOTAL (g)**	**55.3**		
5.- Mass Balance (g)				
5.1.- General				
Inlet (FV_1 + $nC_{12}V_1$-FV_2 - $nC_{12}V_2$ - LR)	**282.04**			
Outlet (LP+Coke+SS_2-SS_1)	**239.13**			
MB	**84.79**			
GSY: (SS_2 - SS_1)/(Inlet)*100	**0.16**			
GDY: (LP)/(Inlet)*100	**75.99**			
GCY: (Coke)/(Inlet)*100	**8.64**			
GG: (100 - H_2S - Distillates - Coke)	**15.21**			
5.2. Products (wt%): Assuming that n-Dodecane is in the distillates				
Feed (FV_1 -FV_2-LR)*$X_{Residue}$	**67.38**			
SY: [SS_2 - SS_1]/Feed*100	**0.67**			
DY: [(LP -($nC_{12}V_2$ - $nC_{12}V_1$) - Feed*$X_{n\text{-dodecane}}$]/Feed*100	**-0.51**			
CY: (Coke/Feed*100)	**36.15**			
G: (100 - H_2S - Distillates - Coke)	**63.69**			
Pumping time (minutes)	**45**			
Flow (gr/min)	**3.75**			

Date	1-14-02			
Experiment ID	15			
Name	n-C12 20 w% 500 psig			
Vacuum residue ID	ABVB			
1.- KOH solution preparation:	Recipient filled	Recipient emptied	w%	
1.1.- KOH (g)				
1.2.- Water (g)	59.42	0.16		
SS_1	**TOTAL (g)**	**59.26**		
2.- Feed preparation	**FV_1**	**FV_2**	w%	
2.1.- n-Dodecane (g)	145.14	107.18	19.85	$X_{n\text{-dodecane}}$*100
2.2.- Vacuum residue (g)	586.05	432.79	80.15	$X_{Residue}$*100
	731.19	539.97		
	TOTAL (g)	**191.22**		
3.- Unit preparation	Recipient emptied	Recipient filled		
3.1.- n-Dodecane used to increase pressure (g)	151.24	0.26		
$nC_{12}V_1$	**TOTAL (g)**	**150.98**		
4.- Shutdown	Empty recipient	Recipient filled		
4.1.- n-Dodecane remaining in n-Dodecane vessel (g)	0	53.95		
$nC_{12}V_2$	**TOTAL (g)**	**53.95**		
4.2.- Flusing mixture collected (g)	0	0	Purge of pump and lines before reactor	
LR	**TOTAL (g)**	**0**		
4.3.- Liquid products (g)	0	166.77		
LP	**TOTAL (g)**	**166.77**		
4.4.- Coke collected (g)	138.72	212.57		
Coke	**TOTAL (g)**	**73.85**		
4.5.- KOH solution after the test (g)	0	59.82		
SS_2	**TOTAL (g)**	**59.82**		
5.- Mass Balance (g)				
5.1.- General				
Inlet (FV_1 + $nC_{12}V_1$-FV_2 - $nC_{12}V_2$ - LR)	**288.25**			
Outlet (LP+Coke+SS_2-SS_1)	**241.18**			
MB	**83.67**			
GSY: (SS_2 - SS_1)/(Inlet)*100	**0.19**			
GDY: (LP)/(Inlet)*100	**57.86**			
GCY: (Coke)/(Inlet)*100	**25.62**			
GG: (100 - H_2S - Distillates - Coke)	**16.33**			
5.2. Products (wt%): Assuming that n-Dodecane is in the distillates				
Feed (FV_1 -FV_2-LR)*$X_{Residue}$	**153.26**			
SY: [SS_2 - SS_1]/Feed*100	**0.37**			
DY: [(LP -($nC_{12}V_2$ - $nC_{12}V_1$) - Feed*$X_{n\text{-dodecane}}$]/Feed*100	**20.74**			
CY: (Coke/Feed*100)	**48.18**			
G: (100 - H_2S - Distillates - Coke)	**30.71**			
Pumping time (minutes)	**45**			
Flow (gr/min)	**4.25**			

Date	1-31-02			
Experiment ID	19			
Name	n-C12 40 w% 870 psig			
Vacuum residue ID	ABVB			
1.- KOH solution preparation:	Recipient filled	Recipient emptied	w%	
1.1.- KOH (g)				
1.2.- Water (g)	28.7	0.16		
SS$_1$	**TOTAL (g)**	**28.54**		
2.- Feed preparation	**FV$_1$**	**FV$_2$**	w%	
2.1.- n-Dodecane (g)	287.24	208.74	39.94	$X_{n\text{-dodecane}}$*100
2.2.- Vacuum residue (g)	431.94	313.90	60.06	$X_{Residue}$*100
	719.18	522.64		
	TOTAL (g)	**196.54**		
3.- Unit preparation	Recipient emptied	Recipient filled		
3.1.- n-Dodecane used to increase pressure (g)	343.18	138.82		
nC$_{12}$V$_1$	**TOTAL (g)**	**204.36**		
4.- Shutdown	Empty recipient	Recipient filled		
4.1.- n-Dodecane remaining in n-Dodecane vessel (g)	0	63.11		
nC$_{12}$V$_2$	**TOTAL (g)**	**63.11**		
4.2.- Flusing mixture collected (g)	138.1	152.9	Purge of pump and lines before reactor	
LR	**TOTAL (g)**	**14.8**		
4.3.- Liquid products (g)	0	260.96		
LP	**TOTAL (g)**	**260.96**		
4.4.- Coke collected (g)	138.86	176.48		
Coke	**TOTAL (g)**	**37.62**		
4.5.- KOH solution after the test (g)	0	28.6		
SS$_2$	**TOTAL (g)**	**28.6**		
5.- Mass Balance (g)				
5.1.- General				
Inlet (FV$_1$ + nC$_{12}$V$_1$-FV$_2$ - nC$_{12}$V$_2$ - LR)	**322.99**			
Outlet (LP+Coke+SS$_2$-SS$_1$)	**298.64**			
MB	**92.46**			
GSY: (SS$_2$ - SS$_1$)/(Inlet)*100	**0.02**			
GDY: (LP)/(Inlet)*100	**80.80**			
GCY: (Coke)/(Inlet)*100	**11.65**			
GG: (100 - H$_2$S - Distillates - Coke)	**7.54**			
5.2. Products (wt%): Assuming that n-Dodecane is in the distillates				
Feed (FV$_1$ -FV$_2$-LR)*$X_{Residue}$	**109.15**			
SY: [SS$_2$ - SS$_1$]/Feed*100	**0.05**			
DY: [(LP -(nC$_{12}$V$_2$ - nC$_{12}$V$_1$) - Feed*$X_{n\text{-dodecane}}$]/Feed*100	**43.17**			
CY: (Coke/Feed*100)	**34.47**			
G: (100 - H$_2$S - Distillates - Coke)	**22.31**			
Pumping time (minutes)	**45**			
Flow (gr/min)	**4.37**			

Date	02/02/2002			
Experiment ID	20			
Name	n-C12 40 w% 500 psig			
Vacuum residue ID	ABVB			
1.- KOH solution preparation:	Recipient filled	Recipient emptied	w%	
1.1.- KOH (g)				
1.2.- Water (g)	46.87	0.25		
SS$_1$	**TOTAL (g)**	**46.62**		
2.- Feed preparation	**FV$_1$**	**FV$_2$**	w%	
2.1.- n-Dodecane (g)	290.64	209.20	40.32	$X_{n\text{-dodecane}}$*100
2.2.- Vacuum residue (g)	430.20	309.66	59.68	$X_{Residue}$*100
	720.84	518.86		
	TOTAL (g)	**201.98**		
3.- Unit preparation	Recipient emptied	Recipient filled		
3.1.- n-Dodecane used to increase pressure (g)	129.04	0.02		
nC$_{12}$V$_1$	**TOTAL (g)**	**129.02**		
4.- Shutdown	Empty recipient	Recipient filled		
4.1.- n-Dodecane remaining in n-Dodecane vessel (g)	0	21.99		
nC$_{12}$V$_2$	**TOTAL (g)**	**21.99**		
4.2.- Flusing mixture collected (g)	138	143.29	Purge of pump and lines before reactor	
LR	**TOTAL (g)**	**5.29**		
4.3.- Liquid products (g)	0	217.42		
LP	**TOTAL (g)**	**217.42**		
4.4.- Coke collected (g)	138.89	194.89		
Coke	**TOTAL (g)**	**56**		
4.5.- KOH solution after the test (g)	0	46.63		
SS$_2$	**TOTAL (g)**	**46.63**		
5.- Mass Balance (g)				
5.1.- General				
Inlet (FV$_1$ + nC$_{12}$V$_1$-FV$_2$ - nC$_{12}$V$_2$ - LR)	**303.72**			
Outlet (LP+Coke+SS$_2$-SS$_1$)	**273.43**			
MB	**90.03**			
GSY: (SS$_2$ - SS$_1$)/(Inlet)*100	**0.00**			
GDY: (LP)/(Inlet)*100	**71.59**			
GCY: (Coke)/(Inlet)*100	**18.44**			
GG: (100 - H$_2$S - Distillates - Coke)	**9.97**			
5.2. Products (wt%): Assuming that n-Dodecane is in the distillates				
Feed (FV$_1$ -FV$_2$-LR)*$X_{Residue}$	**117.38**			
SY: [SS$_2$ - SS$_1$]/Feed*100	**0.01**			
DY: [(LP -(nC$_{12}$V$_2$ - nC$_{12}$V$_1$) - Feed*$X_{n\text{-dodecane}}$]/Feed*100	**26.48**			
CY: (Coke/Feed*100)	**47.71**			
G: (100 - H$_2$S - Distillates - Coke)	**25.80**			
Pumping time (minutes)	**45**			
Flow (gr/min)	**4.49**			

Date	02/06/2002			
Experiment ID	21			
Name	n-C12 60 w% 870 psig			
Vacuum residue ID	ABVB			
1.- KOH solution preparation:	Recipient filled	Recipient emptied	w%	
1.1.- KOH (g)				
1.2.- Water (g)	40.35	0.17		
SS_1	**TOTAL (g)**	**40.18**		
2.- Feed preparation	**FV_1**	**FV_2**	w%	
2.1.- n-Dodecane (g)	433.07	328.923456	59.97	$X_{n\text{-dodecane}}$*100
2.2.- Vacuum residue (g)	289.07	219.556544	40.03	$X_{Residue}$*100
	722.14	548.48		
	TOTAL (g)	**173.66**		
3.- Unit preparation	Recipient emptied	Recipient filled		
3.1.- n-Dodecane used to increase pressure (g)	171.3	0.2		
$nC_{12}V_1$	**TOTAL (g)**	**171.1**		
4.- Shutdown	Empty recipient	Recipient filled		
4.1.- n-Dodecane remaining in n-Dodecane vessel (g)	0	28.8		
$nC_{12}V_2$	**TOTAL (g)**	**28.8**		
4.2.- Flusing mixture collected (g)	138.02	142.07	Purge of pump and lines before reactor	
LR	**TOTAL (g)**	**4.05**		
4.3.- Liquid products (g)	0	265.21		
LP	**TOTAL (g)**	**265.21**		
4.4.- Coke collected (g)	138.82	154.91		
Coke	**TOTAL (g)**	**16.09**		
4.5.- KOH solution after the test (g)	0	40.32		
SS_2	**TOTAL (g)**	**40.32**		
5.- Mass Balance (g)				
5.1.- General				
Inlet (FV_1 + $nC_{12}V_1$-FV_2 - $nC_{12}V_2$ - LR)	**311.91**			
Outlet (LP+Coke+SS_2-SS_1)	**281.44**			
MB	**90.23**			
GSY: (SS_2 - SS_1)/(Inlet)*100	**0.04**			
GDY: (LP)/(Inlet)*100	**85.03**			
GCY: (Coke)/(Inlet)*100	**5.16**			
GG: (100 - H_2S - Distillates - Coke)	**9.77**			
5.2. Products (wt%): Assuming that n-Dodecane is in the distillates				
Feed (FV_1 -FV_2-LR)*$X_{Residue}$	**67.89**			
SY: [SS_2 - SS_1]/Feed*100	**0.21**			
DY: [(LP -($nC_{12}V_2$ - $nC_{12}V_1$) - Feed*$X_{n\text{-dodecane}}$]/Feed*100	**31.22**			
CY: (Coke/Feed*100)	**23.70**			
G: (100 - H_2S - Distillates - Coke)	**44.88**	(Around 11% or less when working at 20 psig or less)		
Pumping time (minutes)	**45**			
Flow (gr/min)	**3.86**			

Date	02/12/2002			
Experiment ID	22			
Name	n-C12 60 w% 500 psig			
Vacuum residue ID	ABVB			
1.- KOH solution preparation:	Recipient filled	Recipient emptied	w%	
1.1.- KOH (g)				
1.2.- Water (g)	55.12	0.19		
SS$_1$	**TOTAL (g)**	**54.93**		
2.- Feed preparation	**FV$_1$**	**FV$_2$**	w%	
2.1.- n-Dodecane (g)	420.93	309.80961	59.95	$X_{n\text{-dodecane}}$*100
2.2.- Vacuum residue (g)	281.21	206.97039	40.05	$X_{Residue}$*100
	702.14	516.78		
	TOTAL (g)	**185.36**		
3.- Unit preparation	Recipient emptied	Recipient filled		
3.1.- n-Dodecane used to increase pressure (g)	133.73	0.42		
nC$_{12}$V$_1$	**TOTAL (g)**	**133.31**		
4.- Shutdown	Empty recipient	Recipient filled		
4.1.- n-Dodecane remaining in n-Dodecane vessel (g)	0	30.4		
nC$_{12}$V$_2$	**TOTAL (g)**	**30.4**		
4.2.- Flusing mixture collected (g)	139.7	145.61	Purge of pump and lines before reactor	
LR	**TOTAL (g)**	**5.91**		
4.3.- Liquid products (g)	0	231.47		
LP	**TOTAL (g)**	**231.47**		
4.4.- Coke collected (g)	138.8	165.06		
Coke	**TOTAL (g)**	**26.26**		
4.5.- KOH solution after the test (g)	0	54.97		
SS$_2$	**TOTAL (g)**	**54.97**		
5.- Mass Balance (g)				
5.1.- General				
Inlet (FV$_1$ + nC$_{12}$V$_1$-FV$_2$ - nC$_{12}$V$_2$ - LR)	**282.36**			
Outlet (LP+Coke+SS$_2$-SS$_1$)	**257.77**			
MB	**91.29**			
GSY: (SS$_2$ - SS$_1$)/(Inlet)*100	**0.01**			
GDY: (LP)/(Inlet)*100	**81.98**			
GCY: (Coke)/(Inlet)*100	**9.30**			
GG: (100 - H_2S - Distillates - Coke)	**8.71**			
5.2. Products (wt%): Assuming that n-Dodecane is in the distillates				
Feed (FV$_1$ -FV$_2$-LR)*$X_{Residue}$	**71.87**			
SY: [SS$_2$ - SS$_1$]/Feed*100	**0.06**			
DY: [(LP -(nC$_{12}$V$_2$ - nC$_{12}$V$_1$) - Feed*$X_{n\text{-dodecane}}$]/Feed*100	**29.19**			
CY: (Coke/Feed*100)	**36.54**			
G: (100 - H_2S - Distillates - Coke)	**34.21**			
Pumping time (minutes)	**45**			
Flow (gr/min)	**4.12**			

Date	2-19-02			
Experiment ID	24			
Name	n-C12 40 w% 20 psig			
Vacuum residue ID	Cerro Negro			
1.- KOH solution preparation:	Recipient filled	Recipient emptied	w%	
1.1.- KOH (g)				
1.2.- Water (g)	65.69	0.45		
SS_1	**TOTAL (g)**	**65.24**		
2.- Feed preparation	**FV_1**	**FV_2**	w%	
2.1.- n-Dodecane (g)	336.48	259.42	38.78	$X_{n\text{-}dodecane}$*100
2.2.- Vacuum residue (g)	531.27	409.58	61.22	$X_{Residue}$*100
	867.75	669.00		
	TOTAL (g)	**198.75**		
3.- Unit preparation	Recipient emptied	Recipient filled		
3.1.- n-Dodecane used to increase pressure (g)	34.8	0.35		
$nC_{12}V_1$	**TOTAL (g)**	**34.45**		
4.- Shutdown	Empty recipient	Recipient filled		
4.1.- n-Dodecane remaining in n-Dodecane vessel (g)	0	5.8		
$nC_{12}V_2$	**TOTAL (g)**	**5.8**		
4.2.- Flusing mixture collected (g)	138.05	144.42	Purge of pump and lines before reactor	
LR	**TOTAL (g)**	**6.37**		
4.3.- Liquid products (g)	0	165.43		
LP	**TOTAL (g)**	**165.43**		
4.4.- Coke collected (g)	138.84	181.02		
Coke	**TOTAL (g)**	**42.18**		
4.5.- KOH solution after the test (g)	0	66.34		
SS_2	**TOTAL (g)**	**66.34**		
5.- Mass Balance (g)				
5.1.- General				
Inlet (FV_1 + $nC_{12}V_1$-FV_2 - $nC_{12}V_2$ - LR)	**221.03**			
Outlet (LP+Coke+SS_2-SS_1)	**208.71**			
MB	**94.43**			
GSY: (SS_2 - SS_1)/(Inlet)*100	**0.50**			
GDY: (LP)/(Inlet)*100	**74.85**			
GCY: (Coke)/(Inlet)*100	**19.08**			
GG: (100 - H_2S - Distillates - Coke)	**5.57**			
5.2. Products (wt%): Assuming that n-Dodecane is in the distillates				
Feed (FV_1 -FV_2-LR)*$X_{Residue}$	**117.78**			
SY: [SS_2 - SS_1]/Feed*100	**0.93**			
DY: [(LP -($nC_{12}V_2$ - $nC_{12}V_1$) - Feed*$X_{n\text{-}dodecane}$]/Feed*100	**52.79**			
CY: (Coke/Feed*100)	**35.81**			
G: (100 - H_2S - Distillates - Coke)	**10.46**			
Pumping time (minutes)	**45**			
Flow (gr/min)	**4.42**			

Date	2-21-02			
Experiment ID	25			
Name	n-C12 0 w% 20 psig			
Vacuum residue ID	Heater's feedstock			
1.- KOH solution preparation:	Recipient filled	Recipient emptied	w%	
1.1.- KOH (g)				
1.2.- Water (g)	66.94	0.37		
SS_1	**TOTAL (g)**	**66.57**		
2.- Feed preparation	**FV_1**	**FV_2**	w%	
2.1.- n-Dodecane (g)	0.00	0	0.00	$X_{n\text{-dodecane}}$*100
2.2.- Vacuum residue (g)	724.50	599.1	100.0	$X_{Residue}$*100
	724.50	599.10		
	TOTAL (g)	**125.40**		
3.- Unit preparation	Recipient emptied	Recipient filled		
3.1.- n-Dodecane used to increase pressure (g)	50	0.27		
$nC_{12}V_1$	**TOTAL (g)**	**49.73**		
4.- Shutdown	Empty recipient	Recipient filled		
4.1.- n-Dodecane remaining in n-Dodecane vessel (g)	0	1.78		
$nC_{12}V_2$	**TOTAL (g)**	**1.78**		
4.2.- Flusing mixture collected (g)	139.81	141.85	Purge of pump and lines before reactor	
LR	**TOTAL (g)**	**2.04**		
4.3.- Liquid products (g)	0	113.64		
LP	**TOTAL (g)**	**113.64**		
4.4.- Coke collected (g)	138.79	179.02		
Coke	**TOTAL (g)**	**40.23**		
4.5.- KOH solution after the test (g)	0	67.51		
SS_2	**TOTAL (g)**	**67.51**		
5.- Mass Balance (g)				
5.1.- General				
Inlet (FV_1 + $nC_{12}V_1$-FV_2 - $nC_{12}V_2$ - LR)	**171.31**			
Outlet (LP+Coke+SS_2-SS_1)	**154.81**			
MB	**90.37**			
GSY: (SS_2 - SS_1)/(Inlet)*100	**0.55**			
GDY: (LP)/(Inlet)*100	**66.34**			
GCY: (Coke)/(Inlet)*100	**23.48**			
GG: (100 - H_2S - Distillates - Coke)	**9.63**			
5.2. Products (wt%): Assuming that n-Dodecane is in the distillates				
Feed (FV_1 -FV_2-LR)*$X_{Residue}$	**123.36**			
SY: [SS_2 - SS_1]/Feed*100	**0.76**			
DY: [(LP -($nC_{12}V_2$ - $nC_{12}V_1$) - Feed*$X_{n\text{-dodecane}}$]/Feed*100	**53.25**			
CY: (Coke/Feed*100)	**32.61**			
G: (100 - H_2S - Distillates - Coke)	**13.38**			
Pumping time (minutes)	**45**			
Flow (gr/min)	**2.79**			

Date	2-26-02					
Experiment ID	26					
Name	HF 100 wt% 20psig High temperature					
Vacuum residue ID	Heater's feedstock					
1.- KOH solution preparation:	Recipient filled	Recipient emptied	w%			
1.1.- KOH (g)						
1.2.- Water (g)	63.8	0.24				
SS_1	**TOTAL (g)**	**63.56**				
2.- Feed preparation	**FV_1**	**FV_2**	w%			
2.1.- n-Dodecane (g)	0.00	0	0.00	$X_{n\text{-dodecane}}$*100		
2.2.- Vacuum residue (g)	730.96	590.18	100.0	$X_{Residue}$*100		
	730.96	590.18				
	TOTAL (g)	**140.78**				
3.- Unit preparation	Recipient emptied	Recipient filled				
3.1.- n-Dodecane used to increase pressure (g)	56.56	0.37				
$nC_{12}V_1$	**TOTAL (g)**	**56.19**				
4.- Shutdown	Empty recipient	Recipient filled				
4.1.- n-Dodecane remaining in n-Dodecane vessel (g)	0	12.74				
$nC_{12}V_2$	**TOTAL (g)**	**12.74**				
4.2.- Flusing mixture collected (g)	138.06	139.12	Purge of pump and lines before reactor			
LR	**TOTAL (g)**	**1.06**				
4.3.- Liquid products (g)	0	124.72				
LP	**TOTAL (g)**	**124.72**				
4.4.- Coke collected (g)	138.88	181.16				
Coke	**TOTAL (g)**	**42.28**				
4.5.- KOH solution after the test (g)	0	64.77				
SS_2	**TOTAL (g)**	**64.77**				
5.- Mass Balance (g)						
5.1.- General						
Inlet ($FV_1 + nC_{12}V_1 - FV_2 - nC_{12}V_2$ - LR)	**183.17**					
Outlet (LP+Coke+SS_2-SS_1)	**168.21**					
MB	**91.83**					
GSY: (SS_2 - SS_1)/(Inlet)*100	**0.66**					
GDY: (LP)/(Inlet)*100	**68.09**					
GCY: (Coke)/(Inlet)*100	**23.08**					
GG: (100 - H_2S - Distillates - Coke)	**8.17**					
5.2. Products (wt%): Assuming that n-Dodecane is in the distillates						
Feed (FV_1 -FV_2-LR)*$X_{Residue}$	**139.72**					
SY: [SS_2 - SS_1]/Feed*100	**0.87**					
DY: [(LP -($nC_{12}V_2$ - $nC_{12}V_1$) - Feed*$X_{n\text{-dodecane}}$]/Feed*100	**58.17**					
CY: (Coke/Feed*100)	**30.26**					
G: (100 - H_2S - Distillates - Coke)	**10.71**					
Pumping time (minutes)	**45**					
Flow (gr/min)	**3.13**					

Date	2-28-02			
Experiment ID	27			
Name	n-C12 55 wt% 870 psig			
Vacuum residue ID	ABVB			
1.- KOH solution preparation:	Recipient filled	Recipient emptied	w%	
1.1.- KOH (g)				
1.2.- Water (g)	65.57	0.22		
SS$_1$	**TOTAL (g)**	**65.35**		
2.- Feed preparation	**FV$_1$**	**FV$_2$**	w%	
2.1.- n-Dodecane (g)	396.71	292.42	55.0	$X_{n\text{-dodecane}}$*100
2.2.- Vacuum residue (g)	324.59	239.26	45.0	$X_{Residue}$*100
	721.30	531.68		
	TOTAL (g)	**189.62**		
3.- Unit preparation	Recipient emptied	Recipient filled		
3.1.- n-Dodecane used to increase pressure (g)	170.92	0.34		
nC$_{12}$V$_1$	**TOTAL (g)**	**170.58**		
4.- Shutdown	Empty recipient	Recipient filled		
4.1.- n-Dodecane remaining in n-Dodecane vessel (g)	0	28.63		
nC$_{12}$V$_2$	**TOTAL (g)**	**28.63**		
4.2.- Flusing mixture collected (g)	139.78	146.71	Purge of pump and lines before reactor	
LR	**TOTAL (g)**	**6.93**		
4.3.- Liquid products (g)	0	269.27		
LP	**TOTAL (g)**	**269.27**		
4.4.- Coke collected (g)	138.79	157.71		
Coke	**TOTAL (g)**	**18.92**		
4.5.- KOH solution after the test (g)	77.26	142.7		
SS$_2$	**TOTAL (g)**	**65.44**		
5.- Mass Balance (g)				
5.1.- General				
Inlet (FV$_1$ + nC$_{12}$V$_1$-FV$_2$ - nC$_{12}$V$_2$ - LR)	**324.64**			
Outlet (LP+Coke+SS$_2$-SS$_1$)	**288.28**			
MB	**88.80**			
GSY: (SS$_2$ - SS$_1$)/(Inlet)*100	**0.03**			
GDY: (LP)/(Inlet)*100	**82.94**			
GCY: (Coke)/(Inlet)*100	**5.83**			
GG: (100 - H$_2$S - Distillates - Coke)	**11.20**			
5.2. Products (wt%): Assuming that n-Dodecane is in the distillates				
Feed (FV$_1$ -FV$_2$-LR)*$X_{Residue}$	**82.21**			
SY: [SS$_2$ - SS$_1$]/Feed*100	**0.11**			
DY: [(LP -(nC$_{12}$V$_2$ - nC$_{12}$V$_1$) - Feed*$X_{n\text{-dodecane}}$]/Feed*100	**32.65**			
CY: (Coke/Feed*100)	**23.01**			
G: (100 - H$_2$S - Distillates - Coke)	**44.23**			
Pumping time (minutes)	**45**			
Flow (gr/min)	**4.21**			

Date	03/02/2002			
Experiment ID	28			
Name	n-C12 55 wt% 500 psig			
Vacuum residue ID	ABVB			
1.- KOH solution preparation:	Recipient filled	Recipient emptied	w%	
1.1.- KOH (g)				
1.2.- Water (g)	65.89	0.2		
SS$_1$	**TOTAL (g)**	**65.69**		
2.- Feed preparation	**FV$_1$**	**FV$_2$**	w%	
2.1.- n-Dodecane (g)	396.95	292.92	55.0	$X_{n\text{-dodecane}}$*100
2.2.- Vacuum residue (g)	324.71	239.62	45.0	$X_{Residue}$*100
	721.66	532.54		
	TOTAL (g)	**189.12**		
3.- Unit preparation	Recipient emptied	Recipient filled		
3.1.- n-Dodecane used to increase pressure (g)	130.79	0.37		
nC$_{12}$V$_1$	**TOTAL (g)**	**130.42**		
4.- Shutdown	Empty recipient	Recipient filled		
4.1.- n-Dodecane remaining in n-Dodecane vessel (g)	0	36.93		
nC$_{12}$V$_2$	**TOTAL (g)**	**36.93**		
4.2.- Flusing mixture collected (g)	139.74	147.36	Purge of pump and lines before reactor	
LR	**TOTAL (g)**	**7.62**		
4.3.- Liquid products (g)	0	209.31		
LP	**TOTAL (g)**	**209.31**		
4.4.- Coke collected (g)	138.81	178.97		
Coke	**TOTAL (g)**	**40.16**		
4.5.- KOH solution after the test (g)	0	66.08		
SS$_2$	**TOTAL (g)**	**66.08**		
5.- Mass Balance (g)				
5.1.- General				
Inlet (FV$_1$ + nC$_{12}$V$_1$-FV$_2$ - nC$_{12}$V$_2$ - LR)	**274.99**			
Outlet (LP+Coke+SS$_2$-SS$_1$)	**249.86**			
MB	**90.86**			
GSY: (SS$_2$ - SS$_1$)/(Inlet)*100	**0.14**			
GDY: (LP)/(Inlet)*100	**76.12**			
GCY: (Coke)/(Inlet)*100	**14.60**			
GG: (100 - H$_2$S - Distillates - Coke)	**9.14**			
5.2. Products (wt%): Assuming that n-Dodecane is in the distillates				
Feed (FV$_1$ -FV$_2$-LR)*$X_{Residue}$	**81.67**			
SY: [SS$_2$ - SS$_1$]/Feed*100	**0.48**			
DY: [(LP -(nC$_{12}$V$_2$ - nC$_{12}$V$_1$) - Feed*$X_{n\text{-dodecane}}$]/Feed*100	**19.58**			
CY: (Coke/Feed*100)	**49.18**			
G: (100 - H$_2$S - Distillates - Coke)	**30.77**			
Pumping time (minutes)	**45**			
Flow (gr/min)	**4.20**			

Date	03/07/2002			
Experiment ID	29			
Name	n-C12 50 wt% 870 psig			
Vacuum residue ID	ABVB			
1.- KOH solution preparation:	Recipient filled	Recipient emptied	w%	
1.1.- KOH (g)				
1.2.- Water (g)	63.5	0.34		
SS_1	**TOTAL (g)**	**63.16**		
2.- Feed preparation	**FV_1**	**FV_2**	w%	
2.1.- n-Dodecane (g)	360.74	267.69	50.0	$X_{n\text{-}dodecane}$*100
2.2.- Vacuum residue (g)	360.20	267.29	50.0	$X_{Residue}$*100
	720.94	534.98		
	TOTAL (g)	**185.96**		
3.- Unit preparation	Recipient emptied	Recipient filled		
3.1.- n-Dodecane used to increase pressure (g)	165.8	0.24		
$nC_{12}V_1$	**TOTAL (g)**	**165.56**		
4.- Shutdown	Empty recipient	Recipient filled		
4.1.- n-Dodecane remaining in n-Dodecane vessel (g)	0	33.32		
$nC_{12}V_2$	**TOTAL (g)**	**33.32**		
4.2.- Flusing mixture collected (g)	139.8	148.52	Purge of pump and lines before reactor	
LR	**TOTAL (g)**	**8.72**		
4.3.- Liquid products (g)	0	253.13		
LP	**TOTAL (g)**	**253.13**		
4.4.- Coke collected (g)	138.9	163.64		
Coke	**TOTAL (g)**	**24.74**		
4.5.- KOH solution after the test (g)	0	63.3		
SS_2	**TOTAL (g)**	**63.3**		
5.- Mass Balance (g)				
5.1.- General				
Inlet (FV_1 + $nC_{12}V_1$-FV_2 - $nC_{12}V_2$ - LR)	**309.48**			
Outlet (LP+Coke+SS_2-SS_1)	**278.01**			
MB	**89.83**			
GSY: (SS_2 - SS_1)/(Inlet)*100	**0.05**			
GDY: (LP)/(Inlet)*100	**81.79**			
GCY: (Coke)/(Inlet)*100	**7.99**			
GG: (100 - H_2S - Distillates - Coke)	**10.17**			
5.2. Products (wt%): Assuming that n-Dodecane is in the distillates				
Feed (FV_1 -FV_2-LR)*$X_{Residue}$	**88.55**			
SY: [SS_2 - SS_1]/Feed*100	**0.16**			
DY: [(LP -($nC_{12}V_2$ - $nC_{12}V_1$) - Feed*$X_{n\text{-}dodecane}$]/Feed*100	**36.37**			
CY: (Coke/Feed*100)	**27.94**			
G: (100 - H_2S - Distillates - Coke)	**35.54**			
Pumping time (minutes)	**45**			
Flow (gr/min)	**4.13**			

Date	03/09/2002			
Experiment ID	30			
Name	n-C12 50 wt% 500 psig			
Vacuum residue ID	ABVB			
1.- KOH solution preparation:	Recipient filled	Recipient emptied	w%	
1.1.- KOH (g)				
1.2.- Water (g)	67.48	0.23		
SS_1	**TOTAL (g)**	**67.25**		
2.- Feed preparation	**FV_1**	**FV_2**	w%	
2.1.- n-Dodecane (g)	360.74	275.35	50.02	$X_{n\text{-dodecane}}$*100
2.2.- Vacuum residue (g)	360.46	275.15	49.98	$X_{Residue}$*100
	721.20	550.50		
	TOTAL (g)	**170.70**		
3.- Unit preparation	Recipient emptied	Recipient filled		
3.1.- n-Dodecane used to increase pressure (g)	127.12	0.21		
$nC_{12}V_1$	**TOTAL (g)**	**126.91**		
4.- Shutdown	Empty recipient	Recipient filled		
4.1.- n-Dodecane remaining in n-Dodecane vessel (g)	0	35.06		
$nC_{12}V_2$	**TOTAL (g)**	**35.06**		
4.2.- Flusing mixture collected (g)	138.27	144.55	Purge of pump and lines before reactor	
LR	**TOTAL (g)**	**6.28**		
4.3.- Liquid products (g)	0	189.28		
LP	**TOTAL (g)**	**189.28**		
4.4.- Coke collected (g)	138.82	179.19		
Coke	**TOTAL (g)**	**40.37**		
4.5.- KOH solution after the test (g)	0	67.64		
SS_2	**TOTAL (g)**	**67.64**		
5.- Mass Balance (g)				
5.1.- General				
Inlet (FV_1 + $nC_{12}V_1$-FV_2 - $nC_{12}V_2$ - LR)	**256.27**			
Outlet (LP+Coke+SS_2-SS_1)	**230.04**			
MB	**89.76**			
GSY: (SS_2 - SS_1)/(Inlet)*100	**0.15**			
GDY: (LP)/(Inlet)*100	**73.86**			
GCY: (Coke)/(Inlet)*100	**15.75**			
GG: (100 - H_2S - Distillates - Coke)	**10.24**			
5.2. Products (wt%): Assuming that n-Dodecane is in the distillates				
Feed (FV_1 -FV_2-LR)*$X_{Residue}$	**82.18**			
SY: [SS_2 - SS_1]/Feed*100	**0.47**			
DY: [(LP -($nC_{12}V_2$ - $nC_{12}V_1$) - Feed*$X_{n\text{-dodecane}}$]/Feed*100	**18.48**			
CY: (Coke/Feed*100)	**49.12**			
G: (100 - H_2S - Distillates - Coke)	**31.92**			
Pumping time (minutes)	**45**			
Flow (gr/min)	**3.79**			

Date	03/12/2002			
Experiment ID	31			
Name	n-C12 50 wt% 100 psig			
Vacuum residue ID	ABVB			
1.- KOH solution preparation:	Recipient filled	Recipient emptied	w%	
1.1.- KOH (g)				
1.2.- Water (g)	57.76	0.27		
SS_1	**TOTAL (g)**	**57.49**		
2.- Feed preparation	**FV_1**	**FV_2**	w%	
2.1.- n-Dodecane (g)	360.99	270.52	50.00	$X_{n\text{-dodecane}}$*100
2.2.- Vacuum residue (g)	360.95	270.50	50.00	$X_{Residue}$*100
	721.94	541.02		
	TOTAL (g)	**180.92**		
3.- Unit preparation	Recipient emptied	Recipient filled		
3.1.- n-Dodecane used to increase pressure (g)	56.08	0.29		
$nC_{12}V_1$	**TOTAL (g)**	**55.79**		
4.- Shutdown	Empty recipient	Recipient filled		
4.1.- n-Dodecane remaining in n-Dodecane vessel (g)	0	15.62		
$nC_{12}V_2$	**TOTAL (g)**	**15.62**		
4.2.- Flusing mixture collected (g)	139.86	146.64	Purge of pump and lines before reactor	
LR	**TOTAL (g)**	**6.78**		
4.3.- Liquid products (g)	0	149.01		
LP	**TOTAL (g)**	**149.01**		
4.4.- Coke collected (g)	138.8	180.48		
Coke	**TOTAL (g)**	**41.68**		
4.5.- KOH solution after the test (g)	0	58.11		
SS_2	**TOTAL (g)**	**58.11**		
5.- Mass Balance (g)				
5.1.- General				
Inlet (FV_1 + $nC_{12}V_1$-FV_2 - $nC_{12}V_2$ - LR)	**214.31**			
Outlet (LP+Coke+SS_2-SS_1)	**191.31**			
MB	**89.27**			
GSY: (SS_2 - SS_1)/(Inlet)*100	**0.29**			
GDY: (LP)/(Inlet)*100	**69.53**			
GCY: (Coke)/(Inlet)*100	**19.45**			
GG: (100 - H_2S - Distillates - Coke)	**10.73**			
5.2. Products (wt%): Assuming that n-Dodecane is in the distillates				
Feed (FV_1 -FV_2-LR)*$X_{Residue}$	**87.07**			
SY: [SS_2 - SS_1]/Feed*100	**0.71**			
DY: [(LP -($nC_{12}V_2$ - $nC_{12}V_1$) - Feed*$X_{n\text{-dodecane}}$]/Feed*100	**25.00**			
CY: (Coke/Feed*100)	**47.87**			
G: (100 - H_2S - Distillates - Coke)	**26.42**			
Pumping time (minutes)	**45**			
Flow (gr/min)	**4.02**			

Date	3-15-02			
Experiment ID	32			
Name	n-C12 55 wt% 100 psig			
Vacuum residue ID	ABVB			
1.- KOH solution preparation:	Recipient filled	Recipient emptied	w%	
1.1.- KOH (g)				
1.2.- Water (g)	54.95	0.45		
SS_1	**TOTAL (g)**	**54.5**		
2.- Feed preparation	**FV_1**	**FV_2**	w%	
2.1.- n-Dodecane (g)	396.37	299.40	55.00	$X_{n\text{-dodecane}}$*100
2.2.- Vacuum residue (g)	324.31	244.98	45.00	$X_{Residue}$*100
	720.68	544.38		
	TOTAL (g)	**176.30**		
3.- Unit preparation	Recipient emptied	Recipient filled		
3.1.- n-Dodecane used to increase pressure (g)	53.41	0.2		
$nC_{12}V_1$	**TOTAL (g)**	**53.21**		
4.- Shutdown	Empty recipient	Recipient filled		
4.1.- n-Dodecane remaining in n-Dodecane vessel (g)	0	13.91		
$nC_{12}V_2$	**TOTAL (g)**	**13.91**		
4.2.- Flusing mixture collected (g)	139.88	144.65	Purge of pump and lines before reactor	
LR	**TOTAL (g)**	**4.77**		
4.3.- Liquid products (g)	0	152.06		
LP	**TOTAL (g)**	**152.06**		
4.4.- Coke collected (g)	138.85	171.22		
Coke	**TOTAL (g)**	**32.37**		
4.5.- KOH solution after the test (g)	0	55.1		
SS_2	**TOTAL (g)**	**55.1**		
5.- Mass Balance (g)				
5.1.- General				
Inlet (FV_1 + $nC_{12}V_1$-FV_2 - $nC_{12}V_2$ - LR)	**210.83**			
Outlet (LP+Coke+SS_2-SS_1)	**185.03**			
MB	**87.76**			
GSY: (SS_2 - SS_1)/(Inlet)*100	**0.28**			
GDY: (LP)/(Inlet)*100	**72.12**			
GCY: (Coke)/(Inlet)*100	**15.35**			
GG: (100 - H_2S - Distillates - Coke)	**12.24**			
5.2. Products (wt%): Assuming that n-Dodecane is in the distillates				
Feed (FV_1 -FV_2-LR)*$X_{Residue}$	**77.19**			
SY: [SS_2 - SS_1]/Feed*100	**0.78**			
DY: [(LP -($nC_{12}V_2$ - $nC_{12}V_1$) - Feed*$X_{n\text{-dodecane}}$]/Feed*100	**23.86**			
CY: (Coke/Feed*100)	**41.94**			
G: (100 - H_2S - Distillates - Coke)	**33.42**			
Pumping time (minutes)	**45**			
Flow (gr/min)	**3.92**			

Date	3-19-02			
Experiment ID	33			
Name	n-C12 50 wt% 100 psig			
Vacuum residue ID	ABVB			
1.- KOH solution preparation:	Recipient filled	Recipient emptied	w%	
1.1.- KOH (g)				
1.2.- Water (g)	56.37	0.37		
SS_1	**TOTAL (g)**	**56**		
2.- Feed preparation	**FV_1**	**FV_2**	w%	
2.1.- n-Dodecane (g)	361.00	262.00	50.00	$X_{n\text{-}dodecane}$*100
2.2.- Vacuum residue (g)	361.04	262.03	50.00	$X_{Residue}$*100
	722.04	524.03		
	TOTAL (g)	**198.01**		
3.- Unit preparation	Recipient emptied	Recipient filled		
3.1.- n-Dodecane used to increase pressure (g)	57.19	0.05		
$nC_{12}V_1$	**TOTAL (g)**	**57.14**		
4.- Shutdown	Empty recipient	Recipient filled		
4.1.- n-Dodecane remaining in n-Dodecane vessel (g)	0	17.4		
$nC_{12}V_2$	**TOTAL (g)**	**17.4**		
4.2.- Flusing mixture collected (g)	139.86	145.78	Purge of pump and lines before reactor	
LR	**TOTAL (g)**	**5.92**		
4.3.- Liquid products (g)	0	169.92		
LP	**TOTAL (g)**	**169.92**		
4.4.- Coke collected (g)	138.82	178.46		
Coke	**TOTAL (g)**	**39.64**		
4.5.- KOH solution after the test (g)	0	56.86		
SS_2	**TOTAL (g)**	**56.86**		
5.- Mass Balance (g)				
5.1.- General				
Inlet (FV_1 + $nC_{12}V_1$-FV_2 - $nC_{12}V_2$ - LR)	**231.83**			
Outlet (LP+Coke+SS_2-SS_1)	**210.42**			
MB	**90.76**			
GSY: (SS_2 - SS_1)/(Inlet)*100	**0.37**			
GDY: (LP)/(Inlet)*100	**73.30**			
GCY: (Coke)/(Inlet)*100	**17.10**			
GG: (100 - H_2S - Distillates - Coke)	**9.24**			
5.2. Products (wt%): Assuming that n-Dodecane is in the distillates				
Feed (FV_1 -FV_2-LR)*$X_{Residue}$	**96.05**			
SY: [SS_2 - SS_1]/Feed*100	**0.90**			
DY: [(LP -($nC_{12}V_2$ - $nC_{12}V_1$) - Feed*$X_{n\text{-}dodecane}$]/Feed*100	**35.54**			
CY: (Coke/Feed*100)	**41.27**			
G: (100 - H_2S - Distillates - Coke)	**22.29**			
Pumping time (minutes)	**45**			
Flow (gr/min)	**4.40**			

Date	3-21-02			
Experiment ID	34			
Name	n-C12 50 wt% 20 psig			
Vacuum residue ID	ABVB			
1.- KOH solution preparation:	Recipient filled	Recipient emptied	w%	
1.1.- KOH (g)				
1.2.- Water (g)	62.55	0		
SS_1	**TOTAL (g)**	**62.55**		
2.- Feed preparation	**FV_1**	**FV_2**	w%	
2.1.- n-Dodecane (g)	361.56	277.17	50.00	$X_{n\text{-dodecane}}$*100
2.2.- Vacuum residue (g)	361.50	277.11	50.00	$X_{Residue}$*100
	723.06	554.28		
	TOTAL (g)	**168.78**		
3.- Unit preparation	Recipient emptied	Recipient filled		
3.1.- n-Dodecane used to increase pressure (g)	48.22	0.26		
$nC_{12}V_1$	**TOTAL (g)**	**47.96**		
4.- Shutdown	Empty recipient	Recipient filled		
4.1.- n-Dodecane remaining in n-Dodecane vessel (g)	0	17.98		
$nC_{12}V_2$	**TOTAL (g)**	**17.98**		
4.2.- Flusing mixture collected (g)	138.14	139.81	Purge of pump and lines before reactor	
LR	**TOTAL (g)**	**1.67**		
4.3.- Liquid products (g)	0	155.22		
LP	**TOTAL (g)**	**155.22**		
4.4.- Coke collected (g)	138.73	165.24		
Coke	**TOTAL (g)**	**26.51**		
4.5.- KOH solution after the test (g)	0	63.1		
SS_2	**TOTAL (g)**	**63.1**		
5.- Mass Balance (g)				
5.1.- General				
Inlet (FV_1 + $nC_{12}V_1$-FV_2 - $nC_{12}V_2$ - LR)	**197.09**			
Outlet (LP+Coke+SS_2-SS_1)	**182.28**			
MB	**92.49**			
GSY: (SS_2 - SS_1)/(Inlet)*100	**0.28**			
GDY: (LP)/(Inlet)*100	**78.76**			
GCY: (Coke)/(Inlet)*100	**13.45**			
GG: (100 - H_2S - Distillates - Coke)	**7.51**			
5.2. Products (wt%): Assuming that n-Dodecane is in the distillates				
Feed (FV_1 -FV_2-LR)*$X_{Residue}$	**83.55**			
SY: [SS_2 - SS_1]/Feed*100	**0.66**			
DY: [(LP -($nC_{12}V_2$ - $nC_{12}V_1$) - Feed*$X_{n\text{-dodecane}}$]/Feed*100	**49.88**			
CY: (Coke/Feed*100)	**31.73**			
G: (100 - H_2S - Distillates - Coke)	**17.73**			
Pumping time (minutes)	**45**			
Flow (gr/min)	**3.75**			

Date	3-23-02			
Experiment ID	35			
Name	n-C12 50 wt% 20 psig Reactor inlet at the botom			
Vacuum residue ID	ABVB			
1.- KOH solution preparation:	Recipient filled	Recipient emptied	w%	
1.1.- KOH (g)				
1.2.- Water (g)	64.58	0.57		
SS_1	**TOTAL (g)**	**64.01**		
2.- Feed preparation	**FV_1**	**FV_2**	w%	
2.1.- n-Dodecane (g)	361.69	280.41	50.00	$X_{n\text{-dodecane}}$*100
2.2.- Vacuum residue (g)	361.65	280.39	50.00	$X_{Residue}$*100
	723.34	560.80		
	TOTAL (g)	**162.54**		
3.- Unit preparation	Recipient emptied	Recipient filled		
3.1.- n-Dodecane used to increase pressure (g)	59.25	0.35		
$nC_{12}V_1$	**TOTAL (g)**	**58.9**		
4.- Shutdown	Empty recipient	Recipient filled		
4.1.- n-Dodecane remaining in n-Dodecane vessel (g)	0	12.58		
$nC_{12}V_2$	**TOTAL (g)**	**12.58**		
4.2.- Flusing mixture collected (g)	138.29	139.38	Purge of pump and lines before reactor	
LR	**TOTAL (g)**	**1.09**		
4.3.- Liquid products (g)	0	160.91		
LP	**TOTAL (g)**	**160.91**		
4.4.- Coke collected (g)	138.8	165.47		
Coke	**TOTAL (g)**	**26.67**		
4.5.- KOH solution after the test (g)	0	64.94		
SS_2	**TOTAL (g)**	**64.94**		
5.- Mass Balance (g)				
5.1.- General				
Inlet (FV_1 + $nC_{12}V_1$-FV_2 - $nC_{12}V_2$ - LR)	**207.77**			
Outlet (LP+Coke+SS_2-SS_1)	**188.51**			
MB	**90.73**			
GSY: (SS_2 - SS_1)/(Inlet)*100	**0.45**			
GDY: (LP)/(Inlet)*100	**77.45**			
GCY: (Coke)/(Inlet)*100	**12.84**			
GG: (100 - H_2S - Distillates - Coke)	**9.27**			
5.2. Products (wt%): Assuming that n-Dodecane is in the distillates				
Feed (FV_1 -FV_2-LR)*$X_{Residue}$	**80.72**			
SY: [SS_2 - SS_1]/Feed*100	**1.15**			
DY: [(LP -($nC_{12}V_2$ - $nC_{12}V_1$) - Feed*$X_{n\text{-dodecane}}$]/Feed*100	**41.95**			
CY: (Coke/Feed*100)	**33.04**			
G: (100 - H_2S - Distillates - Coke)	**23.86**			
Pumping time (minutes)	**45**			
Flow (gr/min)	**3.61**			

Date	3-26-02			
Experiment ID	36			
Name	100 wt% HF 20 psig and less Reactor inlet at the botom			
Vacuum residue ID	DC heater's throughput			
1.- KOH solution preparation:	Recipient filled	Recipient emptied	w%	
1.1.- KOH (g)				
1.2.- Water (g)	52.6	0.4		
SS$_1$	**TOTAL (g)**	**52.2**		
2.- Feed preparation	**FV$_1$**	**FV$_2$**	w%	
2.1.- n-Dodecane (g)	0.00	0.00	0.00	$X_{n\text{-dodecane}}$*100
2.2.- Vacuum residue (g)	748.14	567.16	100.0	$X_{Residue}$*100
	748.14	567.16		
	TOTAL (g)	**180.98**		
3.- Unit preparation	Recipient emptied	Recipient filled		
3.1.- n-Dodecane used to increase pressure (g)	61.47	0.44		
nC$_{12}$V$_1$	**TOTAL (g)**	**61.03**		
4.- Shutdown	Empty recipient	Recipient filled		
4.1.- n-Dodecane remaining in n-Dodecane vessel (g)	0	30.28		
nC$_{12}$V$_2$	**TOTAL (g)**	**30.28**		
4.2.- Flusing mixture collected (g)	139.81	152.66	Purge of pump and lines before reactor	
LR	**TOTAL (g)**	**12.85**		
4.3.- Liquid products (g)	0	130.83		
LP	**TOTAL (g)**	**130.83**		
4.4.- Coke collected (g)	138.93	181.14		
Coke	**TOTAL (g)**	**42.21**		
4.5.- KOH solution after the test (g)	0	53.32		
SS$_2$	**TOTAL (g)**	**53.32**		
5.- Mass Balance (g)				
5.1.- General				
Inlet (FV$_1$ + nC$_{12}$V$_1$-FV$_2$ - nC$_{12}$V$_2$ - LR)	**198.88**			
Outlet (LP+Coke+SS$_2$-SS$_1$)	**174.16**			
MB	**87.57**			
GSY: (SS$_2$ - SS$_1$)/(Inlet)*100	**0.56**			
GDY: (LP)/(Inlet)*100	**65.78**			
GCY: (Coke)/(Inlet)*100	**21.22**			
GG: (100 - H$_2$S - Distillates - Coke)	**12.43**			
5.2. Products (wt%): Assuming that n-Dodecane is in the distillates				
Feed (FV$_1$ -FV$_2$-LR)*$X_{Residue}$	**168.13**			
SY: [SS$_2$ - SS$_1$]/Feed*100	**0.67**			
DY: [(LP -(nC$_{12}$V$_2$ - nC$_{12}$V$_1$) - Feed*$X_{n\text{-dodecane}}$]/Feed*100	**59.53**			
CY: (Coke/Feed*100)	**25.11**			
G: (100 - H$_2$S - Distillates - Coke)	**14.70**			
Pumping time (minutes)	**40**			
Flow (gr/min)	**4.52**			

Date	4-24-02			
Experiment ID	38			
Name	n-C12 50 wt%; 350 psig			
Vacuum residue ID	ABVB			
1.- KOH solution preparation:	Recipient filled	Recipient emptied	w%	
1.1.- KOH (g)				
1.2.- Water (g)	45.26	0.6		
SS_1	**TOTAL (g)**	**44.66**		
2.- Feed preparation	**FV_1**	**FV_2**	w%	
2.1.- n-Dodecane (g)	360.17	264.80	50.00	$X_{n\text{-dodecane}}$*100
2.2.- Vacuum residue (g)	360.17	264.80	50.00	$X_{Residue}$*100
	720.34	529.60		
	TOTAL (g)	**190.74**		
3.- Unit preparation	Recipient emptied	Recipient filled		
3.1.- n-Dodecane used to increase pressure (g)	120.8	0.05		
$nC_{12}V_1$	**TOTAL (g)**	**120.75**		
4.- Shutdown	Empty recipient	Recipient filled		
4.1.- n-Dodecane remaining in n-Dodecane vessel (g)	0	53.86		
$nC_{12}V_2$	**TOTAL (g)**	**53.86**		
4.2.- Flusing mixture collected (g)	139.84	147.46	Purge of pump and lines before reactor	
LR	**TOTAL (g)**	**7.62**		
4.3.- Liquid products (g)	0	184.92		
LP	**TOTAL (g)**	**184.92**		
4.4.- Coke collected (g)	138.81	182.67		
Coke	**TOTAL (g)**	**43.86**		
4.5.- KOH solution after the test (g)	0	44.8		
SS_2	**TOTAL (g)**	**44.8**		
5.- Mass Balance (g)				
5.1.- General				
Inlet (FV_1 + $nC_{12}V_1$-FV_2 - $nC_{12}V_2$ - LR)	**250.01**			
Outlet (LP+Coke+SS_2-SS_1)	**228.92**			
MB	**91.56**			
GSY: (SS_2 - SS_1)/(Inlet)*100	**0.06**			
GDY: (LP)/(Inlet)*100	**73.97**			
GCY: (Coke)/(Inlet)*100	**17.54**			
GG: (100 - H_2S - Distillates - Coke)	**8.44**			
5.2. Products (wt%): Assuming that n-Dodecane is in the distillates				
Feed (FV_1 -FV_2-LR)*$X_{Residue}$	**91.56**			
SY: [SS_2 - SS_1]/Feed*100	**0.15**			
DY: [(LP -($nC_{12}V_2$ - $nC_{12}V_1$) - Feed*$X_{n\text{-dodecane}}$]/Feed*100	**28.91**			
CY: (Coke/Feed*100)	**47.90**			
G: (100 - H_2S - Distillates - Coke)	**23.03**			
Pumping time (minutes)	**40**			
Flow (gr/min)	**4.77**			

Date	05/03/2002			
Experiment ID	40			
Name	n-C12 70 wt%; 870 psig			
Vacuum residue ID	ABVB			
1.- KOH solution preparation:	Recipient filled	Recipient emptied	w%	
1.1.- KOH (g)				
1.2.- Water (g)	50.58	0.71		
SS$_1$	**TOTAL (g)**	**49.87**		
2.- Feed preparation	**FV$_1$**	**FV$_2$**	w%	
2.1.- n-Dodecane (g)	511.06	395.63	69.99	$X_{n-dodecane}$*100
2.2.- Vacuum residue (g)	219.08	169.59	30.01	$X_{Residue}$*100
	730.14	565.22		
	TOTAL (g)	**164.92**		
3.- Unit preparation	Recipient emptied	Recipient filled		
3.1.- n-Dodecane used to increase pressure (g)	159.16	0.39		
nC$_{12}$V$_1$	**TOTAL (g)**	**158.77**		
4.- Shutdown	Empty recipient	Recipient filled		
4.1.- n-Dodecane remaining in n-Dodecane vessel (g)	0	22.31		
nC$_{12}$V$_2$	**TOTAL (g)**	**22.31**		
4.2.- Flusing mixture collected (g)	139.81	151.84	Purge of pump and lines before reactor	
LR	**TOTAL (g)**	**12.03**		
4.3.- Liquid products (g)	0	251.16		
LP	**TOTAL (g)**	**251.16**		
4.4.- Coke collected (g)	138.9	149.05		
Coke	**TOTAL (g)**	**10.15**		
4.5.- KOH solution after the test (g)	0	44.8		
SS$_2$	**TOTAL (g)**	**49.9**		
5.- Mass Balance (g)				
5.1.- General				
Inlet (FV$_1$ + nC$_{12}$V$_1$-FV$_2$ - nC$_{12}$V$_2$ - LR)	**289.35**			
Outlet (LP+Coke+SS$_2$-SS$_1$)	**261.34**			
MB	**90.32**			
GSY: (SS$_2$ - SS$_1$)/(Inlet)*100	**0.01**			
GDY: (LP)/(Inlet)*100	**86.80**			
GCY: (Coke)/(Inlet)*100	**3.51**			
GG: (100 - H$_2$S - Distillates - Coke)	**9.68**			
5.2. Products (wt%): Assuming that n-Dodecane is in the distillates				
Feed (FV$_1$ -FV$_2$-LR)*$X_{Residue}$	**45.87**			
SY: [SS$_2$ - SS$_1$]/Feed*100	**0.07**			
DY: [(LP -(nC$_{12}$V$_2$ - nC$_{12}$V$_1$) - Feed*$X_{n-dodecane}$]/Feed*100	**16.75**			
CY: (Coke/Feed*100)	**22.13**			
G: (100 - H$_2$S - Distillates - Coke)	**61.06**			
Pumping time (minutes)	**45**			
Flow (gr/min)	**3.66**			

Date	05/07/2002			
Experiment ID	41			
Name	n-C12 70 wt%; 20 psig			
Vacuum residue ID	ABVB			
1.- KOH solution preparation:	Recipient filled	Recipient emptied	w%	
1.1.- KOH (g)				
1.2.- Water (g)	75.99	0.79		
SS_1	**TOTAL (g)**	**75.2**		
2.- Feed preparation	**FV_1**	**FV_2**	w%	
2.1.- n-Dodecane (g)	510.88	392.34	70.00	$X_{n\text{-dodecane}}$*100
2.2.- Vacuum residue (g)	218.98	168.16	30.00	$X_{Residue}$*100
	729.86	560.50		
	TOTAL (g)	**169.36**		
3.- Unit preparation	Recipient emptied	Recipient filled		
3.1.- n-Dodecane used to increase pressure (g)	42.5	0.04		
$nC_{12}V_1$	**TOTAL (g)**	**42.46**		
4.- Shutdown	Empty recipient	Recipient filled		
4.1.- n-Dodecane remaining in n-Dodecane vessel (g)	0	9.39		
$nC_{12}V_2$	**TOTAL (g)**	**9.39**		
4.2.- Flusing mixture collected (g)	139.8	150.37	Purge of pump and lines before reactor	
LR	**TOTAL (g)**	**10.57**		
4.3.- Liquid products (g)	0	160.53		
LP	**TOTAL (g)**	**160.53**		
4.4.- Coke collected (g)	138.87	155.16		
Coke	**TOTAL (g)**	**16.29**		
4.5.- KOH solution after the test (g)	0	75.7		
SS_2	**TOTAL (g)**	**75.7**		
5.- Mass Balance (g)				
5.1.- General				
Inlet (FV_1 + $nC_{12}V_1$-FV_2 - $nC_{12}V_2$ - LR)	**191.86**			
Outlet (LP+Coke+SS_2-SS_1)	**177.32**			
MB	**92.42**			
GSY: (SS_2 - SS_1)/(Inlet)*100	**0.26**			
GDY: (LP)/(Inlet)*100	**83.67**			
GCY: (Coke)/(Inlet)*100	**8.49**			
GG: (100 - H_2S - Distillates - Coke)	**7.58**			
5.2. Products (wt%): Assuming that n-Dodecane is in the distillates				
Feed (FV_1 -FV_2-LR)*$X_{Residue}$	**47.64**			
SY: [SS_2 - SS_1]/Feed*100	**1.05**			
DY: [(LP -($nC_{12}V_2$ - $nC_{12}V_1$) - Feed*$X_{n\text{-dodecane}}$]/Feed*100	**34.24**			
CY: (Coke/Feed*100)	**34.19**			
G: (100 - H_2S - Distillates - Coke)	**30.52**			
Pumping time (minutes)	**45**			
Flow (gr/min)	**3.76**			

Date	05/09/2002			
Experiment ID	42			
Name	n-C12 70 wt%; 500 psig			
Vacuum residue ID	ABVB			
1.- KOH solution preparation:	Recipient filled	Recipient emptied	w%	
1.1.- KOH (g)				
1.2.- Water (g)	65.66	0.11		
SS_1	**TOTAL (g)**	**65.55**		
2.- Feed preparation	**FV_1**	**FV_2**	w%	
2.1.- n-Dodecane (g)	510.72	388.85	70.00	$X_{n\text{-dodecane}}$*100
2.2.- Vacuum residue (g)	218.90	166.67	30.00	$X_{Residue}$*100
	729.62	555.52		
	TOTAL (g)	**174.10**		
3.- Unit preparation	Recipient emptied	Recipient filled		
3.1.- n-Dodecane used to increase pressure (g)	166.38	0.27		
$nC_{12}V_1$	**TOTAL (g)**	**166.11**		
4.- Shutdown	Empty recipient	Recipient filled		
4.1.- n-Dodecane remaining in n-Dodecane vessel (g)	0	58.44		
$nC_{12}V_2$	**TOTAL (g)**	**58.44**		
4.2.- Flusing mixture collected (g)	138.26	150.18	Purge of pump and lines before reactor	
LR	**TOTAL (g)**	**11.92**		
4.3.- Liquid products (g)	0	232.18		
LP	**TOTAL (g)**	**232.18**		
4.4.- Coke collected (g)	138.96	155.15		
Coke	**TOTAL (g)**	**16.19**		
4.5.- KOH solution after the test (g)	0	65.54		
SS_2	**TOTAL (g)**	**65.54**		
5.- Mass Balance (g)				
5.1.- General				
Inlet (FV_1 + $nC_{12}V_1$-FV_2 - $nC_{12}V_2$ - LR)	**269.85**			
Outlet (LP+Coke+SS_2-SS_1)	**248.36**			
MB	**92.04**			
GSY: (SS_2 - SS_1)/(Inlet)*100	**0.00**			
GDY: (LP)/(Inlet)*100	**86.04**			
GCY: (Coke)/(Inlet)*100	**6.00**			
GG: (100 - H_2S - Distillates - Coke)	**7.96**			
5.2. Products (wt%): Assuming that n-Dodecane is in the distillates				
Feed (FV_1 -FV_2-LR)*$X_{Residue}$	**48.66**			
SY: [SS_2 - SS_1]/Feed*100	**-0.02**			
DY: [(LP -($nC_{12}V_2$ - $nC_{12}V_1$) - Feed*$X_{n\text{-dodecane}}$]/Feed*100	**22.58**			
CY: (Coke/Feed*100)	**33.27**			
G: (100 - H_2S - Distillates - Coke)	**44.17**			
Pumping time (minutes)	**45**			
Flow (gr/min)	**3.87**			

Date	05/10/2002			
Experiment ID	43			
Name	n-C12 20 wt%; 870 psig			
Vacuum residue ID	ABVB			
1.- KOH solution preparation:	Recipient filled	Recipient emptied	w%	
1.1.- KOH (g)				
1.2.- Water (g)	64.02	0.7		
SS$_1$	**TOTAL (g)**	**63.32**		
2.- Feed preparation	**FV$_1$**	**FV$_2$**	w%	
2.1.- n-Dodecane (g)	145.64	107.12	20.00	$X_{n\text{-dodecane}}$*100
2.2.- Vacuum residue (g)	582.62	428.52	80.00	$X_{Residue}$*100
	728.26	535.64		
	TOTAL (g)	**192.62**		
3.- Unit preparation	Recipient emptied	Recipient filled		
3.1.- n-Dodecane used to increase pressure (g)	178.74	0.58		
nC$_{12}$V$_1$	**TOTAL (g)**	**178.16**		
4.- Shutdown	Empty recipient	Recipient filled		
4.1.- n-Dodecane remaining in n-Dodecane vessel (g)	0	44.57		
nC$_{12}$V$_2$	**TOTAL (g)**	**44.57**		
4.2.- Flusing mixture collected (g)	138.27	152.12	Purge of pump and lines before reactor	
LR	**TOTAL (g)**	**13.85**		
4.3.- Liquid products (g)	0	202.99		
LP	**TOTAL (g)**	**202.99**		
4.4.- Coke collected (g)	138.96	198.45		
Coke	**TOTAL (g)**	**59.49**		
4.5.- KOH solution after the test (g)	0	63.63		
SS$_2$	**TOTAL (g)**	**63.63**		
5.- Mass Balance (g)				
5.1.- General				
Inlet (FV$_1$ + nC$_{12}$V$_1$-FV$_2$ - nC$_{12}$V$_2$ - LR)	**312.36**			
Outlet (LP+Coke+SS$_2$-SS$_1$)	**262.79**			
MB	**84.13**			
GSY: (SS$_2$ - SS$_1$)/(Inlet)*100	**0.10**			
GDY: (LP)/(Inlet)*100	**64.99**			
GCY: (Coke)/(Inlet)*100	**19.05**			
GG: (100 - H_2S - Distillates - Coke)	**15.87**			
5.2. Products (wt%): Assuming that n-Dodecane is in the distillates				
Feed (FV$_1$ -FV$_2$-LR)*$X_{Residue}$	**143.02**			
SY: [SS$_2$ - SS$_1$]/Feed*100	**0.22**			
DY: [(LP -(nC$_{12}$V$_2$ - nC$_{12}$V$_1$) - Feed*$X_{n\text{-dodecane}}$]/Feed*100	**23.53**			
CY: (Coke/Feed*100)	**41.60**			
G: (100 - H_2S - Distillates - Coke)	**34.66**			
Pumping time (minutes)	**45**			
Flow (gr/min)	**4.28**			

Appendix I: Coke Breakage Method

According to the experimental section, one of the physical differences between shot coke and sponge coke is their hardness. This property is one of the important parameters used to differentiate shot coke from sponge coke. Although coke hardness can be measured using standard ASTM methods (ASTM-D5003-95 and ASTM-D409-97), these methods can not be used to process the coke samples produced here because the amount of sample required is larger than the mass of sample. Therefore, the development of a non-standard but reliable method was necessary.

Procedure:

The development of this method was carried out using a coke sample from a pilot plant (Petróleos de Venezuela-Intevep, 2002) composed of a mixture of sponge and shot coke. The procedure followed is indicated below:

1. The coke sample was classified as shot coke and sponge coke following the observable description as indicated in the introductory chapter. Figure I-1 shows a picture of each sample where the visual difference is noticeable. The shot coke sample appears as small spheres stuck together like a bunch of grapes; whereas the sponge coke sample looks like a highly porous solid material.

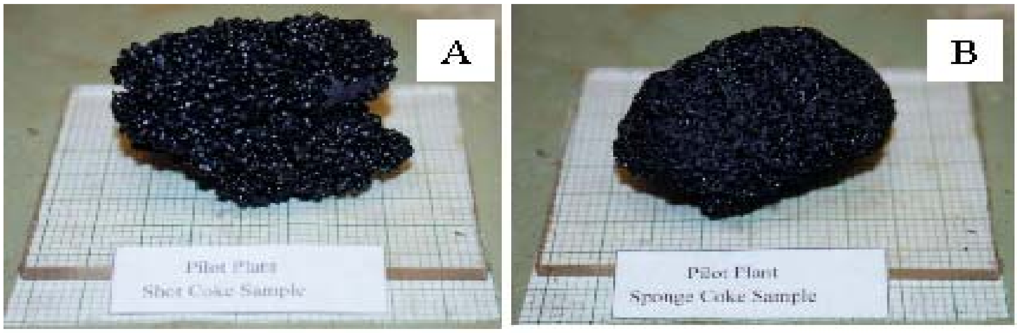

Figure I-1: Shot coke (A) and sponge coke (B) samples from the same source.

2. After classifying the coke as shot or sponge, small samples were separated from the big pieces. The shot coke particles were easy to separate because each one

was perfectly delimited from each other; on the other hand, sponge coke particles were difficult to separate. This big sample was an entire piece without delimitation between particles; thus, the sponge coke particles were taken from the big piece with dimensions similar to the shot coke clusters (between 2 and 8 mm). In total, 20 particles of each coke type were gathered.

3. Each particle was subject to increasing weights until it was broken. The weight was increased according to the scale shown in Table I-1.

Table I-1: Weight scale to determine the coke particles resistance.

Order	1st	2nd	3rd	4th	TOTAL
1	354				354
2	664				664
3	354	478			832
4	417	478			895
5	664	281			945
6	664	281	417		1362
7	1590				1590
8	1638				1638
9	1638	478			2116
10	1638	478	186		2302
11	1638	1590			3228
12	1638	1590	478		3706
13	1638	1590	478	186	3892
14	1638	1590	478	354	4060
15	1638	1590	664	354	4245
16	1638	1590	664	417	4309

The application of weight was performed following the order indicated in the first column. In some cases, specifically from order 3 to 6 and 9 to 15, the weight increments were done by superposition of up to four pieces. The weight of such pieces are indicated from the second column to the fifth column.

Results and Discussion

The measurements were obtained randomly with the previous knowledge that the particle evaluated was a representative sample of shot coke or sponge coke. Table I-2 shows these results.

Table I-2 includes, for each coke particle evaluated, the order of measurement, approximate dimensions, description of their appearances and the weight required to break it.

Table I-2: Shot coke and sponge coke harness measurement.

Number	Dimensions (mm)	Description	Breakage Mass (g)
1	4	Shot. Big pores. Sphere. Smooth surface	3228
2	2 & 4	Shot. Big pores. Sphere. Smooth surface	3228
3	4 & 6 x 2	Sponge. Irregular form.	832
4	6 x 4	Sponge. Big pores. Irregular form.	832
5	2 & 4	Shot. No pores. Sphere. Smooth surface	3228
6	2& 4	Shot. Pores.	3706
7	4 & 6 x 2 & 4	Sponge. Big pores. Irregular form.	664
8	6 x 4	Sponge. Big pores. Irregular form.	832
9	4 x 2	Shot. No pores. Oval. Smooth surface	1638
10	2 & 4	Shot. Some pores. Sphere	3228
11	4 & 6 x 4 & 6	Sponge. Many pores. Irregular form	832
12	4	Shot. Many pores. Sphere	3228
13	4 x 2	Shot. Big pores. Oval. Smooth surface	3706
14	4	Sponge. Pores and irregular form	832
15	4 x 4	Sponge. Big pores. Irregular form.	664
16	2 & 4	Shot. Pores. Non-spherical. Compact	3228
17	2 & 4	Sponge. Big pores. Irregular form.	832
18	4 x 2	Sponge. Big pores. Irregular form.	832
19	6 x 4	Shot. Pores but compact. Spherical	3892
20	4 x 2	Sponge. Pores and irregular form	832

21	2	Shot. Pores. Spherical. Compact	1638
22	4 x 2	Shot. Pores. Oval	1638
23	4	Sponge. Pores and irregular form	832
24	2 & 4	Shot. Few pores. Sphere. Smooth	3228
25	2 & 4	Shot. Sphere. Small pores	3228
26	4 x 2	Sponge. Pores and irregular form	1362
27	6 x 4	Sponge. Pores. Dish form	895
28	6 x 6	Sponge. Pores and irregular form	664
29	4 x 2	Shot. Pores. Oval	4309
30	6 x 6-8	Sponge. Big pores. Irregular form.	2116
31	4	Shot. Pores. Compact sphere	3228
32	6 x 2-4	Sponge. Pores. Irregular form	664
33	2 & 4	Shot. Many pores. Sphere	4245
34	4 x 8	Sponge. Big pores. Irregular form	832
35	2 & 4	Shot. Pores. Spherical.	4060
36	6 x 4	Sponge. Big pores. Irregular form	832
37	4 x 2-4	Shot. Small pores. Oval	3228
38	4 x 2	Shot. Small pores. Oval	1638
39	4 x 4	Sponge. Big pores. Irregular surface	832
40	6 x 4	Sponge. Big pores. Irregular form	832

Figure I-2 shows the breakage mass of shot coke and sponge coke particles. It is worth noting that shot coke particles resist more weight than sponge coke particles. Sponge coke particles present an isolated case where the breakage mass is 2116 g, which could be related to the big particle size; but in general, the breakage mass is below 1000 g. Meanwhile, the breakage mass for shot coke particles is above 1500 g and more frequently above 3000 g.

Therefore, based on the results indicated above, this non-standard method could be useful to differentiate shot coke and sponge coke particles. If the evaluation of particles between 2 – 8 mm gives a breakage mass smaller than 1000 g, the coke can be considered as sponge coke; on the other hand, if such particle can resist more than 1500 g, it can be considered as shot coke.

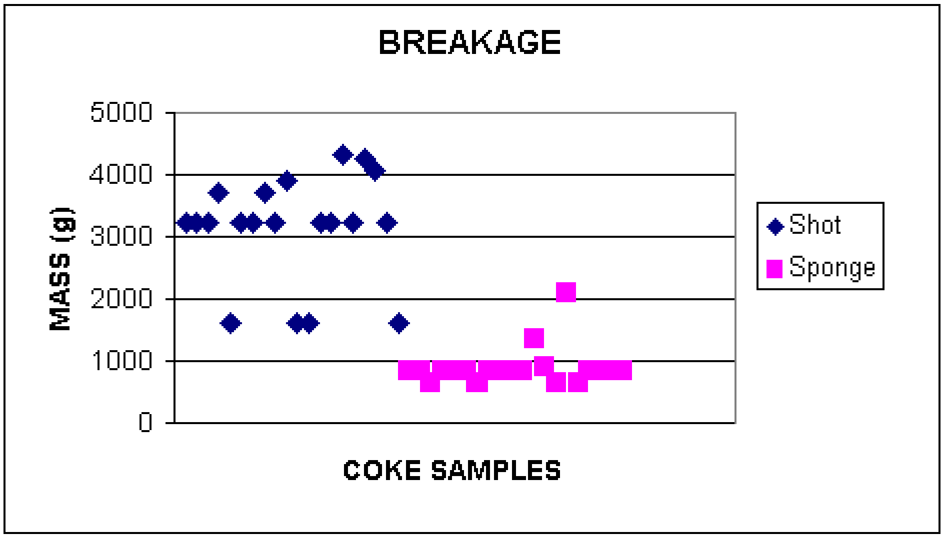

Figure I-2: Breakage mass for shot coke and sponge coke particles.

Appendix J: Coke Analyses

This appendix contains the information to analyze the structure of the coke samples. This information is based on the observation of the samples to identify characteristics associated to shot coke and sponge coke; and on the application of the hardness test to verify the results from the microscope observations. The data presented for each experiment include pictures taken with the electronic microscope QX3+™ and the results from the hardness test. The pictures presented include a group of particles studied with referential measurements and pictures of individual particles.

Microscope Pictures

Experiment 09:

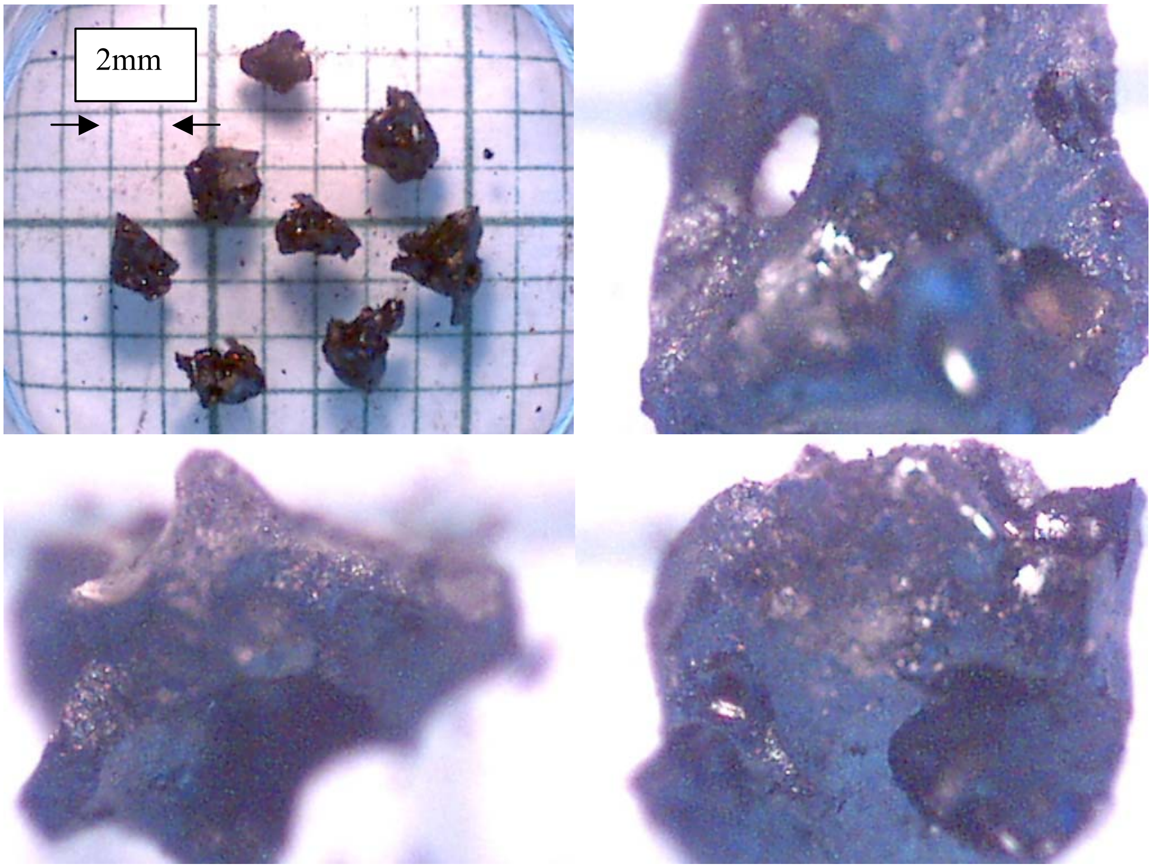

Experiment 11:

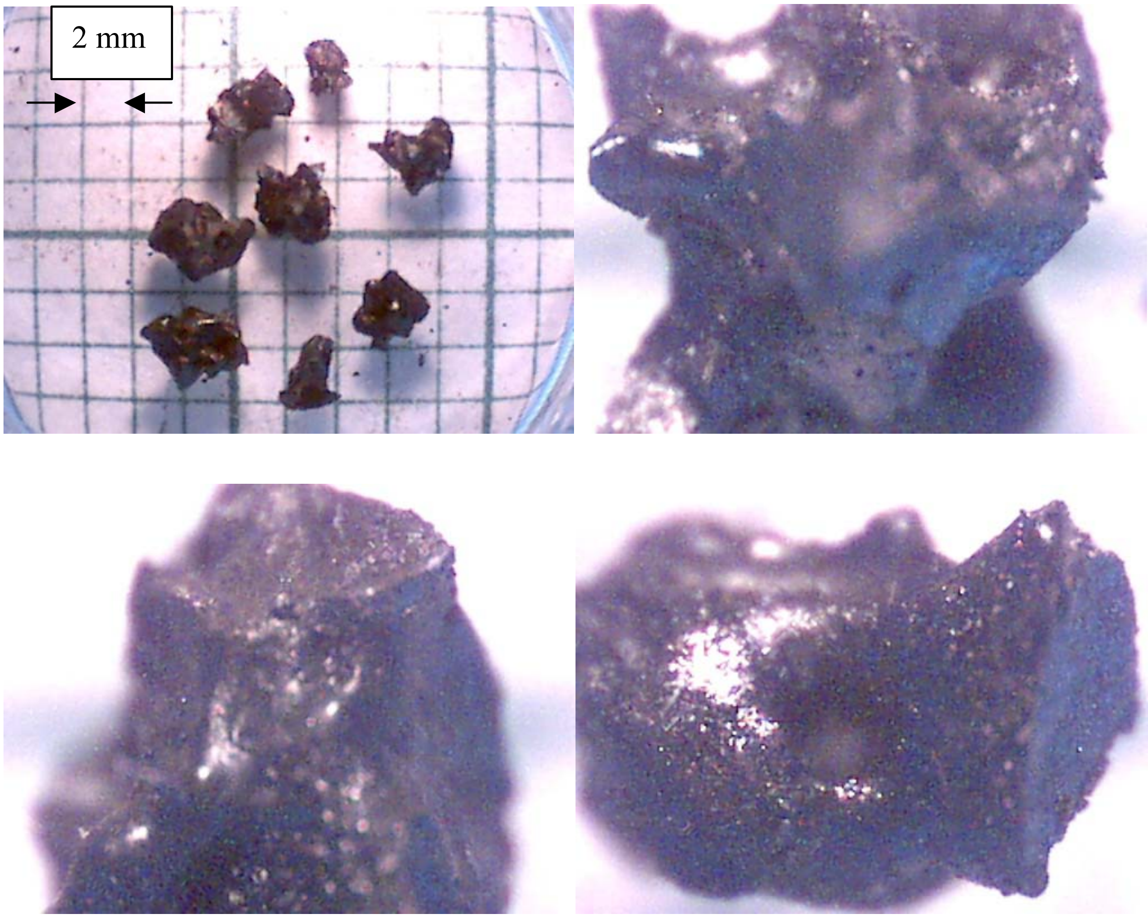

Experiment 15:

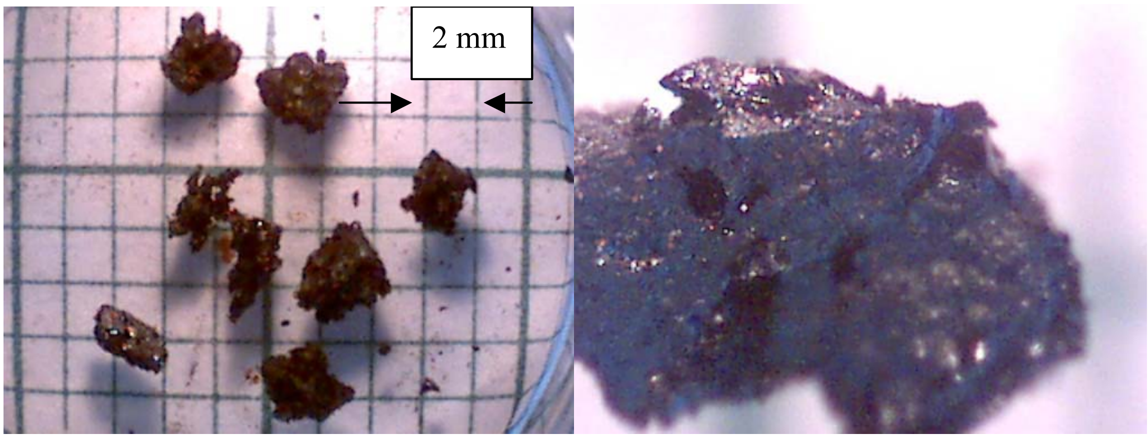

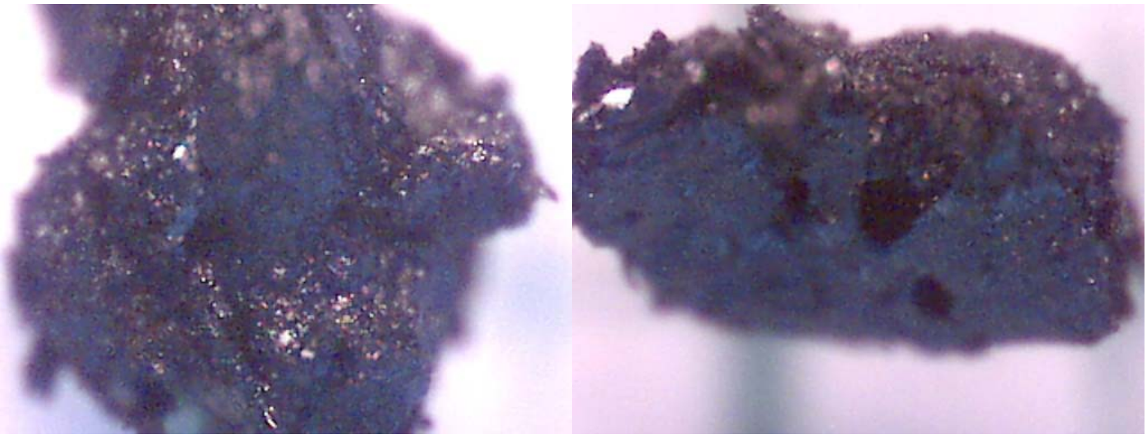

Experiment 19:

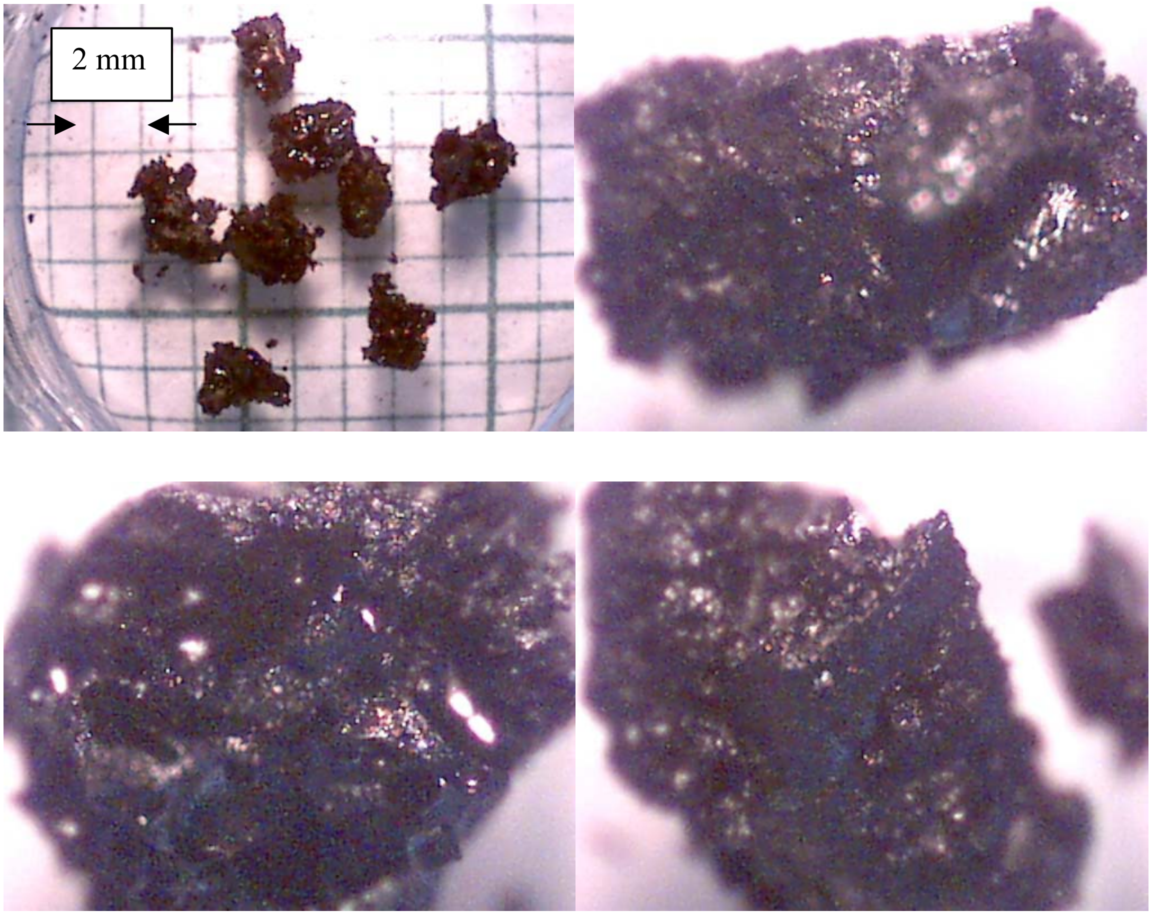

Experiment 20:

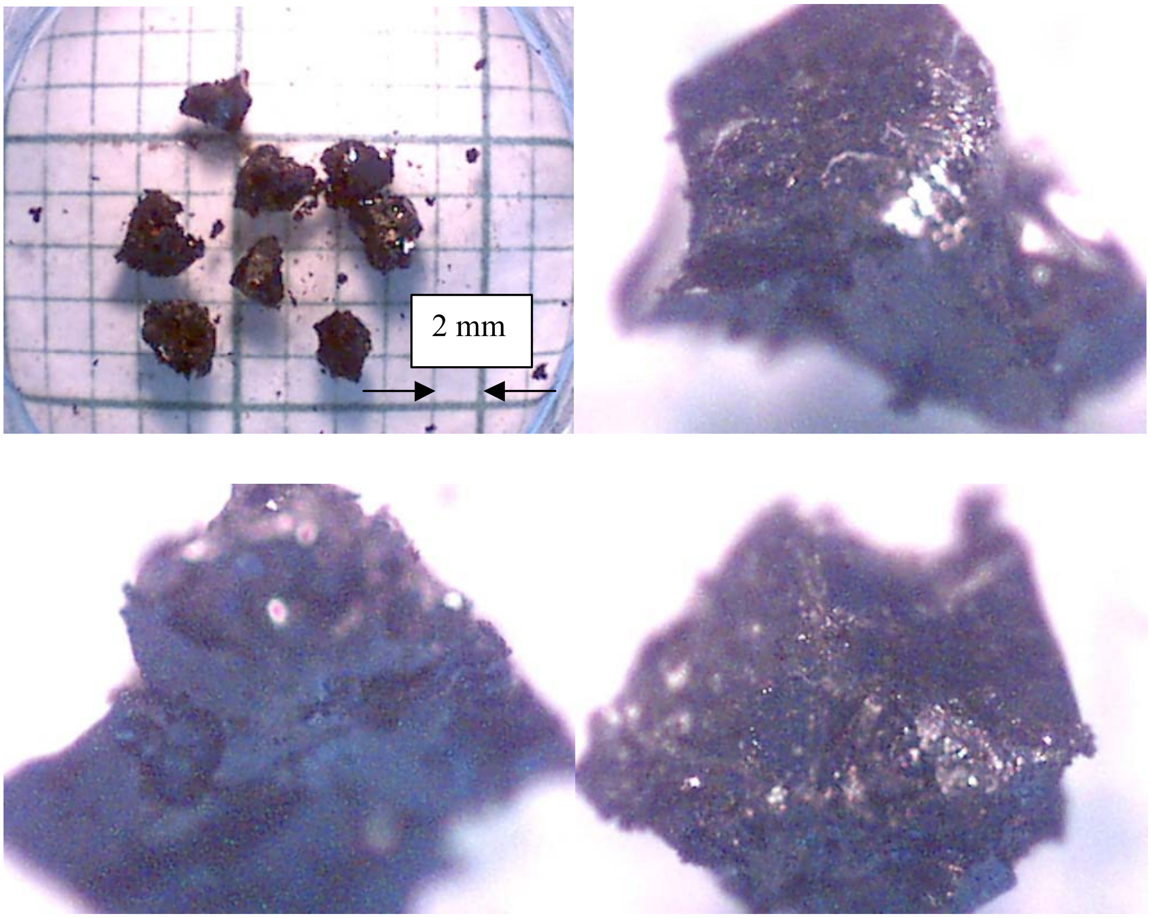

Experiment 21:

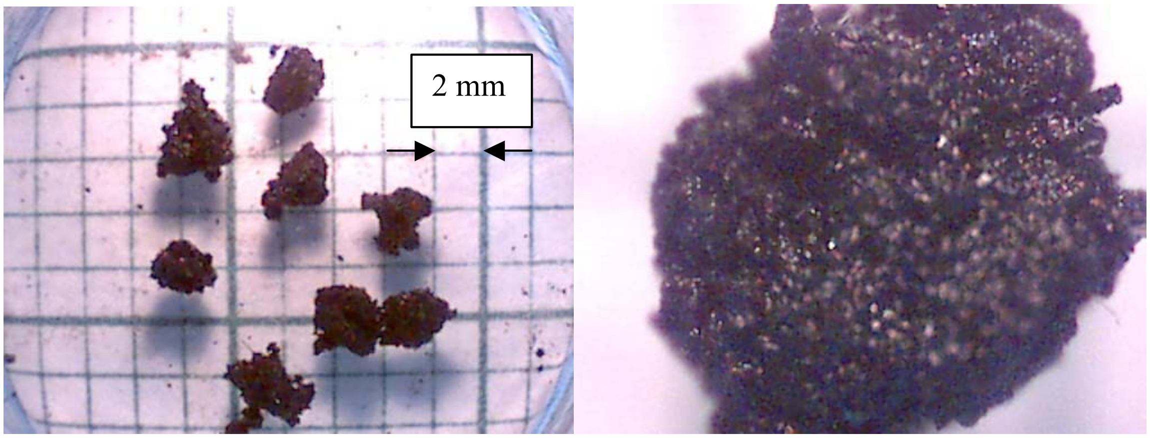

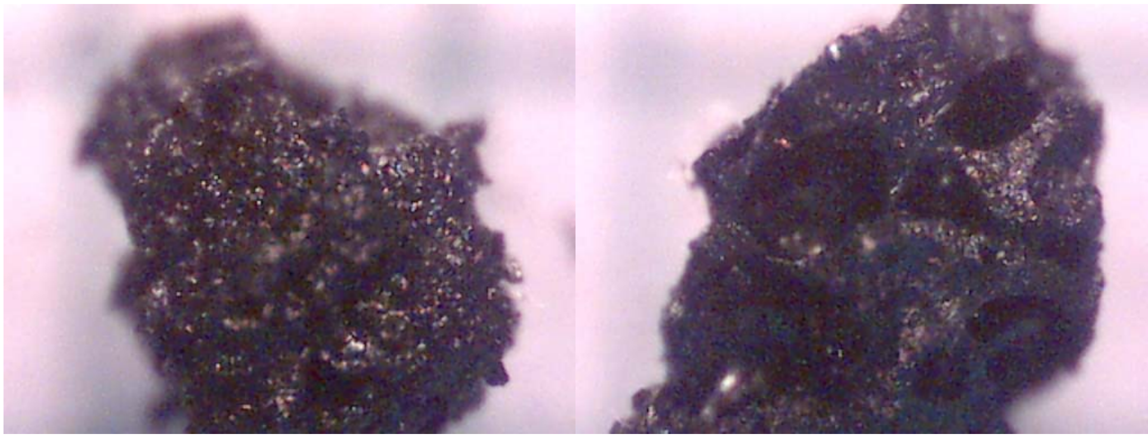

Experiment 22:

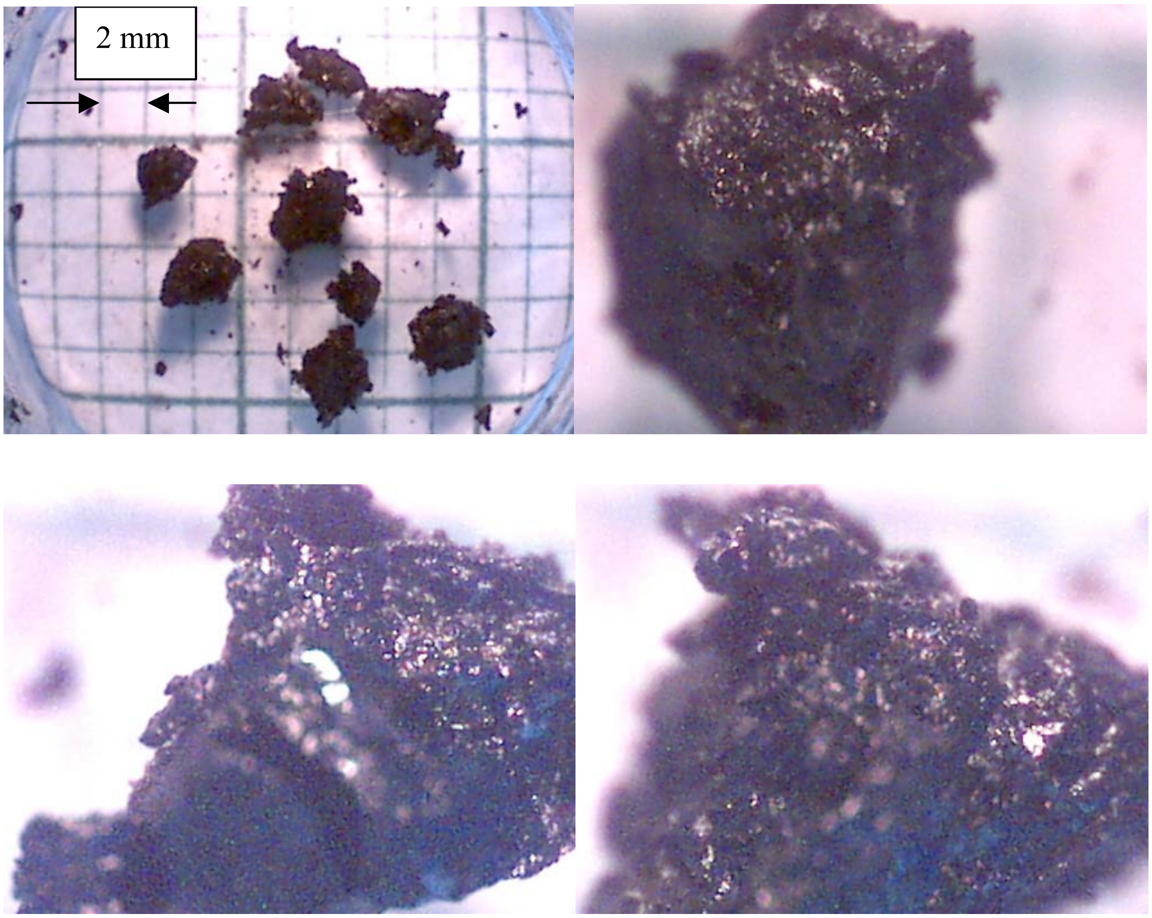

Experiment 24:

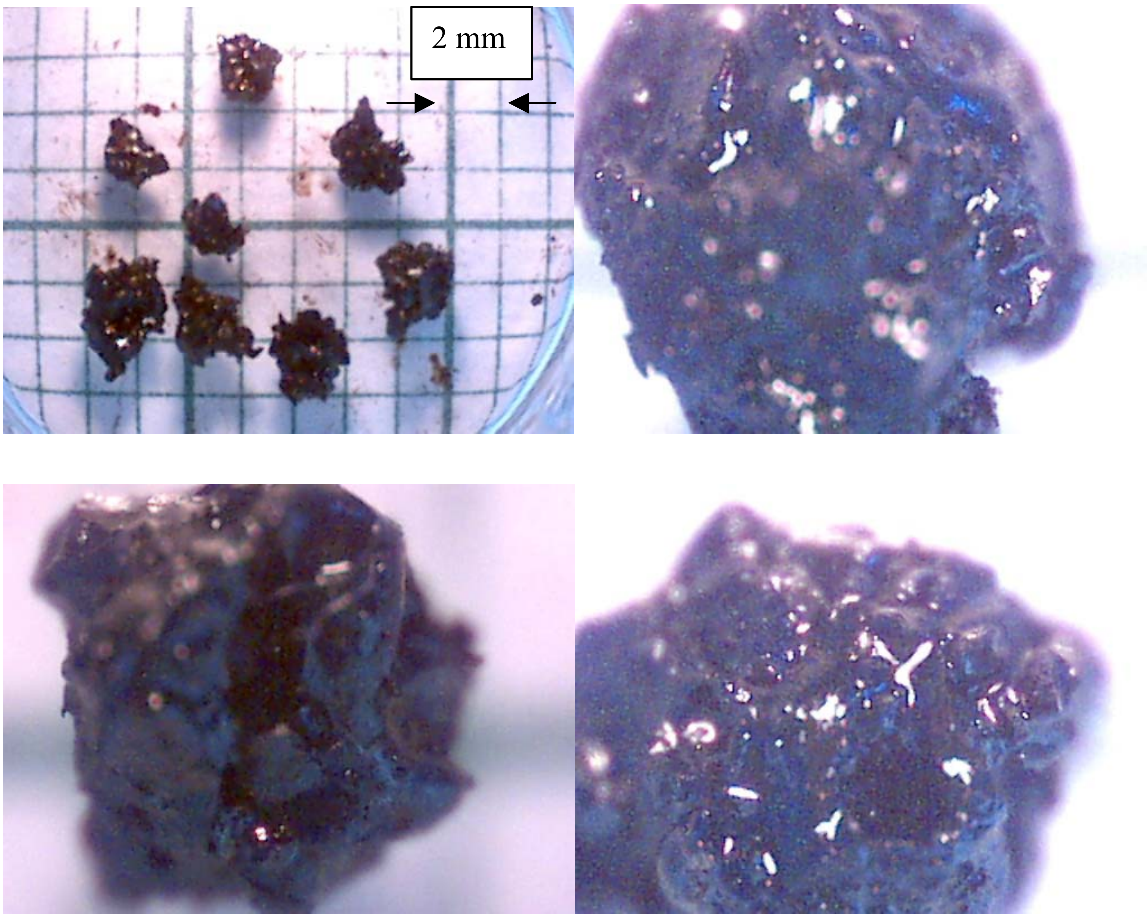

Experiment 25:

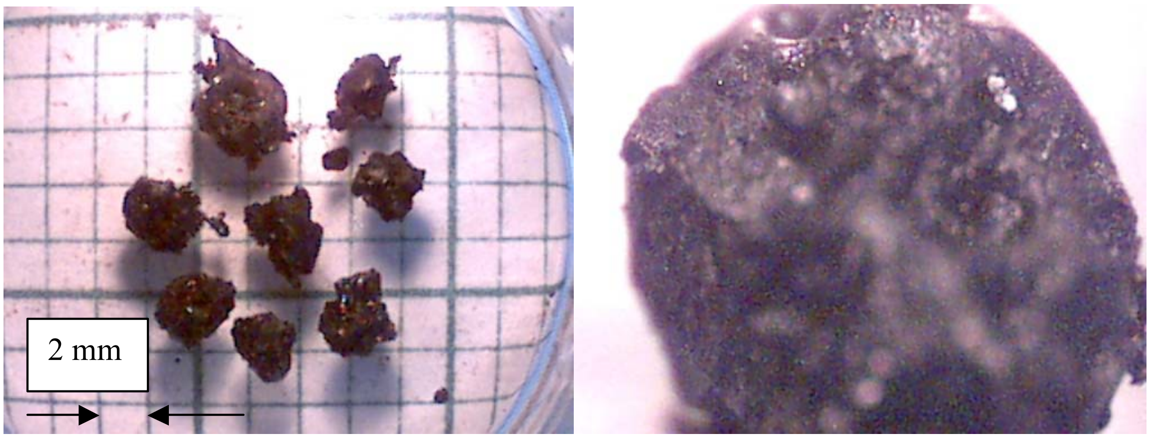

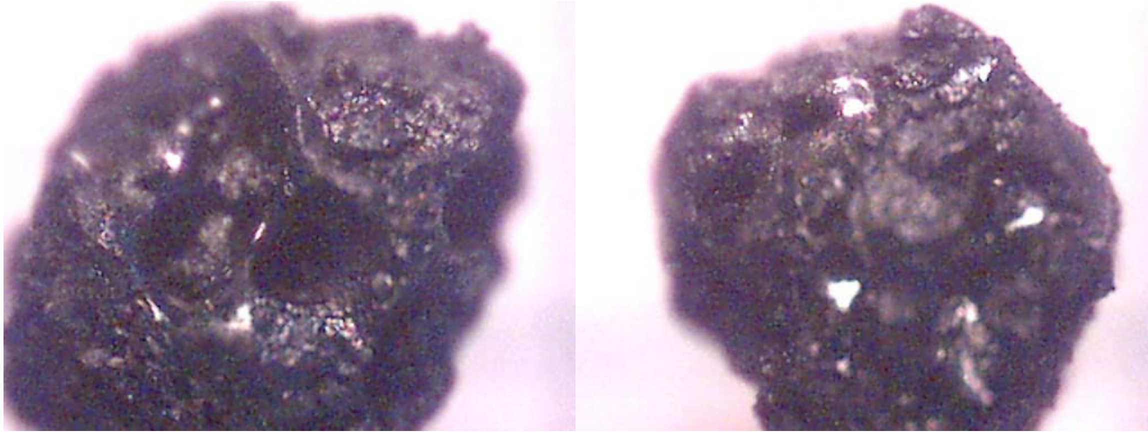

Experiment 26:

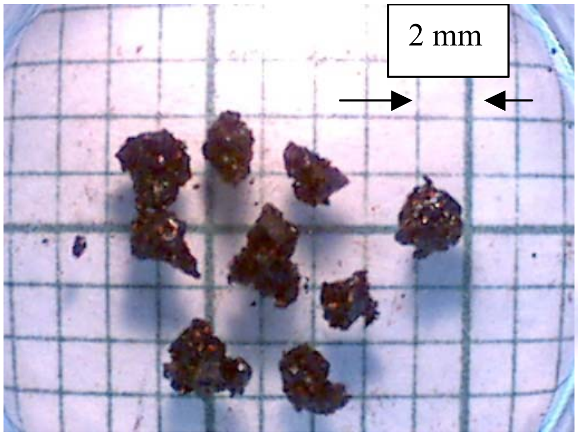

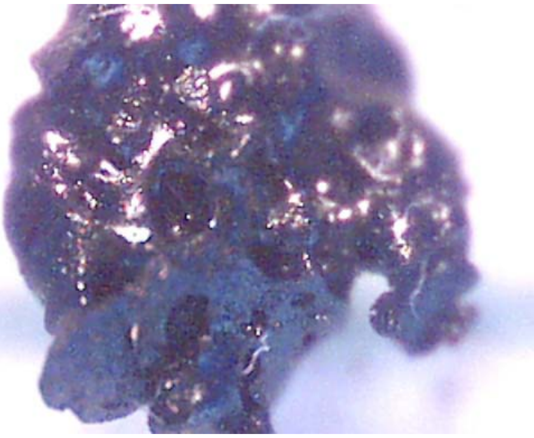

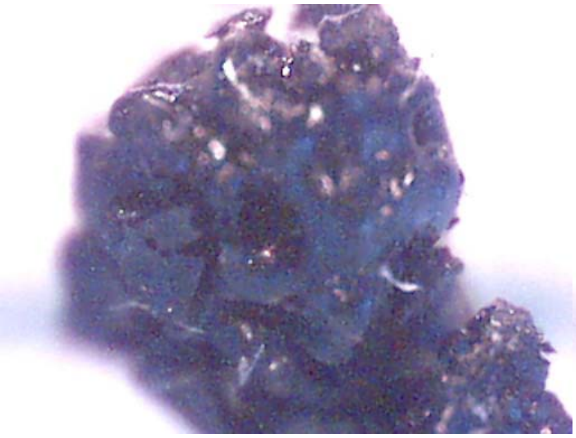

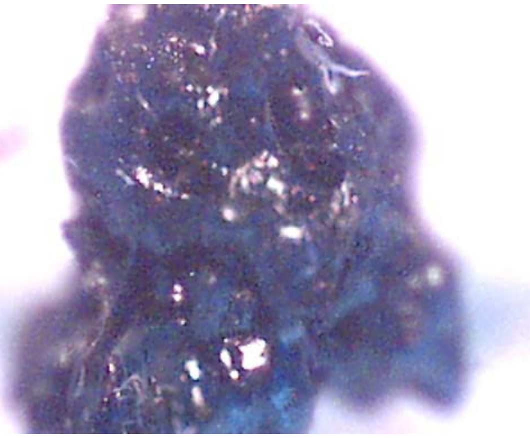

Experiment 27:

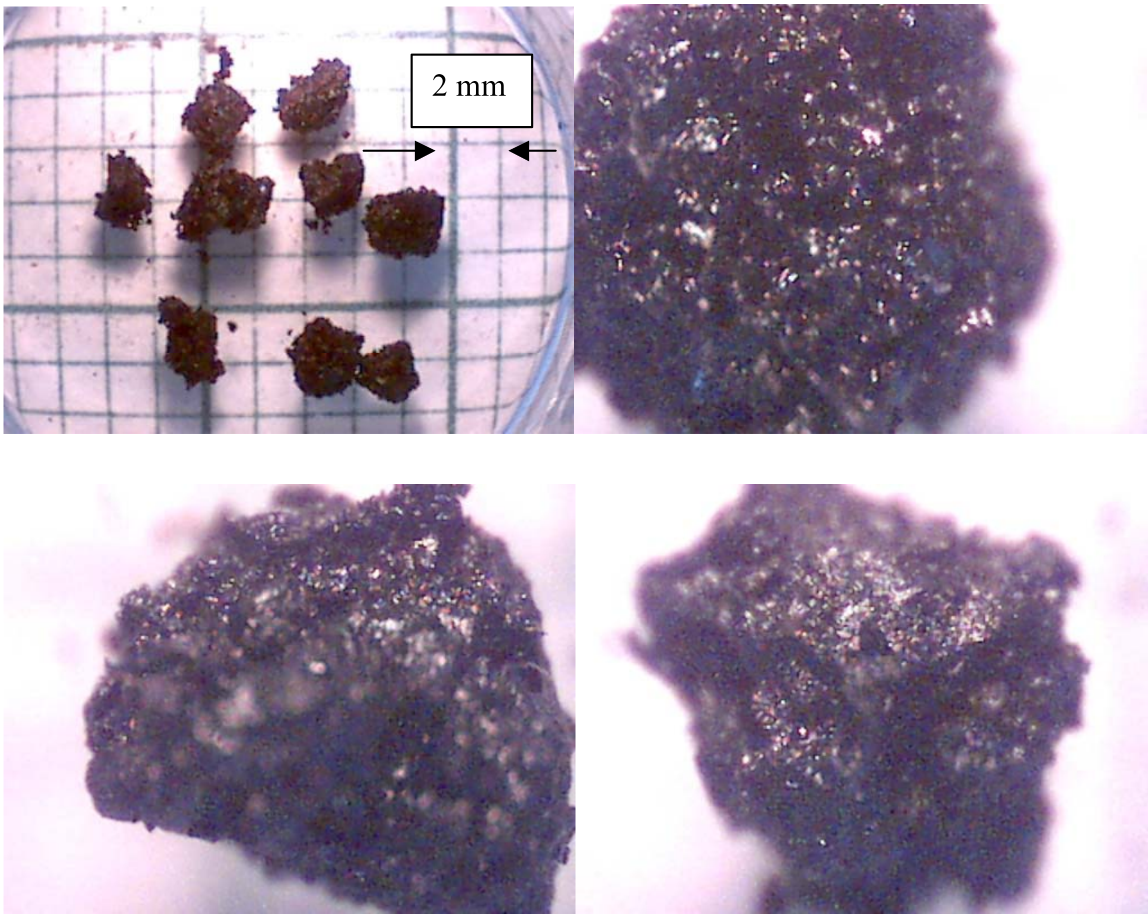

Experiment 28:

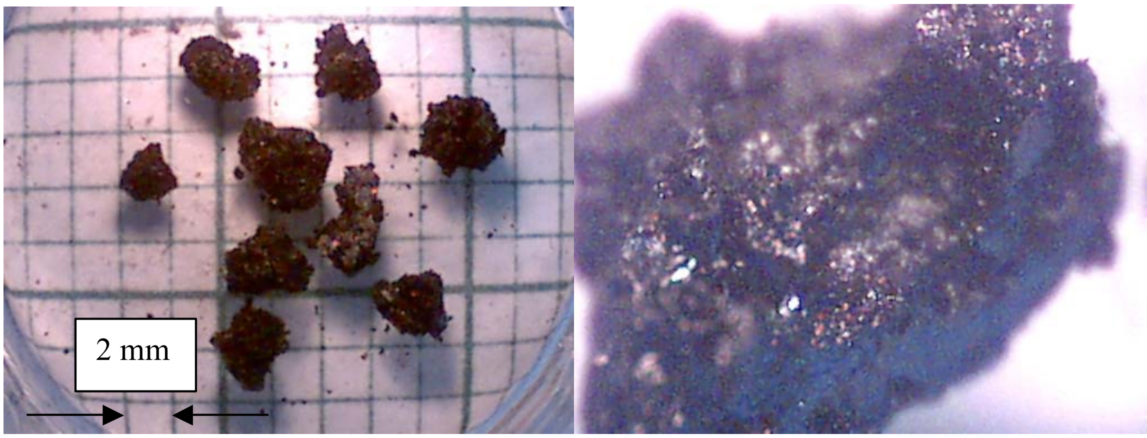

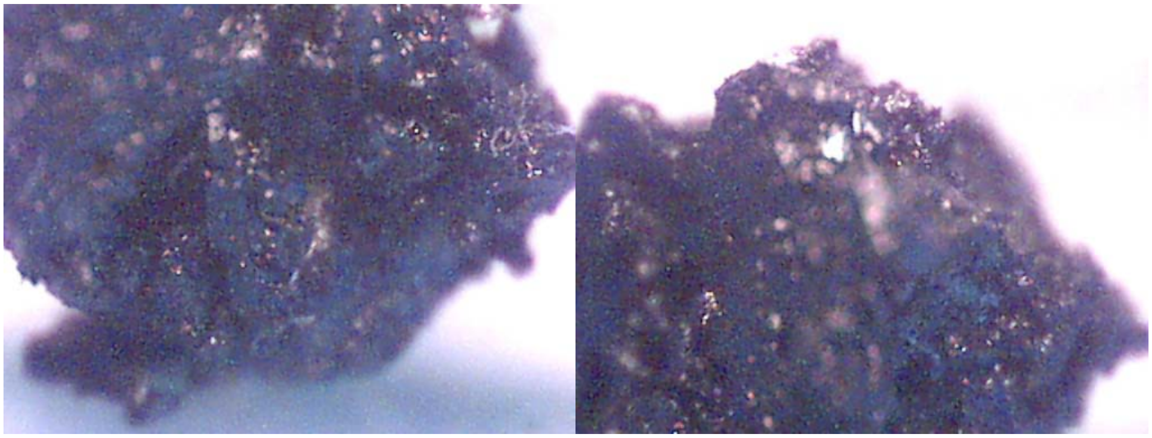

Experiment 29:

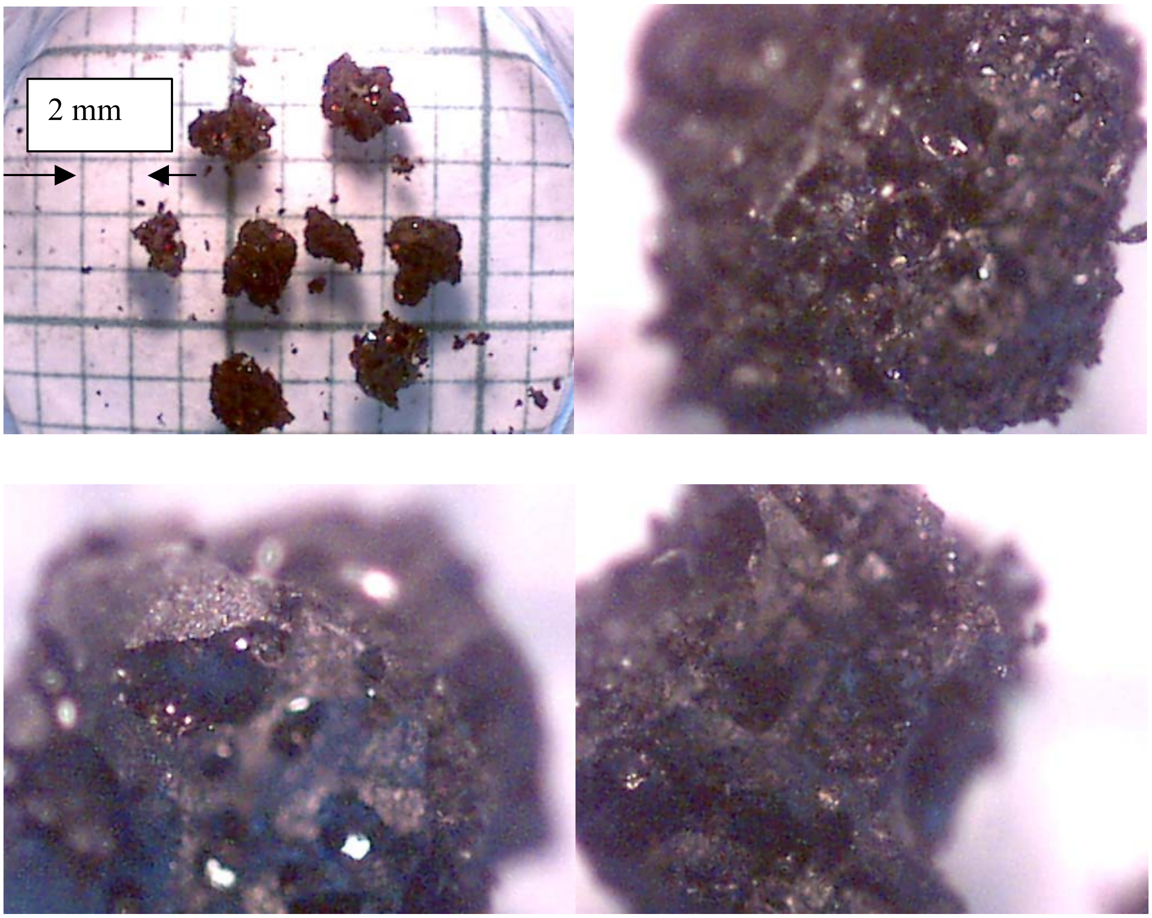

Experiment 30:

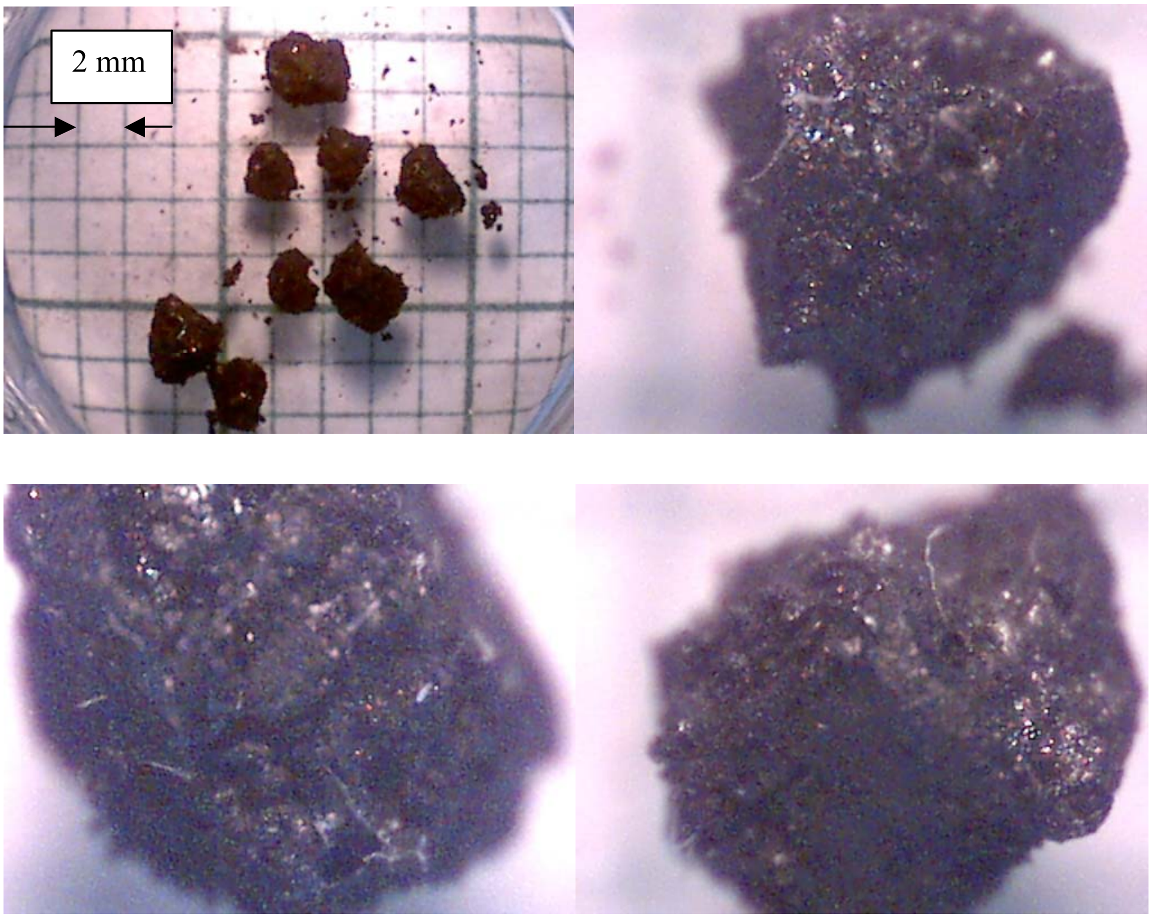

Experiment 31:

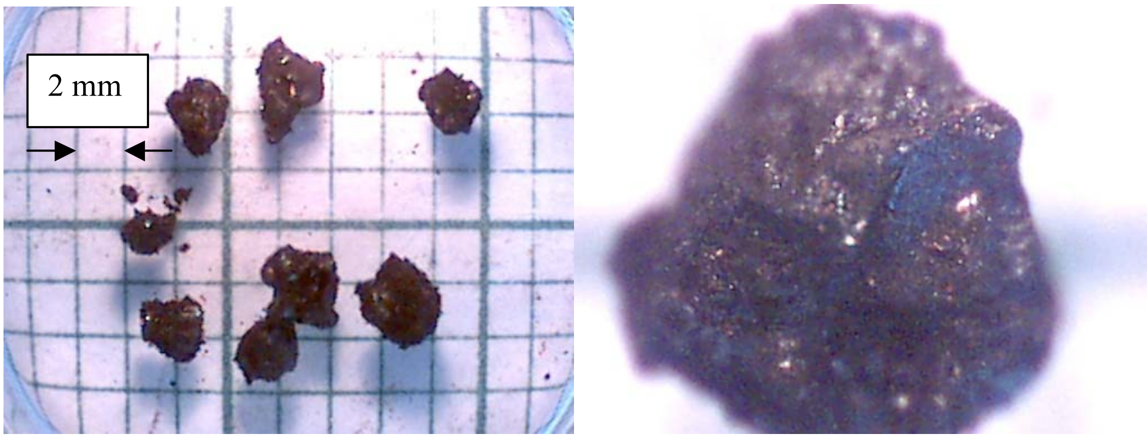

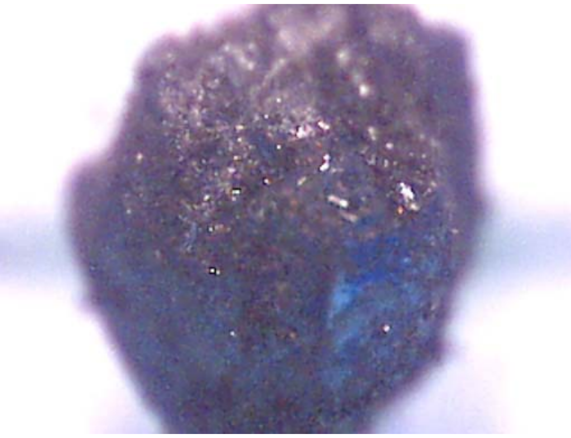

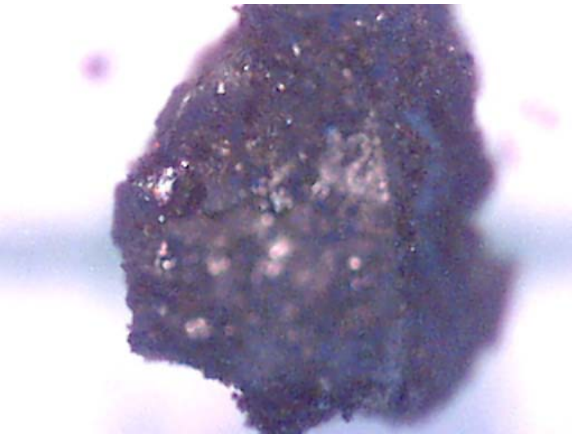

Experiment 32:

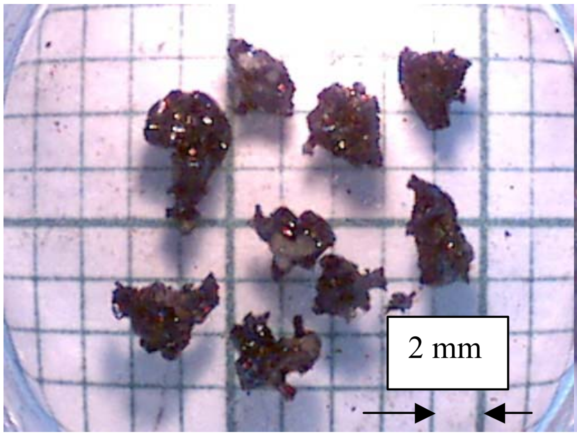

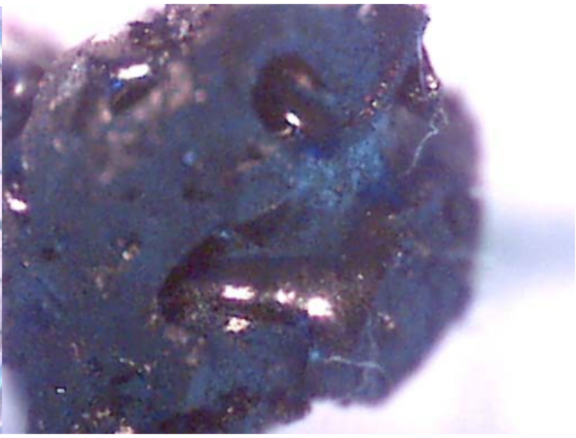

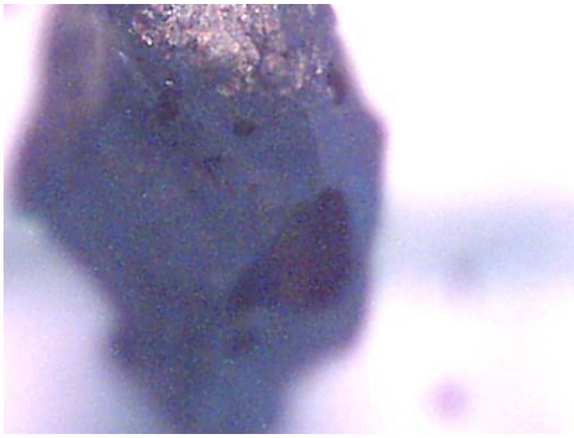

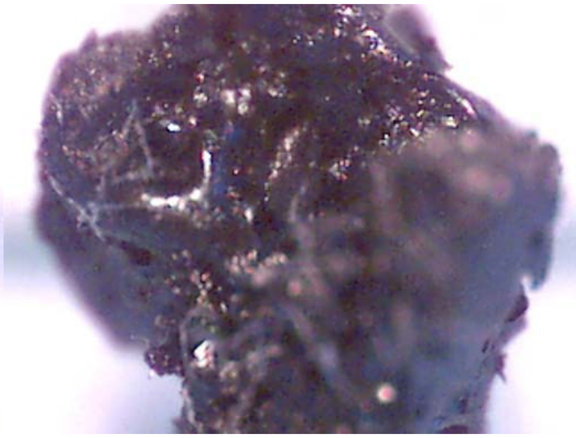

Experiment 33:

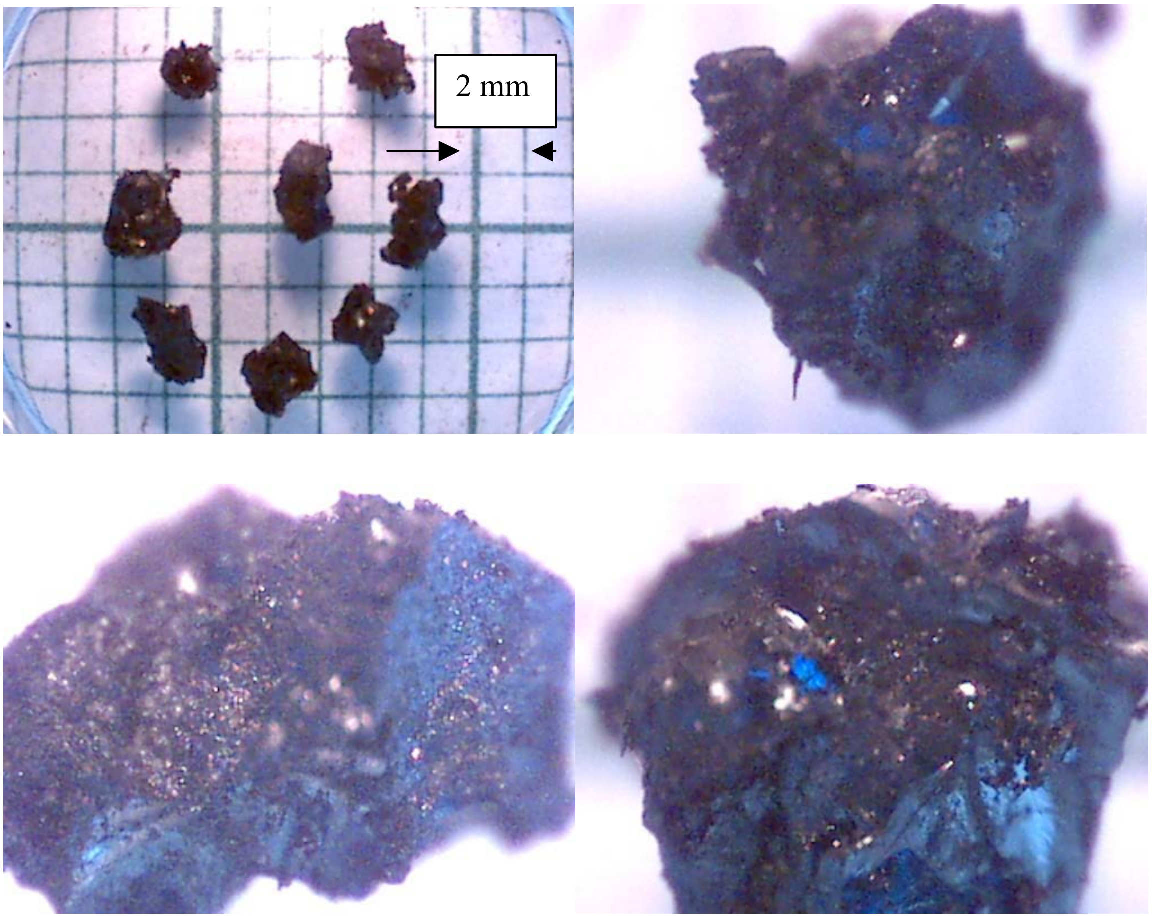

Experiment 34:

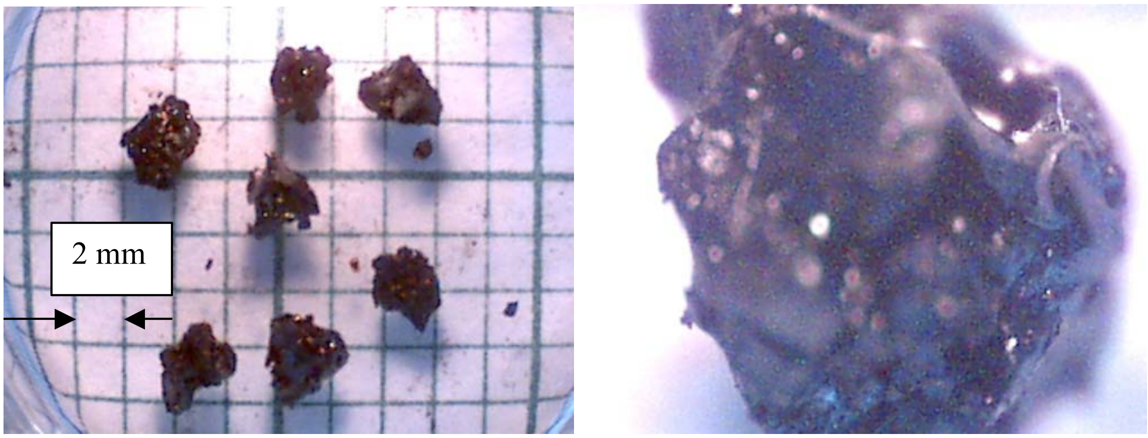

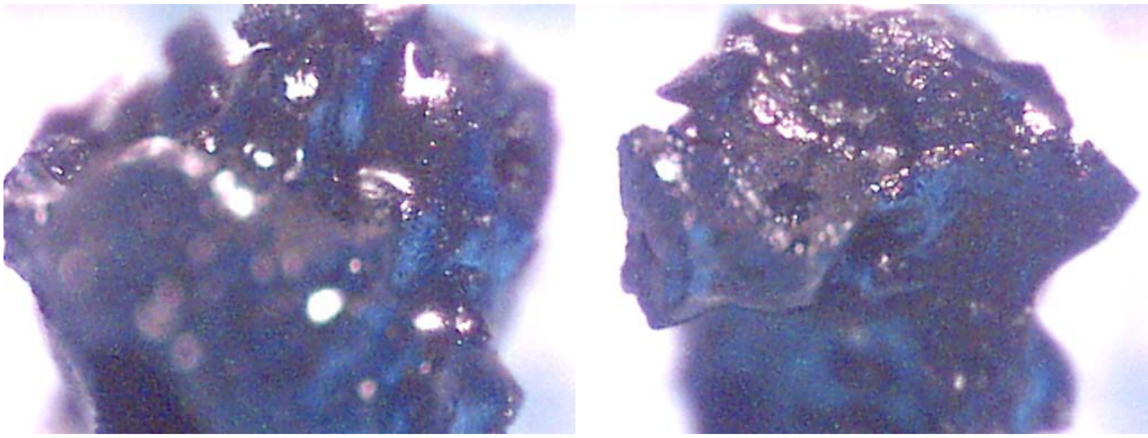

Experiment 35:

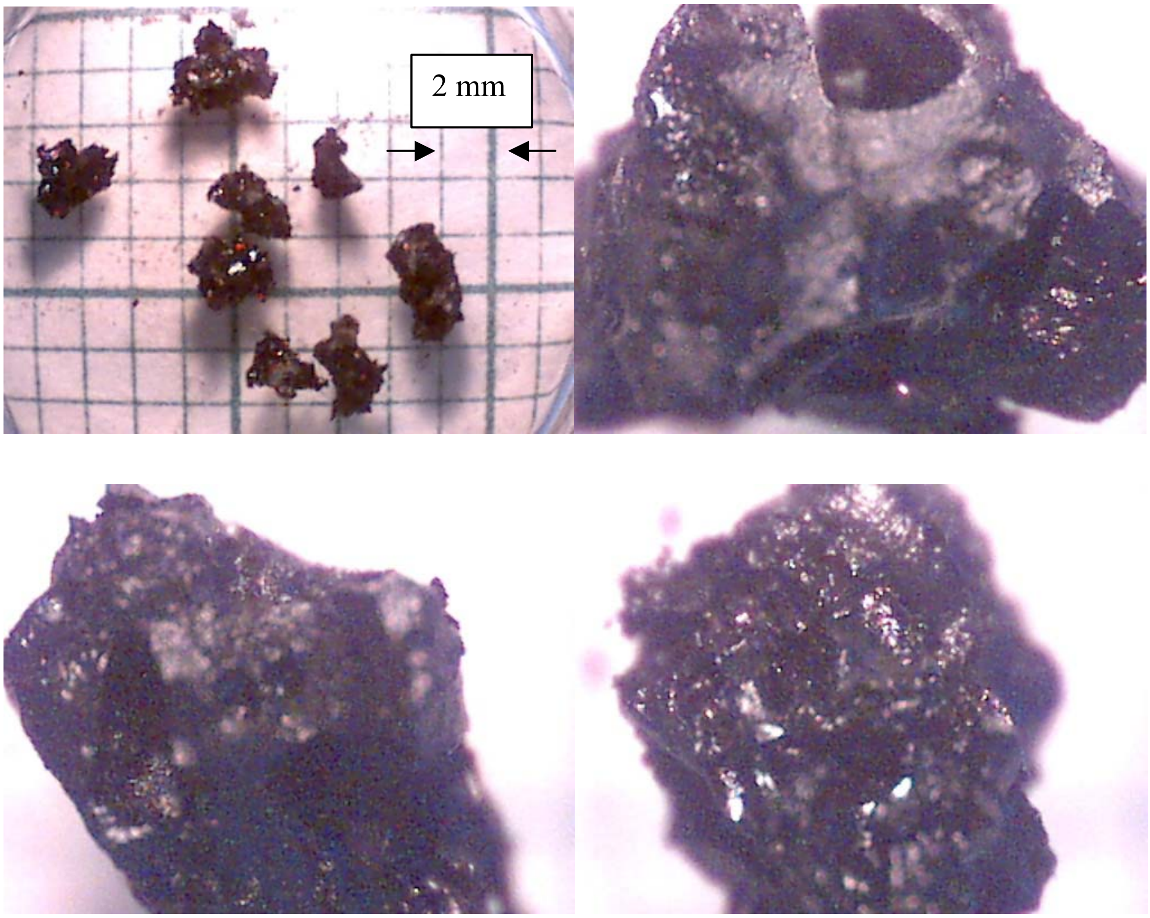

Experiment 36

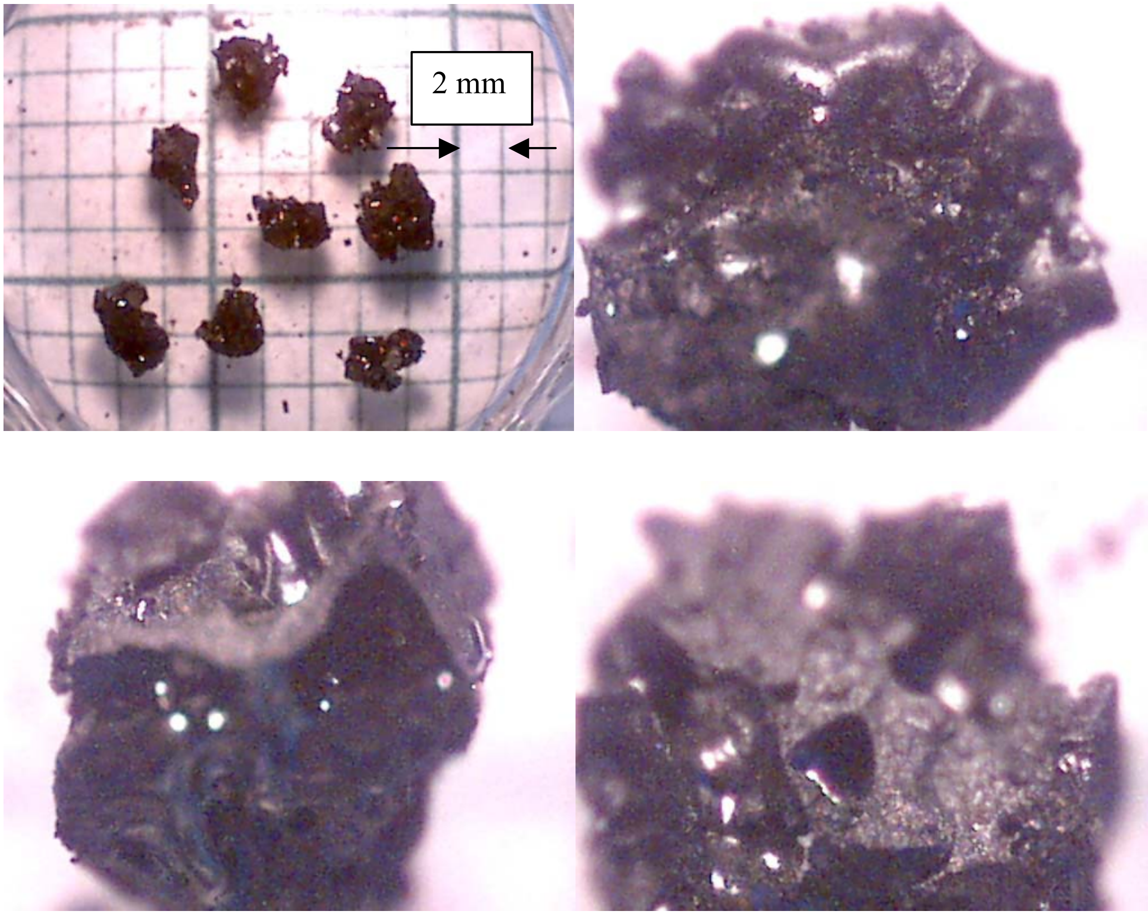

Experiment 38

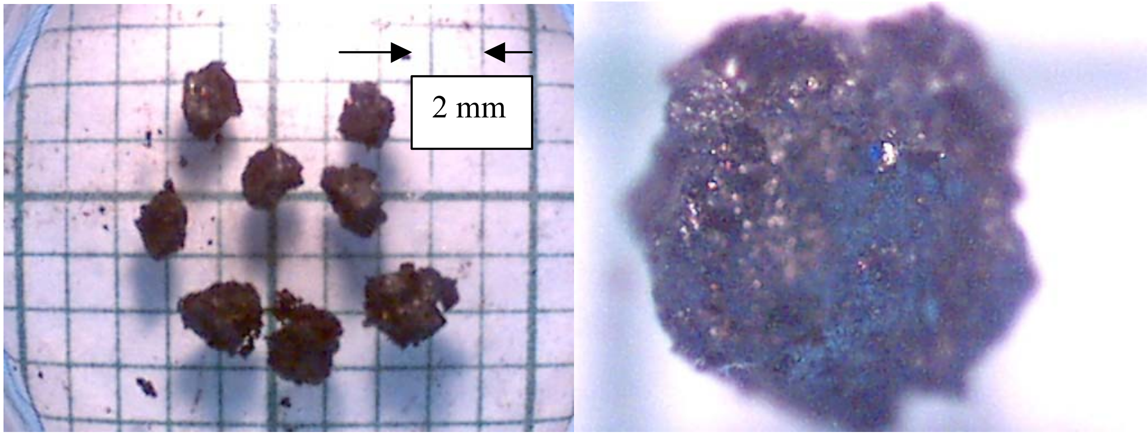

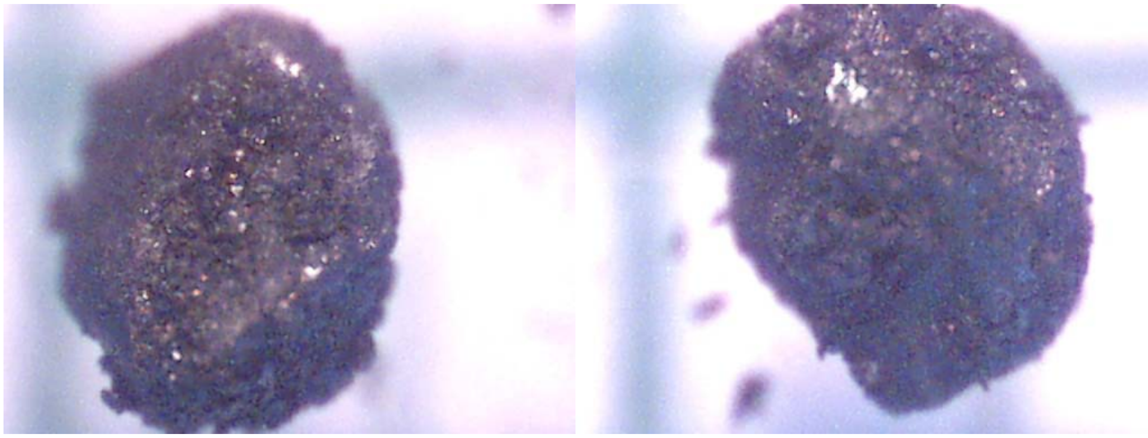

Experiment 40

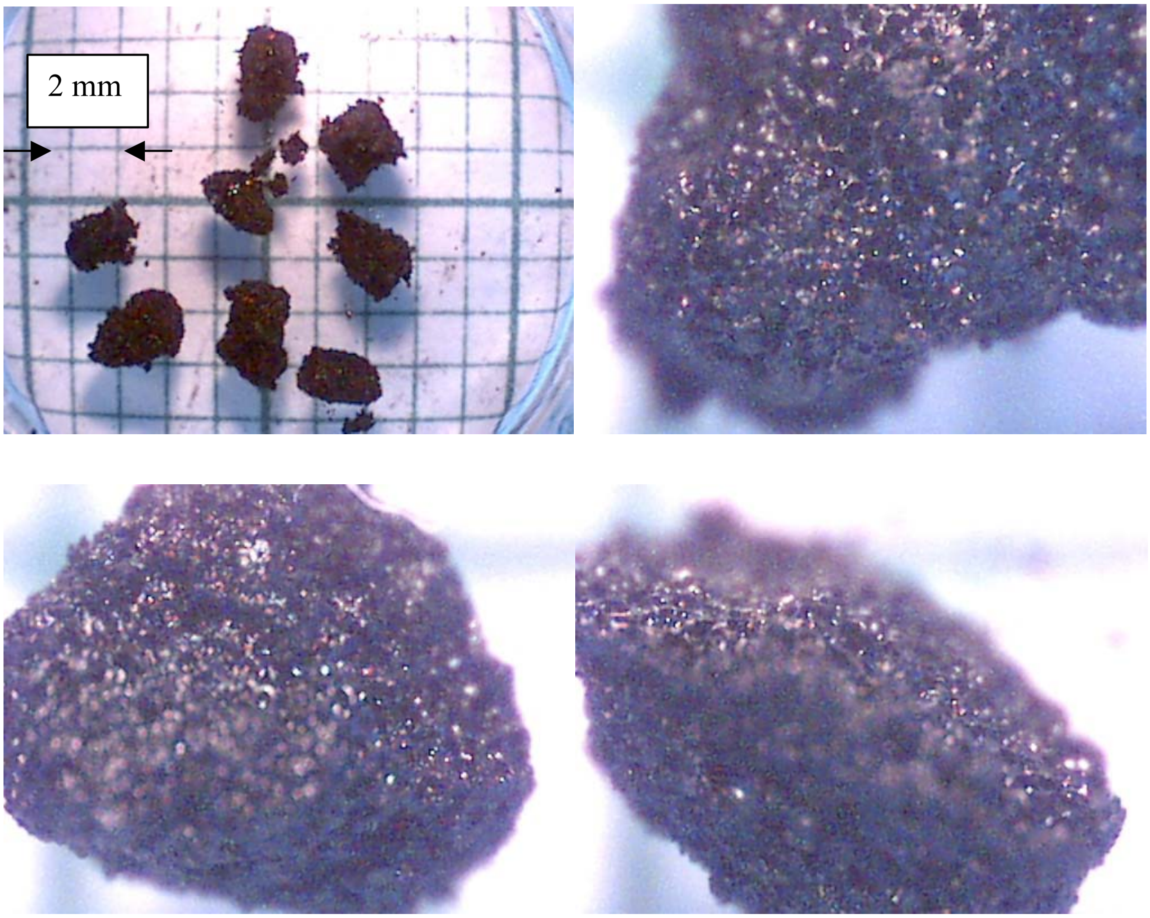

Experiment 41:

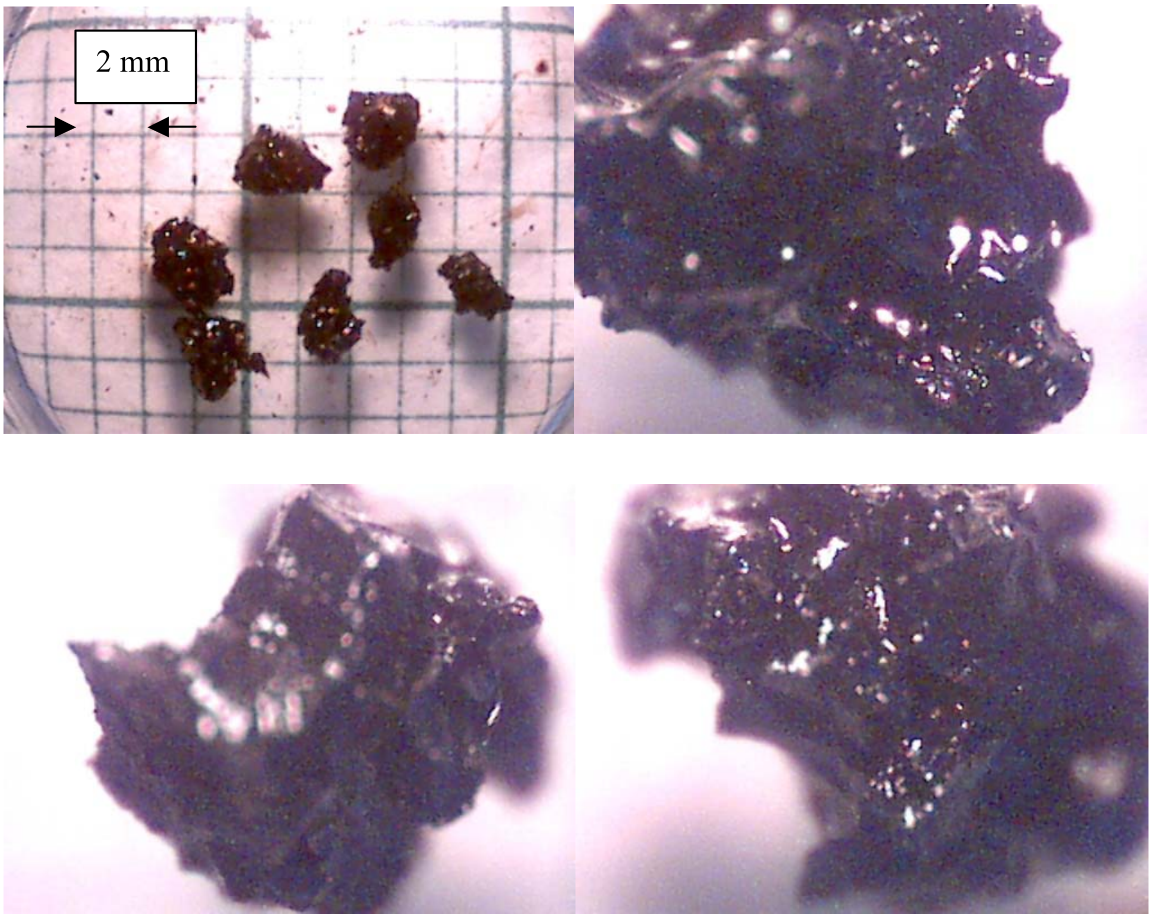

Experiment 42:

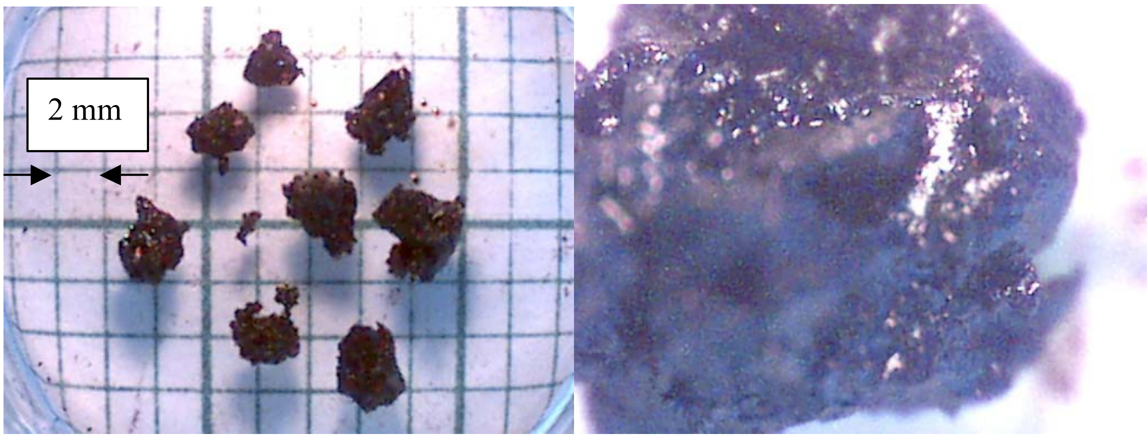

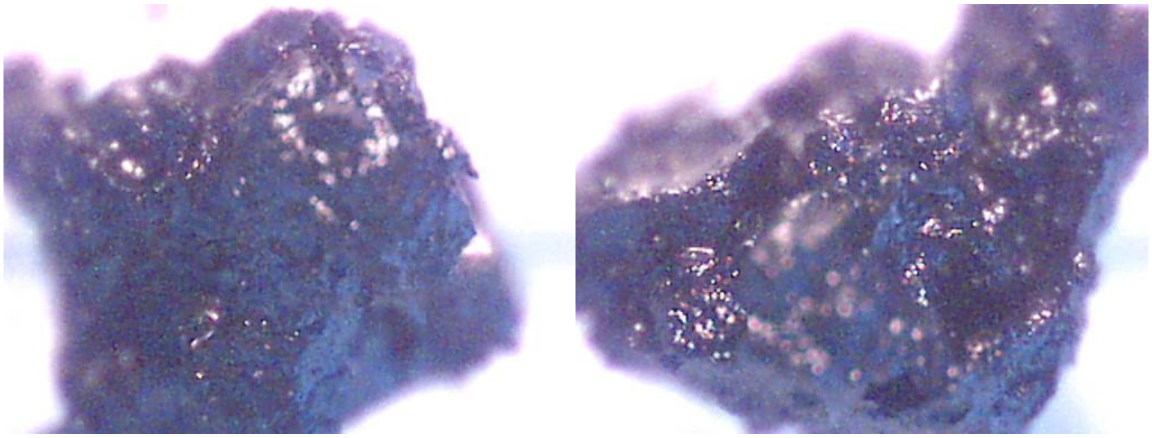

Hardness Test Results

This property was not measured for all experiments. Instead, this test was applied to those samples considered as key experiments for the appearance of both shot coke and sponge coke. The coke hardness test results follow. Also, the average breakage mass and the standard deviation of these measurements are included.

Experiment 09			
Test No.	Breakage Weight (g)	Test No.	Breakage Weight (g)
1	354	6	832
2	664	7	945
3	354	8	832
4	945	9	664
5	1362	10	664
Average (g)		762	
Standard Deviation (g)		298	

Experiment 12			
Test No.	Breakage Weight (g)	Test No.	Breakage Weight (g)
1	664	6	832
2	664	7	664
3	664	8	832
4	354	9	664
5	664	10	664
Average (g)		667	
Standard Deviation (g)		130	

Experiment 20			
Test No.	Breakage Weight (g)	Test No.	Breakage Weight (g)
1	664	6	664
2	945	7	945
3	945	8	832
4	664	9	945
5	945	10	664
Average (g)		821	
Standard Deviation (g)		140	

Experiment 21			
Test No.	Breakage Weight (g)	Test No.	Breakage Weight (g)
1	354	6	664
2	664	7	664
3	895	8	832
4	664	9	664
5	832	10	664
Average (g)		690	
Standard Deviation (g)		149	

Experiment 22			
Test No.	Breakage Weight (g)	Test No.	Breakage Weight (g)
1	664	6	664
2	664	7	945
3	832	8	832
4	895	9	664
5	832	10	354
Average (g)		735	
Standard Deviation (g)		171	

Experiment 25			
Test No.	Breakage Weight (g)	Test No.	Breakage Weight (g)
1	832	6	895
2	664	7	664
3	832	8	664
4	664	9	945
5	895	10	664
Average (g)		772	
Standard Deviation (g)		118	

Experiment 26			
Test No.	Breakage Weight (g)	Test No.	Breakage Weight (g)
1	664	6	945
2	664	7	664
3	1362	8	832
4	664	9	945
5	664	10	664
Average (g)		807	
Standard Deviation (g)		228	

Experiment 27			
Test No.	Breakage Weight (g)	Test No.	Breakage Weight (g)
1	664	6	354
2	664	7	664
3	832	8	895
4	895	9	945
5	664	10	664
Average (g)		724	
Standard Deviation (g)		174	

Experiment 28			
Test No.	Breakage Weight (g)	Test No.	Breakage Weight (g)
1	832	6	664
2	664	7	664
3	354	8	664
4	664	9	895
5	945	10	664
Average (g)		701	
Standard Deviation (g)		164	

Experiment 29			
Test No.	Breakage Weight (g)	Test No.	Breakage Weight (g)
1	664	6	945
2	945	7	664
3	832	8	832
4	664	9	945
5	895	10	945
Average (g)		833	
Standard Deviation (g)		125	

Experiment 30			
Test No.	Breakage Weight (g)	Test No.	Breakage Weight (g)
1	1362	6	895
2	664	7	945
3	945	8	664
4	895	9	832
5	945	10	664
Average (g)		881	
Standard Deviation (g)		208	

Experiment 31			
Test No.	Breakage Weight (g)	Test No.	Breakage Weight (g)
1	664	6	945
2	664	7	664
3	664	8	832
4	945	9	945
5	945	10	664
Average (g)		793	
Standard Deviation (g)		140	

Experiment 32			
Test No.	Breakage Weight (g)	Test No.	Breakage Weight (g)
1	664	6	832
2	664	7	664
3	664	8	832
4	664	9	664
5	664	10	664
Average (g)		698	
Standard Deviation (g)		71	

Experiment 33			
Test No.	Breakage Weight (g)	Test No.	Breakage Weight (g)
1	664	6	354
2	354	7	664
3	664	8	832
4	664	9	664
5	664	10	664
Average (g)		619	
Standard Deviation (g)		149	

Experiment 34			
Test No.	Breakage Weight (g)	Test No.	Breakage Weight (g)
1	945	6	664
2	354	7	664
3	664	8	945
4	1362	9	664
5	664	10	664
Average (g)		759	
Standard Deviation (g)		269	

Experiment 35			
Test No.	Breakage Weight (g)	Test No.	Breakage Weight (g)
1	354	6	664
2	664	7	664
3	945	8	664
4	945	9	664
5	664	10	664
Average (g)		689	
Standard Deviation (g)		166	

Experiment 36			
Test No.	Breakage Weight (g)	Test No.	Breakage Weight (g)
1	895	6	945
2	1423	7	1362
3	1590	8	1362
4	664	9	664
5	1362	10	664
Average (g)		1093	
Standard Deviation (g)		363	

Experiment 38			
Test No.	Breakage Weight (g)	Test No.	Breakage Weight (g)
1	945	6	664
2	832	7	664
3	664	8	945
4	895	9	664
5	664	10	832
Average (g)		777	
Standard Deviation (g)		125	